Additions and corrections

Page	Line	Replace	with
30	8	...its responce being...	...and its response is...
31	1	Dispite...	Despite...
32	10	These channels were...	This channel was...
33	5	...and can be envisaged...	...and it can be envisaged...
38	13	...with rise...	...with a rise...
42	11	et al	et al.
42	13	...of Lys_4...	...or Lys_4...
43	15	et al	et al.
44	16	et al	et al.
45	7	et al	et al.
48	13	Concequently...	Consequently...
49	1	et al	et al.
52	14	et al	et al.
52	25	...suggeted...	...suggested...
60	2	et al	et al.
77	14	...quatermary...	...quaternary...
79	3	...whch...	...which...
82	9	...appart...	...apart...
99	6	...excert...	...exert...
104	entry **14**	26.0 ± 14	26 ± 14
109	9	...properies...	...properties...
122	7	...accosiated...	...associated...
123	4	...E_{LUMO} consists...	...E_{LUMO} provides...
123	5	...ralationships...	...relationships...
124	12	et al	et al.
131	4	...section **2.3**...	...section **2.4**...
133	12	...K_is...	...K_i values...
133	13	...500 times...	...50 times...
135	Table	Kcal/mol	kcal/mol
135	11	Kcal/mol	kcal/mol
136	6	Kcal/mol	kcal/mol
136	23	Kcal/mol	kcal/mol
136	26	Kcal/mol	kcal/mol
136	27	Kcal/mol	kcal/mol
137	13	Kcal/mol	kcal/mol
137	14	Kcal/mol	kcal/mol
137	15	Kcal/mol	kcal/mol
137	16	Kcal/mol	kcal/mol
138	6	Kcal/mol	kcal/mol
138	Table	Kcal/mol	kcal/mol
139	9	Kcal/mol	kcal/mol
139	Table	Kcal/mol	kcal/mol
140	Table	Kcal/mol	kcal/mol
141	10	Kcal/mol	kcal/mol
141	12	Kcal/mol	kcal/mol
143	6	...space i.e....	...space, i.e....
152	15	...comparable but not identical...	...comparable, but not identical,...
155	26	et al	et al.
164	1	4-chloroquinoline	4-Chloroquinoline
164	3	4-hydroxyquinoline	4-Hydroxyquinoline
184	4	Genaral...	General...
184	7	4-chloroquinaldine...	4-Chloroquinaldine
216	3	4-Bromobut-1-yl	4-bromobut-1-yl
233	17	1 g of epoxy-activated Sepharose 6B (Pharmacia)...	Epoxy-activated Sepharose 6B (Pharmacia) (1 g)...
238	6	et al	et al.

SYNTHESIS AND STRUCTURE - ACTIVITY STUDIES OF NOVEL POTASSIUM ION CHANNEL BLOCKERS

(K+)

A thesis presented in partial fulfilment

of the requirements for the

Doctor of Philosophy Degree

of the University of London

DIMITRIOS GALANAKIS

Department of Chemistry

University College London

April 1995

Signature : 

Date : 11-5-1995

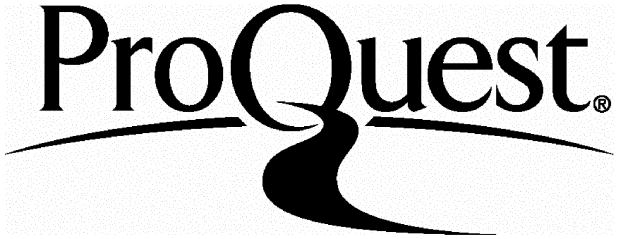

Acknowledgements

I am indebted to Professor C.R. Ganellin for giving me the opportunity to work on this project, for the award of a grant, which enabled me to carry out the work and for his advice, insight and encouragement.

I am grateful to Dr Phil Dunn of the Department of Pharmacology for performing the electrophysiological testing of the compounds and to Professor Donald Jenkinson for helpful discussions.

I would also like to thank Dr Peter Strong of the Neuromuscular Unit of Hammersmith Hospital for offering me the chance to perform radioligand binding studies in his laboratory and Dr Jonathan Wadsworth for help with the practical aspects of binding experiments.

Compounds **32** - **35** were synthesised by Mr Sajeed Malik as part of his 3rd year undergraduate project, working under the supervision of Prof. Ganellin and myself.

Special thanks are due to Drs Ramesh Bambal, Paul Bishop and Andrew Moore for their assistance during my first months in the lab; Dr Julie Calder for introducing me to molecular modelling techniques and Drs Keith Wibley and Andy Vinter for helpful discussions on the modelling.

I thank Alan Stones, Steve Corker, Jill Maxwell and Dr Margaret Mruzek for providing analytical and spectroscopic data.

Finally, but by no means least, I would like to thank Mr Wasyl Tertiuk for his help and support and all members of the Ganellin group for making my stay enjoyable.

The Upjohn Company is acknowledged for the purchase of HPLC equipment and a Silicon Graphics IRIS 4D workstation. I am grateful to the Wellcome Trust for the purchase of a Silicon Graphics Indigo/2 workstation and for a grant for consumables.

This work has been accomplished thanks to the devotion, love and support of my parents.

To them this thesis is dedicated.

Abstract

K^+ channels are found in all animal cells where they play a key role in controlling the excitability of the cell. They exist as multiple subtypes most of which have yet to be exploited for therapeutic use. An area in need of pharmacological exploration is that of Ca^{2+} - activated K^+ channels. One of the subtypes, the small conductance (apamin - sensitive) Ca^{2+} - activated K^+ (SK_{Ca}) channel is blocked by dequalinium (**I**, $R^1 = CH_3$, $R^2 = NH_2$, $R^3 = H$) at micromolar concentrations.

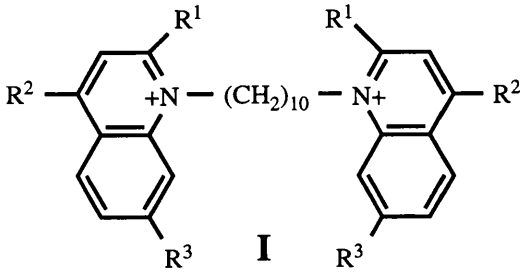

I

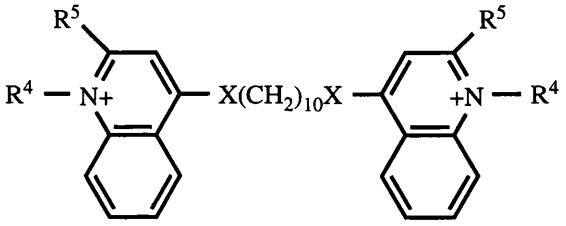

II

Dequalinium is not adequately potent. Having this as the lead structure, novel analogues of the general type **I** have been synthesised and submitted for testing for their ability to block the slow after - hyperpolarisation that follows the action potential measured on rat sympathetic neurones. This series was designed to explore whether particular chemical properties of the substituents might affect activity and quantitative structure - activity correlations were sought. Good correlations were obtained between blocking potency and the energies of either of the frontier orbitals (HOMO and LUMO) for the compounds.

Furthermore, compounds of the general structure **II**, where the aminoquinoline rings have been "inverted", have been synthesised and submitted for testing. Again, good correlations were obtained between blocking potency and the energies of either of the frontier orbitals for the compounds. It was also possible to combine the results for both series **I** and **II** (i.e. 24 compounds) into a single correlation of potency against the energies of either of the frontier orbitals.

Rigidification of the alkyl chain of dequalinium did not alter potency significantly. Furthermore, compounds belonging to series **I** with $R^1 = R^3 = H$, $R^4 = NH_2$ having 5, 6,

8, 10 and 12 methylene groups in the alkyl chain had similar activities. The above suggest that the conformational mobility of the alkyl chain as well as the maximum distance between the quinolinium groups are not critical for SK_{Ca} channel blockade.

Compounds in which the quinolinium groups of dequalinium have been replaced by other charged heterocycles, have also been synthesised and submitted for testing. The aim has been to reveal any special features associated with the quinolinium group. It was shown that compounds with different heterocycles are able to block the SK_{Ca} channel but that quinoline was the best heterocycle.

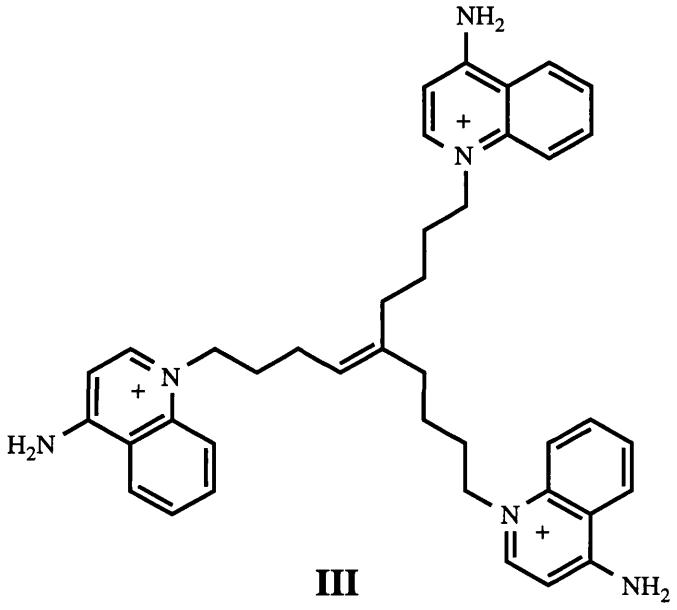

III

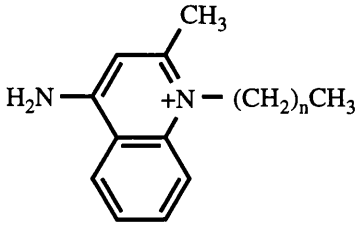

IV: n = 3
V : n = 9

Finally, to examine whether both quinolinium groups of dequalinium contribute to SK_{Ca} channel blockade and to investigate the nature of their contribution, compound **III** (having three quinolinium groups) was synthesised and compared with compounds **IV** and **V** (having one quinolinium group, previously made) and dequalinium. The affinities of the compounds were determined from inhibition of the specific ^{125}I - apamin binding to SK_{Ca} channels of rat brain synaptic plasma membranes. Increasing the number of quinolinium groups increased potency and it is suggested that the contribution of the second and third quinolinium groups in the molecules of dequalinium and **III** may not be the consequence of direct binding to the channel but may arise from a statistical effect. Compound **III** is the most potent non - peptidic blocker of the SK_{Ca} channel on this assay so far reported.

CONTENTS

PAGE

PAGE

Abbreviations

abs. EtOH	absolute ethanol
ACh	acetylcholine
AD	Alzheimer's disease
ADP	adenosine-5'-diphosphate
AHP	after - hyperpolarisation
Ala	alanine
AM1	Austin Model 1
ANBNOS	5-azido-2-nitrobenzoic acid, succinimidyl ester
ANPAA	[(4-azido-2-nitrophenyl)amino]acetic acid, succinimidyl ester
4-AP	4-aminopyridine
Ar	aryl, argon
Arg	arginine
Asn	asparagine
Asp	aspartic acid
ATP	adenosine-5'-triphosphate
BR	identification tag (B. Del Rey Herrero)
br	broad
BK_{Ca}	high conductance Ca^{2+} - activated K^+ channel
BSA	bovine serum albumin
$[Ca^{2+}]_i$	intracellular concentration of Ca^{2+}
cAMP	cyclic adenosine-3',5'-monophosphate
CD	identification tag (C. Davis), circular dichroism
cDNA	complementary DNA
ChTX	charybdotoxin
CI	chemical ionisation
CNS	central nervous system
CO	identification tag (C. Owen)
Cys	cysteine
d	doublet
Da	Dalton (molecular mass unit)
DBU	1,8-diazabicyclo[5.4.0]undec-7-ene
dd	doublet of doublets
DG	identification tag (D. Galanakis)
ΔG	free energy change
ΔG_{sol}	free energy of solvation
ΔH	enthalpy change
DMF	dimethyl formamide
DMSO	dimethyl sulfoxide

DMSO-d_6	deuterated dimethyl sulfoxide
DPM	disintegrations per min
DS	bis(sulphosuccinimidyl)suberate
DSS	disuccinimidyl suberate
ED_{50}	dose (of drug) that causes 50% of maximum responce
EDA	electron donor - acceptor
EDRF	endothelium - derived relaxing factor
EI	electron impact
EMR	equieffective molar ratio
FAB	fast atom bombardment
fmol	femtomole, 10^{-15} mole
g	gramme
GIRK1	cloned G - protein coupled K_{ACh} channel
Gln	glutamine
Glu	glutamic acid
GTP	guanosine-5'-triphosphate
h	hour
H5	putative pore - forming region of K^+ channel proteins
Har	homoarginine
His	histidine
HOMO	highest occupied molecular orbital
HPLC	high performance liquid chromatography
HSAB	4-azidobenzoic acid, succinimidyl ester
5-HT	5-hydroxytryptamine (serotonin)
Hz	Hertz
IbTX	iberiotoxin
IC_{50}	concentration (of drug) that causes 50% inhibition (of response)
icv	intracerebroventricularly
IK_{Ca}	intermediate conductance Ca^{2+} - activated K^+ channel
IR	infrared
IRK1	cloned K_{IR} channel
iv	intravenously
J	coupling constant (NMR)
JCR	identification tag (J. Campos Rosa)
K_A	A - channel (transient outward, K^+ channel subtype)
K_{ACh}	atrial muscarinic - activated K^+ channel
K_{ATP}	ATP - sensitive K^+ channel
K_D	dissociation constant
kDa	kiloDalton (10^3 Daltons)
$K_{5\text{-}HT}$	5-HT - inactivated K^+ channel

K_i	dissociation constant of inhibitor
K_{IR}	inward rectifier (K^+ channel subtype)
kJ	kiloJoule, 10^3 Joules
K_M	muscarinic - inactivated K^+ channel
K_{Na}	Na^+ - activated K^+ channel
K_{SR}	sarcoplasmic reticulum K^+ channel
K_V	delayed rectifier (K^+ channel subtype)
K_{vol}	cell - volume - sensitive K^+ channel
K_{VR}	rapid delayed rectifier (K^+ channel subtype)
K_{VS}	slow delayed rectifier (K^+ channel subtype)
LD_{50}	dose (of drug) that causes death in 50% of the animals
LDA	lithium diisopropylamide
Leu	leucine
LUMO	lowest unoccupied molecular orbital
Lys	lysine
m	multiplet
M	molar
M0	segment of ROMK1 channel protein
M1	segment of IRK1 protein
M2	subtype of muscarinic receptors, segment of IRK1 protein
MCD	mast cell degranulating
Me	methyl
m/e	mass to charge ratio
MEK	methyl ethyl ketone (butanone)
mg	milligramme, 10^{-3} gramme
MHz	megaHertz, 10^6 Hertz
ml	millilitre, 10^{-3} litre
mmol	millimole, 10^{-3} mole
min	minute
MINDO/3	modified intermediate neglect of differential overlap 3
MM2	molecular mechanics 2
MNDO	modified neglect of diatomic (differential) overlap
MNOBA	m-nitrobenzyl alcohol
MO	molecular orbital
MOPAC	molecular orbital package (name of computer program for MO calculations)
mp	melting point
MS	mass spectrum
MW	molecular weight
µl	microlitre, 10^{-6} litre
µM	micromole, 10^{-6} mole

nM	nanomole, 10^{-9} mole
nm	nanometer, 10^{-9} meter
NMR	nuclear magnetic resonance
NOE	nuclear Overhauser enhancement
NTX	noxiustoxin
PC12	phaeochromocytoma cell line
Ph	phenyl
Phe	phenylalanine
pK_i	$-\log K_i$
PM3	parametric method 3
PO5	peptide toxin isolated from the venom of the scorpion *Androctonus mauretanicus mauretanicus*
prep	preparative
Pro	proline
pS	picosiemens (10^{-12} siemens)
py	pyridine
q	quartet
QSAR	quantitative structure - activity relationships
quin	quinoline
ROMK1	cloned ATP - regulated K^+ channel
RP	reverse phase
rpm	rounds per min
RT	room temperature
s	singlet
S1 - S6	segments of voltage - dependent K^+ channel proteins
SANPAH	[6-(4-azido-2-nitrophenyl)amino]hexanoic acid, succinimidyl ester
SAR	structure - activity relationships
SB	identification tag (S. Beels)
sc	subcutaneously
SCF	self - consistent field
SCyTx	scyllatoxin (leiurotoxin I)
SD	standard deviation
SEM	standard error of the mean
SK_{Ca}	small conductance Ca^{2+} - activated K^+ channel
SM	identification tag (S. Malik)
t	triplet
TEA	triethylammonium
TFA	trifluoroacetic acid
TFAA	trifluoroacetic anhydride

THF	tetrahydrofuran
Thr	threonine
TLC	thin layer chromatography
TMEDA	N,N,N',N'-tetramethylethylenediamine
TMS	tetramethylsilane
Tris	tris(hydroxymethyl)aminomethane
TsOH	p-toluenesulfonic acid
Tyr	tyrosine
UCL	identification tag (University College London)
UV	ultraviolet
Val	valine

Thesis compounds

UCL No	Thesis compound No	Page of experimental
1407	**36**	203
1417	**15**	184
1426	**37**	204
1427	**38**	205
1436	**16**	186
1437	**31**	198
1438	**17**	188
1439	**18**	189
1440	**19**	190
1445	**20**	191
1450	**39**	207
1454	**21**	192
1455	**41**	210
1460	**42**	212
1463	**1**	165
1467	**22**	193
1468	**48**	219
1469	**66**	232
1480	**43**	214
1491	**2**	167
1504	**3**	170
1507	**7**	183
1533	**67**	233
1541	**3a**	168
1553	**49**	221
1560	**4**	177
1562	**50**	223

UCL No	Thesis compound No	Page of experimental
1580	**5**	179
1586	**51**	225
1598	**6**	182
1601	**23**	194
1602	**24**	196
1605	**47**	217
1622	**52**	227
1635	**32**	200
1636	**33**	201
1637	**34**	201
1638	**35**	202

THESIS TABLES

Table 1 Structure and biological results for the compounds considered in this study.

Compd No	UCL No	Notebook No	Structure	EMR (±SD)
1	1463	DG-155A	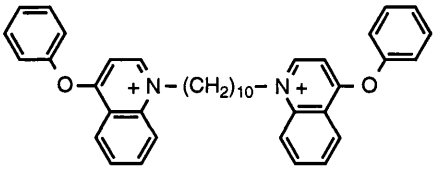	6.5 ± 1.9
2	1491	DG-367B	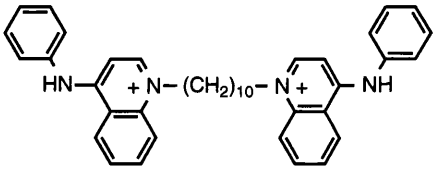	3.4 ± 1.8
3	1504	DG-459A	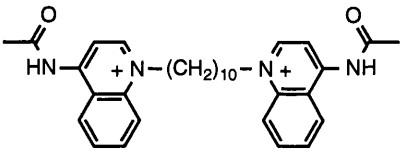	5.5 ± 1.0
4	1560	DG-589B	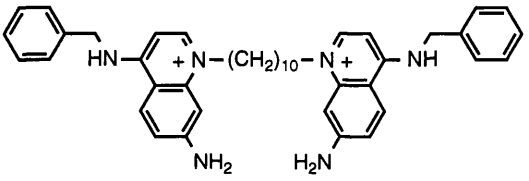	0.9 ± 0.5
5	1580	DG-703C	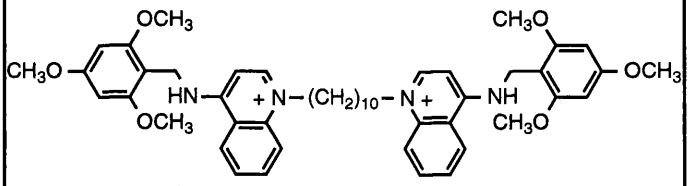	1.0 ± 0.6
6	1598	DG-739B	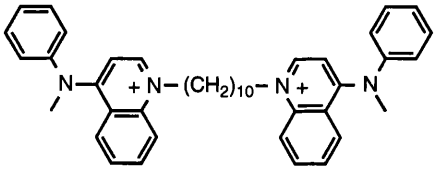	1.8±0.8
7	1507	DG-467A	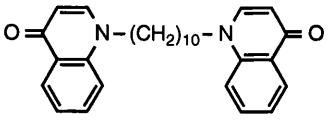	>>10
8	Deq.	—	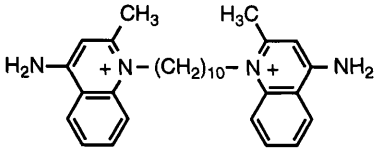	1
9	1072	CD-9A	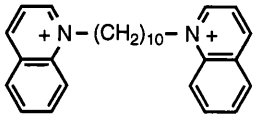	15 ± 7.9
10	1127	CD-45	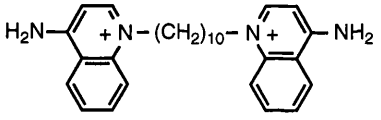	1.3 ± 0.5

Table 1 (continued)

Compd No	UCL No	Notebook No	Structure	EMR (±SD)
11	1130	CD-43B	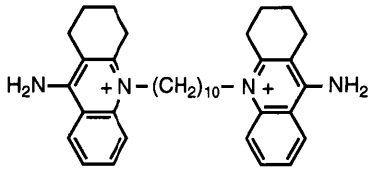	0.9 ± 0.7
12	1173	CD-74	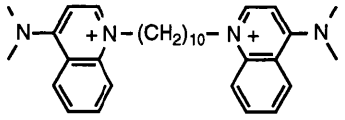	1.4 ± 0.6
13	1359	CO-199B	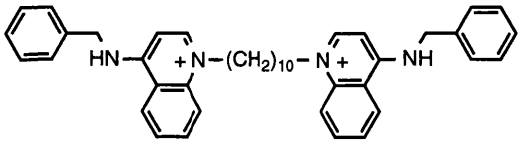	0.7 ± 0.3
14	1431	BR-19A	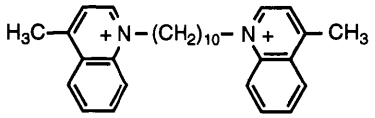	26 ± 14
15	1417	DG-13C	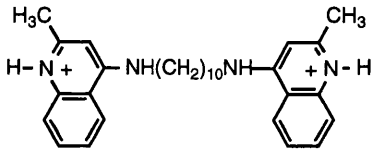	3.6 ± 1.2
16	1436	DG-81D	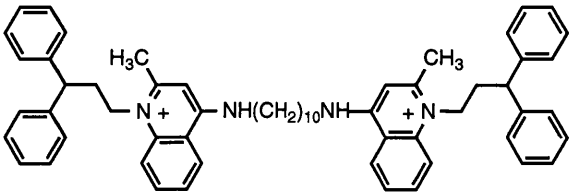	6.2 ± 3.2
17	1438	DG-115C	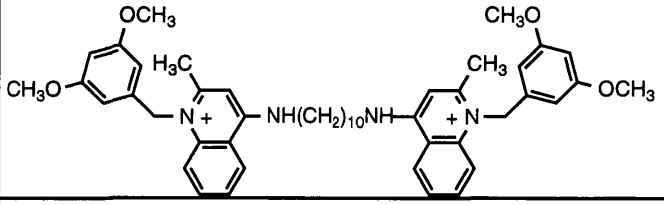	2.1 ± 0.9
18	1439	DG-127C	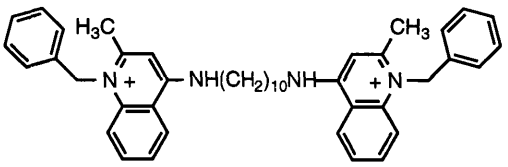	0.6 ± 0.3
19	1440	DG-115B	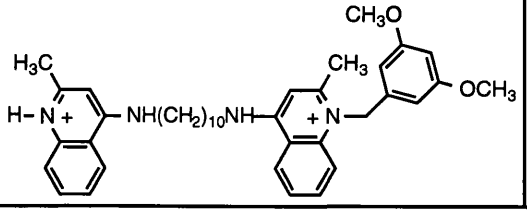	1.2 ± 0.8

Table 1 (continued)

Compd No	UCL No	Notebook No	Structure	EMR (±SD)
20	1445	DG-167A	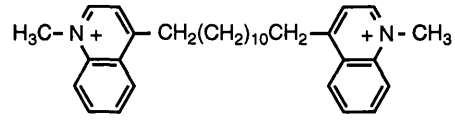	5.9 ± 3.9
21	1454	DG-127B	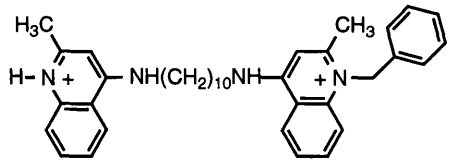	2.4 ± 0.5
22	1467	DG-223A	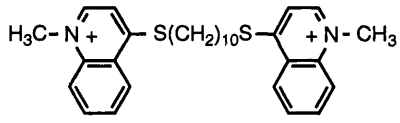	6.2 ± 1.7
23	1601	DG-219B	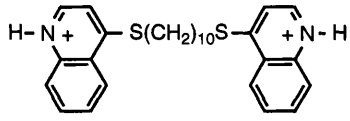	>10
24	1602	DG-159B	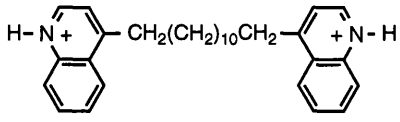	>>10
25	1091	SB-10A	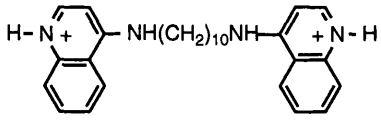	3.5 ± 1.2
26	1118	CD-40	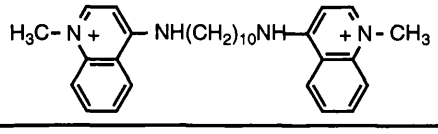	1.9 ± 1.0
27	1144	CD-59	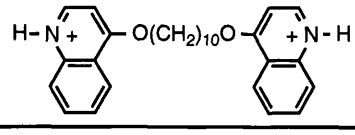	16 ± 21
28	1156	CD-62	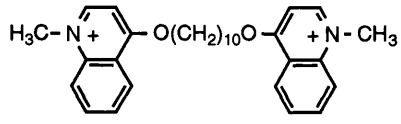	7.2 ± 3.4
29	1360	CO-141A	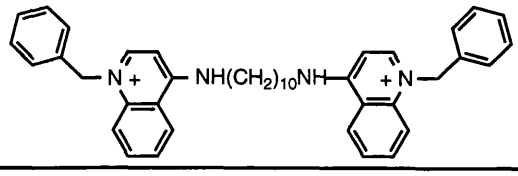	1.0 ± 0.4
30	1449	BR-67C	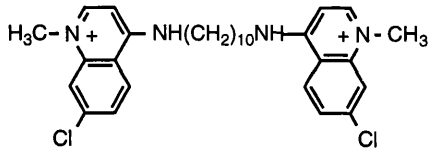	1.5 ± 0.6

Table 1 (continued)

Compd No	UCL No	Notebook No	Structure	EMR (±SD)
31	1437	DG-109A	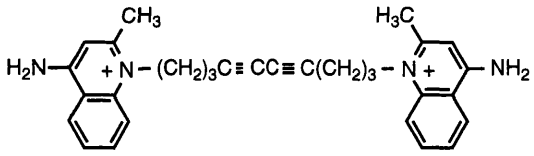	2.4 ± 0.9
32	1635	SM-114B	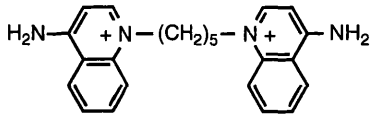	1.0 ± 0.2
33	1636	SM-109A	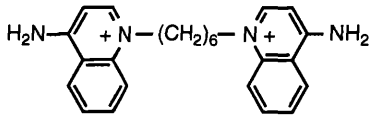	~1
34	1637	SM-104A	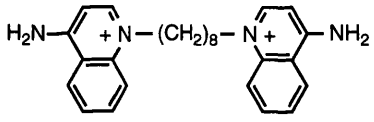	~1
35	1638	SM-106A	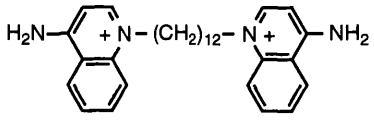	1.8 ± 0.5
36	1407	DG-23B	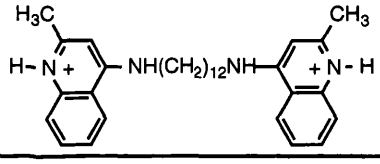	7.1 ± 2.8
37	1426	DG-33C	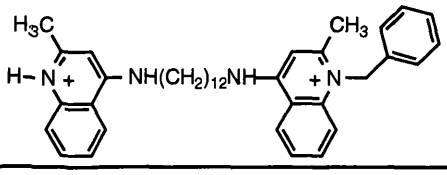	8.0 ± 5.9
38	1427	DG-33D	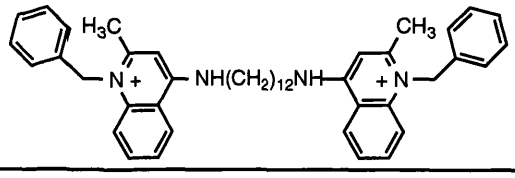	4.0 ± 2.0
39	1450	DG-199A	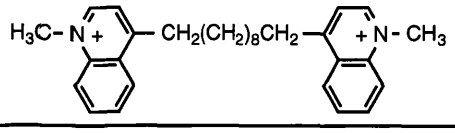	26 ± 9.8
40	1172	CD-71	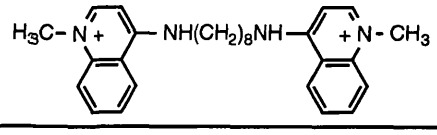	3.1 ± 1.4
41	1455	DG-183B	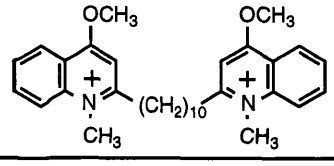	27 ± 9.2

Table 1 (continued)

Compd No	UCL No	Notebook No	Structure	EMR (±SD)
42	1460	DG-207D	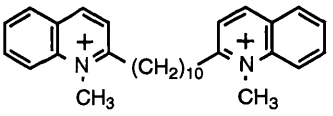	130 ± 34
43	1480	DG-287B	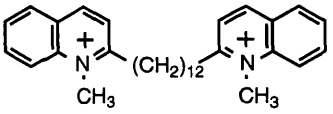	33 ± 10
44	1129	CD-42	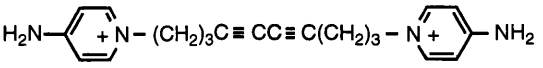	4.7 ± 1.6
45	1092	CD-29	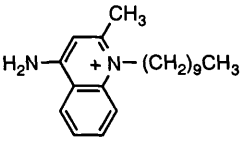	4.7 ± 1.7
46	1171	CD-69	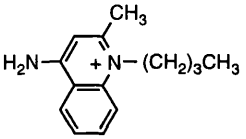	11.9 ± 5.9
47	1605	DG-723B	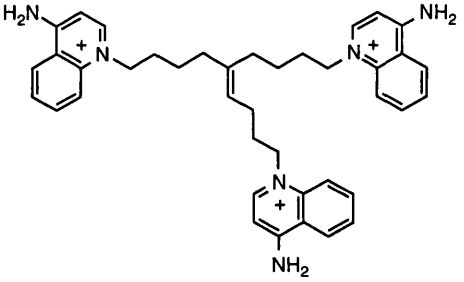	0.24 ± 0.11
48	1468	DG-251A	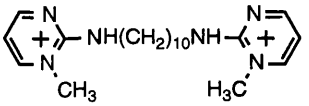	>>10
49	1553	DG-637A	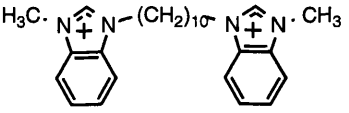	77 ± 23
50	1562	DG-649C	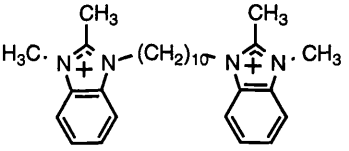	>10
51	1586	DG-735B	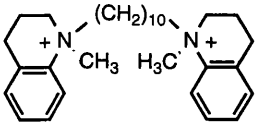	36 ± 20

Table 1 (continued)

Compd No	UCL No	Notebook No	Structure	EMR (±SD)
52	1622	DG-831B	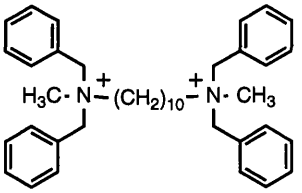	~50
53	1054	CD-1	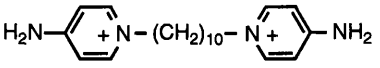	33 ± 13
54	1119	CD-39A	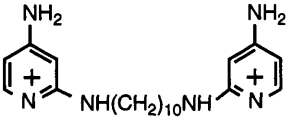	5.0 ± 1.8
55	1143	CD-52	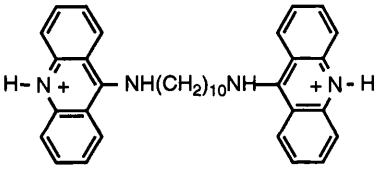	12 ± 4.9
56	1461	BR-103B	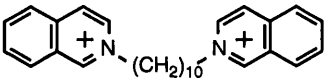	80 ± 42
66	1469	DG-267B	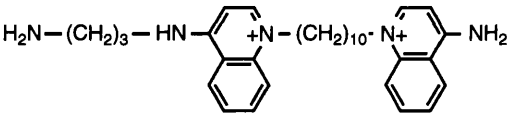	0.78 ± 0.26

CHAPTER 1

INTRODUCTION

Recently, there has been an increasing interest in compounds that modulate K^+ ion channels as potential therapeutic agents.[1,2] K^+ channels are present in all mammalian cells and play a key role in controlling the excitability of the cell. They comprise the most diverse family of ion channels. The most widely used classification of K^+ channels is based on their gating mechanism (the mechanism by which they open or close). This creates a few broad classes of K^+ channels which are further subdivided according to the different kinetics with which they activate, open and inactivate, according to their conductance and according to their pharmacology (compounds which modulate them). An excellent categorization of K^+ channels can be found in the Trends in Pharmacological Sciences Receptor and Ion Channel Nomenclature Supplement (1994) and it is this classification which will be followed here.

1.1 VOLTAGE - DEPENDENT K^+ CHANNELS

1.1.1 DELAYED RECTIFIER (K_V)

K_V channels are activated with some delay (after which they are named) following membrane depolarization. They show outward rectification, carrying K^+ currents which are responsible for membrane repolarization, their conductance being 5 - 60 pS. The first K_V channel to be described was that of the squid giant axon.[3] They are found in a variety of excitable (nerve and muscle) as well as non excitable tissues[4] including frog node of ranvier,[5] bulfrog sympathetic neurones,[6] rat sympathetic neurones,[7] hippocampal pyramidal neurones,[8] cardiac muscle,[9] rat skeletal muscle,[10] and some of these cells may contain more than one delayed rectifier current. Channel inactivation is slow (seconds) or may occur only on repolarization.[4]

Channel structure. K_V channels belong to the family of voltage - gated K^+ channels of which transient outward (K_A) channels are the most extensively studied (see section 1.1.4). The characterization of voltage - gated K^+ channels has been considerably advanced by the identification of a gene of the *Shaker* mutant of the fruitfly *Drosophila melanogaster* which codes for K_A channels (*Shaker* - type K_A channels). As K_V and K_A channels belong to the same family, they exhibit extensive structural similarity[11] (for discussion see section 1.1.4).

Blockers. The blockers of all ion channels can be broadly divided into three main groups: i. Inorganic ions, ii. organic non - peptidic compounds and iii. natural peptidic toxins. Of the first class, Cs^+, Ba^{2+} and Zn^{2+} block K_V channels. Tetraethylammonium (TEA) is an important representative of the second class which effectively blocks a number of K^+ channels, including K_V channels. It appears that the latter possess two TEA binding sites, one extracellular and one intracellular.[11] 4-Aminopyridine (4-AP) and 3,4-diaminopyridine are more selective blockers of the K_V channels, the latter being the most potent of this class.[12] 9-Aminoacridine and the hallucinogen phencyclidine also block K_V channels.[13] Although the physiological effects of local anesthetics are due predominantly to Na^+ channel blockade, these compounds have been also shown to block K_V channels.[14]

As far as peptide toxins are concerned, K_V channels are selectively blocked by *Tityus* toxins (from the scorpion *Tityus serrulatus*),[15] charybdotoxin (from the venom of scorpion *Leiurus quinquestriatus habraeus*)[16] which also blocks BK_{Ca} channels (see below), margatoxin (from the venom of the scorpion *Centruroides margaritatus*),[17] noxiustoxin (from the venom of the scorpion *Centruroides noxius*)[18] and β- and γ-dendrotoxins (from mamba snake venom).[19]

1.1.2 RAPID DELAYED RECTIFIER (K_{VR})

These are found in heart cells and are responsible for the rapidly activating component of the cardiac delayed rectifier K^+ current.[20] They show strong inward rectification.

Blockers. These include the benzenesulphonamide antiarrhythmic drug E-4031 as well as dofetilide, sotalol, tedisamil and quinidine.

1.1.3 SLOW DELAYED RECTIFIER (K_{VS})

Together with K_{VR}, K_{VS} channels exist in the heart and carry a very slowly activating and inactivating K^+ current which is the second component of the cardiac delayed rectifier K^+ current.[20] They show less rectification than K_{VR} channels and the current is ~10 times larger.

Blockers. Compounds LY97241 and NE10118 block K_{VS} channels while the K_{VR} channel blocker E-4031 is ineffective as a K_{VS} channel blocker.

1.1.4 A-CHANNEL (K_A)

This is a very important class of K^+ channels. They are activated by depolarization after a period of hyperpolarization and carry fast, outward K^+ currents, thus driving the potential towards more negative values. They play a crucial role in the regulation of firing rate at spontaneously active cells by delaying depolarization, thus prolonging the interspike interval. They are found in neurones[21] where they modulate neuronal firing rate.

Channel structure. Recently, a number of cDNAs encoding K^+ channels have been cloned from various species, including human, and very similar primary sequences for the derived K^+ channels were revealed.[22] The primary sequences of all these channels

consist of a hydrophilic N- and C-terminus and a highly conserved core region. The latter is composed of six hydrophobic segments (S1 - S3, S5, H5 and S6) and a positively charged amphipathic segment (S4). Segments S1 - S6 possibly traverse the cell membrane, while H5 is not long enough to form two transmembrane segments and is probably tucked into the lipid bilayer (**Figure 1.1**).[11] Segment S4 contains a number of positively charged residues and is thought to comprise the voltage sensor of the channel. As it is highly charged and at the same time inmersed into the membrane, it is capable of sensing changes in the transmembrane voltage, its responce being an appropriate movement which in turn causes a conformational change of the channel. This opens or closes the channel and is the basis of the voltage - gating mechanism of this class of K^+ channels. Furthermore, segment H5 is highly conserved amongst voltage - gated K^+ channels and is most likely part of the pore.

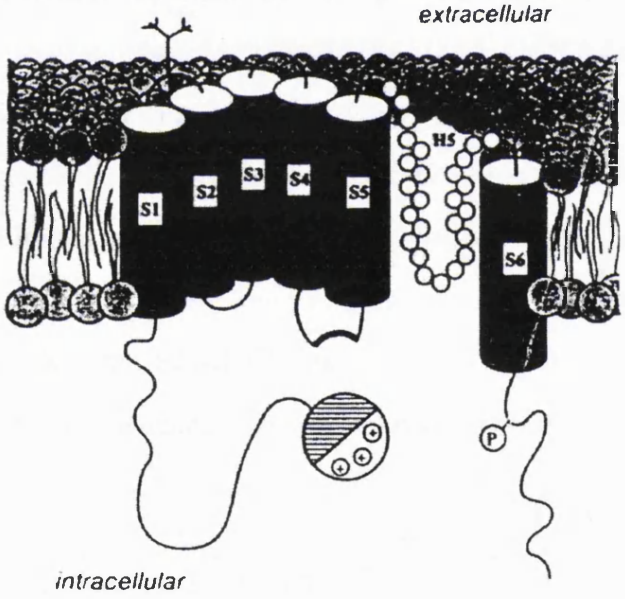

Figure 1.1 Proposed membrane - spanning orientation of one protein subunit of a voltage - gated K^+ channel (taken from ref. 11)

The current structural model of Shaker voltage - gated K^+ channels involves four subunits each comprising of segments S1 - S6 and H5 mentioned above, arranged in a cylindrical fashion with segments S4 being the voltage sensor and segments H5 forming the pore of the channel. It appears that this may be a common structural model for voltage - gated Na^+, Ca^{2+} and K^+ channels.[23] Recently, however, a β-subunit of a voltage -

dependent Shaker - type K^+ channel has been cloned and sequenced.[24] Dispite these common structural features, there is considerable diversity amongst voltage - gated ion channels. This arises from their selectivity for a cation, from the different kinetics with which they activate, open and inactivate and from their different pharmacology.

Blockers. 4-Aminopyridine blocks A-channels (IC_{50} ~ 2 mM).[25] 9-Amino-1,2,3,4-tetrahydroacridine has been shown to block A-channels in hippocampal neurones (IC_{50} = 30 μM)[26] and so has the hallucinogenic phencyclidine.[27] TEA is only a weak blocker of this class of K^+ channels (IC_{50} = 50 μM).[28] As far as peptide toxins are concerned, K_A channels are blocked by dendrotoxin (50 - 350 nM)[29] and mast cell derganulating (MCD) peptide (from the venom of the honey bee *Apis mellifera*, IC_{50} = 37 nM).[30] Charybdotoxin has also been shown to block K_A channels expressed in *Xenopus* oocytes[31] and the mechanism of block has been studied.[32-35]

1.1.5 INWARD RECTIFIER (K_{IR})

In contrast to K_V, K_{IR} channels are activated at hyperpolarized potentials (they are open at the resting potential) and inactivated by depolarization. They conduct inward K^+ currents (5 - 30 pS) and are found in cardiac[36] and skeletal muscle cells[37] where they contribute to the maintenance of long plateaux in the action potential of the cells. They are also involved in cardiac pacemaker activity. Since K_{IR} channels are open at resting potentials they contribute to K^+ conductance.

Structure. A K_{IR} channel from a mouse macrophage cell line has recently been cloned, sequenced and functionally expressed in *Xenopus* oocytes.[38] The primary sequence of this K_{IR} channel (IRK1) shows 40% amino acid identity with that of an ATP - regulated K^+ channel (ROMK1).[39] However, the proposed structure of the IRK1 channel is different from that of voltage - gated K^+ channels. In particular, IRK1 contains two hydrophobic segments (M1 and M2) which may be aligned with the S5 and S6 segments of voltage - gated K^+ channels, as well as a sequence between M1 and M2 which shows extensive similarity with the putative pore - forming H5 region of voltage - gated K^+ channels. It has been proposed that the functional channel has a tetrameric structure similar to that of voltage - gated K^+ channels. Thus, segments M1, H5 and M2

of IRK1 have a similar role to S5, H5 and S6 of the K_V channels. IRK1, however, lacks the "outer shell" of K_V channels which is formed by segments S1 - S3 and the voltage sensor S4. The extensive sequence similarity between IRK1 and ROMK1 suggests that these channels belong to a new superfamily of K^+ channels which are related to, but are distinct from, voltage - gated K^+ channels.

Blockers. TEA blocks K_{IR} channels of skeletal muscle with an IC_{50} of 20 mM.[40] The crude venom of the *Gaboon* viper has been shown to block K_{IR} channels irreversibly, although not selectively.[41]

1.1.6 SARCOPLASMIC RETICULUM CHANNEL (K_{SR})

These channels were first identified on rabbit sarcoplasmic reticulum membranes[42] where it is believed to play a role in the release of Ca^{2+}.[43] It exhibits relatively low K^+/Na^+ selectivity.

Blockers. K_{SR} channels are blocked in a voltage - dependent manner by gallamine[44] and TEA.[45]

1.2 RECEPTOR - COUPLED K^+ CHANNELS

1.2.1 MUSCARINIC - INACTIVATED K^+ CHANNEL (K_M)

This channel is closed by acetylcholine (ACh) acting through muscarinic receptors and is believed to underly, in part, muscarinic excitation.[6,46-48] The K_M channel is activated at potentials more positive to -60 mV and can be envisaged that the K^+ current (I_M) through K_M channels opposes depolarising input currents. Thus K_M channel inhibition facilitates the generation of action potentials. Furthermore, K_M channels may play a role in regulating repetitive firing.[6] Since K_M channels do not inactivate, they contribute to the resting K^+ conductance of the cell.[6,48]

Blockers. Ba^{2+} blocks K_M channels.

1.2.2 ATRIAL MUSCARINIC - ACTIVATED K^+ CHANNEL (K_{ACh})

K_{ACh} channels are present in sinoatrial[49] and atrial[50] cells of the heart, where their activation by ACh released from the vagal nerves slows spontaneous rate in the sinoatrial node, prolongs conduction in the atrioventricular node and shortens the action potential in the atria. These effects of ACh are mediated through binding to M2 muscarinic receptors to activate a pertussis toxin - sensitive G - protein, which in turn gates the K_{ACh} channel. The latter shows inward rectification and has been cloned[51] (GIRK1). Adenosine, which, like ACh, hyperpolarizes and shortens the action potential, has been shown to activate K_{ACh} channels,[52] although ACh and adenosine bind to different receptors. It has been suggested[52] that as for the M2 receptors, the adenosine receptors are linked to K_{ACh} channels via GTP-binding proteins as well.

Blockers. Blockers of the K_{ACh} channel include Cs^{2+}, Ba^{2+}, 4-AP, TEA and quinine.

1.2.3 5-HT-INACTIVATED K^+ CHANNEL ($K_{5\text{-}HT}$)

5-HT produces presynaptic facilitation of transmitter release in *Aplysia* sensory neurones. It has been suggested that this action of 5-HT is mediated through inhibition of $K_{5\text{-}HT}$ channels.[53] $K_{5\text{-}HT}$ channels contribute to the resting conductance of the membrane and action potential repolarization. Serotonin inactivates $K_{5\text{-}HT}$ channels via cAMP -

dependent protein phosphorylation[54] resulting in depolarisation and neuronal excitability.

Blockers. Ba^{2+} blocks the $K_{5\text{-}HT}$ channel[55] while TEA and 4-AP are only weak blockers.

1.3 VARIOUS K^+ CHANNELS

1.3.1 ATP - SENSITIVE K^+ CHANNEL (K_{ATP})

K_{ATP} channels are found in many cell types including pancreatic β-cells,[56,57] myocardial cells,[58,59] skeletal muscle cells[60] and neurones.[61]

The physiological role of K_{ATP} channels is well established only in pancreatic β-cells,[62] where they are involved in the regulation of insulin secretion. Increased plasma levels of glucose result through its catabolism in elevation of [ATP] in pancreatic β-cells. ATP then closes K_{ATP} channels and as a result depolarisation of the membrane occurs, which causes voltage - gated Ca^{2+} channels to open, Ca^{2+} enters the cell and triggers the release of insulin. K_{ATP} channels show strong inward rectification[56] and this is relevant to their structural resemblance with K_{IR} channels (see section 1.1.5 on K_{IR} channels and also below). It is interesting to note that K_{ATP} channels are activated by ADP binding to a site probably distinct from the ATP - binding site[63,64] and it has been suggested that the ratio ATP/ADP modulates K_{ATP} activity.[65,66]

In the heart, activation of K_{ATP} channels increases the outward K^+ current, shortens the action potential duration and decreases the influx of Ca^{2+}, leading to reduced contraction. Thus, activation of K_{ATP} channels may provide an energy - saving mechanism during conditions of metabolic insufficiency. Indeed, it has been suggested that K_{ATP} channels protect heart cells against ischaemia and hypoxia.[67-69] A similar role to that of heart K_{ATP} channels has been suggested for skeletal muscle K_{ATP} channels.[70-72]

As far as neuronal K_{ATP} channels are concerned, their properties are different from the K_{ATP} channels discussed above and their physiological role has not been fully elucidated.[61] It has been suggested, however, that opening of K_{ATP} channels may prevent cell death under conditions of cerebral hypoxia.[73-76] In substantia nigra, on the other hand, K_{ATP} channels have been implicated in seizures which hypoglycaemic diabetic patients develop.[77,78]

Structure. A cDNA encoding an inwardly rectifying ATP - regulated K^+ channel (ROMK1) has recently been isolated, sequenced and functionally expressed in *Xenopus*

oocytes.[39] The primary sequence of ROMK1 has 40% amino acid identity with the above mentioned IRK1 channel. As for the IRK1 channel, ROMK1 contains two hydrophobic, putative transmembrane segments M1 and M2, the segment between M1 and M2 (H5) corresponding to the pore - forming H5 region of K_V channels. However, an additional M0 region of amphipathic nature, preceding the M1 segment, exists in the sequence of ROMK1. It is postulated that this is not a transmembrame segment. The structural organization which has been proposed for the ROMK1 subunits to form a functional channel is similar to that for the IRK1 channel discussed above.

Blockers. Sulphonylureas comprise a class of hypoglycaemic drugs which have been extensively used in the management of type II diabetes but of which the mechanism of action had been unknown. Some typical examples of this class of agents are shown in **Figure 1.2.** Recently, it was shown that the primary site of action of tolbutamide in pancreatic β-cells is the K_{ATP} channel, which it blocks with an IC_{50} of ~7 μM.[79,80]

Furthermore, excellent correlations have been obtained for a number of hypoglycaemic drugs between their ability to block K_{ATP} channels, their affinity for a [^{3}H]glibenclamide binding site, inhibition of $^{86}Rb^+$ efflux and stimulation of insulin secretion from insulinoma cell lines.[81-83]

The sulphonylureas also block cardiac K_{ATP} channels and it has been suggested that such K_{ATP} inhibitors may be useful in suppressing ischaemia - induced dysrhythmias.[1,84]

1.3.2 Na^+ - ACTIVATED K^+ CHANNEL (K_{Na})

K_{Na} channels have been little studied. They have been reported to occur in guinea - pig heart myocytes,[85] avian neurones[86] and brainstem neurones.[87] Their physiological role awaits elucidation.

Blockers. Very little is known about the pharmacology of K_{Na} channels. Only TEA and 4-AP are known to act as blockers.[88]

1.3.3 CELL - VOLUME - SENSITIVE K^+ CHANNEL (K_{vol})

This channel has been characterised in guinea - pig and rat hepatocytes.[89] Swelling of these cells activates K_{vol} channels having a conductance of 7 pS, the activation being

Ca^{2+} independent. The physiological role of K_{vol} channels has not been well established.

Blockers. K_{vol} channels are blocked by (in brackets the IC_{50} value) cetiedil (2.3 μM), bepridil (2.7 μM), quinine (12 μM) and Ba^{2+} (67 μM).

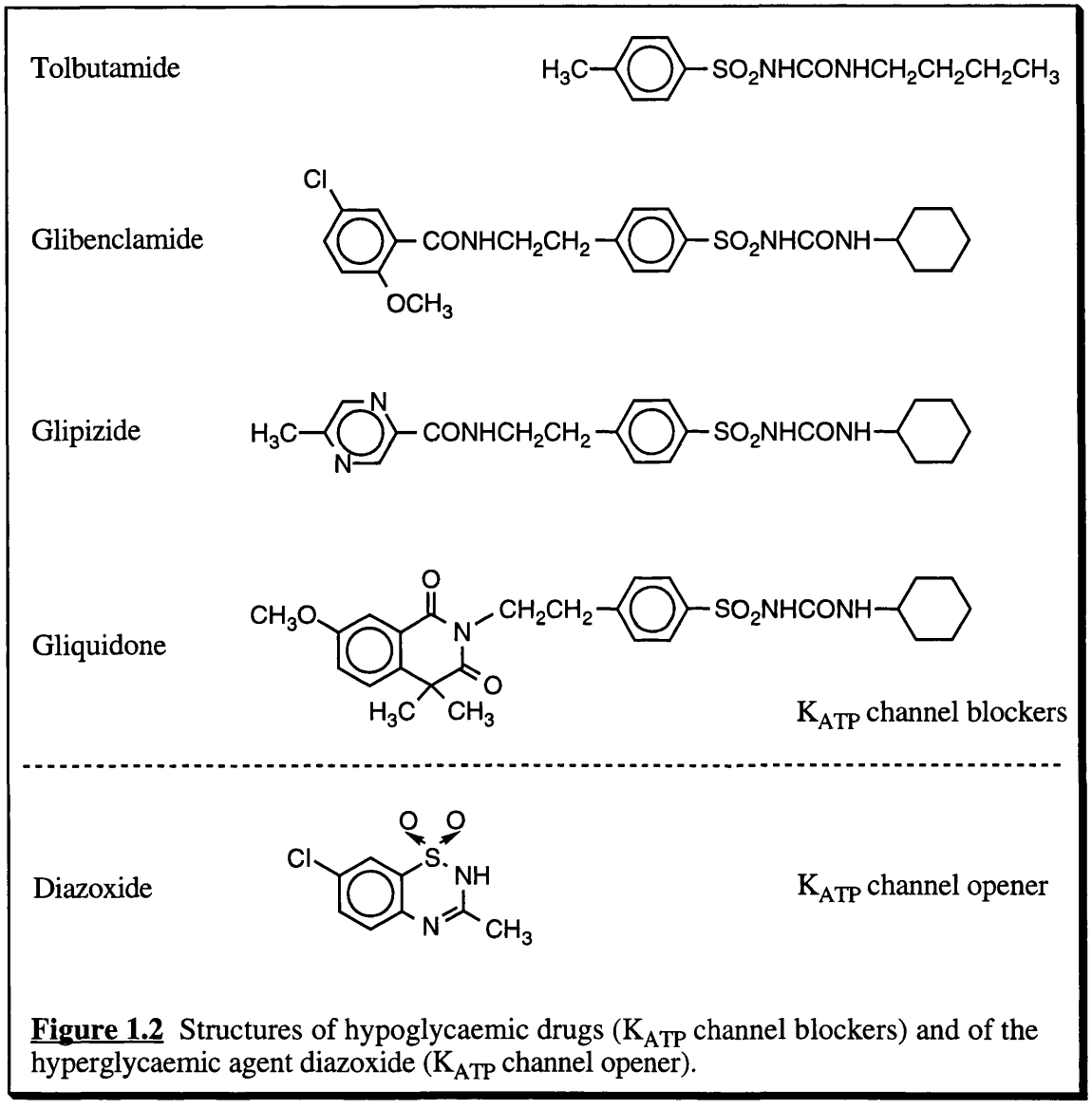

Figure 1.2 Structures of hypoglycaemic drugs (K_{ATP} channel blockers) and of the hyperglycaemic agent diazoxide (K_{ATP} channel opener).

1.4 Ca^{2+} - ACTIVATED K^+ CHANNELS

These are subdivided according the their conductance in high, intermediate and small conductance channels and there is also a Ca^{2+} - activated non specific cation channel. They form a very important class of K^+ channels and their properties have been reviewed.[90]

1.4.1 HIGH CONDUCTANCE Ca^{2+}-ACTIVATED K^+ CHANNEL (BK_{Ca})

BK_{Ca} channels have been identified in a variety of tissues including chromafin cells,[91] skeletal muscle myotubes,[92] pituitary cells,[93] sympathetic neurones, where they contribute to the rapid phase of the action potential repolarisation,[94] exocrine gland cells, where they are involved in ion secretion[95] and pancreatic β-cells, where they play a key role in controlling the secretion of insulin.[96,97] BK_{Ca} channels are modulated both by intracellular Ca^{2+} ($[Ca^{2+}]_i$) and membrane potential. The open probability of the channel increases with rise in $[Ca^{2+}]_i$ and with membrane depolarisation at constant $[Ca^{2+}]_i$.[98] As the name implies, BK_{Ca} channels have a high conductance of the order of 100 - 300 pS depending on the cell type.[90]

Structure. Recently, a gene encoding for BK_{Ca} channels was isolated from mouse brain and skeletal muscle, sequenced and expressed in *Xenopus* oocytes.[99] Furthermore, a BK_{Ca} channel from bovine tracheal smooth muscle has been purified to homogeneity by a combination of conventional chromatography and sucrose gradient sentrifugation.[100] It was found that the BK_{Ca} channel consists of two subunits of 62 (α)- and 31(β)- KDa. Reconstitution of the purified channel proteins into artificial bilayers yielded a functional channel with all the characteristics of a BK_{Ca} channel. The β-subunit has subsequently been cloned and sequenced.[101]

Blockers. With respect to small organic molecules, TEA has found some use as a blocker of the BK_{Ca} channel.[90] The neuroleptics haloperidol, trifluoperazine, chloropromazine and thioridazine have been shown to block BK_{Ca} channels of tracheal smooth muscle with K_D's of 1, 1.4, 2 and 2.4 μM respectively.[102] On the other hand, peptide toxins exist which are potent blockers of the BK_{Ca} channel and have found wide

application for the study of these channels. Charybdotoxin (ChTX) has been the most widely used. It is a 37 amino acid peptide isolated from the venom of the scorpion *Leiurus quinquestriatus hebraeus*[103] and has been shown to block BK_{Ca} channels.[104] Subsequently, ChTX has been synthesised using solid phase techniques[105] and its three dimensional structure has been studied by a combination of NMR and molecular modelling.[106-108] The mechanism of block of BK_{Ca} channels by ChTX has been studied in some detail.[109,110] Furthermore, ChTX mutants have been invaluable, not only for the study of structure - activity relationships on ChTX, but also for structural investigations of the ChTX binding site, which is part of the BK_{Ca} channel.[111-113] However, the usefulness of ChTX is limited by its lack of selectivity, since it also blocks voltage - dependent *Shaker* K^+ channels (see above) and IK_{Ca} channels.[114]

Iberiotoxin (IbTX), another 37 amino acid peptide which shows 68% homology with ChTX and is isolated from the venom of the scorpion *Buthus tamulus*, blocks BK_{Ca} channels potently.[115] In contrast to ChTX, IbTX is a selective blocker of the BK_{Ca} channel. Some efforts have been undertaken to identify regions on ChTX and IbTX with impact on selectivity by synthesizing chimeric ChTX - IbTX peptides. The results suggest that the C-terminal domain of ChTX homologues defines the toxin - channel interaction which distinguishes between BK_{Ca} and voltage - dependent K^+ channels.[116] The solution 3-D structure of IbTX has been studied by a combination of 2-D NMR and molecular modelling[117] and has been found to be similar to that of ChTX.

Finally, a third toxin, noxiustoxin (NTX), a 39 amino acid peptide isolated from the venom of the scorpion *Centruroides noxius*, has been shown to block BK_{Ca} channels.[118] However, this peptide lacks selectivity (since it blocks K_V channels as well, see above) and is much less potent than ChTX.

Openers. Recently, the benzimidazolone NS004 (**Figure 1.3**) has been reported to be an effective activator of BK_{Ca} channels in arterial smooth muscle cells, causing smooth muscle relaxation.[119] Furthermore, the triterpenoid glycosides dehydrosoyasaponin I, soyasaponin I and soyasaponin III, shown in **Figure 1.3**, have been shown to be effective activators of BK_{Ca} channels in tracheal smooth muscle.[120] Finally, nitric oxide (NO), which is the major endothelium - derived relaxing factor

(EDRF), can directly activate single BK_{Ca} channels from rabbit aorta, an effect which could cause hyperpolarization and relaxation of vascular smooth muscle.[121]

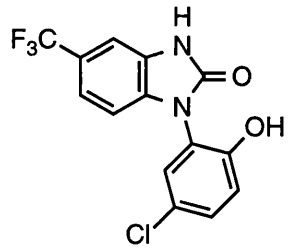

NS004

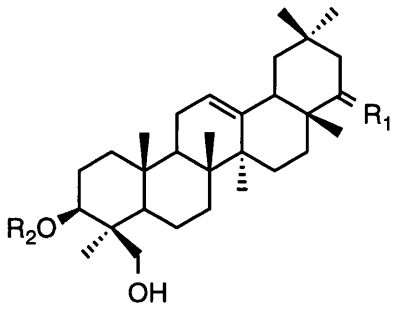

Compound	R_1	R_2	R_3
Soyasaponin I	H, OH	I	II
Dehydrosoyasaponin I	O	I	II
Soyasaponin III	H, OH	I	H

I =

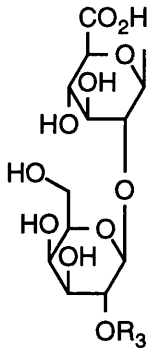

II =

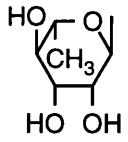

Figure 1.3 BK_{Ca} channel activators.

1.4.2 INTERMEDIATE CONDUCTANCE Ca^{2+}-ACTIVATED K^+ CHANNEL (IK_{Ca})

There are two subtypes of IK_{Ca} channels according to their voltage sensitivity.

1.4.2.1 Voltage - insensitive IK_{Ca} channel.

This channel is found in red blood cells of most animals where it has been well studied.[122] Similar channels may be present in other cell types but their characteristics are much less well established. The conductance of voltage - insensitive IK_{Ca} channels varies

from 10 to 50 pS.[90]

Blockers. Blockers of this channel include quinine and quinidine,[123] carbocyanine dyes[124] and the anti - sickling agent cetiedil.[125] ChTX, which blocks BK_{Ca} and voltage - dependent K^+ channels (see above), also blocks IK_{Ca} channels in red blood cells.[114]

1.4.2.2 Voltage - sensitive IK_{Ca} channel.

These channels were first described in *Aplysia*[126] and *Helix*[127] neurones. Their physiological role is thought to lie in the control of the bursts of action potentials that characterise the activity of these molluscan neurones. The conductance of this channel varies between 35 and 60 pS depending on the cell type and experimental conditions.[90]

Blockers. TEA and quinine block the IK_{Ca} channel.[128] In addition, ChTX has been shown to block voltage - insensitive IK_{Ca} channels in *Aplysia californica.*[129]

1.4.3 SMALL CONDUCTANCE Ca^{2+}-ACTIVATED K^+ CHANNEL (SK_{Ca})

SK_{Ca} channels are present in intestinal smooth muscle where their activation mediates the inhibitory action of α_1-adrenoceptors and of the receptors for neurotensin and ATP.[130-132] In many neurones, including those of the sympathetic ganglia,[133,134] opening of SK_{Ca} channels mediates long afterhyperpolarizations that follow the action potential. The distribution of SK_{Ca} channels in rat brain has been studied using autoradiographic techniques.[135] That SK_{Ca} channels have a physiological role in the central nervous system is supported by the isolation of an endogenous ligand with apamin - like activity from pig brain.[136] An endogenous equivalent of scyllatoxin has also been characterized in phaeochromocytoma cells[137] (apamin and scyllatoxin are specific blockers of the SK_{Ca} channel and are discussed below). In hepatocytes, SK_{Ca} channels mediate adrenaline hyperkalaemia.[138,139] Furthermore, opening of SK_{Ca} channels in brown fat cells contributes to the mobilization of intracellular Ca^{2+}.[140] SK_{Ca} channels have also been described in neuroblastoma[141] and skeletal muscle cells.[142] Single channel recordings have suggested a conductance of 6 - 14 pS for the SK_{Ca} channel.[142-145]

Structure. Despite the existence of specific neurotoxin blockers (apamin,

leiurotoxin I, PO5, see below) of the SK_{Ca} channel which can be used as probes for the elucidation of its structure through biochemical purification procedures, progress in this direction has been hampered by the low density of expression of the SK_{Ca} channel and by its apparent instability after solubilization from the membrane.[146] Therefore, attention has been focused mainly on the analysis of ^{125}I-apamin and ^{125}I-scyllatoxin binding proteins which have been modified by covalent attachment of the toxin via cross - linking reagents. Nevertheless, even in this relatively narrow line of research, some discrepancies exist in the results published by different groups and/or when different species or conditions were used.

Using the photoreactive aryl azide ANPAA [[(4-azido-2-nitrophenyl)amino]acetic acid succinimidyl ester] (**Figure 1.4**) Seagar et al[147,148] have covalently linked ^{125}I-apamin to its receptor in rat cultured neurones and rat synaptic plasma membranes either through Cys_1 [^{125}I-(α-ANPAA-Cys_1) apamin] of Lys_4 [^{125}I-(α-ANPAA-Lys_4) apamin]. ^{125}I-(α-ANPAA-Cys_1) apamin labeled an 86 KDa protein in cultured neurones and two proteins of 86 and 59 KDa in synaptic plasma membranes. The 59 KDa polypeptide was suggested by the authors to be a degradation product of the 86 KDa protein. ^{125}I-(α-ANPAA-Lys_4) apamin on the other hand, labeled 33 and 22 KDa polypeptides in both tissue preparations. Subsequently, results from the same group[149] using ^{125}I-ANPAA-apamin and cultured astrocytes from rat brain, confirmed the presence of the 86 and 33 KDa proteins. However, a 59 KDa protein was also clearly labeled, a fact which led the authors to reconsider their suggestion that the 59 KDa protein is a proteolytic fragment of the 86 KDa peptide. The 86 KDa protein has been consistently identified in liver, intestinal smooth muscle and heart membranes, while the 59 KDa polypeptide has been labeled in liver but not intestinal smooth muscle and heart membranes.[150] These discrepancies led to further proteolytic work in the same group, the results of which strongly suggest that the 59 KDa is in fact a proteolytic fragment of the 86 KDa protein.[151]

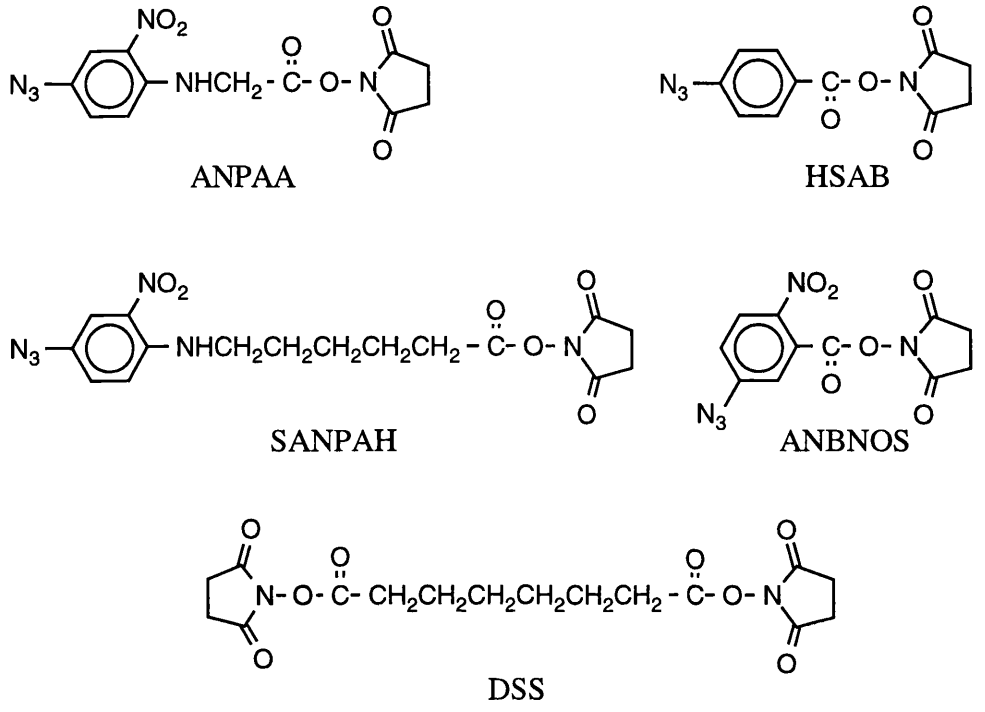

Figure 1.4 Crosslinking reagents that have been used in the characterization of apamin - binding proteins.

The second research group involved in the analysis of apamin binding proteins is that of Lazdunski. Early cross - linking experiments with DSS (disuccinimidyl suberate, **Figure 1.4**) in rat brain synaptosomes identified a 28 KDa protein[152] and later a 33 KDa protein in the same tissue.[153] A systematic study using DSS, ANPAA, SANPAH [[6-(4-azido-2-nitrophenyl)amino]hexanoic acid, succinimidyl ester], HSAB (4-azidobenzoic acid, succinimidyl ester) and ANBNOS (5-azido-2-nitrobenzoic acid, succinimidyl ester) as crosslinking reagents and two different tissue preparations (rat brain synaptic plasma membranes and pheochromocytoma PC12 cells) identified different apamin - binding polypeptides depending on the reagent and tissue.[154] The major component has a mass of ~30 KDa but other components of 45, 58 and 86 KDa were also identified. It is the last three of which the presence varied. These results led the authors to suggest that there are subtypes of apamin receptors. Furthermore, using a radiolabeled derivative of leiurotoxin I [^{125}I-[Tyr$_2$]-leiurotoxin I] and DSS, Lazdunski's group have identified 27 and 57 KDa proteins in rat brain synaptic plasma membranes.[155]

Recently, Wadsworth et al[156] have added to the evidence for the existence of

subtypes of the SK_{Ca} channel discused above. Cross - linking studies using ^{125}I-apamin and DSS or DS [bis(sulphosuccinimidyl)suberate] have identified a 33 KDa apamin binding polypeptide expressed in rat, rabbit, guinea pig and bovine brain, a 30 KDa polypeptide in rabbit and bovine liver and a 25 KDa polypeptide in guinea pig liver. These peptides have distinct biochemical properties and it is suggested that they fulfil equivalent functional roles within putative subtypes of the SK_{Ca} channel. It is further suggested that the SK_{Ca} channel may be composed of two subunits of 86 and ~30 KDa. Further evidence for the involvement of the 33 and 30 KDa proteins within SK_{Ca} channel subtypes is provided by the fact that none of these polypeptides was labeled in rat liver, a tissue known to lack SK_{Ca} channels.[157]

Moreover, there have been attempts to estimate the MW of the apamin receptor, but little agreement exists between different groups. A MW of ~350 KDa has been suggested from density gradient sedimentation analysis[146] while radiation - inactivation techniques proposed MWs of 84 - 115 KDa[148] and 250 KDa.[153]

At the gene level, no information had been available until recently, when Sokol et al published the cloning of an apamin binding protein of smooth muscle.[158] In this paper, an affinity support of immobilized apamin was used to purify a 78 KDa protein from bovine brain. Antibodies against this protein were then employed to clone a cDNA from a porcine vascular smooth muscle expression library. This gene codes for a 438 amino acid protein with four potential transmembrane domains, one putative calcium binding site, a protein kinase C phosphorylation site and a leucine zipper motif.

Peptidic blockers of the SK_{Ca} channel. Apamin, an 18 - amino acid neurotoxin isolated from the venom of the honey bee (*Apis mellifera*) has been shown to block SK_{Ca} channels potently (IC_{50} = 1 nM) and selectively[157,159,160] and has been discussed in several reviews.[160-163] Apamin has been an extremely useful tool for the study of SK_{Ca} channels. Its primary structure is shown in **Figure 1.5**. It is a highly basic peptide as it contains four positively charged amino acids: Cys_1 (NH_2 terminus), Lys_4, Arg_{13}, Arg_{14} and only one negatively charged, the Glu_7 (His_{18}, the CO_2H terminus is amidated). It possesses two disulfide bridges between Cys_1-Cys_{11} and Cys_3-Cys_{15} which render its tertiary structure considerably rigid and stable in a wide range of pH and

organic solvents, even at 6 M guanidinium chloride.

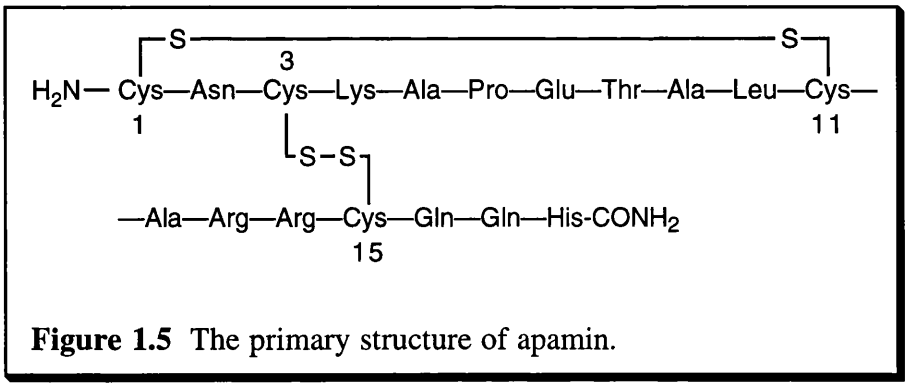

Figure 1.5 The primary structure of apamin.

The tertiary structure of apamin has been studied in some detail using 1-D NMR,[164] circular dichroism (CD),[165] molecular modelling,[166] 2-D NMR,[167] energy minimization techniques[168] and a combination of 2-D NMR and distance geometry.[169] The latter study is perhaps the most systematic, involving less assumptions than the others. There is general agreement between all proposed models concerning the presence of an α-helix at the C-terminus of apamin (residues 9 - 17 according to Pease et al[169]). This is the most rigid part of the peptide which is connected to a less well defined N-terminus. The latter incorporates a β-turn (residues 2 - 5). As far as amino acid side chains are concerned, and especially those of Arg_{13} and Arg_{14} which have been suggested to be crucial for activity (see below), the lack of NOEs strongly suggests that they are mobile in solution.[169]

The chemical synthesis of apamin has been undertaken[170,171] and this has opened the way to structure - activity studies using synthetic analogues of apamin.[172-176] The SAR work on apamin which has been reported to date is summarized in **Table 1.1**.

Table 1.1 Structure - activity relationships of apamin.

1	3	4	7	10	11	13	14	15	16	17	18		LD_{50} (apamin)/LD_{50} (analogue) sc in mice	iv in mice[1]	icv in mice[5]	K_i (nM)[5]
Cys	Cys	Lys	Glu	Leu	Cys	Arg	Arg	Cys	Gln	Gln	His	NH_2	1.0	1.0	1.0	0.012
				Ala								NH_2			0.67	0.048
												NH_2			0.16	0.89
												NH_2			0.0035	120
												NH_2			0.0043	120
						CHD Arg	CHD Arg					NH_2	nd[2]		0.0004	500
Acm Cys	Acm Cys				Acm Cys			Acm Cys				NH_2	nd[2]		nd	79
						Lys							0.67[3]	0.86		
							Lys						0.59[3]	0.49		
						Lys	Lys						0.07[3]			
		Har											1.00[2]			
		Har				Har								0.76		
		Har					Har							0.39		
		Har				Har	Har						0.15[3]			
											Eof His		0.38[2]			
Ac Cys		Ac Lys											0.4[2], 0.8[4]			
Ac Cys		Ac Lys									Eof His		nd[2]			
Ac Cys		Ac Lys				Ac Lys							nd[3]			
Ac Cys		Ac Lys					Ac Lys						nd[3]			
F Cys		F Lys											0.36[2]			
Me_2 Cys		Me_2 Lys											0.55[4]			
											I His		0.27[4]			
			Gly-OEt Glu										0.50[2]			

Notes:

[1] Ref. 172
[2] Ref. 173
[3] Ref. 174
[4] Ref. 176
[5] Ref. 175

nd: not determinable
CHO: 1,2-cyclohexanedione
Acm: acetamido
Eof: ethoxyformylo
Har: homoarginine
Gly-OEt: $-NHCH_2COOEt$

F:

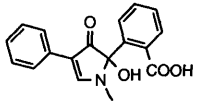

Table 1.2 Structure - activity relationships of leiurotoxin I.

	K_i (nM)		ED_{50} (nM)
	^{125}I-apamin	^{125}I-leiurotoxin I	taenia coli contraction
2 3 6 8 12 13 20 21 25 26 27 28 30 31 Phe—Cys—Arg—Cys—Cys—Arg—Lys—Cys—Lys—Cys—Glu—Cys—Lys—His—NH_2	..0.1[1], 0.13[2]	.....0.2[1], 0.13[2]	.....6[1]
CHD CHD Arg Arg NH_2	.>100[1]*	.....>100[1]*	...>1000[1]*
Har Har Har NH_2	.....0.20[1]	.....0.20[1]	.....400[1]
Gly-OEt Glu NH_2	.....0.16[1]	.....0.16[1]	.....200[1]
I His NH_2	.....4[1]	.....8[1]	.....800[1]
	.....0.53[2]	.....0.48[2]	
Tyr NH_2	.....0.18[2]		
Acm Acm Acm Acm Acm Acm Cys Cys Cys Cys Cys Cys NH_2	.>100[2]*	.....>1000[2]*	

Notes:

[1] Ref. 177
[2] Ref. 155
Har: homoarginine
CHO: 1,2-cyclohexanedione
Gly-OEt: -$NHCH_2COOEt$
Acm: acetamido
* no inhibition up to this concentration

Table 1.3 Structure - activity relationships of PO5.[1]

	K_i (nM) ^{125}I-apamin	LD_{50} (ng) icv in mice
6 7 31 -Arg—Arg—His—CO_2H	0.02	
———————$CONH_2$	<0.0001 (irreversible?)	20
I ———————His—$CONH_2$	0.2	80
-Lys—Lys———————$CONH_2$	2	200
-Leu—Leu———————$CONH_2$	100	>10,000
apamin	0.006	12

Note:

[1] Ref. 178

Table 1.1 which includes 22 apamin analogues merits discussion. Six of the analogues have been tested for their ability to inhibit ^{125}I-apamin binding to rat brain synaptic plasma membranes and the dose of each analogue which causes death in 50% of mice (LD_{50}) after intracerebroventricular (icv) injection has been determined. For four of the analogues the LD_{50} after intravenous (iv) injection in mice has been measured. Finally, for sixteen analogues the LD_{50} after subcutaneous (sc) injection in mice has been obtained, the results being a combination from three different laboratories. There are some points which one should bear in mind when trying to interpret the SAR data presented in **Table 1.1**. The majority of apamin analogues have been tested for their toxicity and, therefore, the SAR obtained concern their toxic effects. Although it is likely that the toxic effects of apamin and analogues are mediated through the blockade of SK_{Ca} channels, to the best of our knowledge there are no reports in the literature correlating quantitatively these two effects. Concequently, the interpretation of the SAR becomes difficult, particularly since the distribution (including blood - brain barrier penetration in the cases of iv and sc injection) and metabolism of the analogues can affect LD_{50} values.

On the other hand, the inhibition of ^{125}I-apamin binding to rat brain synaptic plasma membranes provides affinity constants (K_i) for the binding of the analogues to SK_{Ca} channels. This much more direct and reliable measurement is unfortunately available

for only six of the analogues, from the work of Labbé-Jullié et al[175] who also obtained LD_{50} values for the same analogues after icv injection in mice. This provides the opportunity of attempting to correlate quantitatively K_i and LD_{50} for these six analogues. The plot of $\log(K_i)$ vs $\log(LD_{50})$ is shown in **Figure 1.6** and the plot of the ratios $\log(K_{i(apamin)}/K_{i(analogue)})$ vs $\log(LD_{50(apamin)}/LD_{50(analogue)})$ is shown in **Figure 1.7**. The correlations are reasonably good but caution is required in attempting to extrapolate the results to iv and sc data.

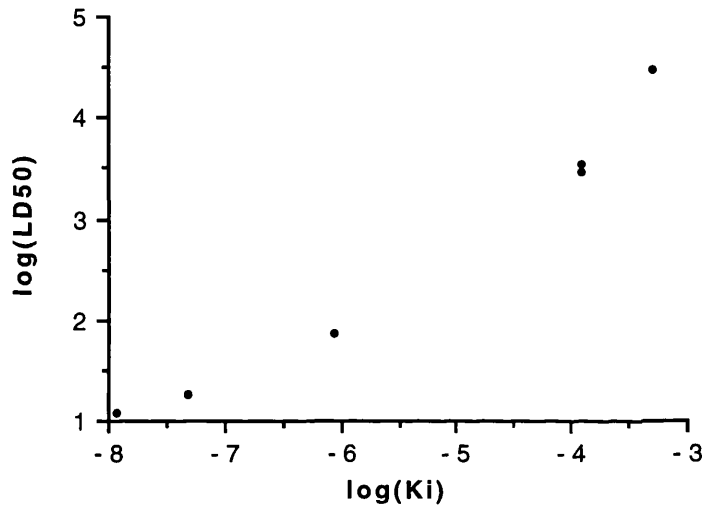

Figure 1.6 Plot of $\log(K_i)$ vs $\log(LD_{50})$ for 6 of the apamin analogues of **Table 1.1**. K_i is in nM and LD_{50} is in ng.

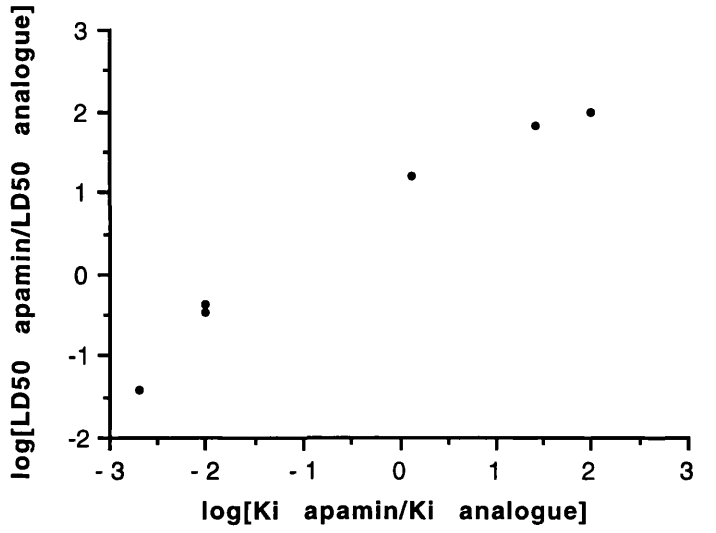

Figure 1.7 Plot of $\log(K_{i(apamin)}/K_{i(analogue)})$ vs $\log(LD_{50(apamin)}/LD_{50(analogue)})$ for 6 of the apamin analogues of **Table 1.1**.

The possibility that LD_{50} values may not be a reliable measure of affinity for the SK_{Ca} channel is demonstrated by the case of the analogue in which the disulphide bonds have been reduced. Although this peptide possesses nanomolar affinity for the SK_{Ca} channel, it shows no lethal effects in mice.[175] From the toxicity data, the two arginines have been suggested to be essential for SK_{Ca} channel blockade since their modification alters toxicity dramatically. However, the analogue in which the side chains of the two arginines have been modified in such a way as to remove the positive charges, despite being 4 orders of magnitute less potent than apamin, retains submicromolar affinity for the SK_{Ca} channel. This strongly suggests that, although the two arginines are part of the pharmacophore of apamin, other amino acids also contribute. This is in line with the finding that simple bis - guanidine dipeptides are not effective blockers of the SK_{Ca} channel.[179] The terminal histidine seems to contribute by a factor of 20 to binding, while Gln_{17} contributes substantially more, by a factor of 700. Clearly, the binding and subsequent blockade of the SK_{Ca} channel by apamin is a complex phenomenon, not well understood at this stage, and the hypothesis that the two arginines are mainly responsible for SK_{Ca} channel blockade is an oversimplification.

As mentioned above, apamin is considered to be a specific blocker of the SK_{Ca} channel. Recently, however, reports have appeared in the literature which attribute Na^+ channel[180] and L-type Ca^{2+} channel[181] blocking activity to apamin.

Leiurotoxin I (LTX I, also referred to as scyllatoxin, SCyTx), isolated from the venom of the scorpion *Leiurus quinquestriatus hebraeus*[182] has also been shown to be a potent inhibitor of ^{125}I-apamin binding to rat brain synaptic plasma membranes (K_i = 130 pM) and to block SK_{Ca} channels.[155] It is a 31 - amino acid peptide (the primary sequence of which is shown in **Figure 1.8**), featuring no sequence homology with apamin, which forms three disulphide bridges and possesses a net charge of +3. This toxin has been chemically synthesized and a modified analogue of scyllatoxin (Phe_2 replaced by Tyr_2) has been radiolabeled with ^{125}I (at Tyr_2).[155] The tertiary structure of leiurotoxin I has been studied by NMR[183] and it has been suggested that it forms an α-helix from residue 6 to 16 and an antiparallel β-sheet from Leu_{18} to Val_{29}. Although Arg_6 and Arg_{13} of scyllatoxin are found two turns apart (on the same side) of the α-helix, it has been proposed that they

may be able to simulate Arg_{13} and Arg_{14} of apamin (found consecutively on an α-helix) due to the conformational mobility of their side chains.[183]

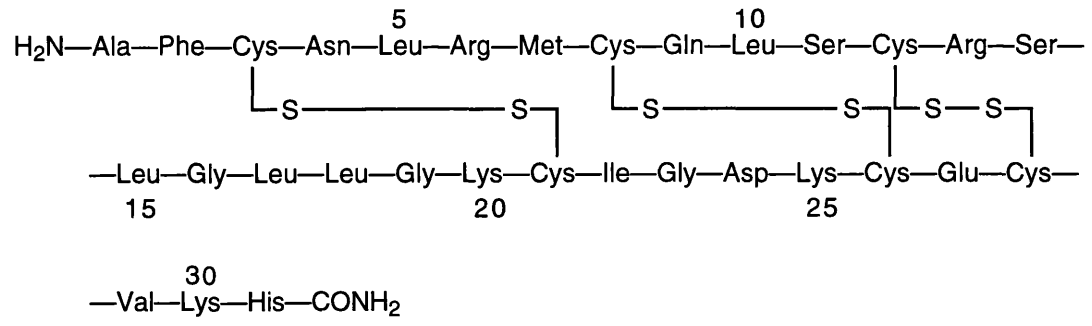

Figure 1.8 The primary structure of Leiurotoxin I

A few SCyTx analogues have been synthesized and tested for their ability to inhibit ^{125}I-apamin or ^{125}I-[Tyr_2]-SCyTx binding to rat brain synaptic plasma membranes and for their ability to contract *taenia coli* with a view to obtaining SAR (**Table 1.2**). The only structural modifications that result in dramatic loss of potency are the cyclohexanedione treatment of Arg_6 and Arg_{13} and the reduction of the 3 disulphide bridges.

In addition to apamin and leiurotoxin I, a third SK_{Ca} channel blocking peptide has been isolated from the venom of the scorpion *Androctonus mauretanicus mauretanicus* and named PO5.[184] It contains 31 amino acids and possesses 87% identity with leiurotoxin I, the most important differences being the presence of an Arg_7 and Val_{24} in PO5 in place of Met_7 and Asp_{24} in leiurotoxin I. Furthermore, the terminal His_{31} in PO5 is not amidated. Consequently, the net charge of PO5 is +4.

The K_i for inhibition of ^{125}I-apamin binding to rat brain synaptic plasma membranes is 20 pM for PO5.[184] Interestingly, the analogue of PO5 which is amidated at the terminal His_{31} (PO5-NH_2) has been found to bind irreversibly to rat brain synaptic plasma membranes.[178] The K_i for inhibition of ^{125}I-apamin binding was less than 0.1 pM. It was not clear however whether PO5-NH_2 binds truly irreversibly or whether the apparent irreversibility results from its extremely high affinity and slow dissociation from the receptor. A few analogues of PO5-NH_2 have been synthesized and tested for their ability to inhibit ^{125}I-apamin binding to rat brain synaptic plasma membranes (**Table**

1.3). Iodination of the terminal His_{31} resulted in at least 3 orders of magnitude drop in potency compaired with PO5-NH_2. The modifications of Arg_6 and Arg_7 had a more dramatic effect on potency. Thus, replacement by Lys caused a four order of magnitude drop in potency while complete elimination of the positive charges of the two Arg effected by replacement by Leu resulted in a six order of magnitude drop in potency.

The 3-D structure of PO5-NH_2 has been studied by CD and molecular dynamics[178] and a combination of 2-D NMR and distance geometry.[185] It consists of an α-helix (residues 5 - 14) connected by a tight turn to a two stranded antiparallel β-sheet (residues 17 - 22 and 25 - 29). The sequence Arg_6-Arg_7-Cys_8-Gln_9 of PO5-NH_2, which is also present in apamin (Arg_{13}-Arg_{14}-Cys_{15}-Gln_{16}), is located on the α-helix, as for apamin. Arg_{13} of PO5-NH_2 is also found close to Arg_6 and Arg_7 in the 3-D structure and the three Args form a positively charged molecular surface which includes Gln_9.[185] It has been suggested that Arg_6, Arg_7 and Gln_9 of PO5-NH_2 occupy similar positions in space to Arg_{13}, Arg_{14} and Gln_{16} of apamin respectively.[178] Meunier et al[185] support the argument that Gln_9 is important for the interaction with the receptor since the greatest positive potential is centered on this residue and since it has been found that Gln_{16} of apamin is necessary for binding. However, the latter is not accurate, as it is Gln_{17} of apamin which has been found to be necessary[175] and Gln_{17} has not been paralleled to Gln_9 of PO5-NH_2. Meunier et al[185] also suggest a multipoint interaction of PO5-NH_2 with the receptor since the binding is sensitive to modifications of His_{31}, which is remote from the positively charged surface created by the 3 Args. This is in line with the results from the SAR on apamin discussed above which clearly show that although Arg_{13} and Arg_{14} are part of the pharmacophore of apamin, alone they cannot account for its potency. It is also interesting to note that the cystine - stabilized α-helix is a common structural feature of many ion channel blocking neurotoxic peptides and has been suggeted to correlate with their common ion channel blocking activity.[186]

Non - peptidic blockers of the SK_{Ca} channel. So far the discussion has focussed on the 3 peptide blockers of the SK_{Ca} channel, apamin, leiurotoxin I and PO5. There are, however, non - peptide blockers of the SK_{Ca} channel as well.

The presence of the bis - charged pharmacophore of apamin prompted tests of a

number of bis - quaternary neuromuscular blockers, some of which were found to be effective blockers of the SK_{Ca} channel.[187,188,133] The 3 most potent were atracurium, tubocurarine and pancuronium (**Figure 1.9**) having K_i's (for inhibition of ^{125}I-apamin binding to guinea pig hepatocytes) of 4.5, 7.5 and 6.8 μM respectively.[188] Furthermore, a correlation was found between the K_i for inhibition of ^{125}I-apamin binding to guinea pig hepatocytes and the IC_{50} for inhibition of the Ca^{2+} - activated K^+ efflux from these cells for all the blockers tested. This strongly suggests that the site of action of these K^+ channel blockers is the apamin - sensitive SK_{Ca} channel.

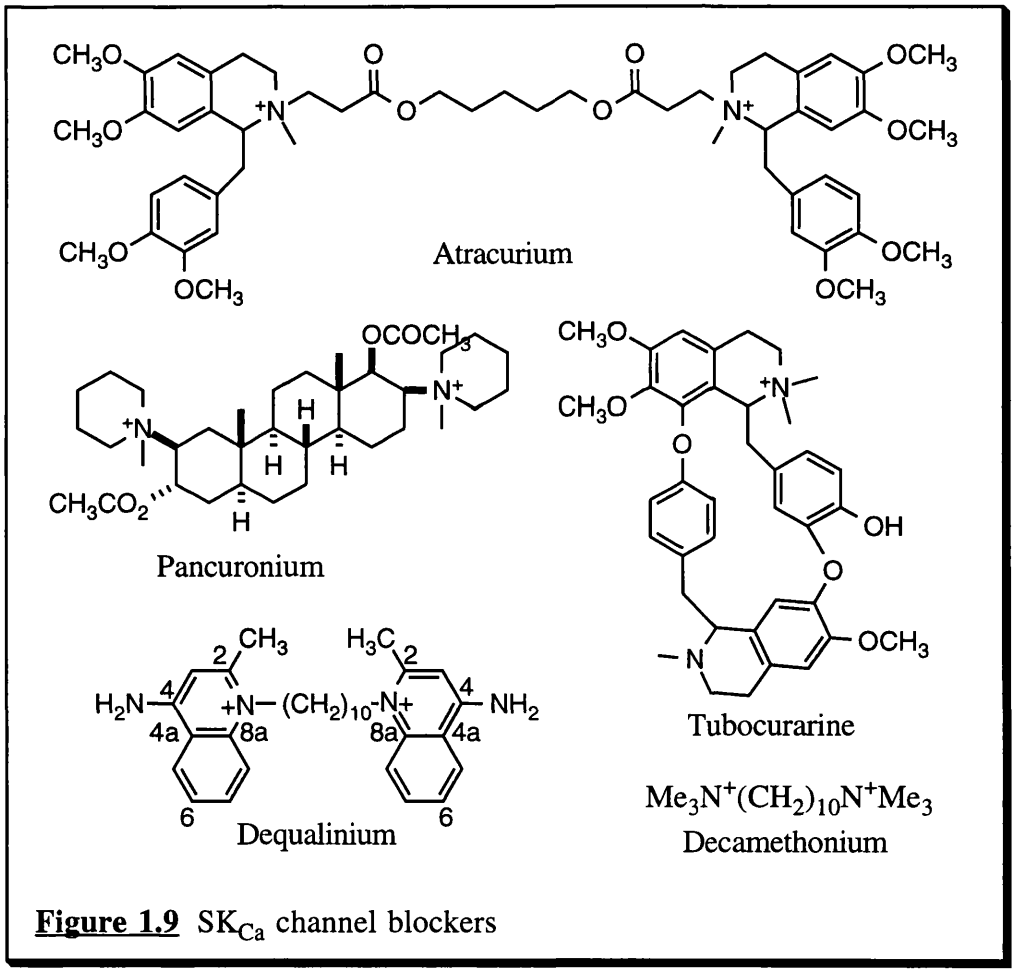

Figure 1.9 SK_{Ca} channel blockers

Furthermore, dequalinium (**Figure 1.9**), another bis - quaternary compound that has been used as an antiseptic,[189] has been shown to be an even more potent blocker of the SK_{Ca} channel in guinea pig hepatocytes,[190] inhibiting ^{125}I-apamin binding with a K_i of 1.1 μM. In rat sympathetic neurones, the action potential is followed by a slow afterhyperpolarization (AHP) which is mediated by the opening of SK_{Ca} channels. Dequalinium has been shown to selectively inhibit the AHP in these neurones with an IC_{50}

(concentration that causes 50% inhibition of the AHP) of 1.1 μM.[191] Therefore, this compound constitutes a useful lead for the development of more potent and selective non - peptidic blockers of the SK_{Ca} channel which will aid the examination of the physiological and pathophysiological roles of this particular channel. It should be noted, however, that dequalinium shows relatively weak antagonistic activity at the nicotinic ACh receptor[192] and this might limit its usefulness as a probe for the SK_{Ca} channel.

The therapeutic potential of SK_{Ca} channel modulation. SK_{Ca} channels have been implicated in *myotonic muscular dystrophy*, since the binding site for apamin is expressed in muscles of patients with this disease while it is completely absent in normal human muscle.[193] In addition, it has been suggested that a neurotrophic factor is involved in the regulation of the expression of apamin binding sites in skeletal muscle membranes[194] but further work is needed to establish a role of the SK_{Ca} channel in this disease.

It has been found that 1 - 10 μM of the *neuroleptic* drugs haloperidol, chloropromazine and trifluoperazine block the calcium - activated AHP in hippocampal pyramidal cells.[195] This, combined with the fact that a Ca^{2+} - activated K^+ conductance is responsible for the generation of the slow AHP in pyramidal neurones[196,197] and with the finding that these neurones possess the receptor for apamin,[135] has led to the suggestion that the neuroleptics may block SK_{Ca} channels.[198] If this is the case then SK_{Ca} channel openers might be useful in controlling some of the adverse effects of neuroleptic treatment.[199] There is, however, strong evidence oposing this suggestion. Cook and Haylett have found no interaction of chloropromazine with apamin binding to guinea - pig hepatocytes.[188] Furthermore, the slow AHP in neurones can be mediated by BK_{Ca} channels[200] and it has been found that haloperidol, trifluoperazine, chloropromazine and thioridazine inhibit the BK_{Ca} channel in tracheal smooth muscle cells.[102] It has also been shown that haloperidol, trifluoperazine and fluphenazine inhibit a Ca^{2+} - activated K^+ efflux from rat brain synaptosomes, probably mediated by BK_{Ca} channels.[201] Therefore, the neuroleptics are capable of blocking BK_{Ca} channels. Alternatively, the depression of Ca^{2+} - dependent K^+ conductance by neuroleptics mentioned above may be due to their acting as calmodulin antagonists at similar concentrations.[195]

^{125}I-apamin binding sites are highly concentrated in the subiculum and CA1 regions of hippocampus and it has been found that there was a marked and selective loss of apamin binding from these two regions in patients with *Alzheimer's disease* (AD).[202] Moreover, ^{125}I-apamin was found to be increased in the temporal and occipital cortex of patients with AD.[203] No definite conclusions as to a role of SK_{Ca} channels in the neuronal degeneration associated with AD can be drawn from these studies and further work is needed to evaluate the importance of these findings and to elucidate the putative role of SK_{Ca} channels in AD.

There have also been attempts to implicate SK_{Ca} channels in *behavioural processes.* Hence, administration of apamin increased behavioral activity in mice and facilitated memory processes.[204] Furthermore, microinjections of apamin into the A10 dopamine region of rat brain resulted in activation of A10 dopamine neurones, increase in dopamine neurotransmission and increase in motor behaviour.[205] These studies constitute evidence for the existence of a physiological role for the SK_{Ca} channel, associated with behavioural and memory processes, and may be of particular interest since, as mentioned above, an endogenous apamin - like peptide exists in mammalian brain.[136]

Finally, *ethanol* has been found to increase the AHP of rat CA1 hippocampal cells[206] as well as the Ca^{2+} - dependent ^{86}Rb (a radioactive substitute for K^+) efflux from both human red blood cells and rodent brain synaptosomes.[207] Apamin inhibited the stimulatory effects of ethanol on the Ca^{2+} - dependent efflux of ^{86}Rb from synaptosomes. It also shortened but not abolished ethanol narcosis. This suggests that stimulation of SK_{Ca} channels is one of several neurochemical changes responsible for *alcohol intoxication.* Therefore, there is potential for therapeutic intervention in cases of ethanol intoxication with selective SK_{Ca} channel blockers.

CHAPTER 2

SELECTION OF COMPOUNDS

As mentioned in the introduction, although being a relatively simple molecule, dequalinium (**8**) is a potent and selective blocker of the SK_{Ca} channel. Hence, studies have been initiated[208,209] to identify the pharmacophore of dequalinium for SK_{Ca} channel blockade. The aim of this work has been to examine whether certain structural features of dequalinium are important for blocking activity, the ultimate objective being the design of a more potent SK_{Ca} blocker. Our efforts have concentrated mainly on five issues:

1. Examination of the role of the NH_2 group of dequalinium. The series of compounds synthesized for this purpose will be refered to as **series I**.
2. Exploration of a second series (**series II**) in which the quinolines have been "inverted" with respect to dequalinium and are joined by position 4.
3. Alterations in the linking chain, including variation of chain length and rigidity as well as linking position to the quinolinium rings (**series III**).
4. The need for two quinolinium groups in the molecule and their role (**series IV**). This should provide information on the mode of binding of dequalinium to the channel.
5. Replacement of the quinolinium groups by other charged heterocycles (**series V**). This should reveal any important features associated with the quinolinium group.

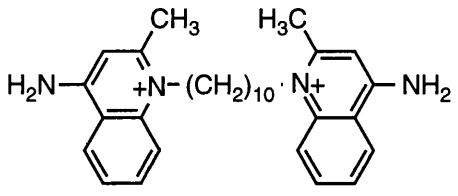

Dequalinium (**8**)

2.1 THE ROLE OF THE NH_2 GROUP.

It has been shown[209] that the NH_2 group of dequalinium is important for SK_{Ca} channel blockade since its removal results in approximately one order of magnitude drop in potency. The NH_2 group may act as an H-bond donor, particularly since its hydrogens are acidic. This is due to the participation of the NH_2 group in the delocalization of the positive charge (**Figure 2.1**) which results in the presence of a fractional positive charge on the group. It has been shown,[210] however, that the NH_2 group does not act as an H - bond donor since replacement by the dimethylamino group gives an equipotent compound (cf. **10** vs **12**):

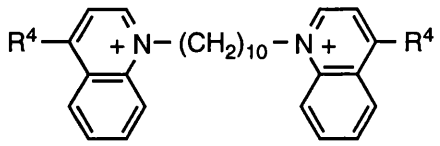

10: $R^4 = NH_2$, EMR = 1.3
12: $R^4 = NMe_2$, EMR = 1.4
9: $R^4 = H$
13: $R^4 = NHCH_2Ph$
14: $R^4 = CH_3$
1: $R^4 = OPh$
2: $R^4 = NHPh$
3: $R^4 = NHCOCH_3$
6: $R^4 = N(CH_3)Ph$

On the other hand it is unlikely that the NH_2 group acts as an H - bond acceptor, since the lone pair of the nitrogen is involved in the delocalisation of the positive charge and is not available for H - bonding. It has been suggested[209] that the delocalisation of the positive charge effected by the NH_2 group (**Figure 2.1**) is important for SK_{Ca} channel blockade. Therefore, it was decided to study systematically the effect of varying the degree of delocalisation of the positive charge on potency, by replacing the NH_2 group by groups of different electronic properties. Along these lines, compounds **1** - **3** and **6** were selected for synthesis which complement compounds **9**, **10** and **12**, previously made by Dr C.A. Davis, **13**, made by Mr C. Owen and **14**, made by Dr Benedicto Del Rey Herrero.

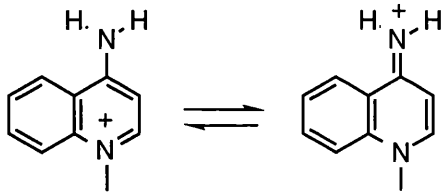

Figure 2.1 Delocalization of the positive charge of the amino-quinolinium group.

Compound **7** was selected after obtaining a correlation of pIC_{50} with σ_R (see results and discussion section) in an attempt to extend the correlation.

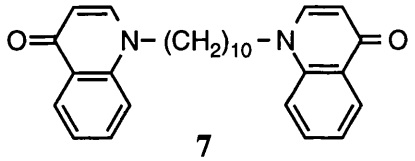

7

Furthermore, compounds **4** and **5** were selected later on in the study in order to follow up a correlation of pIC_{50} with the energy of the LUMO for the compounds (see discussion part).

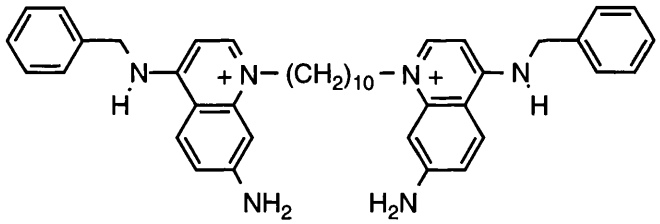

4

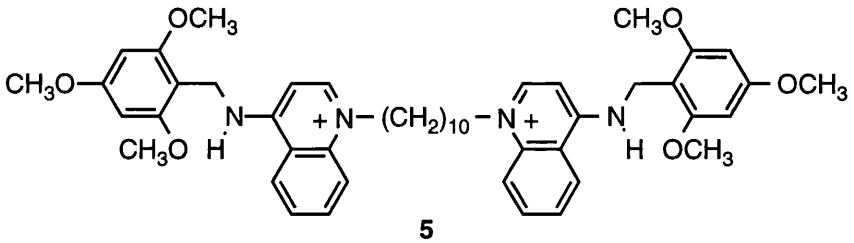

5

2.2 EXPLORATION OF "INVERSE" SERIES

Earlier studies (Davis et al, unpublished results) have also shown that "inversion" of the quinolinium groups of dequalinium, so that these now are joined by the exocyclic rather than the endocyclic nitrogen, gave potent blockers (compounds **25** - **30**, **Table 1**) and it seemed worthwhile to follow up this series. An important structural feature in these is heteroatom X (see below) and its role was investigated by synthesising compounds where X = S (**22**) or X = CH_2 (**20**). These complement the compounds where X = NH (**26**) and X = O (**28**) made earlier by Dr C.A. Davis.

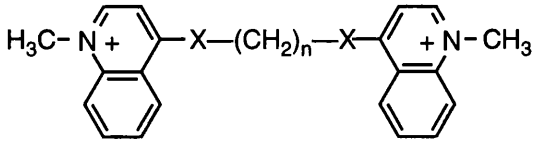

20: X = CH_2
22: X = S
26: X = NH
28: X = O

Another important question addressed in this series was whether the quinoline rings need to be permanently charged for SK_{Ca} channel blockade. Earlier observations[209] suggested that compounds with non - quaternary heterocyclic groups in place of the quinolinium groups (such as **54** and **55**, **Table 1**) were effective blockers. However, the heterocycles used were basic enough to be protonated at physiological pH. In this series, the ring nitrogen of the quinolines can be left non - alkylated and, by varying heteroatom X, the basicity of the quinoline (and therefore its degree of protonation at physiological pH) can be varied. So compounds **23** and **24** were selected which complement compounds **25** and **27** made earlier in our laboratory.

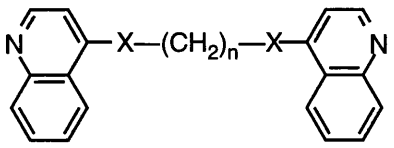

23: X = S
24: X = CH_2
25: X = NH
27: X = O

The ring nitrogen of the quinoline in this series provides a convenient handle upon which a variety of groups can be attached. Seeking lipophilic interactions with the channel, compounds **16** and **18** were synthesised. Moreover, a number of MeO groups are present in atracurium and tubocurarine (**Figure 1.9**), the importance of which has not been investigated. Therefore, it seemed worthwhile to introduce some MeO groups into the

dequalinium - like compounds and compound **17** was selected. Furthermore, the importance of symmetry in the molecule was examined by synthesising the non - symmetrical analogues **19** and **21**.

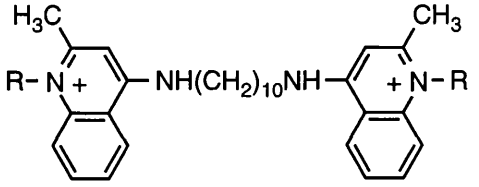

16: R = $CH_2CH_2CHPh_2$

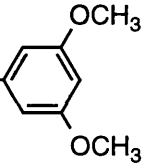

17: R = CH_2-

18: R = CH_2Ph

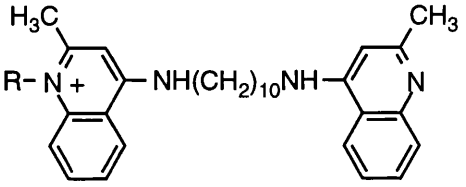

19: R = CH_2-

21: R = CH_2Ph

2.3 ALTERATIONS IN THE LINKING ALIPHATIC CHAIN

Previous studies[209] have shown that introducing rigidity in the alkyl chain of an analogue of dequalinium having aminopyridinium groups (compound **53**) in the form of two triple bonds (**44**) resulted in a 6 - fold increase in potency. It was decided to extend this investigation in the dequalinium series by making an analogue with two triple bonds in the chain. Therefore, compound **31** was selected for synthesis.

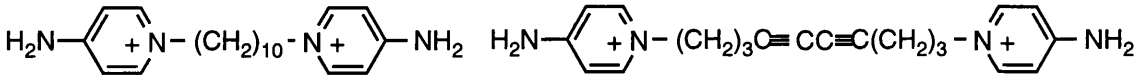

53
(EMR = 33)

44
(EMR = 4.7)

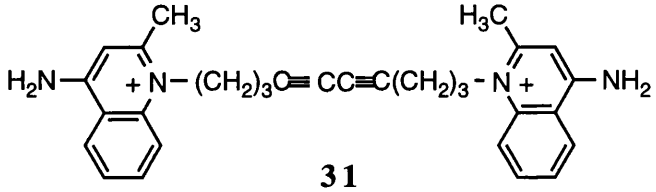

31

It should be noted that although dequalinium has 10 methylene groups in its alkyl chain, the optimum length has not been properly investigated in the "inverse" series. Some hints have been obtained with compound **40** (**Table 1**) but it was felt that this point is worth further investigation. So, further information can be obtained from pairs **36** - **15**, **20** - **39**, and **38** - **18**.

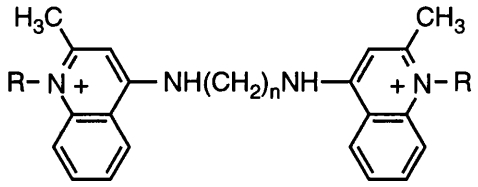

36: R = H, n = 12
15: R = H, n = 10

38: R = CH_2Ph, n = 12
18: R = CH_2Ph, n = 10

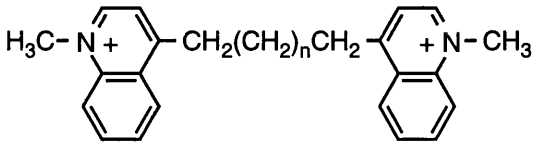

20: n = 10
39: n = 8

Alternative positions of the linking chain have also been investigated by synthesising compounds **41** - **43**.

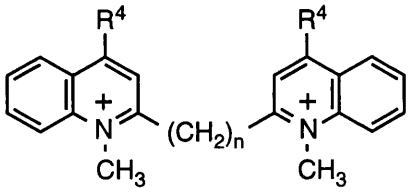

41: $R^4 = OCH_3$, n = 10
42: $R^4 = H$, n = 10
43: $R^4 = H$, n = 12

As it was found that compounds with two quinolinium groups have higher affinity for the SK_{Ca} channel than compounds with one, it was decided to alter the maximum distance between them in the molecule of dequalinium by varying the number of methylene groups in the aliphatic chain. This should provide additional information on the mode of binding of the quinolinium groups. Therefore, compounds **32** - **35** were selected. These do not have the methyl group of dequalinium but are directly comparable with analogue **10**.

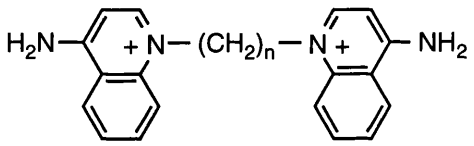

32: n = 5
33: n = 6
34: n = 8
10: n = 10
35: n = 12

2.4 THE NEED FOR TWO QUINOLINIUM RINGS AND THEIR ROLE

The general strategy adopted is as follows: Previous attempts in our laboratory to address the problem have resulted in the synthesis of compounds **45** and **46**.[209]

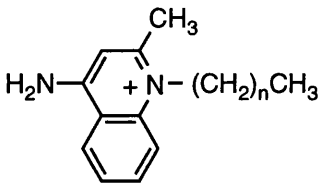

Compd No	UCL No	Notebook No	n	EMR (± SD)
45	1092	CD-29	9	4.7 ± 1.7
46	1171	CD-69	3	11.9 ± 5.9

In **45** one quinolinium group of dequalinium has been removed while in **46** approximately half of the molecule (one quinolinium group and half of the chain) has been removed. These structural changes should provide evidence on the role of the second quinolinium group and also on the possible contribution of the alkyl chain. The results for these two compounds will be discussed in the discussion part. In addition to these changes, indirect evidence on the mode of binding of the quinolinium groups can also be obtained by adding a third quinoline to the molecule. The problem of how this addition should be effected has to be approached with care. In altering the structure of dequalinium to accommodate a third quinoline, as many features present in it as possible should be kept constant. This ensures that changes in the biological activity that will be observed in the new compound will reflect the contribution of the new structural features (third quinoline) to the greatest extent possible. Synthetic accessibility is of course an important issue. After consideration of a number of factors, it was decided to aim at compounds of the type **57**:

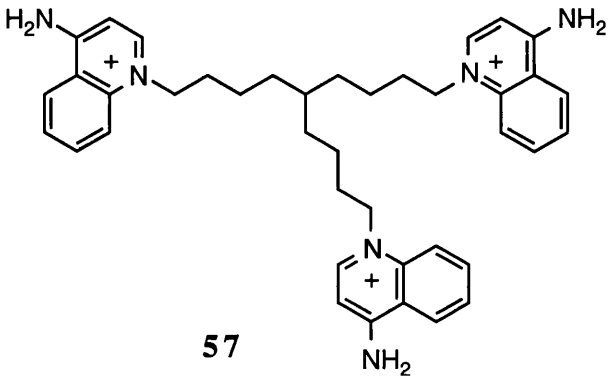

57

In this compound we have maintained an almost unaltered dequalinium structure (two aminoquinolinium rings separated by approximately 10 methylene groups, 9 in this case). We have also kept the ratio of methylene groups per quinolinium group constant and have maintained a separation of approximately 10 methylenes (9 in this case) between each pair of quinolinium groups. It was attempted to synthesise compound **57** but because of difficulties discussed in the synthesis section, compound **47** was made instead.

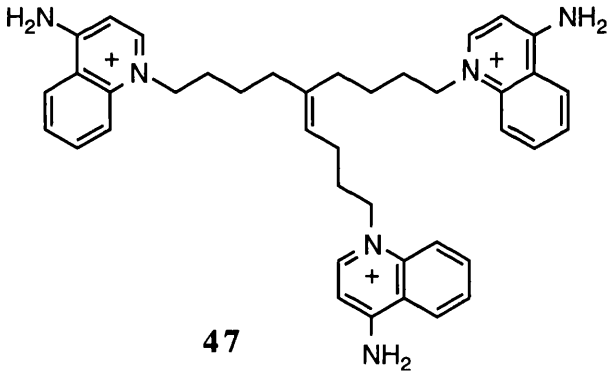

47

2.5 REPLACEMENT OF THE QUINOLINIUM GROUPS

As mentioned in the introduction, the two arginines of apamin are thought to be part of its pharmacophore. Studies to establish a link between the pharmacophore of apamin and the dequalinium - type compounds are of great interest. Bearing this in mind, we partially incorporated a guanidine - type structure into an aromatic ring to give the amino pyrimidinium compound **48**.

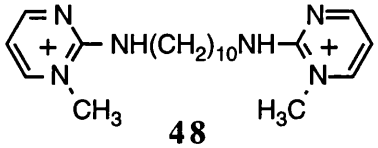

48

Since it was found that the amino group of dequalinium serves to delocalise the positive charge, it seemed appropriate to examine the importance of it being exocyclic. Hence, the benzimidazolium compounds **49** and **50** were synthesized, in which the exocyclic nitrogen of dequalinium has been incorporated into the ring, while keeping its ability to delocalise the charge.

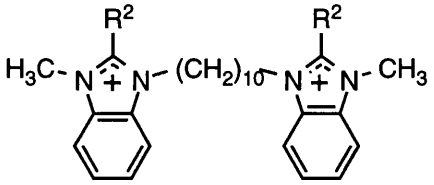

49: $R^2 = H$
50: $R^2 = CH_3$

To examine the importance of the flat aromatic system of the quinolinium rings, compound **51** having a tetrahydroquinolinium ring was selected. This is directly comparable to **9**.[209]

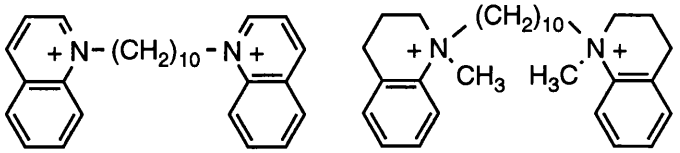

9 **51**

More radical changes to the quinolinium groups were effected in the case of compound **52**. In **52** the two aromatic rings of **9** are no longer fuzed but independently attached to the quaternary nitrogen via a methylene group. These studies on the

replacement of the quinolines by other heterocycles relate to previous work in our laboratory (unpublished results) which yielded compounds **53** - **55** made by Dr C.A. Davis and **56** made by Dr B. Del Rey Herrero (**Table 1**).

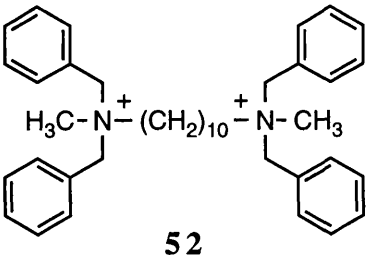

52

Table 2.1. Compounds of series I synthesised in this study.

Compd No	UCL No	Notebook No	Structure
1	1463	DG-155A	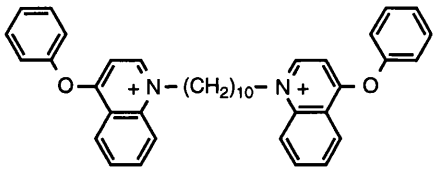
2	1491	DG-367B	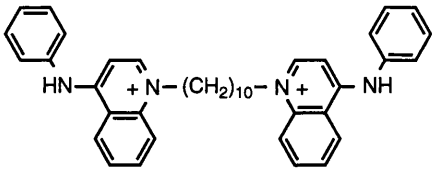
3	1504	DG-459A	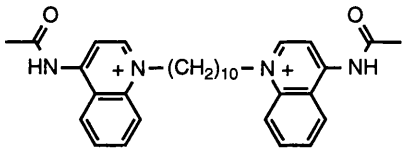
4	1560	DG-589B	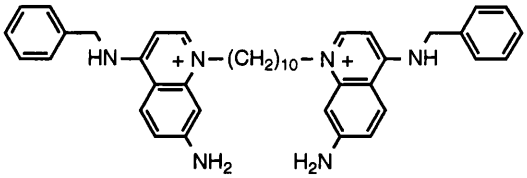
5	1580	DG-703C	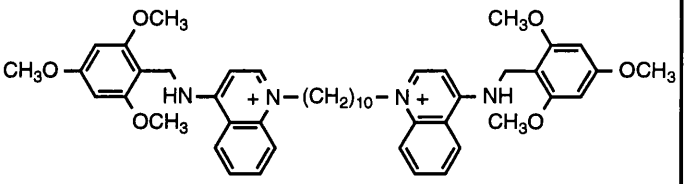
6	1598	DG-739B	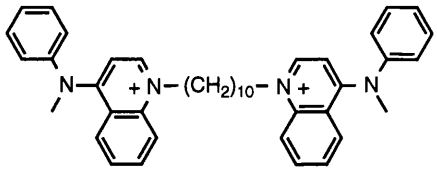
7	1507	DG-467A	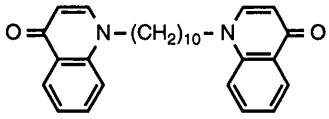

Table 2.2. Compounds of series II synthesised in this study.

Compd No	UCL No	Notebook No	Structure
15	1417	DG-13C	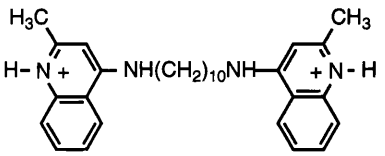
16	1436	DG-81D	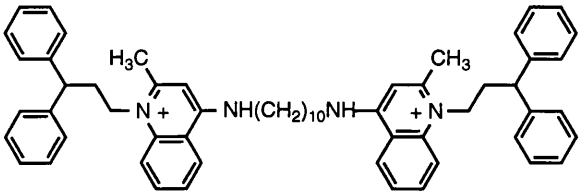
17	1438	DG-115C	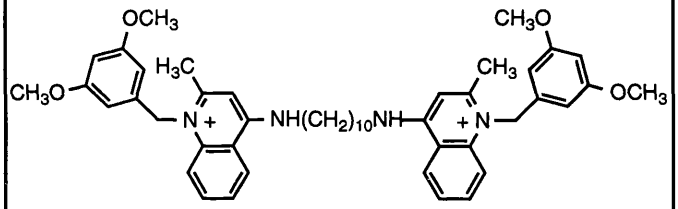
18	1439	DG-127C	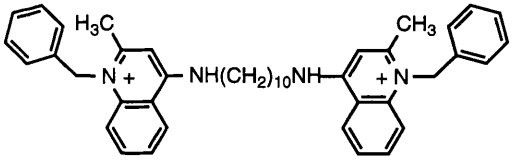
19	1440	DG-115B	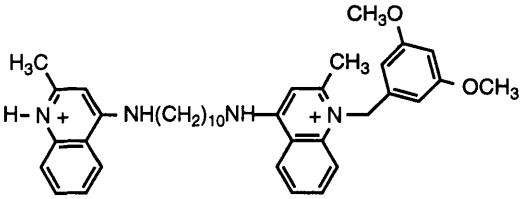
20	1445	DG-167A	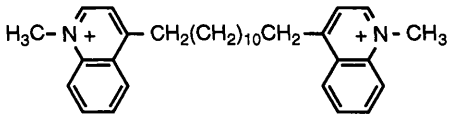
21	1454	DG-127B	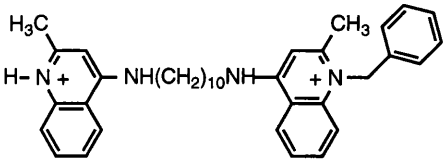
22	1467	DG-223A	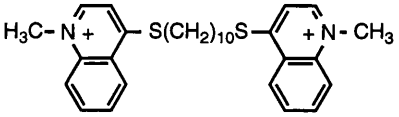
23	1601	DG-219B	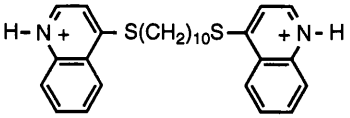
24	1602	DG-159B	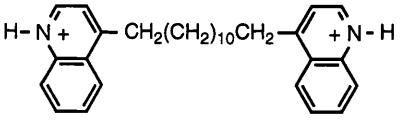

Table 2.3 Compounds of series III synthesised in this study.

Compd No	UCL No	Notebook No	Structure
31	1437	DG-109A	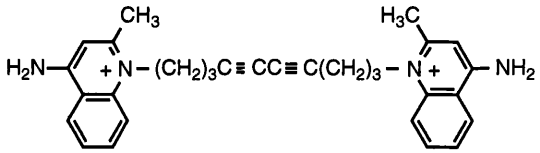
32	1635	SM-114B	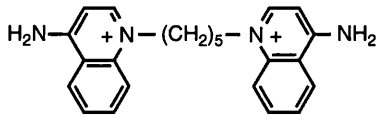
33	1636	SM-109A	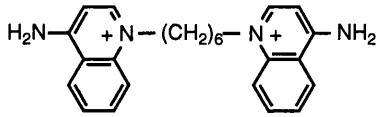
34	1637	SM-104A	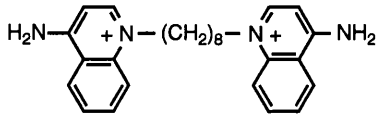
35	1638	SM-106A	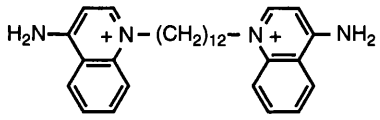
36	1407	DG-23B	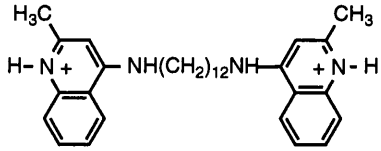
37	1426	DG-33C	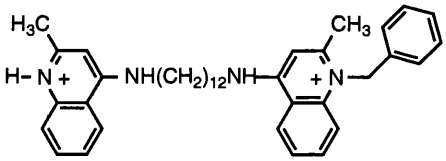
38	1427	DG-33D	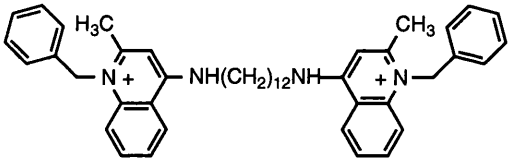
39	1450	DG-199A	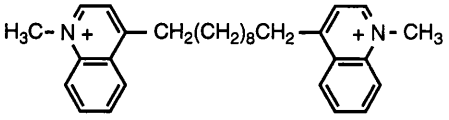

Table 2.3 (continued)

Compd No	UCL No	Notebook No	Structure
41	1455	DG-183B	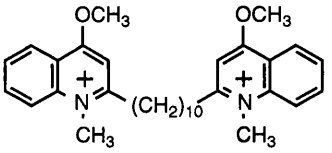
42	1460	DG-207D	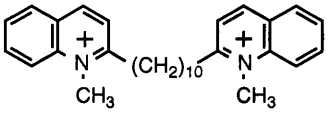
43	1480	DG-287B	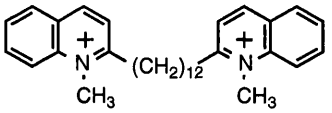

Table 2.4 Compound of series IV synthesised in this study.

Compd No	UCL No	Notebook No	Structure
47	1605	DG-723B	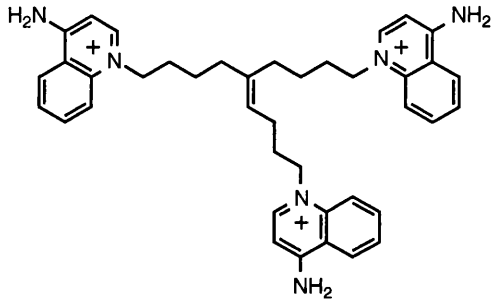

Table 2.5 Compounds of series V synthesised in this study.

Compd No	UCL No	Notebook No	Structure
48	1468	DG-251A	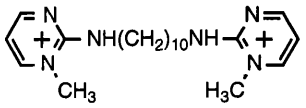
49	1553	DG-637A	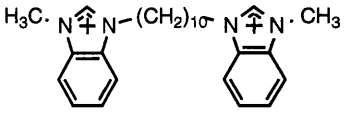
50	1562	DG-649B	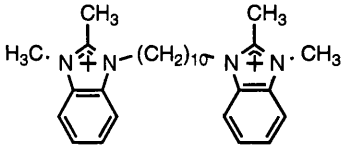
51	1586	DG-735B	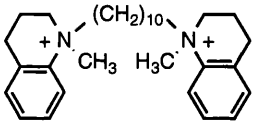
52	1622	DG-831B	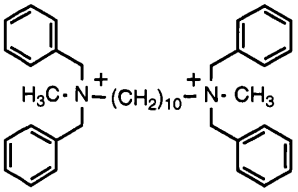

CHAPTER 3

SYNTHESIS OF COMPOUNDS

Compounds **1 - 3, 5, 6** and **32 - 35** (**Table 2.1**) were synthesised according to **Scheme 3.1**. Substituent R^4 was introduced via the displacement of the chlorine atom of 4-chloroquinoline by the respective amine or phenol. In general, these reactions proceed through an addition - elimination mechanism:

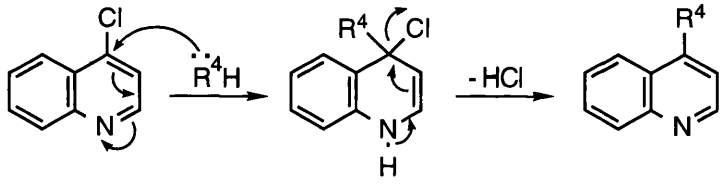

The initial nucleophilic attack of R^4H at position 4 of the quinoline is facilitated if the ring nitrogen is protonated. Thus, the role of PhOH in the synthesis of 4-aminoquinoline (**scheme 3.1**) is to form initially 4-phenoxyquinoline hydrochloride, the phenoxy group of which is easily displaced by NH_3:[211]

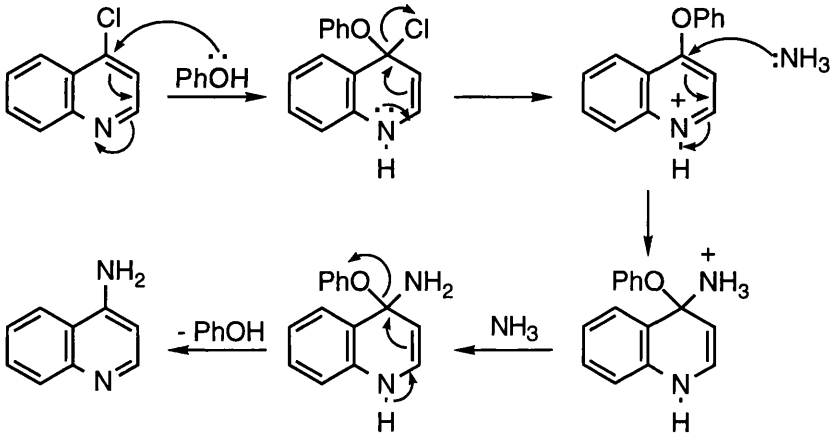

Scheme 3.1[a]

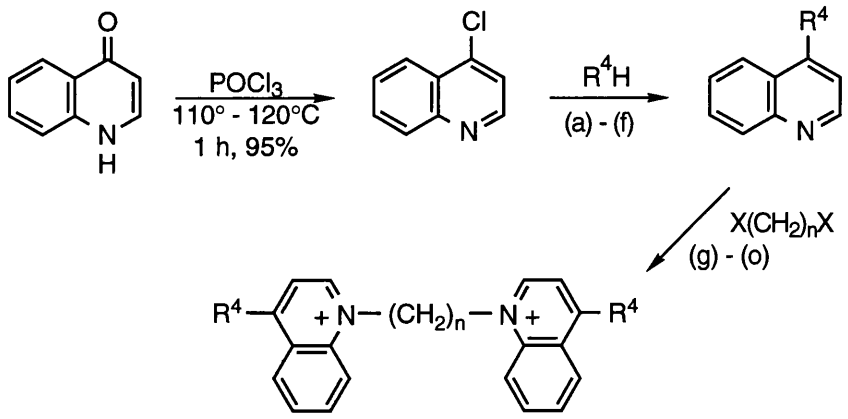

[a]Methods: (a) R^4 = **NH_2**, dry NH_3 (gas)/PhOH, 180°C, 4 h, 99%; (b) R^4 = **N(Me)Ph**, PhNHMe/glacial AcOH, reflux, 3 h, 51%; (c) R^4 = **NHPh**, $PhNH_2$/glacial AcOH, reflux, 3 h, 86%; (d) R^4 = **OPh**, PhOH/KOH, 125° - 130°C, 1 h, 100%; (e) R^4 = **$NHCOCH_3$**, 4-aminoquinoline made under (a) was acetylated using Ac_2O/pyridine, 80°C, 24 h, 100%; (f) R^4 = **(2,4,6-trimethoxybenzyl)amino-**, 2,4,6-trimethoxybenzylamine·HCl/DBU/dry DMSO,120°C, 30 h, 52%; (g) **1**, n = 10, X = I, MEK, reflux, 96 h, 16%; (h) **2**, n = 10, X = I, MEK, reflux, 96 h, 82%; (i) **3**, n = 10, X = I, 4-methyl-pentan-2-ol, reflux, 30 h, 71%; (j) **5**, n = 10, X = Br, MEK, reflux, 240 h, 47%; (k) **6**, X = I, MEK, reflux, 168 h, 47%; (l) **32**, n = 5, X = I, MEK, reflux, 96 h, 49%; (m) **33**, n = 6, X = I, MEK, reflux, 96 h, 58%; (n) **34**, n = 8, X = I, MEK, reflux, 96 h, 57%; (o) **35**, n = 12, X = Br, MEK, reflux, 96 h, 36%.

It should be noted that the ring nitrogen of the 4-aminoquinoline is more basic than the nitrogen of the NH_2 group. In fact, the NH_2 group strengthens the basicity of the ring nitrogen and, as a result, 4-aminoquinoline is a stronger base (pK_a = 9.13) than quinoline (pK_a = 4.90) itself.[212] This is due to the difference in the geometry of the lone pair orbitals of the two nitrogens. The lone pair of the NH_2 group occupies an orbital almost perpendicular to the plane of the quinoline and is conjugated with the π - system. On the other hand, the lone pair of the ring nitrogen occupies an orbital in the plane of the quinoline, does not participate in the conjugation of the rings and is available to attack an electrophile. Furthermore, the compound that results from protonation at the ring nitrogen is stabilized via delocalization of the positive charge:

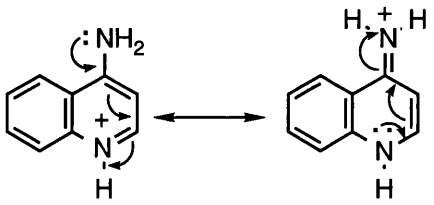

Such resonance stabilisation does not occur when the exocyclic nitrogen is protonated. The same arguments apply to alkylation reactions. Hence, 4-aminoquinolines are alkylated under neutral conditions at the ring nitrogen but are acylated in the presence of a base at the NH_2 group. The acylation is thought to proceed via the following mechanism:

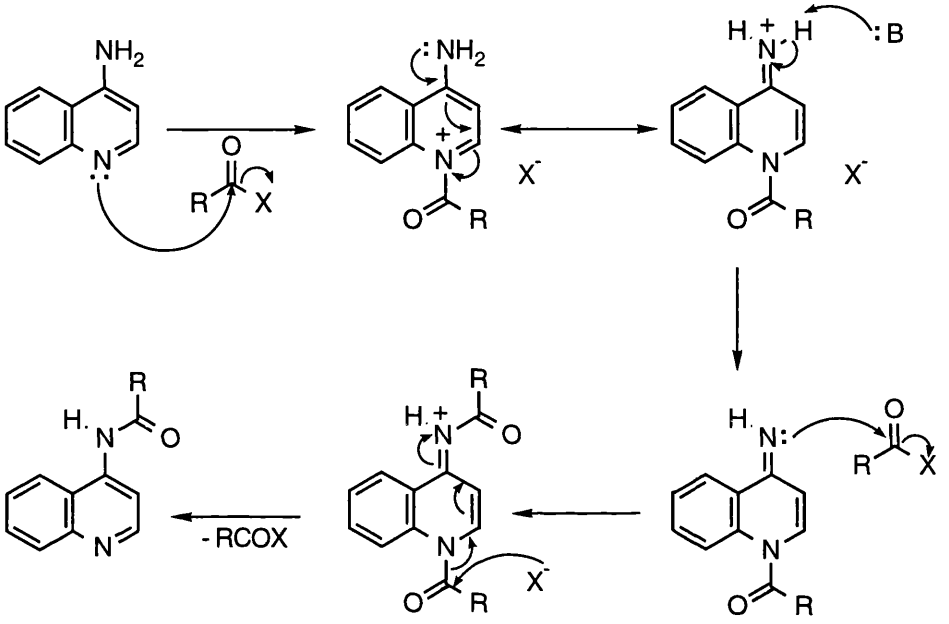

Hence, for the synthesis of compound **3**, the 4-aminoquinoline was acetylated in pyridine to yield the necessary amide. The 4-substituted quinolines were finally alkylated with $I(CH_2)_{10}I$ [$Br(CH_2)_{10}Br$ in the case of compound **5**] either in methyl ethyl ketone (MEK) or in 4-methylpentan-2-ol to afford the final products. All these were purified by recrystallization.

The acetylene compound **31** was synthesised according to **Scheme 3.2**. 4-Aminoquinaldine was alkylated with 5-iodo-1-butyne which was made from the chloride by halogen exchange. Attempts to obtain the quaternary acetylene directly from 5-chloropent-1-yne in refluxing MEK or diisobutyl ketone containing a catalytic amount of $Bu_4N^+I^-$ failed. The quatermary acetylene was then oxidatively coupled. Such reactions are catalyzed by copper complexes of monoamines (e.g. pyridine) or diamines such as TMEDA (N,N,N',N'-tetramethylethylenediamine) and in this case the method of Hay[213] was employed. The advantage of this method compared with the classical coupling of Campbell and Eglinton[214] is the mild conditions and the capability of the CuCl·TMEDA

catalyst to function in a variety of solvents (for another, recent application see ref. 215).

Scheme 3.2

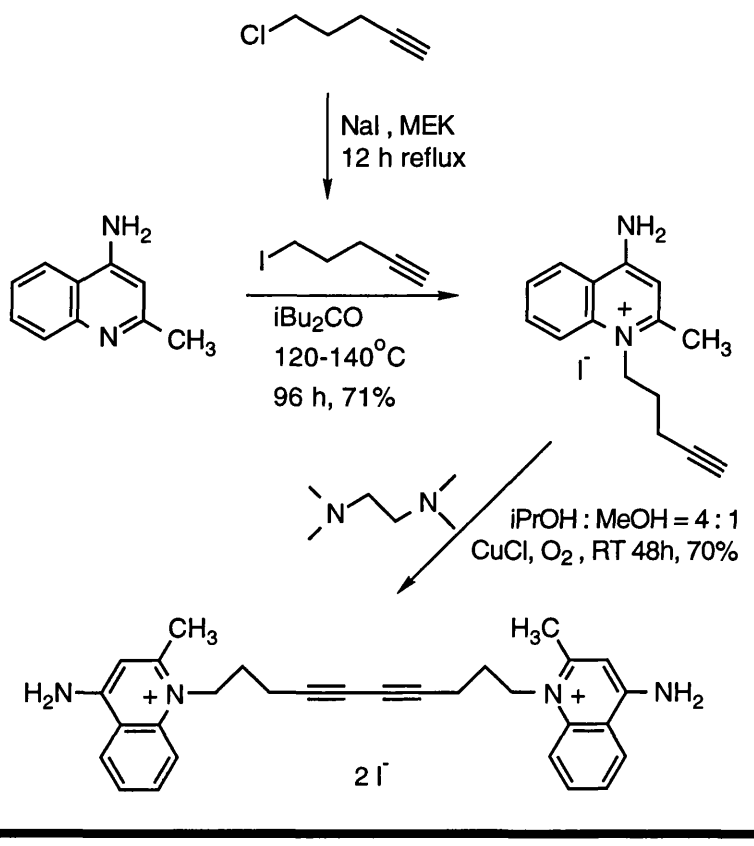

The mechanism of the oxidative coupling has not been fully elucidated.[216] A simple approach proposes that the monoacetylene acts as an acid and dissociates to give the anion **A**:

$$RC{\equiv}CH \rightleftharpoons \underset{\mathbf{A}}{RC{\equiv}C^-} + H^+$$

$$RC{\equiv}C^- + Cu^{2+} \longrightarrow RC{\equiv}C\cdot + Cu^+$$

$$2\ RC{\equiv}C\cdot \longrightarrow RC{\equiv}C\text{-}C{\equiv}CR$$

$$2\ Cu^+ + 1/2\ O_2 + H_2O \longrightarrow 2\ Cu^{2+} + 2\ HO^-$$

The cupric ion abstracts an electron from the anion **A** and is reduced to the cuprous ion, while creating an acetylenic radical which dimerizes to give the diacetylene. Oxygen reoxidizes the cuprous back to the cupric ion and so the catalyst is regenerated.

For the synthesis of compound **4**, the requisite key intermediate 7-nitro-4-

quinolone has been reported only once by Ellis et al.[217] As shown in **Scheme 3.3**, diethyl ethoxymethylenemalonate was condensed with m-nitroaniline to give α-ethoxycarbonyl-β-(3-nitrophenylamino)acrylate whch was cyclised in refluxing diphenyl ether to provide 3-ethoxycarbonyl-7-nitro-4-(1H)quinolone. In the original paper[217] this ester was first hydrolysed to 3-carboxy-7-nitro-4-(1H)quinolone and in a second step decarboxylated to the desired 7-nitro-4-(1H)quinolone. Nevertheless, it was found that the ester can be hydrolysed and decarboxylated in one step by heating in Dowtherm A containing 5% TsOH as a catalyst. Both methods, however, yielded a *mixture* of 5-nitro- and the desired 7-nitro-4-(1H)quinolone, the latter being the predominant product. It is worth noting that Ellis et al[217] have not reported the formation of a mixture but only the 7-nitro-4-(1H)quinolone.

Due to their polar nature, the two isomers were not separated at this stage but after conversion to the coresponding chloro- derivatives. Only small quantities of the 5-nitro-4-chloro- compound were isolated, insufficient to pursue it further. The chlorine of the desired 7- isomer was displaced by benzylamine and the resultant 4-benzylamino-7-nitroquinoline was reduced to the 7-amino analogue using $SnCl_2$.[218] The ring N of the 7-amino-4-benzylaminoquinoline was alkylated with $I(CH_2)_{10}I$ and the resulting foam was purified by preparative HPLC as described in the experimental section.

The general **Scheme 3.4** shows the synthesis of compounds **15 - 19, 21** and **36 - 38** of **series II** (**Table 4.2**). 4-Aminoquinaldine was treated with the necessary diamine to provide **36** and **15** which were then reacted with an appropriate halide to afford **37, 38, 16 - 19** and **21**.

Scheme 3.3

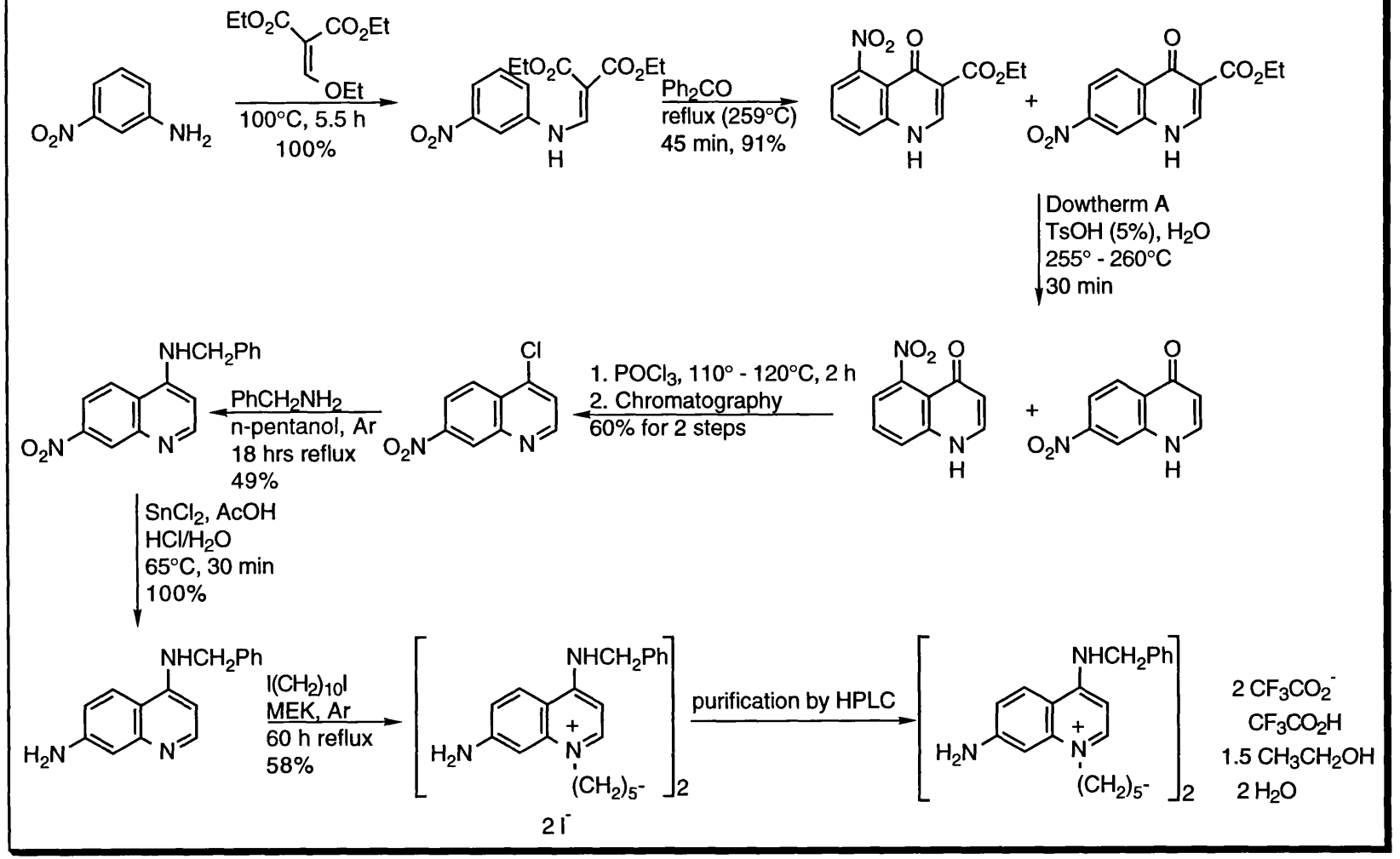
EtO2C CO2Et
OEt
100°C, 5.5 h
100%
Ph2CO
reflux (259°C)
45 min, 91%
Dowtherm A
TsOH (5%), H2O
255° - 260°C
30 min
1. POCl3, 110° - 120°C, 2 h
2. Chromatography
60% for 2 steps
PhCH2NH2
n-pentanol, Ar
18 hrs reflux
49%
SnCl2, AcOH
HCl/H2O
65°C, 30 min
100%
I(CH2)10I
MEK, Ar
60 h reflux
58%
purification by HPLC
2 I-
2 CF3CO2-
CF3CO2H
1.5 CH3CH2OH
2 H2O

Scheme 3.4[a]

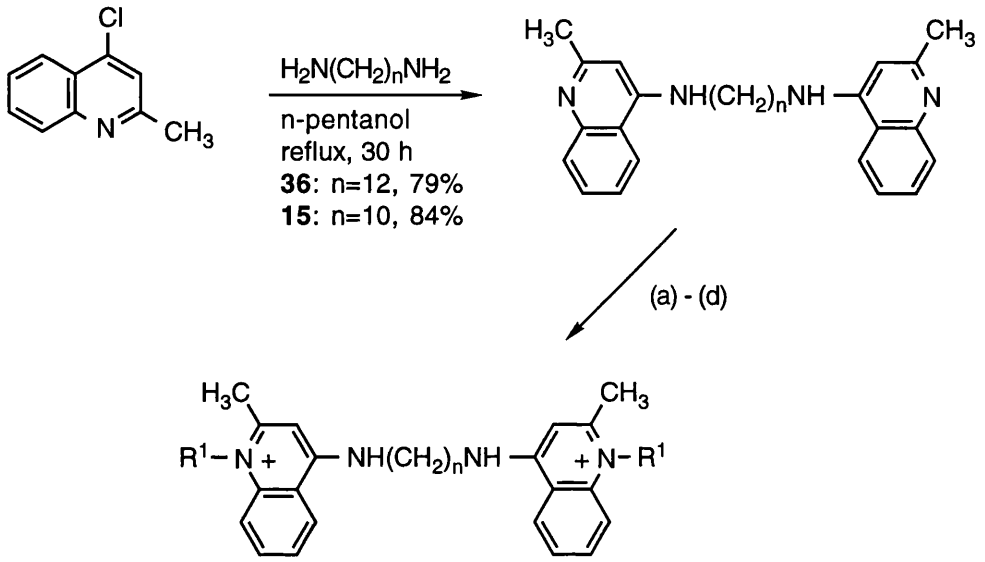

[a]Methods: (a) **37**, **38**: **36**, BnBr, $(iBu)_2CO$, reflux, 24 h; (b) **16**: **15**, 1,1'-(3-iodopropylidene)-bis-benzene, 4-methylpentan-2-ol, reflux, 120 h; (c) **17**, **19**: **15**, 3,5-dimethoxybenzyliodide, $PhNO_2$, 100° - 120°C, 144 h; (d) **18**, **21**: **15**, BnBr, $PhNO_2$, 100° - 120°C, 96 h, 120° - 140°C, 12 h.

In the final quaternization step of **Scheme 3.4** high temperatures were required. The quinoline ring nitrogen atom in these compounds is substantially hindered by the methyl group at position 2 as well as the peri- hydrogen atom (at position 8). In spite of the fact that the nucleophilicity of the ring nitrogen atom is enhanced by the presence of the 4-amino group, the reactions failed to proceed under the normal conditions, employing MEK and reflux (80°C) temperatures. In all cases, mixtures of mono- and bisquaternary compounds were obtained from the final quaternization step. These could only be separated using reverse phase preparative HPLC. Despite considerable efforts to find reaction conditions which would favour the formation of the bisquaternary products by changing the solvent, temperature and reaction time, monoquaternary compounds have always been obtained.

For the synthesis of **16** the requisite 1,1'-(3-iodopropylidene)-bis-benzene was obtained from the corresponding alcohol:

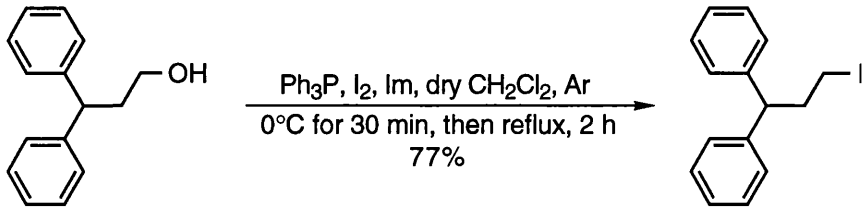

The mechanism of the reaction involves the formation of a pentavalent intermediate from the interaction of the Ph_3P with the I_2, which is attacked by the alcohol to give an alkoxyphosphonium species. The iodide ion then attacks the carbon α- to the oxygen and $Ph_3P{=}O$ is eliminated. The imidazole traps the HI generated in the course of the reaction. The driving force for the conversion is provided by the strength of the P=O bond formed:

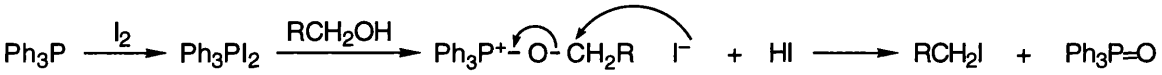

Furthermore, for the synthesis of compounds **20**, **39** and **24** alkylation of the anion of lepidine with a dihalide was effected (**Scheme 3.5**), followed by quaternization of the quinoline groups with MeI.

Scheme 3.5

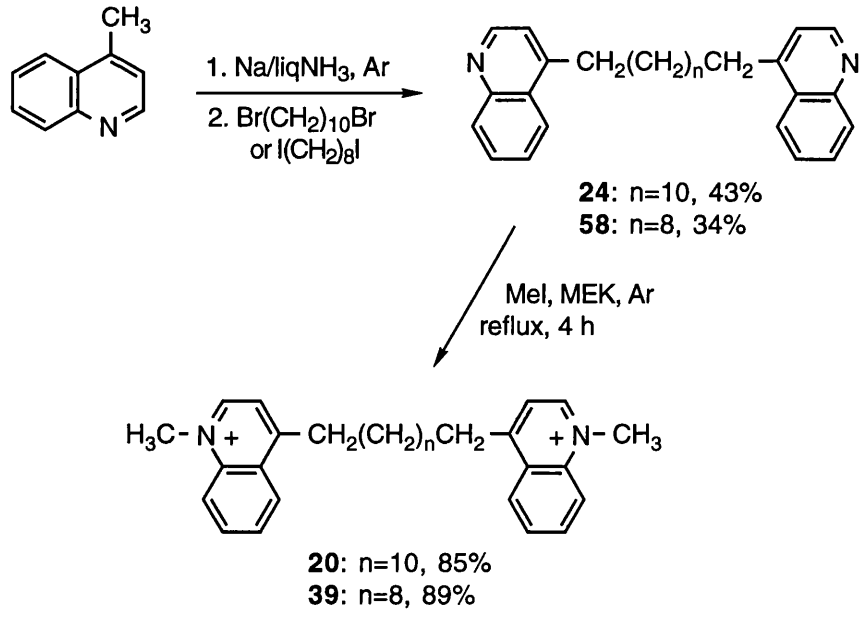

It should be noted that appart from the hydrogens of the methyl group, the hydrogen at position 2 of the quinoline is also acidic. Deprotonation, however, occurs at

the methyl group, since the anion produced is stabilized by resonance:

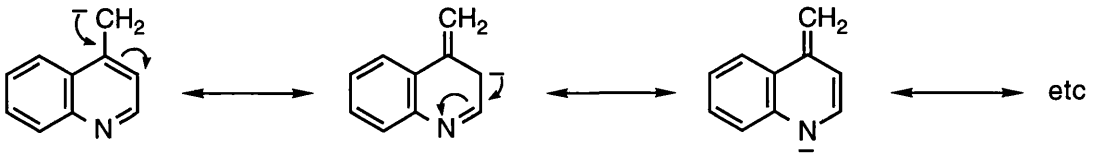

The synthesis of the thio- compounds **22** and **23** is shown in **Scheme 3.6**. Alkylation of 1,10-dichlorodecane with isothiourea was effected in ethanol to yield the respective bis-isothiouronium salt. Hydrolysis of this gave the corresponding bis-thiol which was not isolated but reacted *in situ* with 4-chloroquinoline to afford **23**. Methylation of **23** as usual gave **22**. The latter two complete the discussion of the synthesis of the analogues of **series II**.

Scheme 3.6

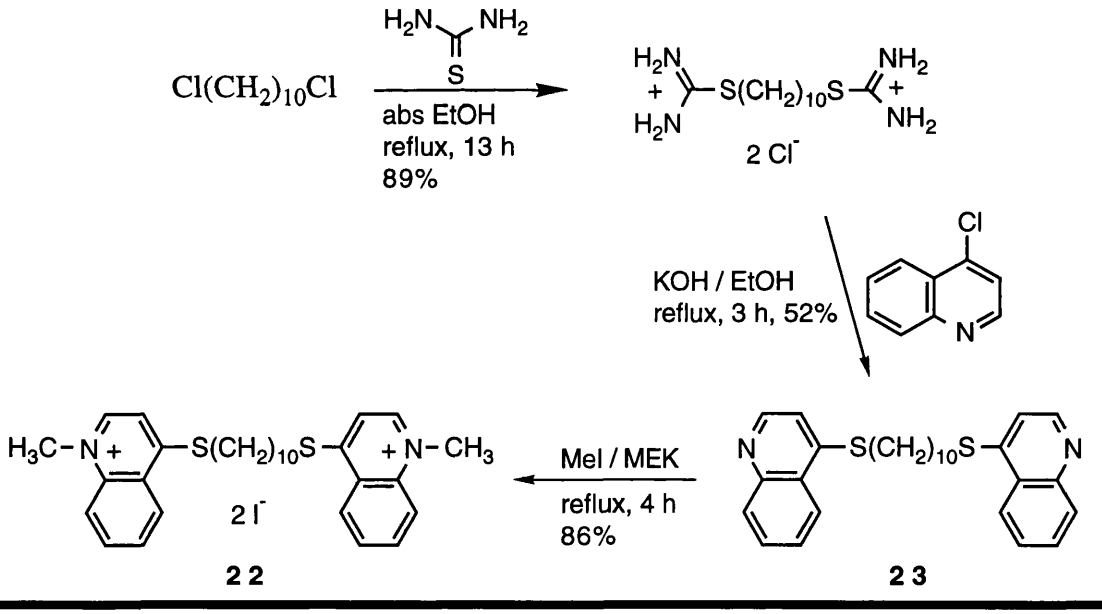

22 **23**

Analogues **41** - **43** belonging to **series III** were obtained by deprotonation of a 2-methylquinoline, alkylation with an appropriate dihalide and quaternization of the resulting bis-quinoline compounds with MeI as described in **Scheme 3.7**.

Scheme 3.7[a]

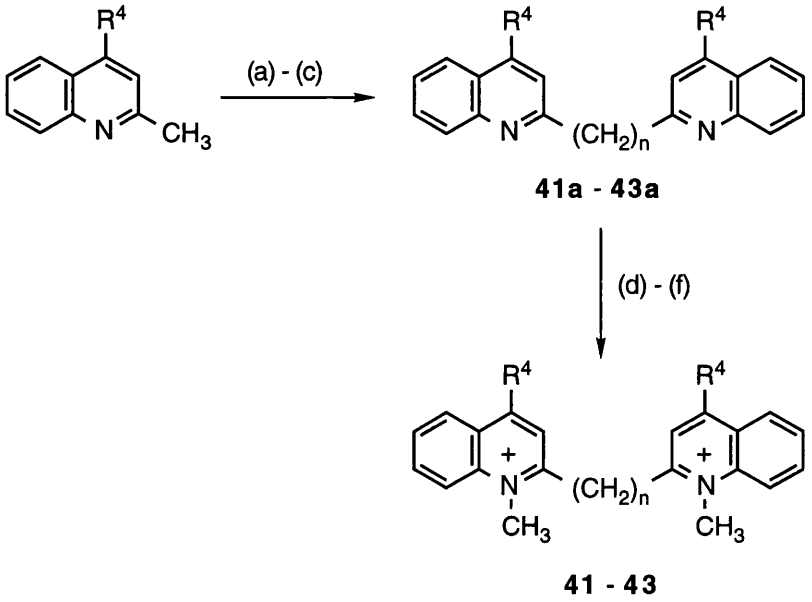

[a]Methods: (a) **41a**: R^4=OMe, 1. Na/liq NH_3/DMF, Ar; 2. $I(CH_2)_8I$, 28%; (b) **42a**: R^4=H, 1. Na/liq NH_3, Ar; 2. $I(CH_2)_8I$, 12%; (c) **43a**: R^4=H 1. LDA/THF; 2. $Br(CH_2)_{10}Br$, -78°C –> RT, 18 h, 78%; (d) **41**: R^4=OMe, MeI/MEK, reflux, 12 h, 52%; (e) **42**: R^4=H, MeI/MEK, reflux, 33 h, 68%; (f) **43**: R^4=H, MeI/MEK, reflux, 72 h, 84%.

The aminopyrimidine analogue **48** was synthesised as shown in **Scheme 3.8**. The chlorine of 2-chloropyrimidine, which is labile due to the presence of the two adjacent ring nitrogens, was displaced with 1,10-diaminodecane to afford the bis-pyrimidine intermediate which was methylated using MeI to give the desired compound **48**.

Scheme 3.8

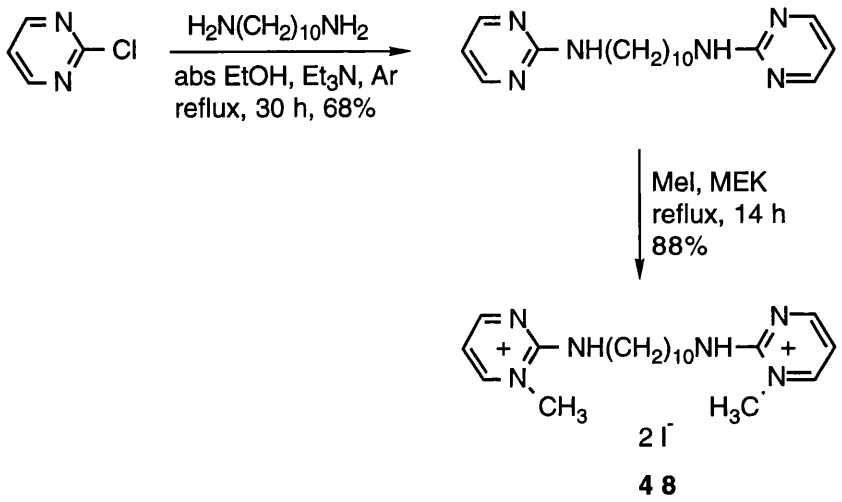

48

For the synthesis of the non - quaternary bis - quinolone **7** it was selected not to alkylate 4-(1H)quinolone with a dihalodecane but to hydrolyse the NH_2 group of **10** (**Scheme 3.9**), previously synthesised by Dr C.A. Davis.

Scheme 3.9

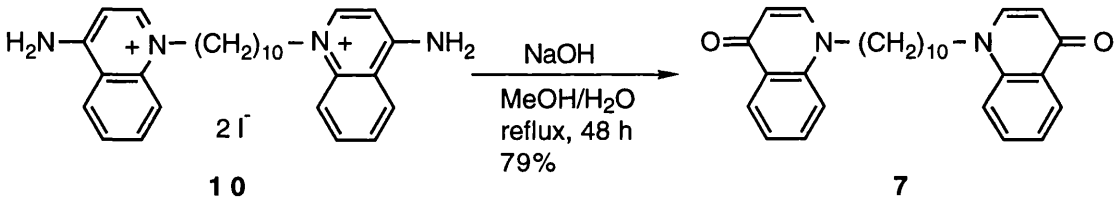

10 **7**

Note that the NH_2 group of 4-aminoquinoline is not a good leaving group. However, in the case of 4-aminoquinolinium compounds such as **10**, the presence of the positive charge facilitates the initial addition step of the addition - elimination process. Furthermore, in the elimination step, elimination of NH_3 is favoured since this results in the disappearance of the positive charge and in the formation of the stable quinolone heterocycle:

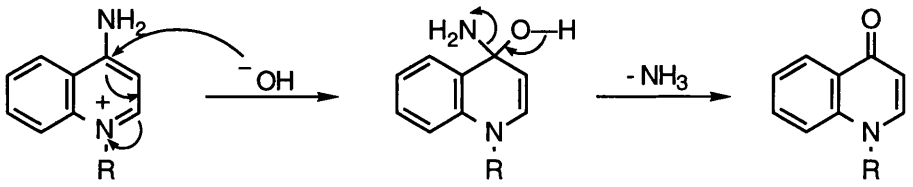

The two benzimidazolium analogues **49** and **50** were synthesised by alkylation of the benzimidazole anion with 1,10-diiododecane to provide intermediates **49a** and **50a** and subsequent methylation of these with MeI (**Scheme 3.10**).

Scheme 3.10

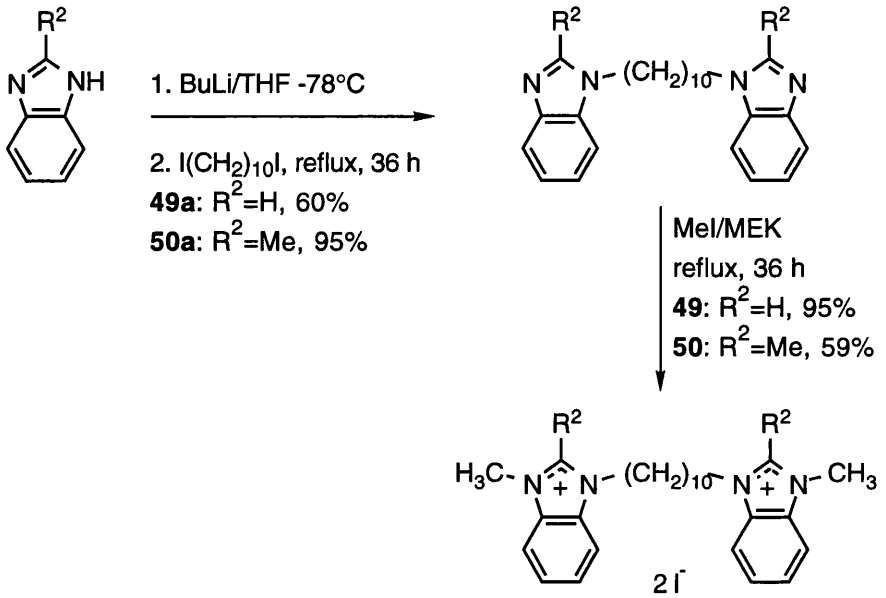

In the first alkylation step of **scheme 3.10** a strong base (n-BuLi) was used to effect quantitative conversion of the benzimidazole to the corresponding anion which was then cleanly alkylated. The alkylation of benzimidazoles (and imidazoles) can also be effected by partial conversion to the anion using a weaker base (in which case an equilibrium is established) or even without the presence of any base. In these cases however, byproducts can be formed and these result from alkylation of one of the nitrogens of benzimidazole and quaternization of the second:

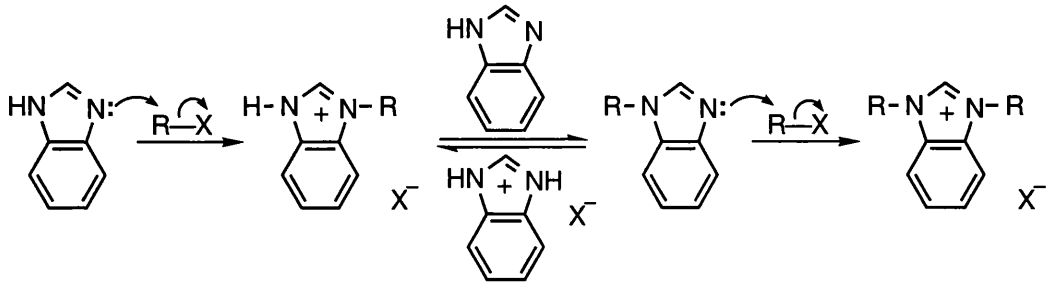

Furthermore, note that proton loss in the deprotonation of 2-methylbenzimidazole occurs at the NH rather than at the CH_3 group, because of the greater stability of the anion produced. This is due to the fact that in anion **A** both ring nitrogens participate in the delocalization of the charge, while in anion **B** the NH cannot take part:

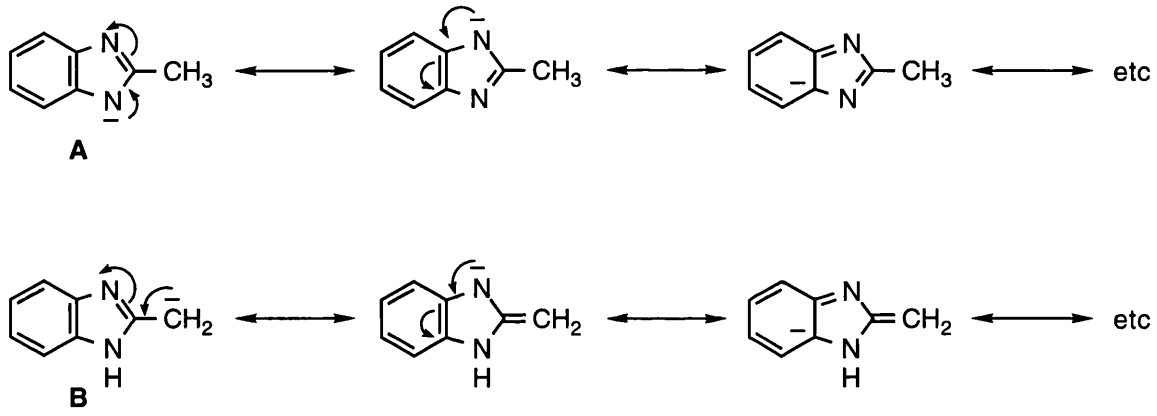

Delocalization over two nitrogens is energetically more favourable than delocalization over one nitrogen and one carbon atoms. It should also be noted that reflux temperature was required for the alkylation of the benzimidazole anion as the reaction did not proceed at room temperature.

For the tetrahydroquinolinium compound **51**, tetrahydroquinoline was deprotonated with n-BuLi and alkylated with 1,10-diiododecane to give intermediate **51a** (**Scheme 3.11**). 1,2,3,4-Tetrahydroquinoline is a weak base (pK_a = 5.03[212]) and this is due to the participation of the lone pair of the nitrogen to the conjugation of the phenyl group. Thus, a strong base (n-BuLi) was used to deprotonate quantitatively the NH group and, hence, to increase the nucleophilicity of the amine. Moreover, in this manner the

formation of quaternary byproducts (for mechanism see above the discussion of the synthesis of the benzimidazolium compounds **49** and **50**) is minimized. **51a** was methylated as usual with MeI in MEK to yield **51** as a hygroscopic solid which was difficult to purify by conventional methods and reverse phase (RP) preparative HPLC was used for this purpose.

Scheme 3.11

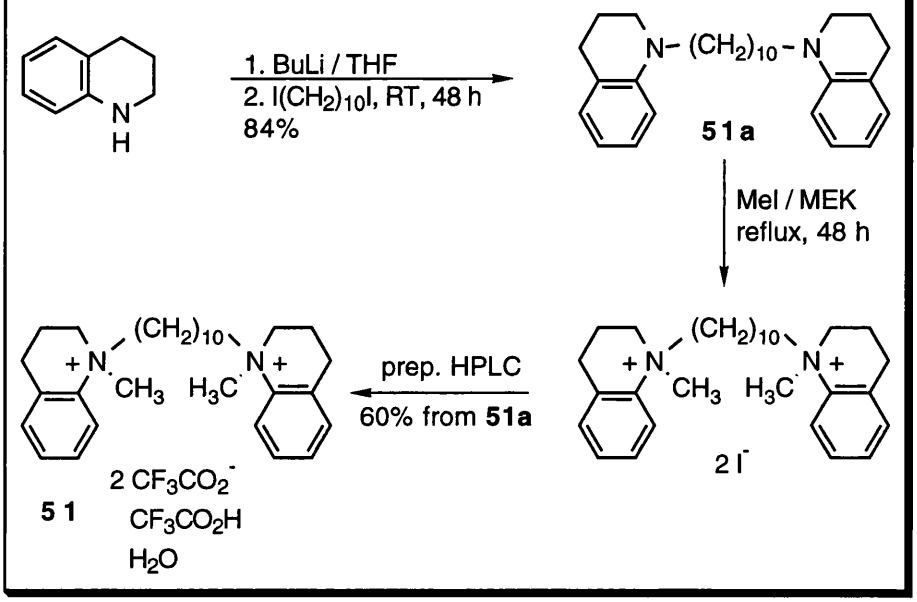

Compound **52a** was synthesised similarly to **51a** (**Scheme 3.12**). However, the methylation of **52a** had to be carried out at room temperature as reflux temperatures resulted in a complicated mixture of products, probably caused by debenzylation. The final compound **52** was an oil which was purified by RP preparative HPLC.

Scheme 3.12

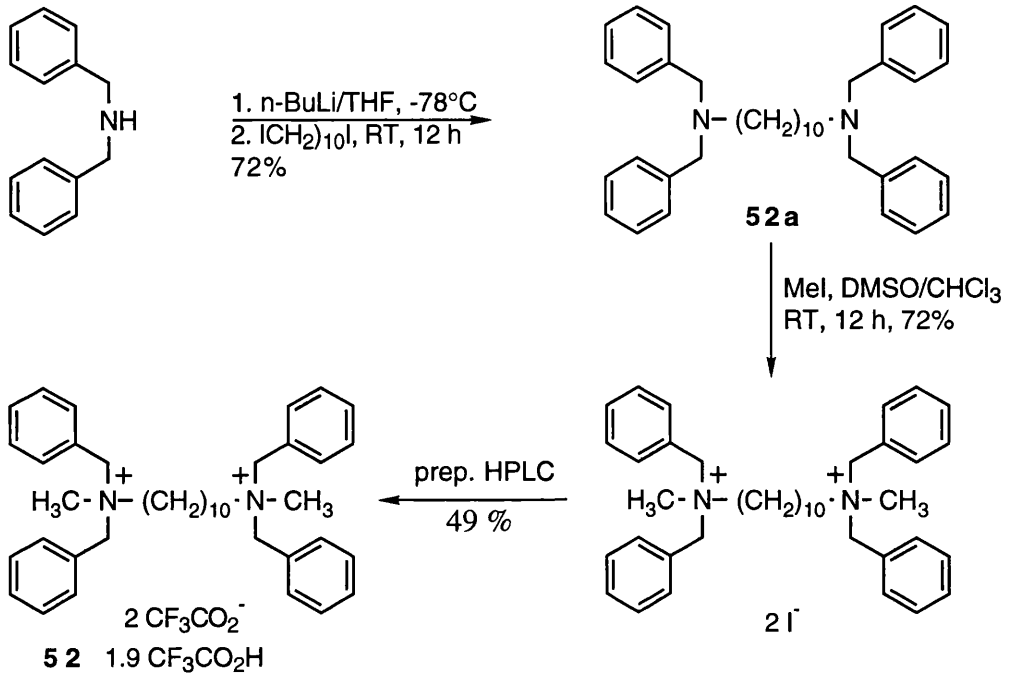

As mentioned in **section 2.3** compound **57** was selected:

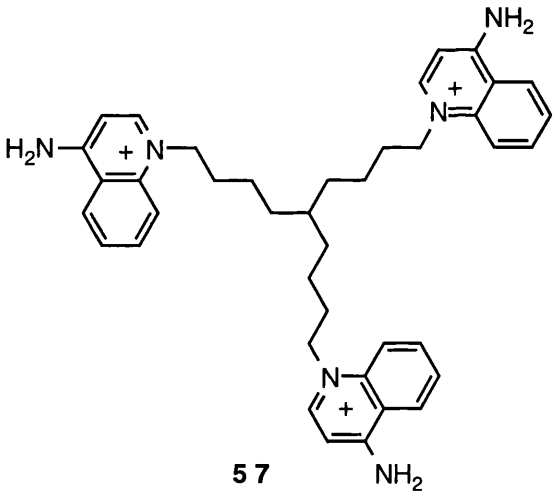

57

For the synthesis of **57** the tribromide **47c** (**scheme 3.13**) was needed. This has been reported once in the literature in a communication[219] and was prepared by the route shown in **scheme 3.13**. Initial hydroboration of the 4-bromobut-1-ene at 0°C yielded the respective trialkylborate. This was converted to the trialkylmethanol **47a** via the sequence shown in **scheme 3.13**. Note that the synthesis of **47a** is a one pot procedure from 4-bromobut-1-ene.

Scheme 3.13

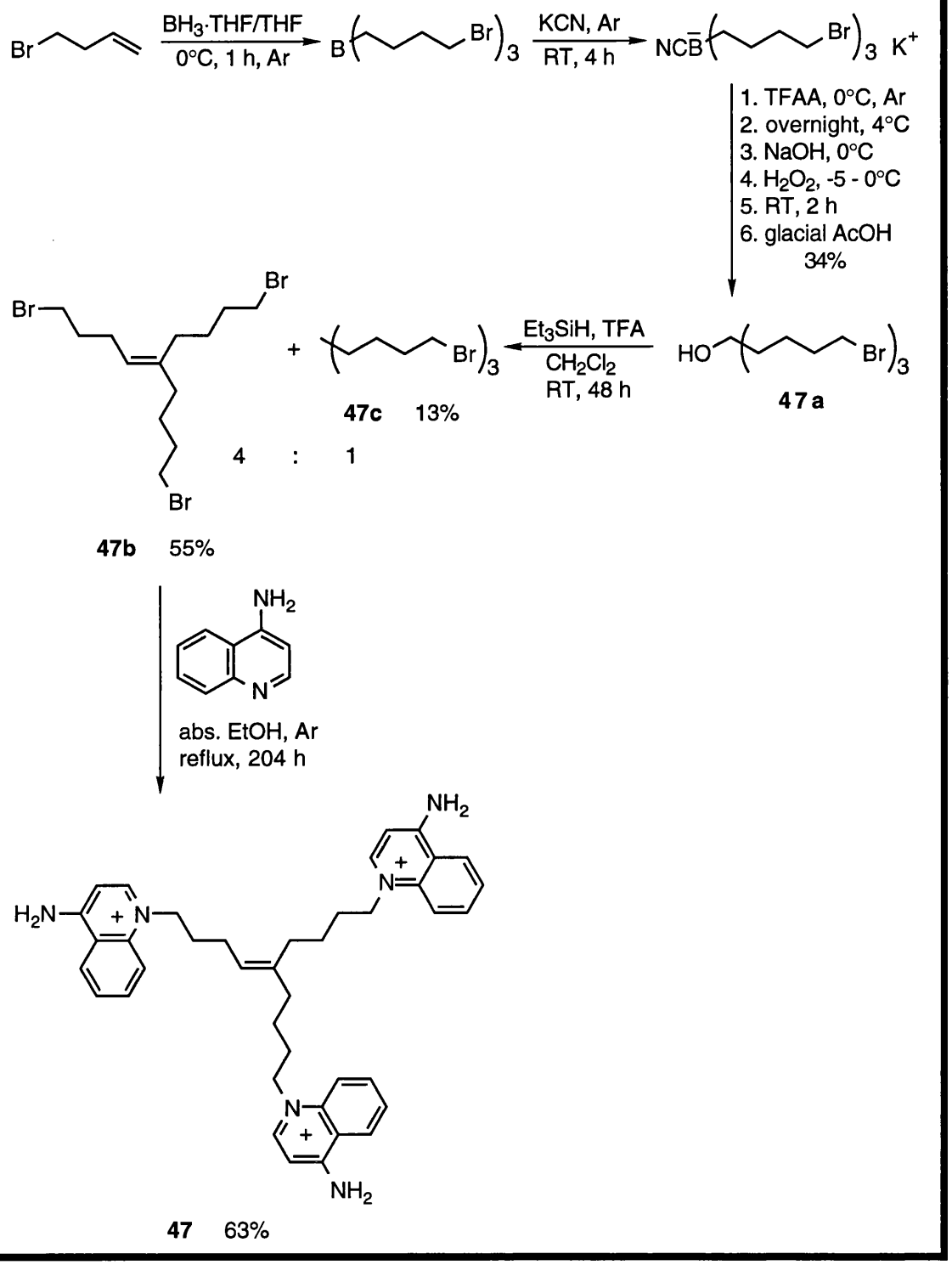

The mechanism of the conversion of trialkylborates to trialkylmethanols has been studied[220,221] and is thought to proceed as follows:

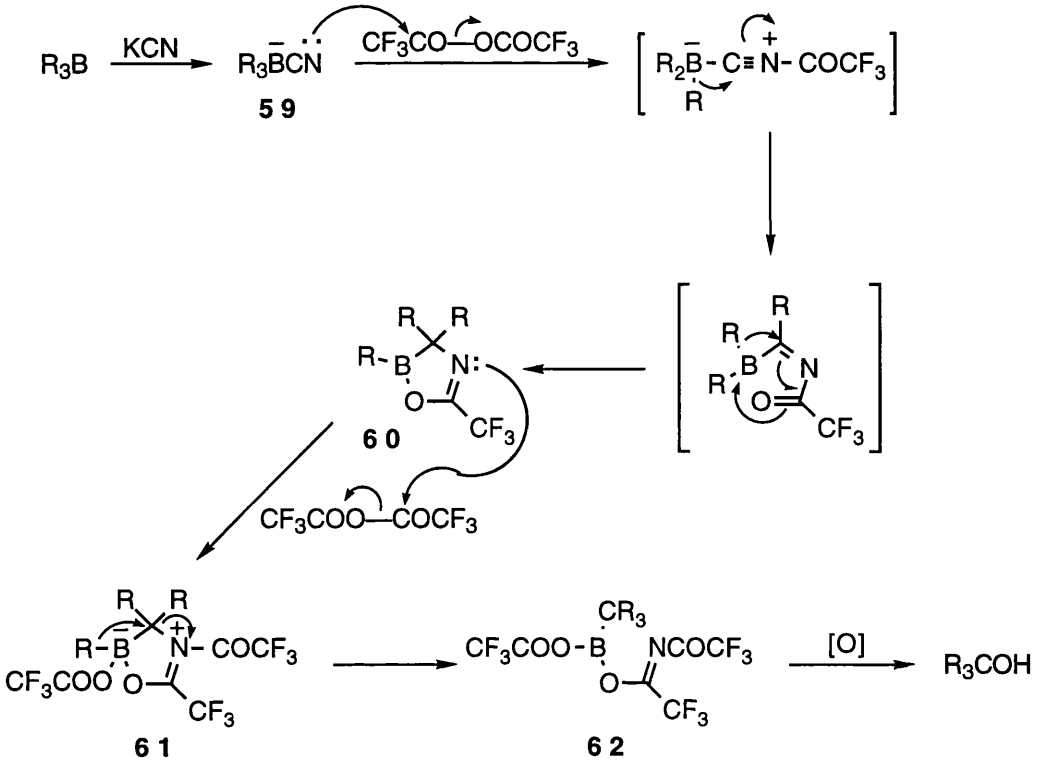

Addition of KCN to the trialkylborate forms the trialkylcyanoborate **59**. Reaction of 1 mole of TFAA with this effects two alkyl migrations from the boron atom to the carbon atom of the CN group to give intermediate **60**. This can be hydrolysed to yield a ketone ($R_2C{=}O$), whereas addition of a second equivalent of TFAA effects a third migration of the alkyl group from the boron atom to the carbon atom of the former CN group. Then, hydrolysis of **62** yields the trialkylmethanol R_3COH.

Hallgren and Lucas[219] report that deoxygenation of **47a** (**scheme 3.13**) using Et_3SiH and TFA gave the tribromide **47c**. However, in our hands this procedure yielded a mixture of **47c** and the elimination product **47b** in approximately 1 : 4 ratio. The mechanism of this reaction involves[222] protonation of the OH group of the tertiary alcohol by TFA and elimination of water to form a carbocation which is then reduced by Et_3SiH:

Since **47b** is a novel compound and larger quantities of it were available, it was reacted with 4-aminoquinoline to give **47** which was obtained as a hygroscopic foam and was

purified by reverse phase preparative HPLC. It may be possible to obtain the initial target compound **57** via hydrogenation of the double bond of **47**. Note, however, that the quinolinium groups, being charged, may be susceptible to reduction and this might be a potential problem. Since only small amounts of **47** were available, the reduction of **47** to **57** has not been pursued, mainly due to time limitations, and will have to be undertaken in the future. But, analogue **57** is not expected to be substantially different in potency than **47**, since it was found that rigidification of the alkyl chain of dequalinium did not alter potency significantly (section **4.3**). Moreover, the length of the alkyl chain was found to be unimportant (section **4.3**).

CHAPTER 4

RESULTS AND DISCUSSION

It was clearly indicated in the selection of compounds section that the aim of this work was mainly five fold: **i.** To investigate the role of the NH_2 group of dequalinium. **ii.** To explore an "inverse" series. **iii.** To effect alterations in the linking alkyl chain. **iv.** To investigate whether both quinolinium groups of dequalinium are needed for SK_{Ca} channel blockade and to attempt to obtain information on their mode of binding as this is of crucial importance in designing a more potent blocker. **v.** To investigate replacements of the quinolinium by other charged groups in order to seek any special features associated with the former group. Therefore, the discussion will focus mainly on these issues and will follow the same order of presentation.

4.1 THE ROLE OF THE NH_2 GROUP OF DEQUALINIUM.

In the course of this investigation, compounds belonging to **series I** have been synthesised. Structural information as well as biological data for the analogues of **series I** can be found in **Table 4.1**. Previous investigations[208] have shown that the contribution of the 2-Me group of dequalinium is very small (cf. compounds **8** and **10**). However, the contribution of the 4-NH_2 group is substantial since its removal results in an order of magnitude drop in potency (cf. compounds **9** and **10**). The hydrogens of the NH_2 group carry substantial positive charges which result from the delocalisation of the ring charge (**Figure 4.1**) and are therefore acidic:

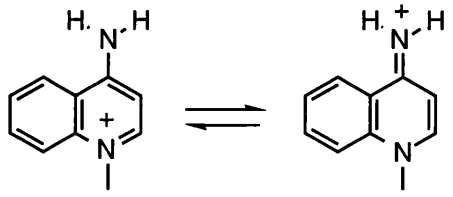

Figure 4.1 Resonance structures of the amino quinolinium group

The NH_2 group is therefore an excellent H - bond donor and it was felt that its contribution to activity may stem from it acting as such. However, it was shown that replacement of the NH_2 by the NMe_2 group, thus eliminating the possibility of H - bond donation, does not result in any loss of potency (cf. compounds **10** and **12**). On the other hand, it seemed unlikely that the NH_2 group can function as an H - bond acceptor since its lone pair is involved in the delocalisation of the positive charge of the ring and is therefore unavailable for H - bonding.

Considering the above, the most likely explanation for the contribution of the NH_2 group comes from its ability to modify the electronic properties of the quinolinium ring. In particular, it provides more extensive delocalisation of the positive charge (**Figure 4.1**) compared with the unsubstituted case (compound **9**). Thus, it was felt that the influence of the degree of the delocalisation of the positive charge on potency is a worthwhile investigation.

Table 4.1 Structure and biological results for the compounds of **series I.**

Compd No	UCL No	Notebook No	Structure	EMR*(±SD)
1	1463	DG-155A	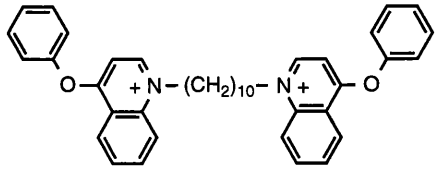	6.5 ± 1.9
2	1491	DG-367B	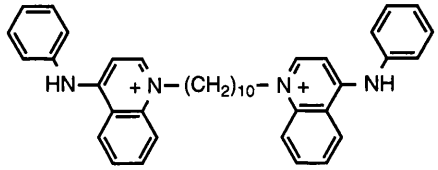	3.4 ± 1.8
3	1504	DG-459A	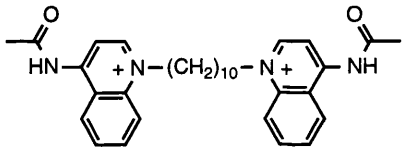	5.5 ± 1.0
4	1560	DG-589B	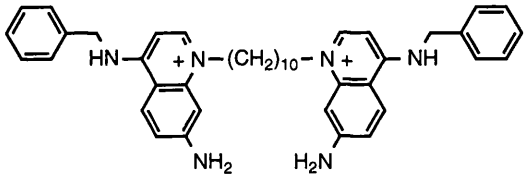	0.9 ± 0.5
5	1580	DG-703C	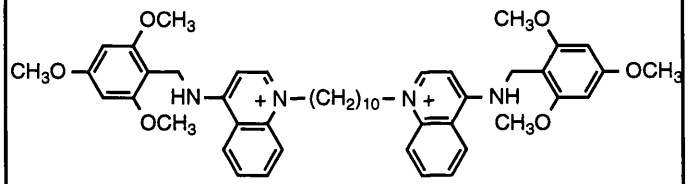	1.0 ± 0.6
6	1598	DG-739B	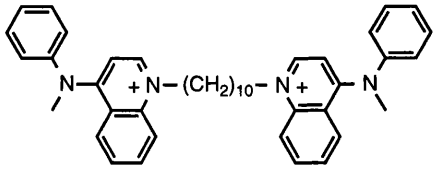	1.8±0.8
7	1507	DG-467A	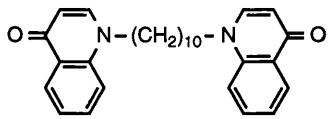	>>10

* Equieffective molar ratio: the ratio of the concentrations of the test compound and dequalinium that cause 50% inhibition of the afterhyperpolarization (AHP), as determined in the same experiment.

Table 4.1 (continued)

Compd No	UCL No	Notebook No	Structure	EMR (±SD)
8	Deq.	—	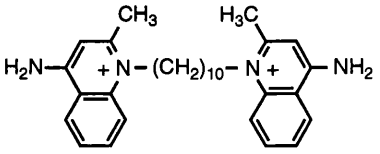	1
9	1072	CD-9A	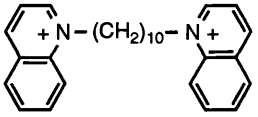	15 ± 7.9
10	1127	CD-45	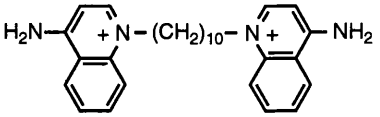	1.3 ± 0.5
11	1130	CD-43B	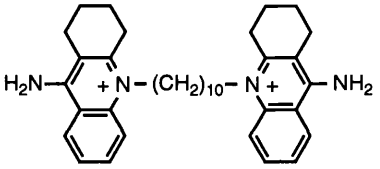	0.9 ± 0.7
12	1173	CD-74	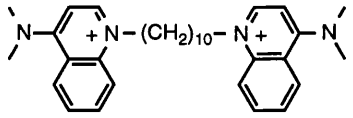	1.4 ± 0.6
13	1359	CO-199B	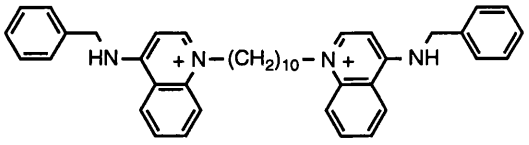	0.7 ± 0.3
14	1431	BR-19A	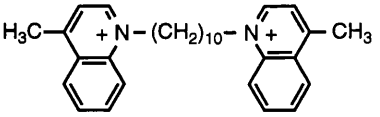	26 ± 14

In order to vary the degree of delocalisation the NH_2 group was replaced by groups of different electronic properties. This task was undertaken by synthesising compounds with a PhO- (**1**), PhNH- (**2**), CH_3CONH- (**3**) and $Ph(CH_3)N$- (**6**) group at position 4, relating to compounds with an NH_2- (**10**), H- (**9**), $(CH_3)_2N$- (**12**) or CH_3- (**14**) group at the same position. Compound **13** with a $PhCH_2NH$- substituent at position 4 was made earlier on in an effort to seek lipophilic interactions but can be included in this discussion. In all these nine compounds the substituent at position 2 was kept constant, being a hydrogen for synthetic accessibility reasons since compounds with a Me group at position 2 are more difficult to synthesise, particularly as the nucleophilicity of the ring nitrogen is decreased by reducing the electron releasing properties of the substituent at position 4. Again related to synthetic problems was the fact that, apart from the hydrogen (compound **9**) all substituents used have an overall electron releasing effect since quinolines with electron withdrawing groups at position 4 are extremely weak nucleophiles and alkylation of the ring nitrogen with a halide is very difficult.

All nine compounds show SK_{Ca} channel blocking activity. There appears to be no correlation between EMR and either the size or lipophilicity of substituent $\mathbf{R^4}$. Nevertheless, they seem to follow a clear trend: The more electron releasing the substituent at position 4, the more potent the compound. Quantification of this trend is of course an important issue and for this a descriptor of the electronic properties of substituent $\mathbf{R^4}$ is needed. Various electronic parameters exist in the literature and have been widely used in QSAR (for a large collection and discussion of substituent constants see references 223-225). These electronic parameters can be classified according to the type of the substituent to which they refer (aliphatic or aromatic). Aromatic substituent constants are further subdivided according to the position of the substituent relative to an important center on the aromatic ring into "meta" or "para" substituent constants. For the purpose of this analysis, "aromatic", "para" constants will be used, as the $\mathbf{R^4}$ substituent is "para" with respect to the quaternary ring nitrogen carrying the positive charge. These parameters are in general of three types:

1. Those describing the overall electronic effect (inductive and mesomeric) of the substituent [e.g. σ_P^{HL} (ref. 225), σ_P^{SW} (ref. 226), σ_P^{M} (ref. 227), σ_P^{E} (ref. 228)].

2. Those related only to the inductive effect of the substituent [e.g. σ_I^M (ref. 227), σ_I^{CH} (ref. 229), F (ref. 230)].
3. Those incorporating only the resonance effect of the substituent [e.g. σ_R^M (ref. 227), σ_R^{CH} (ref. 229), R (ref. 230), R′ (ref. 231)]. **Table 4.2** shows values for these parameters for the substituents considered in this study.

Linear regression was performed on all compounds of **Table 4.2** except for **13** for which values for the parameters are not available. The results are shown in **Table 4.3**. Some conclusions can be drawn from **Table 4.3**. There appear to be modest to good correlations of potency with the overall electronic effect of substituent **R4** depending on the individual σ_P parameter used. However, when the electronic effect of **R4** is separated into its inductive and resonance components as represented by the respective parameters, it becomes clear that there is no correlation with the inductive effect, while the resonance effect correlates well. A plot of pEMR vs σ_R^{CH} is shown in **Figure 4.2**.

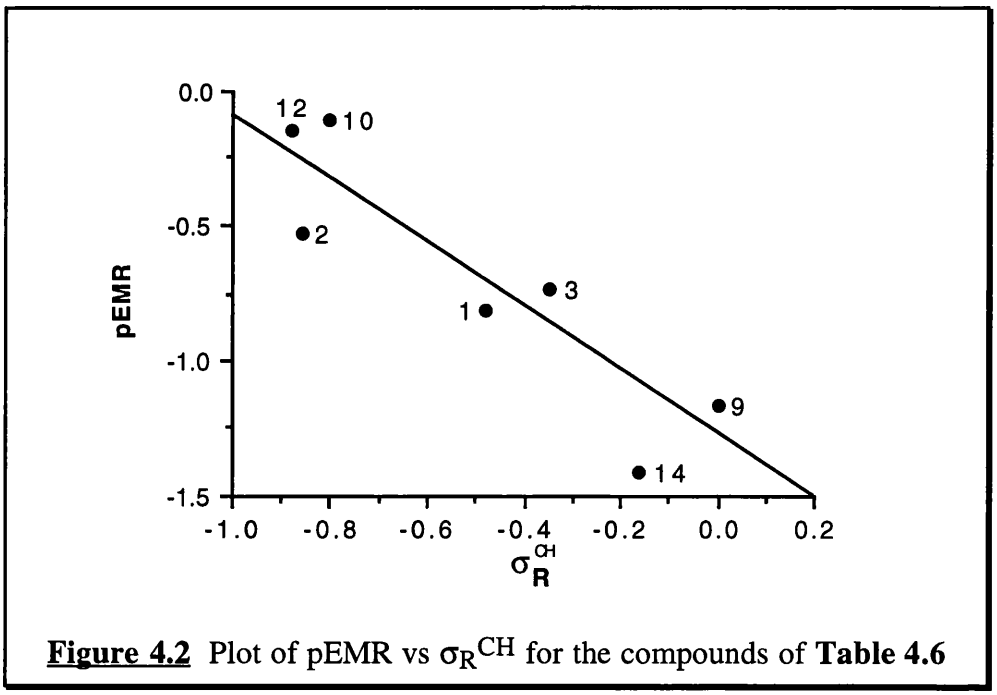

Figure 4.2 Plot of pEMR vs σ_R^{CH} for the compounds of **Table 4.6**

Thus, it seems that the resonance component of the electronic effect of **R4** is the crucial factor that alters potency. This is consistent with conventional chemical concepts. Substituent **R4** is in direct conjugation with the positively charged ring nitrogen and is in a "para" position with respect to the latter. Therefore, it would be expected that the inductive effect of **R4** would only be able to operate to a small extent from such a distance, while its

resonance effect, being less dependent on distance would become the dominant factor.

Following these findings, the predictive value of the correlation to provide more potent compounds was considered. For this purpose, a group with higher electron releasing power than the NH_2 or NMe_2 groups was sought. However, these are virtually the most electron releasing neutral substituents known.[223-225] Nevertheless, negatively charged groups (e.g. the O^- group) can excert a greater electron releasing effect. It was therefore decided to incorporate the $-O^-$ group at position 4 of the quinoline and the structure that results from this substitution is shown in **Figure 4.3**. Of course, **7a** is only a resonance structure of compound **7**.

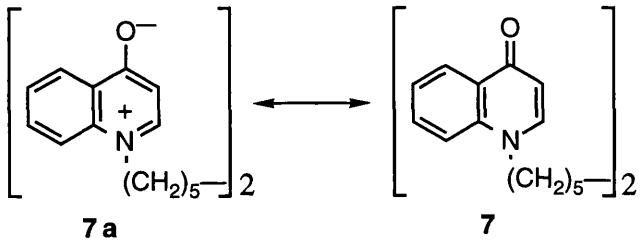

7a **7**

Figure 4.3 Resonance structures of compound **7**

Hence, compound **7** was synthesised but was found to be devoid of any biological activity (**Table 4.1**). Obviously, compound **7** does not have a net positive charge like all the other compounds of this series. Instead, it is a dipole and any fractional positive charges in the ring result from the contribution of resonance structure **7a** to the hybrid. It therefore seems that it is important to maintain a net positive charge in the quinoline nucleus.

Although the use of conventional electronic parameters (such as these of **Table 4.2**) in QSAR can provide initial guidance and useful insight into determinant factors, it is also associated with some limitations. These stem from the limited availability of values for the parameters to a small number of functional groups (e.g. values for the electronic parameters of the benzyl group are not available as mentioned above) and from the need for multiparameter correlations when more than one substituent is being considered. This raises the demand on the number of compounds to be included in the QSAR in order to produce statistically meaningful correlations and to reduce the risk of chance correlations.

Table 4.2. Values of some electronic parameters for substituent R^4.

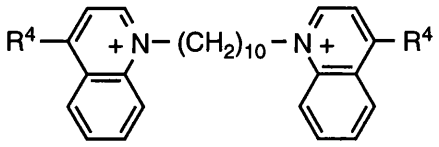

Compd No	UCL No	Notebook No	R^4	σ_P^{HL} 1	σ_P^{SW} 2	σ_P^{M} 3	σ_P^{E} 4
9	1072	CD-9A	H	0	0	0	0
14	1431	BR-19A	CH_3	-0.17	-0.135	-0.17	-0.14
3	1504	DG-459A	$NHCOCH_3$	0	0.002	-0.20	0
1	1463	DG-155A	OPh	-0.03	0.055	-0.35	0.05
2	1491	DG-367B	NHPh	-0.40	-0.160	-0.41	-0.27
10	1127	CD-45	NH_2	-0.66	-0.295	-0.69	-0.30
12	1173	CD-74	NMe_2	-0.83	-0.317	-0.83	-0.32
13	1359	CO-199B	$NHCH_2Ph$	NA[12]	NA[12]	NA[12]	NA[12]

Compd No	σ_I^{M} 5	σ_I^{CH} 6	F 7	σ_R^{M} 8	σ_R^{CH} 9	R 10	R´ 11
9	0	0	0	0	0	0	0
14	-0.04	-0.01	-0.04	-0.14	-0.16	-0.13	-0.41
3	0.28	0.28	0.28	-0.26	-0.35	-0.26	-1.43
1	0.38	0.40	0.34	-0.40	-0.48	-0.35	-1.29
2	0.01	0.30	-0.02	-0.85	-0.86	-0.38	-1.58
10	0.20	0.17	0.02	-0.76	-0.80	-0.68	-2.52
12	0.08	0.17	0.10	-0.92	-0.88	-0.92	-3.81
13	NA[12]	NA[12]	NA[12]	NA[12]	NA[12]	NA[12]	NA[12]

1. Hammet constant for "para" substitution.[225] 2. Hammet constant for "para" substitution.[226] 3. Hammet constant for "para" substitution.[227] 4. Hammet constant for "para" substitution.[228] 5. Hammet constant for inductive effects.[227] 6. Electronic parameter for inductive effects.[229] 7. Field parameter.[230] 8. Hammet constant for resonance effects.[227] 9. Electronic parameter for resonance effects.[229] 10. Resonance parameter.[230] 11. Corrected field parameter.[231] 12. NA: not available.

Table 4.3. Correlation equations for compounds of **Table 4.2.**

Equation	n	r	s
pEMR = -1.16 (± 0.38) σ_P^{HL} - 1.05 (± 0.17)	7	-0.80	0.318
pEMR = -2.21 (± 1.10) σ_P^{SW} - 0.97 (± 0.20)	7	-0.67	0.398
pEMR = -1.49 (± 0.32) σ_P^{M} - 1.27 (± 0.15)	7	-0.90	0.233
pEMR = -2.06 (± 1.03) σ_P^{E} - 0.99 (± 0.21)	7	-0.67	0.399
pEMR = 0.93 (± 1.30) σ_I^{M} - 0.83 (± 0.26)	7	0.30	0.510
pEMR = 1.43 (± 1.27) σ_I^{CH} - 0.97 (± 0.30)	7	0.45	0.478
pEMR = 0.33 (± 1.42) F - 0.74 (± 0.24)	7	0.10	0.532
pEMR = -1.19 (± 0.27) σ_R^{M} - 1.27 (± 0.16)	7	-0.89	0.242
pEMR = -1.24 (± 0.26) σ_R^{CH} - 1.33 (± 0.16)	7	-0.90	0.230
pEMR = -1.40 (± 0.29) R - 1.25 (± 0.14)	7	-0.91	0.225
pEMR = -0.35 (± 0.07) R′ - 1.25 (± 0.14)	7	-0.91	0.221

Taking these limitations into account and to seek a more appropriate electronic descriptor that would refer to the whole molecule rather than just one substituent, it was decided to perform molecular orbital (MO) calculations on the compounds. As an initial step, the calculations were done at the semiempirical level (for speed) using the MOPAC package and the AM1 Hamiltonian.[232] To simplify the computational problem, the calculations were performed on model compounds consisting of only one of the two substituted quinolinium groups and the ten methylene chain was replaced by a methyl. It was felt that this is a reasonable approximation since the two quinolinium groups are well separated to not interact electronically. The replacement of the ten methylene chain by a methyl introduces some errors which arise from the different inductive and hyperconjugation effect of the former compared with the latter, but these are expected to be largely the same for all the compounds. Therefore, the results of the calculations should be comparable. The general formula of the model compounds can be represented by structure **63** (see below).

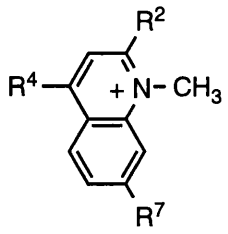

6 3

It should be noted at this point that the newer PM3 Hamiltonian was not used as it gave positive partial charges on the ring nitrogen. This was in contrast to results from MNDO, AM1 and *Ab Initio* (3-21G level) calculations which indicated that the ring nitrogen has a negative partial charge (data not shown). Initially, the variation of the partial charges (obtained from Mulliken population analysis) of the ring nitrogen and of the carbon at position 4 (since to this carbon the substituent is attached) of the quinoline was examined. These are shown in **Table 4.4**. Compounds above the double line will be discussed first as these were initialy available. Compounds **4** and **5** were synthesised subsequently.

As can be seen from equation **R-1** (**Table 4.5**) there is not a significant correlation between pEMR and the partial charge of the carbon at position 4 of the quinoline. On the other hand, there is a good correlation between pEMR and the partial charge on the ring nitrogen of the quinoline (eq. **R-2**). It can be seen from eq. **R-2** that the more negative the partial charge on the ring nitrogen the more potent the compound. A plot of pEMR vs N_1 charge can be found in **Figure 4.4**. The influence of the variation of the partial charge on the ring nitrogen on activity is in agreement with the σ_R correlation discussed earlier. The more electron releasing $\mathbf{R^4}$ is, the more electron density is fed into the ring and the more positive charge is withdrawn from it. As a result, the negative charge on the ring nitrogen is increased and so is potency.

Apart from the charge distribution, the electronic influence of $\mathbf{R^4}$ alters molecular orbital energies. The energies of the frontier orbitals for the model compounds are shown in **Table 4.4** and the correlation equations are **R-3** and **R-4** (**Table 4.5**). Plots of pEMR vs E_{LUMO} or E_{HOMO} are shown in **Figures 4.5** and **4.6** respectively. As can be seen, the blocking potency of the compounds correlates equally well with the partial charge on the ring nitrogen and with the energy of the LUMO, while the correlation with

the energy of the HOMO is less good. These correlations suggest that the higher the energies of the frontier orbitals the more potent are the compounds.

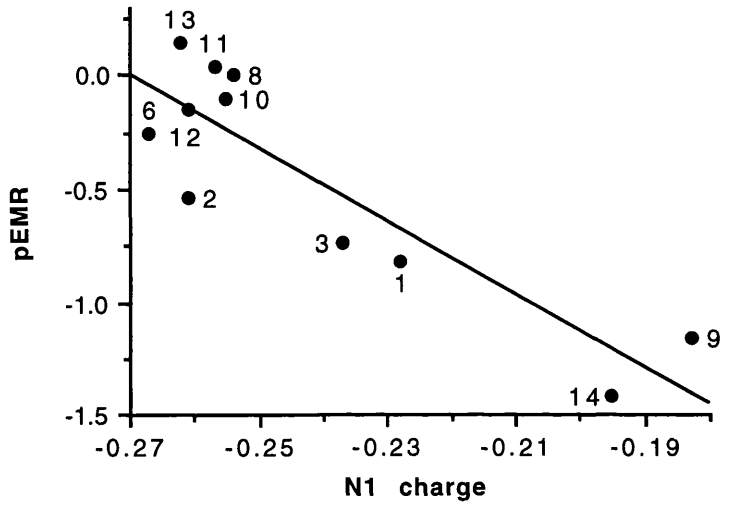

Figure 4.4 Plot of pEMR vs N_1 charge for the compounds of eq. **R-2**

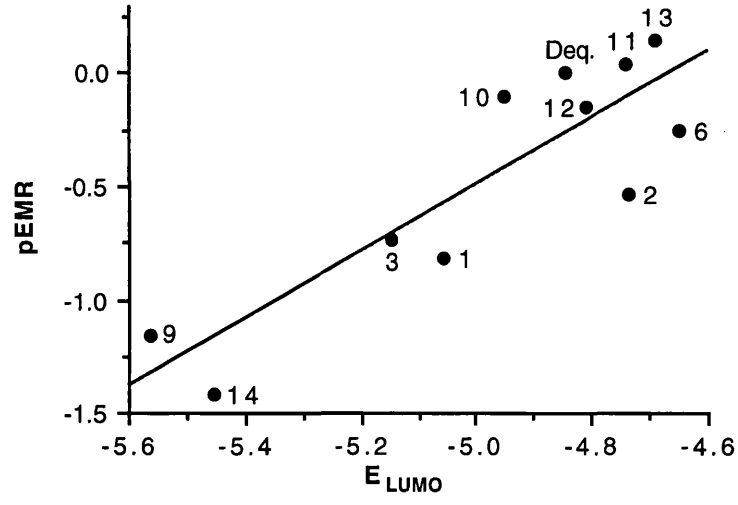

Figure 4.5 Plot of pEMR vs E_{LUMO} for the compounds of eq. **R-3**

Table 4.4 Partial charges and frontier orbital energies for the model compounds of **series I.**

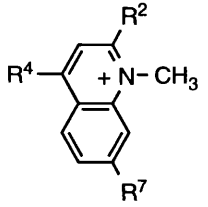

Compd No[1]	UCL No[1]	Notebook No[1]	R^2	R^4	R^7	C_4 charge	N_1 charge	E_{HOMO}*	E_{LUMO}*	EMR (±SD)[2]
1	1463	DG-155A	H	OPh	H	0.257	-0.228	-12.72	-5.058	6.5 ± 1.9
2	1491	DG-367B	H	NHPh	H	0.270	-0.261	-12.41	-4.735	3.4 ± 1.8
3	1504	DG-459A	H	$NHCOCH_3$	H	0.263	-0.237	-12.93	-5.148	5.5 ± 1.0
6	1598	DG-739B	H	N(Me)Ph	H	0.272	-0.267	-12.25	-4.652	1.8 ± 0.8
8	Deq.	—	CH_3	NH_2	H	0.270	-0.254	-12.75	-4.847	1 ± 0.05
9	1072	CD-9A	H	H	H	-0.039	-0.183	-13.54	-5.564	15 ± 7.9
10	1127	CD-45	H	NH_2	H	0.269	-0.255	-12.84	-4.952	1.3 ± 0.5
11	1130	CD-43B	$-(CH_2)_4-$	NH_2	H	0.267	-0.257	-12.50	-4.743	0.9 ± 0.7
12	1173	CD-74	H	NMe_2	H	0.265	-0.261	-12.46	-4.810	1.4 ± 0.6
13	1359	CO-99B	H	$NHCH_2Ph$	H	0.262	-0.262	-12.30	-4.693	0.7 ± 0.3
14	1431	BR-19A	H	CH_3	H	0.083	-0.195	-13.39	-5.456	26.0 ± 14
4	1560	DG-589B	H	$NHCH_2Ph$	NH_2	0.274	-0.277	-11.97	-4.341	0.9 ± 0.5
5	1580	DG-703C	H	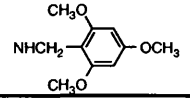	H	0.260	-0.272	-11.45	-4.347	1.0 ± 0.6

* in eV.

1. The compound No, UCL No and notebook No of the corresponding bis - quinolinium compound of **Table 4.1** are used for simplicity.
2. The EMR of the corresponding compound of **Table 4.1** is used for simplicity.

Table 4.5 Correlation equations for the model compounds of **series I** using data from **Table 4.4**.

Equation No	Equation	n	r	s	Excludes	Reason for exclusion
R-1	pEMR = 3.82 (± 1.13) **C_4** charge - 1.30 (± 0.27)	11	0.75	0.366	**4, 5**	initially not synthesised
R-2	pEMR = -16.24 (± 2.80) **N_1** charge - 4.38 (± 0.68)	11	-0.89	0.253	**4, 5**	initially not synthesised
R-3	pEMR = 1.49 (± 0.27) **E_{LUMO}** + 6.94 (± 1.33)	11	0.88	0.262	**4, 5**	initially not synthesised
R-4	pEMR = 0.98 (± 0.25) **E_{HOMO}** + 12.04 (± 3.2)	11	0.79	0.336	**4, 5**	initially not synthesised
R-5	pEMR = -15.93 (± 2.30) **N_1** charge - 4.31 (± 0.57)	13	-0.90	0.230	none	
R-6	pEMR = 1.19 (± 0.21) **E_{LUMO}** + 5.41 (± 1.05)	13	0.86	0.274	none	
R-7	pEMR = 0.69 (± 0.18) **E_{HOMO}** + 8.35 (± 2.28)	13	0.76	0.349	none	

It should be noted at this point that in all compounds of **Table 4.4** the LUMO is an antibonding π orbital localised on the quinolinium ring with major contributions from the ring nitrogen (N_1) and carbons C_2, C_4, C_5, C_7 and C_{8a}. However, the HOMO is a π orbital not always localised on the quinolinium ring. In particular, in the case of compounds **2** and **6** there are considerable contributions from the Ph ring of the NHPh and N(Me)Ph substituent position 4, while in compounds **1**, **5** and **13** the HOMO is a different π orbital with contributions only from the Ph ring of the respective substituent at postition 4 (**Figure 4.8a**). As a result, correlations that use the E_{LUMO} should be qualitatively more consistent than those that use the E_{HOMO}.

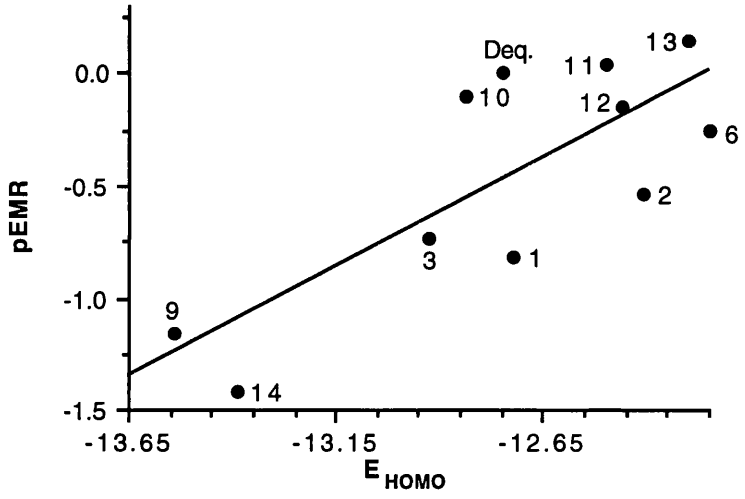

Figure 4.6 Plot of pEMR vs E_{HOMO} for the compounds of eq. **R-4**

It was decided to assess the predictive value of the above correlations in terms of obtaining more potent blockers by synthesising a few representative compounds. MO calculations suggested that the energy of the frontier orbitals can be raised in two ways: Either by introducing further electron releasing substituents at positions 2, 5 and/or 7 of the quinoline (positions in which the substituent would be in direct conjugation with the ring nitrogen) or by introducing electron releasing substituents at positions 2, 4 and/or 6 (ortho or para to the methylene) of the phenyl ring of compound **13**. Hence, a representative compound from each case was synthesised.

Considering the first possibility, it was decided to work with compound **13** since

this is the most potent in this series, and the option of introducing an amino group at position 2, 5 or 7 of the quinoline of this compound was examined. Molecular modelling suggested that an NH_2 group at position 5 would not raise the frontier orbital energies as much as one at positions 2 or 7, due to rotation of the NH_2 group out of the plane of the ring, arising from severe steric interactions with the NH at the peri- (4) position, hence reducing the degree of conjugation between this group and the ring nitrogen. On the other hand, an NH_2 group at position 2 of the quinoline would present synthetic difficulties, not only in synthesising the quinoline ring itself but also in alkylating the ring nitrogen due to steric hindrance (this difficulty was experienced with compounds having a Me group at position 2 of the quinoline). Since an NH_2 group at position 7 raises MO energies approximately by the same amount as one at position 2 without presenting the same synthetic problems, compound **4** (**Table 4.1**) was synthesised.

The second possibility was investigated by introducing electron releasing substituents in the phenyl ring of compound **13**. In particular, three MeO groups were introduced at positions 2, 4 and 6. NH_2 groups were avoided again for synthetic accessibility reasons. These modifications resulted in compound **5** (**Table 4.1**). The predicted EMR value for compounds **4** and **5** is 0.34 on the basis of equation **R-3**. However, it should be noted that the partial charge on the ring nitrogen of these two compounds does not change significantly with respect to the parent compound **13** (as shown in **Table 4.4**) and eq. **R-2** does not predict substantial changes in their biological activities. The predicted EMR values from eq. **R-2** are 0.76 for compound **4** and 0.92 for compound **5**, well within the experimental error of the activities measured experimentally (**Table 4.1**). In fact, the inclusion of compounds **4** and **5** in the correlation with N_1 charge results in slightly improved statictics (cf. equations **R-2** and **R-5**, **Table 4.5**, **Figures 4.4** and **4.7**). On the other hand, inclusion of compounds **4** and **5** into the E_{LUMO} correlation results in slightly worse statistics (cf. equations **R-3** and **R-6**, **Table 4.5**, **Figures 4.5** and **4.8**).

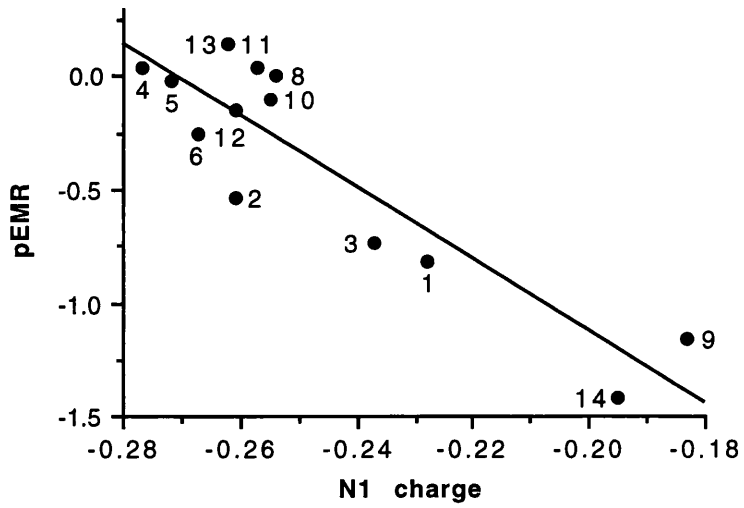

Figure 4.7 Plot of pEMR vs N_1 charge for the compounds of eq. **R-5**

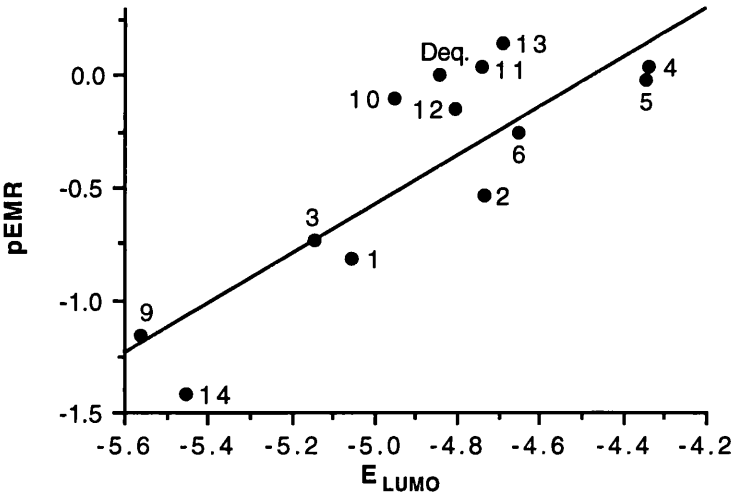

Figure 4.8 Plot of pEMR vs E_{LUMO} for the compounds of eq. **R-6**

It therefore seems that the correlation with N_1 charge has better predictive power than the correlation with E_{LUMO} for this series (**series I**) of analogues.

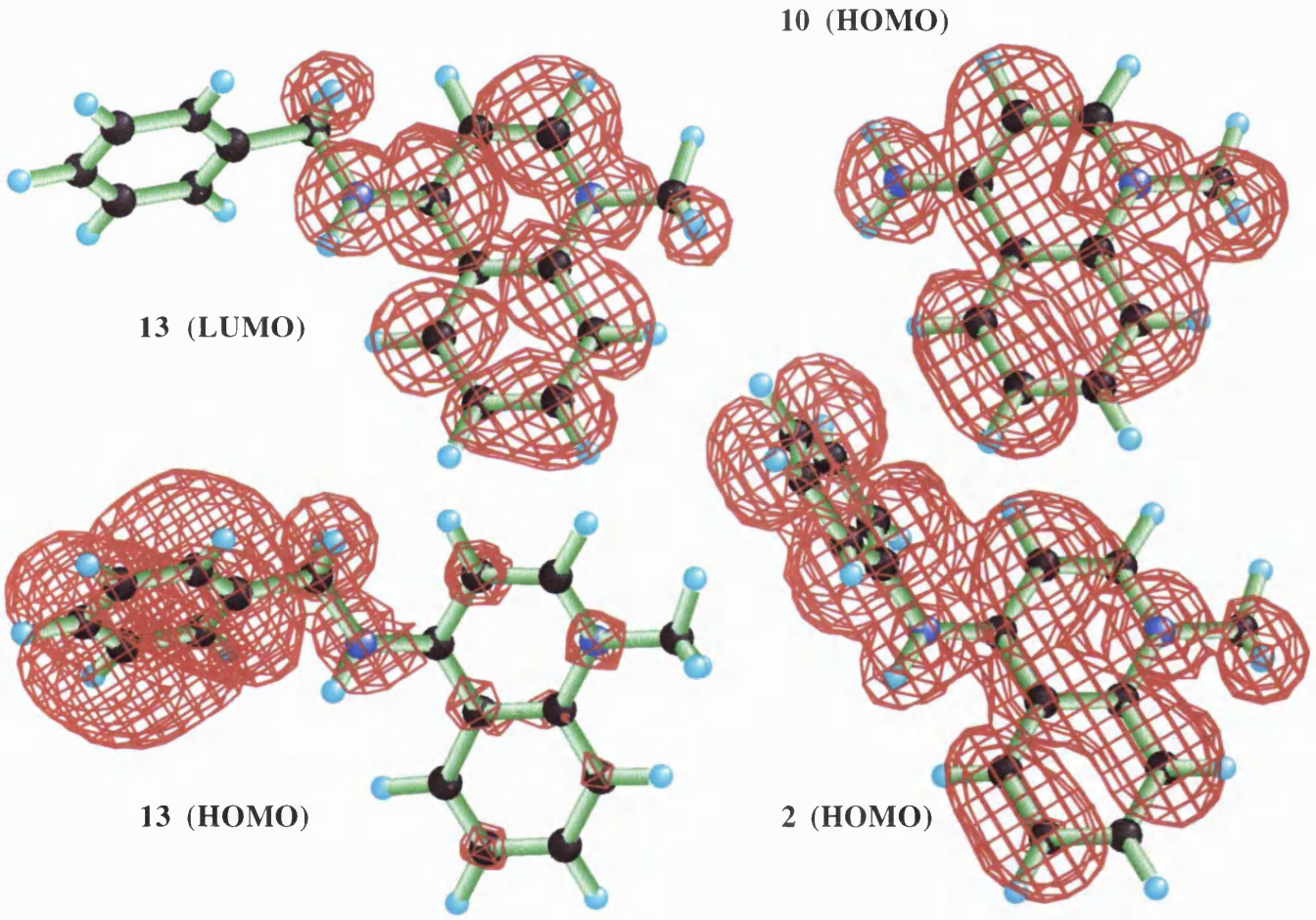

Figure 4.8a MO contour plots for representative model compounds of **Table 4.4**. LUMO contours of all analogues of **Table 4.4** are similar to **13** shown. The different contributions to the HOMO in different molecules is exemplified using **2**, **10** and **13**. The molecules were minimised with AM1. Atoms are coloured black (carbon), blue (nitrogen) and cyan (hydrogen). Contours were drawn in Sybyl 6.03 at the PSI^2 mode, at the 0.0009 electron/$Å^3$ level.

4.2 EXPLORATION OF THE "INVERSE" SERIES

A second series (**series II**) of dequalinium analogues has been synthesised which includes compounds **25** - **28** and **40** made by Dr C.A. Davis, **29** made by Mr C. Owen and **30** made by Dr B. Del Rey Herrero (**Tables 4.6** and **4.12**) which were complemented with compounds **15** - **24** (**Table 4.6**) and **36** - **39** (**Table 4.12**). The compounds of **series II** can be represented by the general formula I.

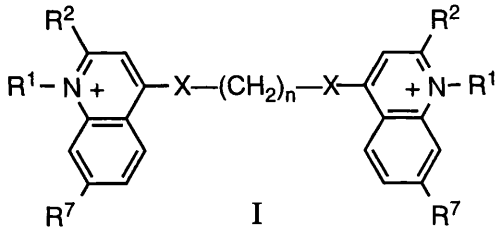

I

A number of issues were examined in this series. At first, the group $\mathbf{R^1}$ attached to the ring nitrogen of the quinoline was varied to see if there is a dependence of activity on the properies of this group. The other three variable groups of the general structure I were kept constant, being an NH for **X**, H for $\mathbf{R^7}$ and Me for $\mathbf{R^2}$. The size and lipophilicity of $\mathbf{R^1}$ was increased going from a H (**15**) to a benzyl (**18**) to a diphenylpropyl (**16**) group. In addition, two MeO groups were introduced into the benzyl group of **18** to give compound **17**, in an attempt to simulate the MeO groups present in atracurium and tubocurarine. Compound **18** is the most potent of this series, but it is doubtful whether the relatively small increase in potency observed on going from compound **15** to **18** should be attributed to the increased lipophilicity or dispersion interactions due to the CH_2Ph group. In general, the maximum difference in potency between these four compounds is an order of magnitude, the least potent being **16** probably due to the size of the diphenylpropyl group. It is evident, however, that there is considerable steric tolerance in the direction of substituent $\mathbf{R^1}$.

Furthermore, by comparing compound pairs **37** - **38** (**Table 4.12**), **17** - **19** and **18** - **21** (**Table 4.6**) one can see that non - symmetrical analogues are either equiactive or a little less potent than their symmetrical counterparts.

Table 4.6 Structure and biological results for the compounds of **series II.**

Compd No	UCL No	Notebook No	Structure	EMR(±SD)
15	1417	DG-13C	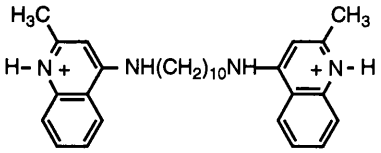	3.6 ± 1.2
16	1436	DG-81D	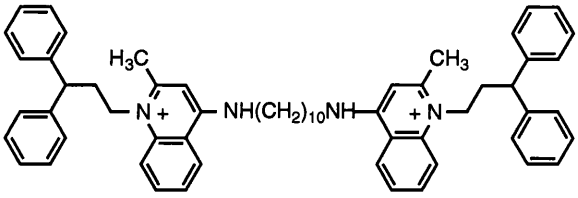	6.2 ± 3.2
17	1438	DG-115C	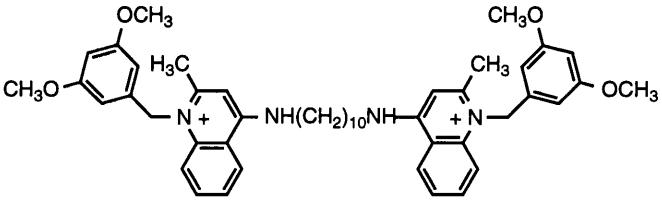	2.1 ± 0.9
18	1439	DG-127C	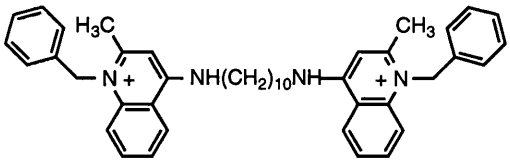	0.6 ± 0.3
19	1440	DG-115B	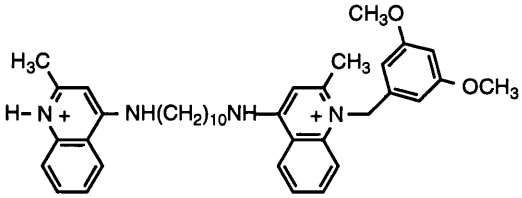	1.2 ± 0.8
20	1445	DG-167A	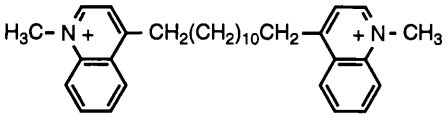	5.9 ± 3.9
21	1454	DG-127B	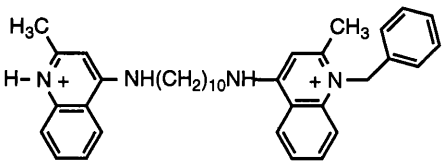	2.4 ± 0.5
22	1467	DG-223A	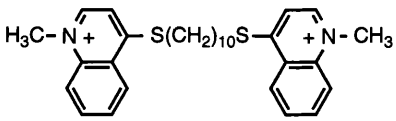	6.2 ± 1.7
23	1601	DG-219B	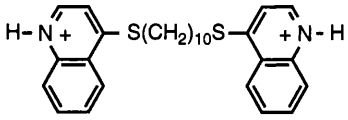	>10

Table 4.6 (continued)

Compd No	UCL No	Notebook No	Structure	EMR(±SD)
24	1602	DG-159B	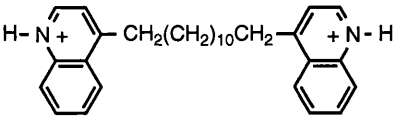	>>10
25	1091	SB-10A	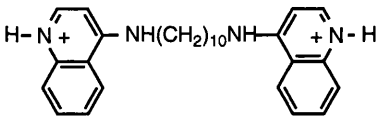	3.5 ± 1.2
26	1118	CD-40	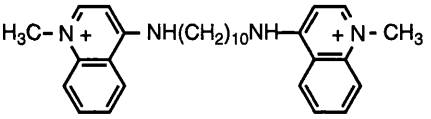	1.9 ± 1.0
27	1144	CD-59	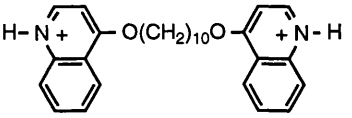	16 ± 21
28	1156	CD-62	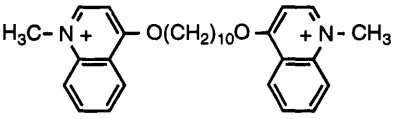	7.2 ± 3.4
29	1360	CO-141A	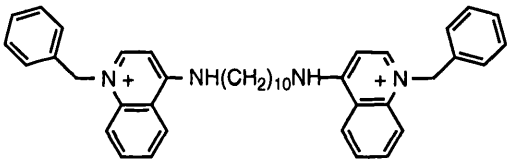	1.0 ± 0.4
30	1449	BR-67C	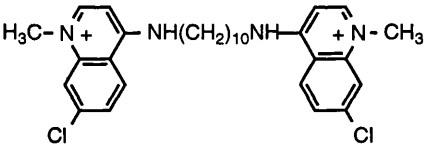	1.5 ± 0.6

Another important structural feature in this series of analogues is heteroatom **X** and its role was examined by synthesising compounds where **X** = CH_2 (**20**) or S (**22**) complementing compounds where **X** = NH (**26**) or O (**28**) previously synthesised in our laboratory. As can be seen from **Table 4.6**, the most potent is compound **26** while the other three have similar activities to each other.

Series II permitted the investigation of a crucial issue and that is whether the quinolines have to be charged for the compounds to be effective blockers of the SK_{Ca} channel. **Series I** did not allow this examination since the ring nitrogen of the quinoline is alkylated and, therefore, the heterocycle is necessarily charged. However, in **series II** the ring nitrogen can be left non - alkylated and by varying hetroatom **X**, the basicity of the quinoline and, hence, the degree of protonation at physiological pH can be altered. For this purpose, compounds **23** (**X** = S) and **24** (**X** = CH_2) were synthesised which relate to compounds **25** (**X** = NH) and **27** (**X** = O) previously made by Dr C.A. Davis. Compound **25** had an EMR of 3.5, **27** had EMR = 16, **23** showed some inhibition at 10 μM but insufficient to obtain a reliable EMR and **24** showed no inhibition at 10 μM. The blocking potencies of these four analogues parallel the pKa of simple model compounds (obtained from ref. 212):

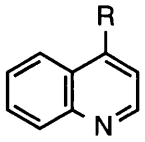

R	pKa
NH_2	9.2
CH_3O	6.5
CH_3S	5.9
CH_3	5.7

Figure 4.9 pKa values for model compounds

It therefore seems that a charged quinoline is a critical feature for SK_{Ca} channel blockade.

The compounds of **series II** have also been subjected to AM1 MO calculations using the same approximations that applied to **series I** and the results are shown in **Table 4.7**. The correlation equations can be found in **Table 4.8**. As in **series I**, in **series II** there is no correlation of pEMR with C_4 charge (eq. **R-8**). Furthermore, and in

contrast to **series I**, there appears to be no correlation with N_1 charge as well (eq. **R-9**, **Figure 4.10**). Compounds **15**, **25** and **27** form a separate group on the plot and these are the non - quaternary compounds. However, the exclusion of these from the plot, does not give a good correlation.

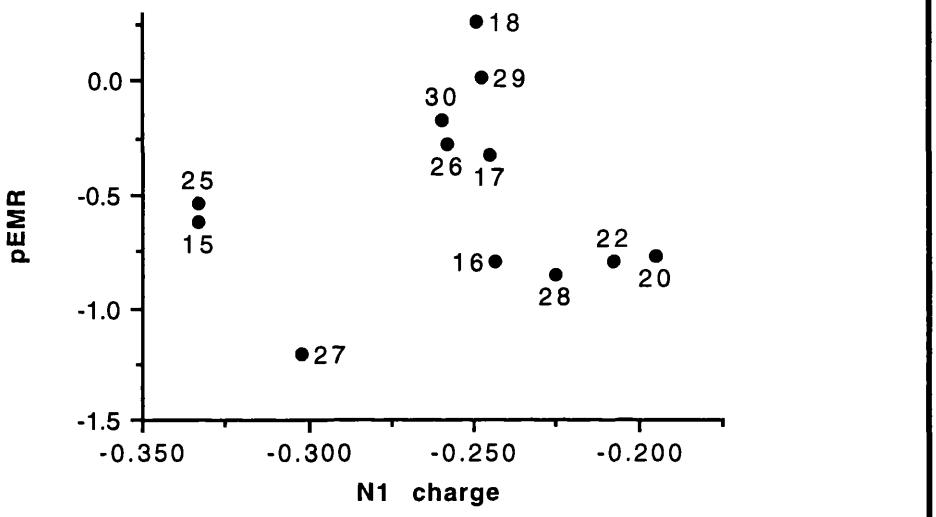

Figure 4.10 Plot of pEMR vs N_1 charge for the compounds of eq. **R-9**

For the frontier orbital energies the correlation equations with E_{LUMO} and E_{HOMO} are **R-10** and **R-11** respectively (**Table 4.8**). The respective plots are **Figures 4.11** and **4.12** respectively.

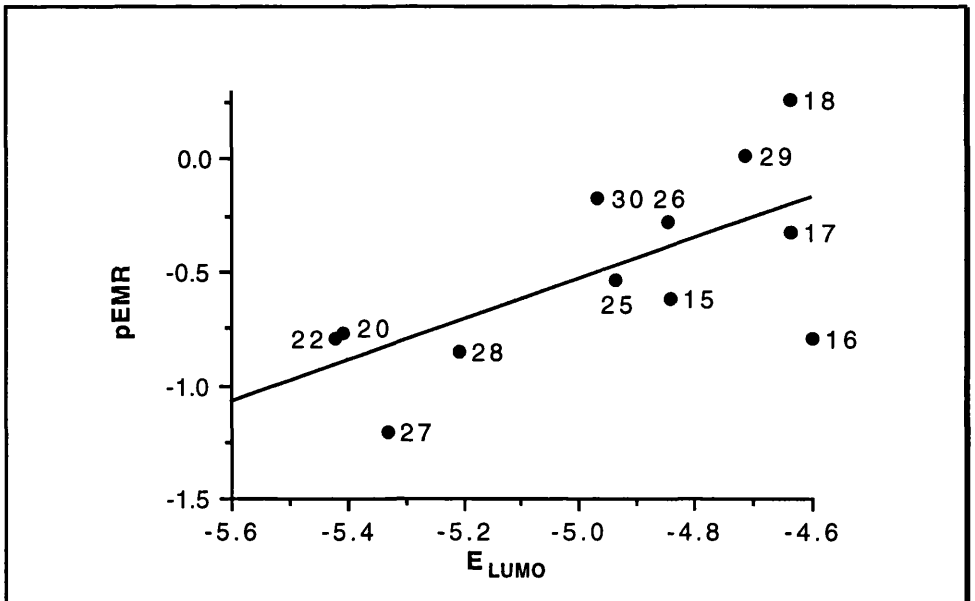

Figure 4.11 Plot of pEMR vs E_{LUMO} for the compounds of eq. **R-10**

Table 4.7 Partial charges and frontier orbital energies for the model compounds of **series II**.

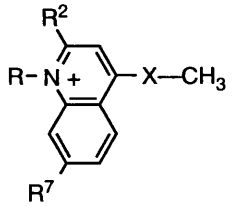

Compd No[1]	UCL No[1]	Notebook No[1]	X	R	R^2	R^7	C_4 charge	N_1 charge	E_{HOMO}*	E_{LUMO}*	EMR (±SD)[1]
15	1417	DG-13C	NH	H	CH_3	H	0.266	-0.333	-12.74	-4.840	3.6 ± 1.2
16	1436	DG-81D	NH	$(CH_2)_2CHPh_2$	CH_3	H	0.260	-0.244	-11.43	-4.600	6.2 ± 3.2
17	1438	DG-115C	NH	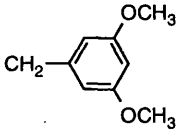	CH_3	H	0.260	-0.245	-11.43	-4.637	2.1 ± 0.9
18	1439	DG-127C	NH	CH_2Ph	CH_3	H	0.261	-0.249	-12.29	-4.638	0.6 ± 0.3
20	1445	DG-167A	CH_2	CH_3	H	H	0.087	-0.195	-13.36	-5.406	5.9 ± 3.9
22	1467	DG-223A	S	CH_3	H	H	-0.121	-0.208	-12.84	-5.424	6.2 ± 1.7
23	1601	DG-219B	S	H	H	H	-0.116	-0.286	-12.99	-5.551	>10
24	1602	DG-159B	CH_2	H	H	H	0.096	-0.271	-13.50	-5.543	>>10
25	1091	SB-10A	NH	H	H	H	0.271	-0.333	-12.82	-4.940	3.5 ± 1.2
26	1118	CD-40	NH	CH_3	H	H	0.268	-0.258	-12.64	-4.846	1.9 ± 1.0
27	1144	CD-59	O	H	H	H	0.265	-0.302	-13.31	-5.329	16 ± 21
28	1156	CD-62	O	CH_3	H	H	0.257	-0.225	-13.15	-5.207	7.2 ± 3.4
29	1360	CO-141A	NH	CH_2Ph	H	H	0.260	-0.248	-12.37	-4.716	1.0 ± 0.4
30	1449	BR-67C	NH	CH_3	H	Cl	0.270	-0.260	-12.76	-4.968	1.5 ± 0.6

* in eV.

1. The compound No, UCL No, notebook No and EMR of the corresponding bis - quinolinium compound of **Table 4.2** are used for simplicity.

Table 4.8 Correlation equations for the model compounds of **series II** using data from **Table 4.7**.

Equation No	Equation	n	r	s	Excludes	Reason for exclusion
R-8	pEMR = 1.03 (± 1.04) **C_4** charge -0.73 (± 0.26)	12	0.30	0.408	none	
R-9	pEMR = 0.19 (± 2.93) **N_1** charge -0.46 (± 0.77)	12	0.02	0.428	none	
R-10	pEMR = 0.89 (± 0.31) **E_{LUMO}** + 3.93 (± 1.55)	12	0.67	0.316	none	
R-11	pEMR = 0.26 (± 0.19) **E_{HOMO}** + 2.71 (± 2.35)	12	0.40	0.392	none	
R-12	pEMR = 1.16 (± 0.26) **E_{LUMO}** + 5.33 (± 1.29)	11	0.83	0.243	**16**	too bulky
R-13	pEMR = 1.10 (± 0.18) **E_{HOMO}** + 13.56 (± 2.35)	10	0.90	0.198	**16** **17**	too bulky ?
R-14	pEMR = 1.30 (± 0.27) **E_{LUMO}** + 6.05 (± 1.37)	10	0.86	0.235	**16** **17**	too bulky ?

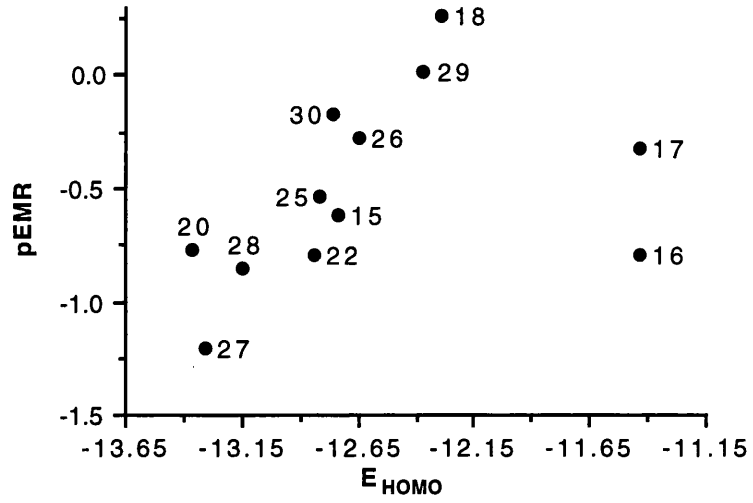

Figure 4.12 Plot of pEMR vs E_{HOMO} for the compounds of eq. **R-11**

With respect to the E_{LUMO} correlation, there appears to be a major outlier and this is compound **16**. This compound is much less active than predicted by the equation; the ring nitrogen of the quinoline has been alkylated with the very large diphenylpropyl group, hence, it is possible that this group interferes sterically in the interaction of the compound with the channel. On this basis, **16** can be excluded from the correlation which then becomes **R-12** (**Figure 4.13**).

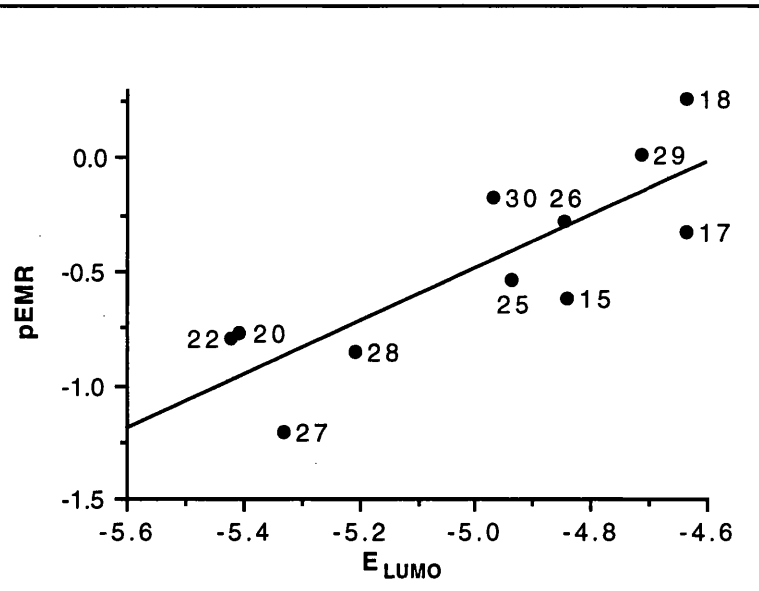

Figure 4.13 Plot of pEMR vs E_{LUMO} for the compounds of eq. **R-12**

Clearly, compounds **16** and **17** are outliers in the E_{HOMO} correlation and these are two of the compounds in which the HOMO is a different orbital not localised on the quinolinium ring (**Figure 4.16a**). If these are excluded from the correlation this becomes **R-13** (**Figure 4.14**). For comparison, the E_{LUMO} correlation becomes **R-14** if compounds **16** and **17** are excluded.

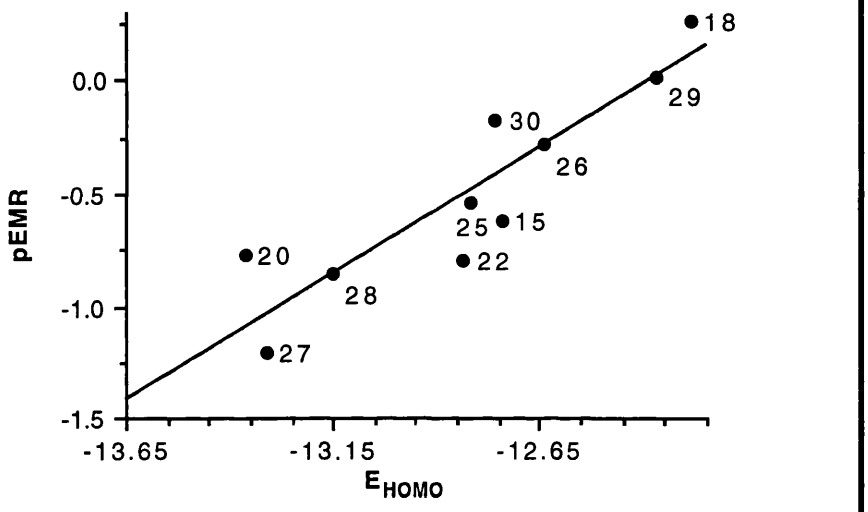

Figure 4.14 Plot of pEMR vs E_{HOMO} for the compounds of eq. **R-13**

By way of conclusion, in **series II** there is no correlation of pEMR with partial charges on atoms of the quinolinium ring. The E_{LUMO} correlation is less good than in **series I** and the E_{HOMO} correlation is better if compounds **16** and **17** are excluded. However, the E_{HOMO} correlation is still qualitatively inconsistent since the energies do not refer to the same orbital in all compounds.

An interesting aspect of the correlation studies is the fact that the E_{LUMO} and E_{HOMO} correlations for **series I** and **II** can be combined to give correlations of pEMR with either E_{LUMO} or E_{HOMO} which include the compounds of **Tables 4.4** and **4.7** in the same equation. These are shown in **Table 4.9**. Thus, equations **R-3** and **R-12** can be combined to eq. **R-19** (**Figure 4.15**). The respective E_{HOMO} correlation **R-20** is worse and this is due to the fact that compound **17** is a major outlier. If this is excluded, both correlations improve (**R-21** and **R-22**), with the E_{HOMO} correlation improving dramatically. It should be noted, however, that at this stage there is no well justified

reason for not including **17** in the correlations. The plot for eq. **R-22** is shown in **Figure 4.16**.

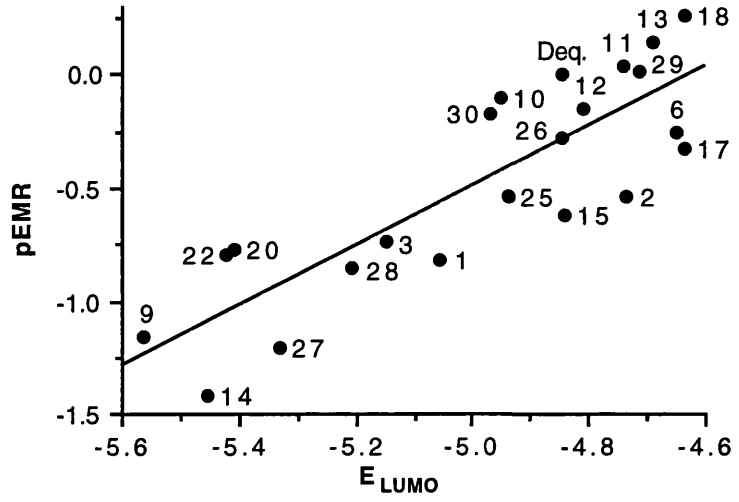

Figure 4.15 Plot of pEMR vs E_{LUMO} for the compounds of eq. **R-19**

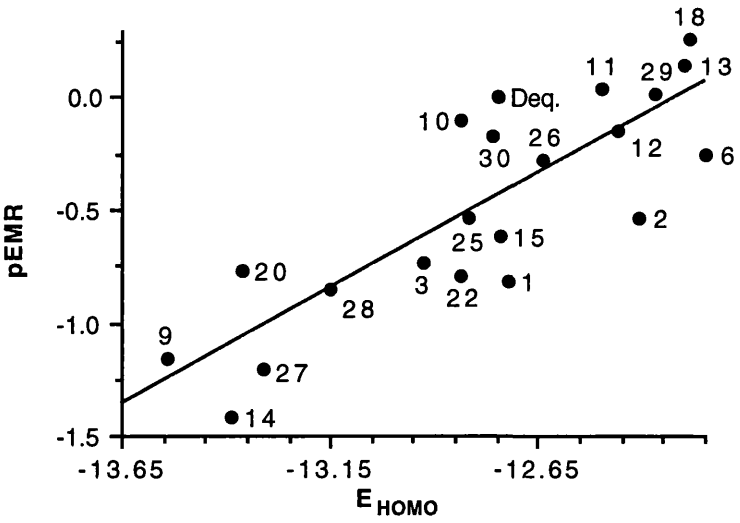

Figure 4.16 Plot of pEMR vs E_{HOMO} for the compounds of eq. **R-22**

Finally, if the two new analogues **4** and **5** are included in the correlations, equations **R-17** and **R-18** result. The plot for **R-17** is shown in **Figure 4.17**.

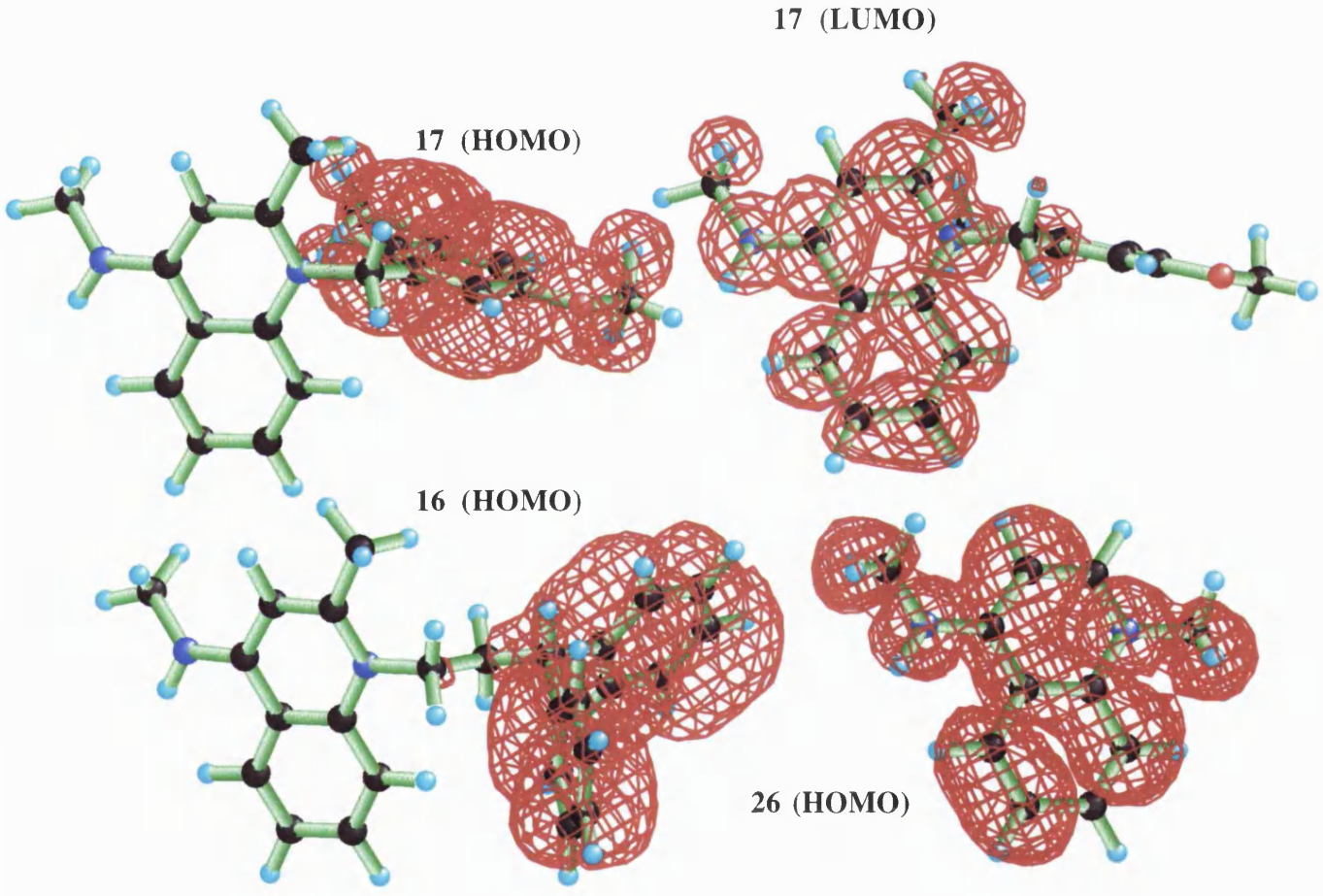

Figure 4.16a MO contour plots for representative model compounds of **Table 4.7**. LUMO contours of all analogues of **Table 4.7** are similar to **17** shown. The different contributions to the HOMO in different molecules is exemplified using **16**, **17** and **26**. The molecules were minimised with AM1. Atoms are coloured black (carbon), blue (nitrogen), red (oxygen) and cyan (hydrogen). Contours were drawn in Sybyl 6.03 at the PSI^2 mode, at the 0.0009 electron/$Å^3$ level.

Table 4.9 Correlation equations for the model compounds of **series I** and **II** using data from **Tables 4.4** and **4.7**.

Equation No	Equation	n	r	s	Excludes	Reason for exclusion
R-15	pEMR = 1.08 (± 0.17) $\mathbf{E_{LUMO}}$ + 4.87 (± 0.86)	25	0.79	0.287	none	
R-16	pEMR = 0.46 (± 0.13) $\mathbf{E_{HOMO}}$ + 5.31 (± 1.69)	25	0.58	0.381	none	
R-17	pEMR = 1.17 (± 0.15) $\mathbf{E_{LUMO}}$ + 5.33 (± 0.76)	24	0.85	0.249	**16**	too bulky
R-18	pEMR = 0.61 (± 0.13) $\mathbf{E_{HOMO}}$ + 7.34 (± 1.60)	24	0.72	0.328	**16**	too bulky
R-19	pEMR = 1.33 (± 0.18) $\mathbf{E_{LUMO}}$ + 6.17 (± 0.90)	22	0.86	0.244	**16** **4, 5**	too bulky not synthesised then
R-20	pEMR = 0.69 (± 0.15) $\mathbf{E_{HOMO}}$ + 8.25 (± 1.96)	22	0.71	0.336	**16** **4, 5**	too bulky not synthesised then
R-21	pEMR = 1.40 (± 0.18) $\mathbf{E_{LUMO}}$ + 6.51 (± 0.91)	21	0.87	0.239	**16** **4, 5** **17**	too bulky not synthesised then ?
R-22	pEMR = 1.02 (± 0.15) $\mathbf{E_{HOMO}}$ + 12.53 (± 1.97)	21	0.84	0.266	**16** **4, 5** **17**	too bulky not synthesised then ?

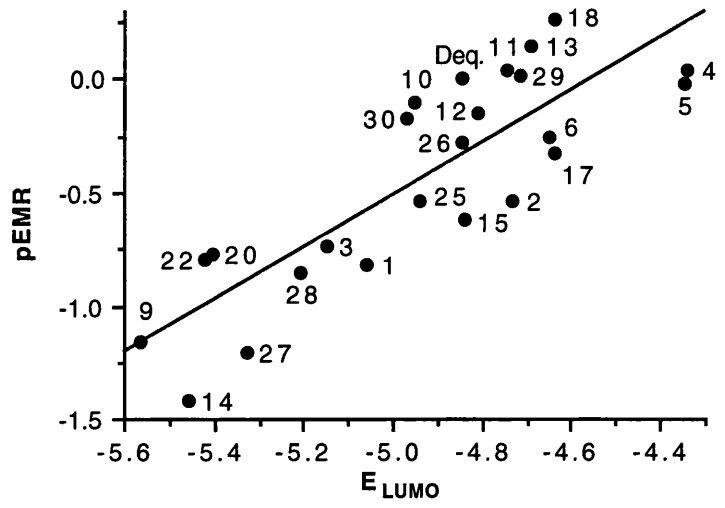

Figure 4.17 Plot of pEMR vs E_{LUMO} for the compounds of eq. **R-17**

In conclusion, there is a good correlation of pEMR with N_1 charge in **series I**, the more negative the charge on the nitrogen the more potent the compound. This correlation seems to have good predictive power as indicated from the cases of compounds **4** and **5**. In the same series, pEMR correlates well with E_{LUMO} although the activities of **4** and **5** are not very well predicted using this correlation. Furthermore, pEMR correlates less well with E_{HOMO} and there is the additional ambiguity of the HOMO being a different orbital in some compounds, which introduces questions with respect to the consistency of the correlation.

On the other hand, there is no correlation between pEMR and N_1 charge in **series II**. pEMR correlates with E_{LUMO} when the bulky analogue **16** is excluded but the correlation is less good than in the previous series. A good correlation with E_{HOMO} (better than with E_{LUMO}) is obtained when compounds **16** and **17** are excluded but there is no justification for excluding **17**. Moreover, the HOMO is again a different orbital in some of the molecules rendering again the correlation qualitatively inconsistent.

Interestingly, the compounds of both series can be included in the same correlation either with E_{LUMO} or E_{HOMO}. Because of the uncertainties associated with the use of E_{HOMO}, and because of the absence of any correlation with partial charges in **series II**,

E_{LUMO} can be considered as the best electronic parameter (amongst those tried) that accounts for changes in the blocking potency of the compounds. More validity to the E_{LUMO} correlation is credited by its qualitative consistency and by the fact that it operates in two series of analogues which have substantial structural differences.

At this point, it is appropriate to comment on the physical meaning of the correlations with frontier MO energies. The E_{HOMO} correlation suggests that the higher the energy of the HOMO the more potent the compound. If the contribution of the HOMO is assumed to be at the level of the interaction of the compound with the channel, then some kind of charge transfer interaction with the latter is implied in which the compound has the role of the electron *donor*. This is in disagreement with fundamental chemical concepts since it is hard to see how these compounds could act as electron *donors* because they are electron *defficient*. The absence of an obvious physical meaning combined with the inconsistencies mentioned in the preceding paragraphs diminish the value of the E_{HOMO} correlation.

With respect to the E_{LUMO} correlation, it suggests that the higher the energy of the LUMO the more potent the compound. If, again, the contribution of the LUMO is assumed to be at the level of the interaction of the compound with the channel, then a charge transfer interaction with the latter is implied in which the compound has the role of the electron *acceptor*. For efficient stabilisation energy to result from the charge - transfer interaction the geometry of the HOMO and of the LUMO must exhibit complementarity features.[233] If this requirement is satisfied then the stability of the electron donor - acceptor complex depends on the E_{LUMO} - E_{HOMO} difference. The smaller the energy gap the stronger the interaction.[234] It is presumed that the compounds act at the same site and therefore interact with the same HOMO. The energy of the latter must be lower than the energy of the LUMO since the opposite would result in complete electron transfer from the HOMO to the LUMO and the compound would be reduced.[235] Hence, the E_{LUMO} - E_{HOMO} gap would be modified by the E_{LUMO} of the compound since E_{HOMO} is constant. This in turn means that lower E_{LUMO} values would lead to smaller E_{LUMO} - E_{HOMO} gap and to a stronger interaction. This is in contrast to the experimental observations suggesting a stronger interaction for compounds with higher E_{LUMO}. As a result, this

particular mode of interaction seems unlikely. To the best of our knowledge, this is the first example of activity increasing with higher E_{LUMO} values. A literature survey on the use of E_{LUMO} as an electronic index in QSAR reveals that it has been employed in the case of mutagenic compounds,[236-239] toxins[234] as well as opiates,[240] anti-inflammatory agents,[241,242] neuroleptics,[243] antibacterials,[244,245] cardiotoxic compounds,[246] antitumor agents,[247] antifungals,[248] anxiolytics,[249] radiosensitizing compounds[250] and psychotomimetics.[251] However, in all these cases, potency is accosiated with a low lying LUMO and the explanation given has always been charge - transfer from the receptor to the compound.

From the above it seems that the LUMO correlation does not imply an electron donor - acceptor (EDA) interaction of the channel with the compounds. An explanation on the physical meaning of the above mentioned correlation may be provided by the principle of maximum hardness initially suggested by Pearson[252,253] and proved by Parr using statistical mechanics and density functional theory.[254] Very briefly, the hardness of a chemical system (a chemical system being an atom, an ion, a radical, a molecule or several molecules, in a state of interaction[253]) can be defined as half the energy gap between the LUMO and the HOMO. The larger the gap, the harder the system and the more stable it is. There appears to be a general trend in nature for chemical systems to adjust themselves so as to maximize the HOMO - LUMO gap and therefore minimize their energy and become more stable.[252-254]

For the application of this principle to the interaction of the quinolinium compounds with the channel it will be assumed that the former bind to an anionic site. This assumption is reasonable since it has been shown above that the positive charge on the quinoline rings is an essential feature for blocking activity and since all K^+ channel subtypes that have been cloned so far have negatively charged amino acids in the sequence of the putative pore - forming region of the protein.[38,39,99,11] The role of these negatively charged amino acids is to facilitate energetically the conduction of the positively charged K^+ ions. The alteration of the frontier orbital energies in the formation of an ion pair is shown in **Figure 4.18.**[253] As the cation (compound) approaches the anion (binding site) the potential of the anion raises the E_{LUMO} and the potential of the cation lowers the

E_{HOMO}. Since in the quinolinium compounds the E_{LUMO} is progressively increased, the E_{LUMO} - E_{HOMO} gap of the ion pair (drug - K^+ channel complex) is also increased and the latter becomes more stable. If this hypothesis is correct, then the correlation of pEMR with E_{LUMO} consists, to the best of our knowledge, the first application of the principle of maximum hardness to structure - activity ralationships in the field of pharmacology.

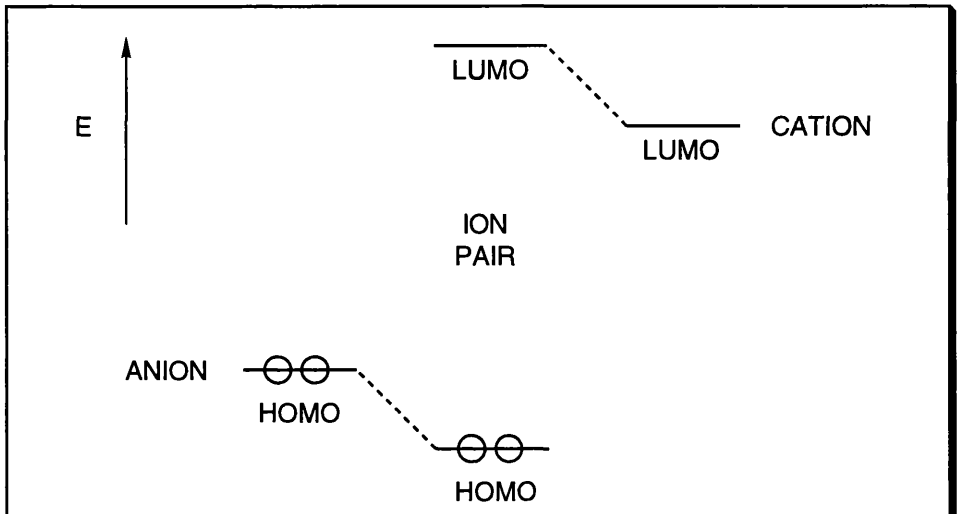

Figure 4.18 A hypothesis on the physical meaning of the correlation of pEMR with E_{LUMO}

So far, the contribution of the LUMO to the SK_{Ca} channel blocking activity of the compounds has been assumed to be at the level of the drug - K^+ channel interaction. Nevertheless, the possibility of the LUMO being involved at a level other than the compound - K^+ channel complex has to be considered. In this case, the LUMO correlation may be implying that an EDA interaction takes place at a site which is remote from the channel and that this interaction reduces the efficiency of the K^+ channel blockade either by reducing the available concentration of the compound or by increasing the free energy change of the binding process. The free energy (ΔG) change of the drug (**D**) - K^+ channel (**K**) complex formation is given by **eq. R-23**:

$$\Delta G = \Delta G_{DK} - (\Delta G_D + \Delta G_K) \qquad \textbf{R-23}$$

where: ΔG_{DK} is the energy of the drug - K^+ channel complex,

ΔG_D is the energy of the uncomplexed drug and

ΔG_K is the energy of the free channel.

For the drug - ion channel interaction to take place, the drug molecule would have to desolvate (wholly or partly) and the same possibly applies to the binding site as well. Therefore, ΔG_D includes the solvation energy of the molecule which is adverse to the binding process because the better the solvation of the drug, the more negative is ΔG_D and ΔG becomes more positive. EDA forces contribute substantially to solvent solute interactions[255,256] and if it is assumed that in the case of the quinolinium compounds the latter act as electron acceptors with the solvent (H_2O) molecules acting as electron donors, then increasing the E_{LUMO} of the molecule would result in its weaker solvation, ΔG_D would become more positive with ΔG getting more negative and thus the interaction with the channel would become stronger.

Bearing this in mind, the solvation free energies ΔG_{sol} for model compounds of **Table 4.4** have been calculated using the solvation model of W.C. Still et al[257] as implemented in MacroModel.[258] This is a continuum model which has been shown to give results comparable to those determined experimentally as well as theoretically using computationally demanding free energy perturbation methods.[257,259] For the model to perform well, good quality partial charges have to be used[257] and in the case of the quinolinium compounds Mulliken charges obtained from AM1[232] calculations have been used. For comparative purposes, ΔG_{sol} have been calculated using the MM2[260] (**Table 4.10**) or the AMBER[261] (**Table 4.11**) forcefield, as implemented in MacroModel.

It is evident from **Tables 4.10** and **4.11** that there is no correlation between the blocking potency of the compounds and their ΔG_{sol}. This may be due to a number of reasons. First of all, the ΔG_{sol} calculated refer to the *whole* molecule, while in the interaction of the compound with the channel only part of it may have to desolvate. On the other hand, this treatment of solvation does not take into account EDA interactions.[257] Hence, if indeed there is a contribution of EDA forces to ΔG_{sol} the model would not be appropriate to use.

Furthermore, it has been attempted to correlate the activity of the compounds with the difference $\Delta H_w - \Delta H_v$ where the former is the enthalpy of the molecule (after energy minimization) in water (using the solvation model) and the latter is the enthalpy in the gas phase. As can be seen from **Tables 4.10** and **4.11** this was not successful.

Table 4.10 Free energy of solvation (in KJ/mol) for model compounds of **Table 4.4**, calculated using Macromodel and the MM2 forcefield.

Compd No	UCL No	Notebook No	EMR(±SD)	ΔG_{sol}	ΔH_v	ΔH_w	ΔH_w-ΔH_v
1	1463	DG-155A	6.5 ± 1.9	-194.5	125.7	31.3	-94.3
2	1491	DG-367B	3.4 ± 1.8	-195.6	99.3	-66.0	-165.3
3	1504	DG-459A	5.5 ± 1.0	-207.7	-23.59	-359.5	-335.9
8	Deq.	—	1 ± 0.05	-198.2	-14.0	-317.1	-303.1
9	1072	CD-9A	15 ± 7.9	-215.7	113.6	47.2	-66.4
10	1127	CD-45	1.3 ± 0.5	-215.4	49.37	-145.7	-195.0
11	1130	CD-43B	0.9 ± 0.7	-184.6	138.2	253.0	114.8
12	1173	CD-74	1.4 ± 0.6	-187.3	134.9	76.47	-58.4
13	1359	CO-199B	0.7 ± 0.3	-195.0	117.8	-9.5	-127.3
14	1431	BR-19A	26 ± 14	-203.7	71.8	-56.5	-128.4

Table 4.11 Free energy of solvation (in KJ/mol) for model compounds of **Table 4.4**, calculated using Macromodel and the AMBER forcefield.

Compd No	UCL No	Notebook No	EMR(±SD)	ΔG_{sol}	ΔH_v	ΔH_w	ΔH_w-ΔH_v
1	1463	DG-155A	6.5 ± 1.9	-197.5	97.8	-6.9	-104.7
2	1491	DG-367B	3.4 ± 1.8	-198.5	118.9	5.9	-113.0
3	1504	DG-459A	5.5 ± 1.0	-207.7	72.1	-92.6	-164.7
8	Deq.	—	1 ± 0.05	-197.2	48.7	-115.3	-163.9
9	1072	CD-9A	15 ± 7.9	-214.7	91.9	-16.6	-108.5
10	1127	CD-45	1.3 ± 0.5	-215.1	72.2	-76.2	-148.4
11	1130	CD-43B	0.9 ± 0.7	-184.7	138.2	-34.0	-172.1
12	1173	CD-74	1.4 ± 0.6	-188.4	98.5	-12.7	-111.2
13	1359	CO-	0.7 ± 0.3	-198.1	89.9	-42.4	-132.3
14	1431	BR-19A	26 ± 14	-203.6	81.55	-36.34	-117.9

4.3 ALTERATIONS IN THE LINKING CHAIN

To increase rigidity of the linking aliphatic chain of the aminopyridine compound **53** (**Table 1**, see section **4.5** for discussion of this analogue) in order to force the charged rings to occupy more strictly defined positions in space relative to each other, triple bonds were introduced (**44, Table 4.12**) and this resulted in a 6 - fold increase in potency.[209] Motivated by this finding, the chain of dequalinium was analogously constrained by making **31** (**Table 4.12**). However, this did not provide the expected increase in activity, but rather a small decrease.

To investigate an alternative position for the aliphatic chain in joining the two quinoline rings some representative compounds were made. Moving the linking point of **9** (**Table 1**) from position 1 to position 2 (**42, Table 4.12**) resulted in loss of potency possibly due to changes in conformation. Introduction of a methoxy group at position 4 of the quinoline rings of **42** improved activity by a factor of 5 (**41, Table 4.12**), possibly due to increased delocalisation of the charge. Adding two more methylene groups to the ten methylene chain of **42** also produced a similar increase in potency (**43, Table 4.12**).

A structural feature in the molecule of dequalinium that merits investigation is the length of the alkyl chain. It was mentioned above that rigidification of this did not alter potency significantly. To gain more understanding into the role of the alkyl chain, a systematic investigation of its length was undertaken and analogues **32 - 35** (**Table 4.12**) of compound **10** (**Table 1**) were synthesised (direct analogues of dequalinium were avoided because of the synthetic difficulties presented by the methyl at position 2 of the quinoline). Surprisingly, varying the number of methylene groups in the aliphatic chain from 5 to 12 hardly had any effect on potency. This is a very important finding which may have important implications for the mode of action of dequalinium and analogues (for a discussion see section **4.4** on the need for the two quinolinium groups and their role). Furthermore, the apparent independence of potency on the length of the linking chain seriously questions the validity of the pharmacophore which has been proposed for the SK_{Ca} channel blockers, in which two positively charged groups are envisaged as being separated by a distance of ~10 Å.[188]

Table 4.12 Structure and biological results for the compounds of **series III.**

Compd No	UCL No	Notebook No	Structure	EMR (±SD)
31	1437	DG-109A	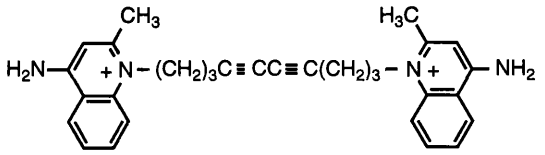	2.4 ± 0.9
32	1635	SM-114B	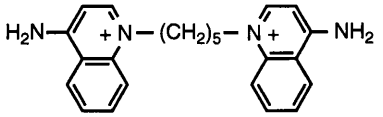	1.0 ± 0.2
33	1636	SM-109A	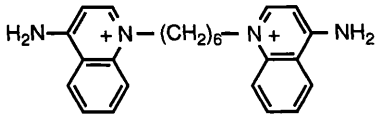	~1
34	1637	SM-104A	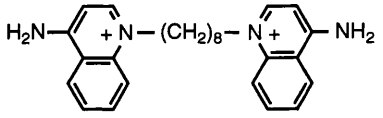	~1
35	1638	SM-106A	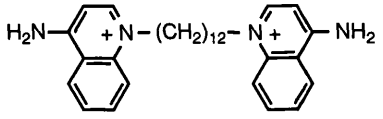	1.8 ± 0.5
36	1407	DG-23B	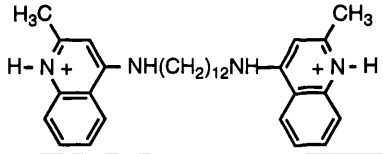	7.1 ± 2.8
37	1426	DG-33C	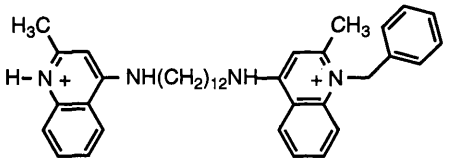	8.0 ± 5.9
38	1427	DG-33D	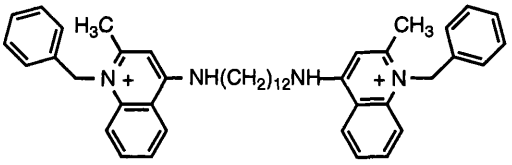	4.0 ± 2.0
39	1450	DG-199A	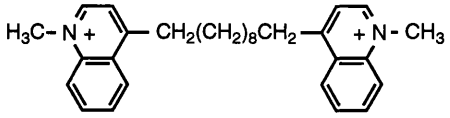	26 ± 9.8
40	1172	CD-71	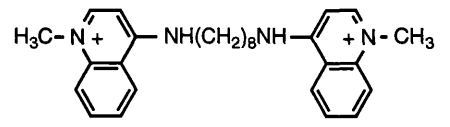	3.1 ± 1.4
41	1455	DG-183B	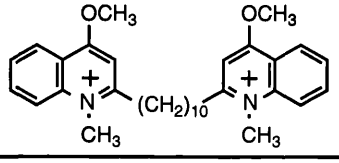	27 ± 9.2

Table 4.12 (continued)

Compd No	UCL No	Notebook No	Structure	EMR (±SD)
42	1460	DG-207D	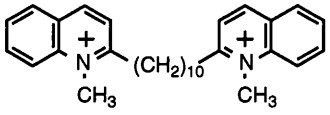	130 ± 34
43	1480	DG-287B	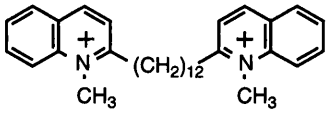	33 ± 10
44	1129	CD-42		4.7 ± 1.6

A question that arises from the "inversion" of the quinolinium rings of compounds belonging to **series I** to effect the transition to **series II** is the number of methylene groups that should be used in the aliphatic chain of compounds belonging to the latter. In **series I** the quinolines were separated by 10 methylene groups. Using 10 methylene groups in **series II** means that the quinolines are separated by (10 CH_2 + 2 **X**) groups. It is also evident that the quaternary ring nitrogens are held further apart in **series II** if the extended conformations of compounds are compared. Although we have not carried out a systematic investigation on the chain length in **series II** (as in **series I** the length of the alkyl chain was found to be unimportant) we have extended the number of CH_2 groups to 12 in two cases (cf. compound pairs **36** - **15** and **38** - **18**) and shortened it to 8 in another two compounds (**20** - **39** and **26** - **40**). Both the shortening and lengthening of the chain resulted in drop in potency, although the dependence does not seem to be too critical. One possible explanation for this is that the chain is long and flexible enough to adopt the right conformation at the receptor and also that in the quinolinium and especially in the aminoquinolinium cation there exists extensive delocalisation of the positive charge (as depicted partially in **Figure 4.1**) which further reduces distance demands of the system.

4.4 THE NEED FOR TWO QUINOLINIUM GROUPS AND THEIR ROLE

The pharmacophore of SK_{Ca} channel blockers, as this has been depicted in the literature, contains two charged groups (let these be the guanidinium groups of the Args of apamin, the alkylammonium groups of the neuromuscular blockers or the quinolinium groups of dequalinium) at a distance of ~10 Å. However, the need for two charged groups has not been firmly established. In view of this, it seemed important to address the questions of the need for two quinolinium groups and of their role. The answer to the first question would establish whether our structural analogues should have one or two quinolinium groups and the answer(s) to the second should reveal the explanation for the importance of the charge being carried by a quinolinium rather than an alkylammonium group and should also guide our thinking in designing more potent blockers of the SK_{Ca} channel.

In work conducted earlier in our laboratory[209] the issue of the need for two quinolinium groups was addressed by removing one such group from the molecule of dequalinium to provide compound **45** (**Table 4.13**). Although the drop in activity that results from this change appears rather small to account for the loss of a binding site, the biological test result for **45** does not reflect pure SK_{Ca} channel blocking activity, for at least two reasons. Firstly, **45** slowed the rising phase of the action potential of the neurone and this in itself would reduce the AHP by lowering Ca^{2+} entry. Secondly, in contrast to dequalinium, the onset of action of **45** was slow (many minutes rather than seconds), suggesting a different mechanism of action. Shortening the chain of **45** from 10 to 4 carbons provided **46** which, although it did not block the action potential of the neurone, again had a slow onset of action. It is important to note that as for dequalinium[191] the analogues of **Table 1** (except **45** and **46**) have a fast onset of action (complete within 90 seconds). It seems that **45** and **46** either bind at a different site on the SK_{Ca} channel or act via a different mechanism.

Table 4.13 Structure and biological results for the compounds of **series IV**.

Compd No	UCL No	Notebook No	Structure	EMR (±SD)
45	1092	CD-29	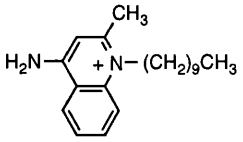	4.7 ± 1.7
46	1171	CD-69	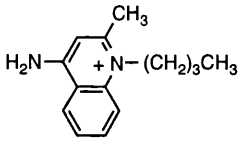	11.9 ± 5.9
10	1127	CD-45	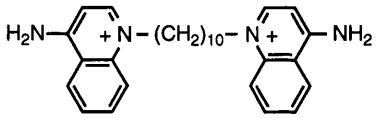	1.3 ± 0.5
47	1605	DG-723B	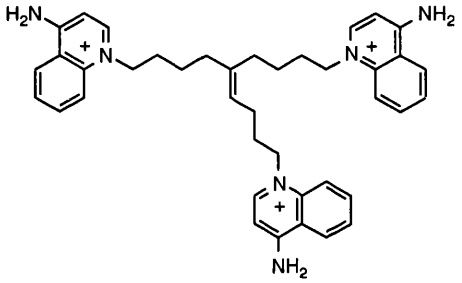	0.24 ± 0.11

On the other hand, additional information on the mode of binding of dequalinium can be provided by the introduction of a third quinolinium group in the molecule. Hence, the trisquinolinium analogue **47** was synthesised (for the rationale behind the selection of **47** as a representative of trisquinolinium compounds see section **2.3**), which was 5 times more potent than **10** (**Table 4.13**). Note that the pharmacological profile of **47** (in terms of selectivity) was similar to that of dequalinium. The increased potency of **47** compared with **10** raises the question of the nature of the contribution of the third quinolinium group. It can be envisaged that this may arise either from direct binding of the third quinolinium group to the channel (gain of an additional binding site compared with **10**) or indirectly from a statistical effect of three rather than two potential binding groups existing in the molecule (no gain of an additional binding site compared with **10**).

Table 4.14 Structures and biological results for mono-, bis- and trisquinolinium compounds.

Compd No	UCL No	Notebook No	Structure	EMR (± SD)	K_i (nM)
45	1092	CD-29	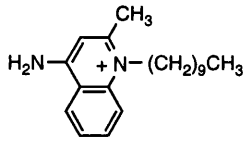	4.7 ± 1.7	12,200
46	1171	CD-69	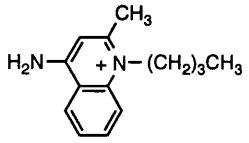	11.9 ± 5.9	25,100
8	Deq.	—	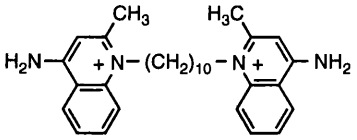	1	291
18	1439	DG-127C	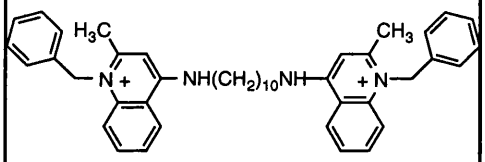	0.6 ± 0.3	529
64	1530	BBH-49B	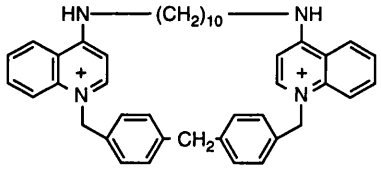	0.16 ± 0.1	95
47	1605	DG-723B	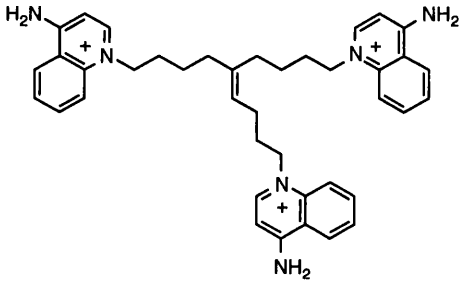	0.24 ± 0.11	34

To attempt to answer this question, it is of critical importance to know the affinities of the two monoquinolinium analogues **45** and **46** for the SK_{Ca} channel. Their uncertain mechanism of action renders the biological activities obtained from the inhibition of the AHP in rat sympathetic neurones unreliable as measures of their affinities for the SK_{Ca} channel and necessitates a more direct measurement. This can be achieved by employing equilibrium radioligand binding studies. As mentioned in section **1.4.3**, apamin is a potent and selective blocker of the SK_{Ca} channel and so is a radiolabeled (with ^{125}I at the

His_{18}) analogue, ^{125}I-apamin. The latter has been used as a specific radiologand for the SK_{Ca} channel and its inhibition of binding to the SK_{Ca} channel by compounds has been considered as strong evinence for these compounds binding to this channel. Again as mentioned in section **1.4.3**, rat brain synaptic plasma membranes are known to possess SK_{Ca} channels and have been used in ^{125}I-apamin binding studies. It was therefore decided to perform radioligand binding studies in order to assess the ability of compounds **45**, **46**, **47** and dequalinium to inhibit ^{125}I-apamin binding to rat synaptic plasma membranes at equilibrium and to obtain the dissociation constants (K_i) of these analogues for the SK_{Ca} channel.

Binding assays were performed as discribed in the experimental section. The dissociation constant (K_D) of apamin was found to be 4.8 pM for the particular membrane preparation used. The K_is of the analogues tested are shown in **Table 4.14**. As can be seen, the monoquinolinium compounds **45** and **46** are 500 times less potent than dequalinium and the trisquinolinium analogue **47** has 10 times higher affinity for the SK_{Ca} channel and constitutes the most potent non - peptidic SK_{Ca} channel blocker tested on this assay system. A plot of the percentage of ^{125}I-apamin that binds to the channel in the presence of varying concentrations of the compounds is shown in **Figure 4.19**.

The affinity constants can be converted to the corresponding free energy changes (ΔG) upon binding of the compounds to the channel using the well known equation:

$$\Delta G = -RT\ln K_i \qquad \textbf{R-24}$$

where: R is the universal gas constant (1.97 cal/mol·°K) and

T is the temperature in °K

The results are shown in **Table 4.15**. There is approximately a 2 Kcal/mol difference in the binding energy between the monoquinolinium compounds and dequalinium which becomes 1.2 Kcal/mol on going from the latter to the trisquinolinium compound **47**. The issue that arises from the results of the binding studies is whether the additional contribution of 2 and 1.2 Kcal/mol of the 2nd and 3rd quinolinium groups of dequalinium and **47** are the result of binding of these groups to the channel or whether they are the outcome of a statistical effect of two or three potential binding groups being

present in the molecule. In other words, an analysis method has to be sought, the results of which would give information as to whether one, two or all three quinolinium groups of **47** actually bind to the channel.

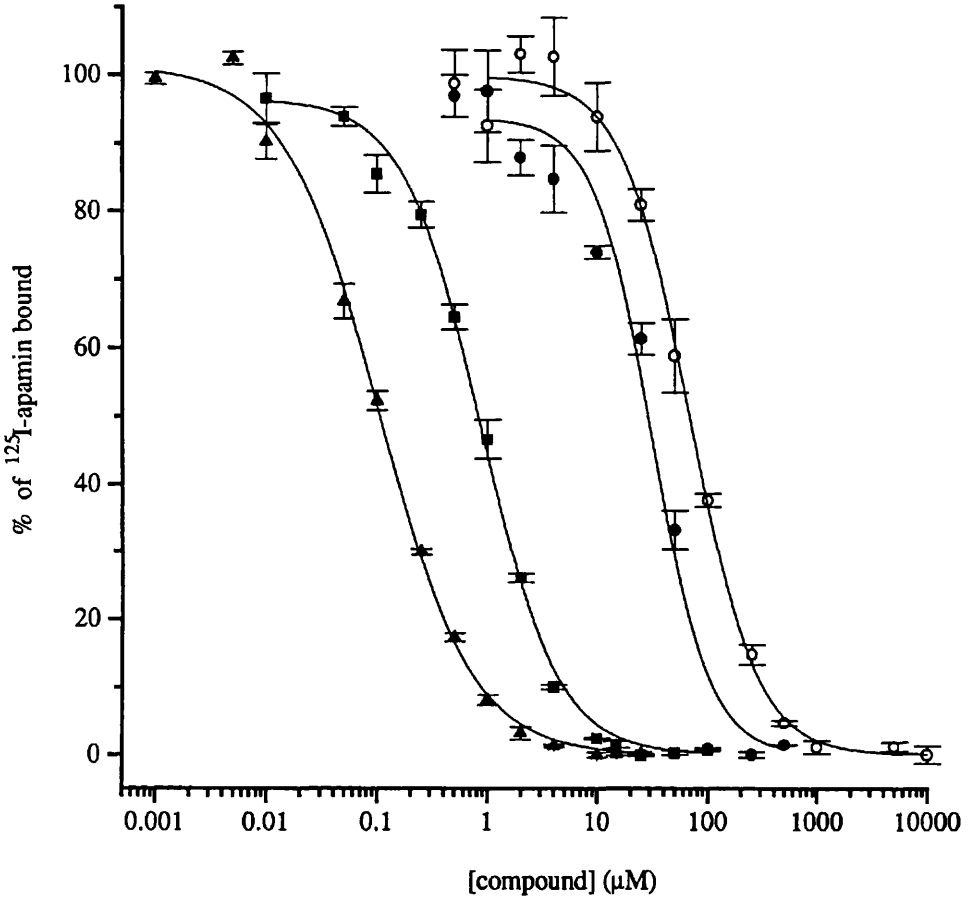

Figure 4.19 ^{125}I-apamin binding to rat brain synaptic plasma membranes in the presence of compounds **47** (▲), dequalinium (■), **45** (●), and **46** (o). Membranes were incubated (on ice for 1 h in 10 mM KCl, 25 mM Tris, containing 0.1% (w/v) BSA, at pH = 8.4) in the presence of 10 pM ^{125}I-apamin and varying concentrations of the compounds. Following collection of membranes by filtration, the amount of bound ^{125}I-apamin was measured and the extend of ^{125}I-apamin binding was expressed as a percent of total binding in the absence of any competing compound. Data points are the means of triplicate determinations ± SD.

Initially Jencks[262] and subsequently Williams and coworkers in a series of publications[263-272] have substantially contributed to the understanding of the contribution of the various functional groups present in a molecule to the overall binding free energy of the molecule. They have suggested that the binding free energy (ΔG) of a small molecule (drug) to a macromolecule (receptor) can be considered as the linear combination of a number of free energies:[262,264]

Table 4.15 EMR, K_i and ΔG values for selected analogues

Compd No	UCL No	Notebook No	EMR (± SD)	K_i (nM)	ΔG (Kcal/mol)
45	1092	CD-29	4.7 ± 1.7	12,200	-6.1
46	1171	CD-69	12 ± 5.9	25,100	-5.7
35	1638	SM-106A	1.8 ± 0.5	—	-7.8
8	Deq.	—	1	291	-8.1
34	1637	SM-104A	~2.0	—	-7.7
33	1636	SM-109A	~1.4	—	-7.9
32	1635	SM-114B	1.0 ± 0.2	—	-8.1
18	1439	DG-127C	0.6 ± 0.3	529	-7.8
64	1530	BBH-49B	0.16 ± 0.1	95	-8.7
47	1605	DG-723B	0.24 ± 0.11	34	-9.2

$$\Delta G = \Delta G_{t+r} + \Delta G_r + \Delta H_{conf} + \Sigma\Delta G_p + \Delta G_{VdW} + \Delta G_h \qquad \textbf{R-25}$$

In eq. **R-25** ΔG_{t+r} is unfavorable and entropic in origin resulting from the loss of three degrees of translational and three degrees of rotational freedom upon a bimolecular association. It is generally assumed that a macromolecule of a large MW, such as an ion channel embeded in the cell membrane, has very limited degrees of freedom and, concequently, ΔG_{t+r} includes mainly the loss of entropy of the drug and can be calculated as it is proportional to the MW of the drug.[269] ΔG_r again opposes binding and relates to the loss of internal degrees of freedom of a drug binding to a receptor. This is the consequence of the "freezing" of otherwise freely rotatable bonds of the drug when this is bound to the receptor. It has been suggested that the value of this term is of the order of 1.2 to 1.44 Kcal/mol per rotor frozen upon complexation.[273] Furthermore, it is often the case that the binding conformation of the drug and/or the receptor do not correspond to their minimum energy conformations. As a result, a certain amount of strain may be present in the drug - receptor complex and term ΔH_{conf} reflects this unfavorable conformational strain enthalpy. The last three terms of eq. **R-25** are negative and favour

the binding process. $\Sigma\Delta G_p$ is the sum of all the *intrinsic binding energies* of the polar (non - hydrocarbon) functional groups present in the drug and hence reflects the contribution of each functional group to binding. ΔG_{VdW} is a measure of the favourable Van der Waals packing forces which may be present in the drug - receptor complex but absent in the uncomplexed receptor. Finally, ΔG_h is mainly entropic in mature and is the consequence of hydrophobic interactions. These have been estimated to contribute 0.03 Kcal/mol per $Å^2$ of hydrocarbon removed from water accessibility upon complex formation.[264] (For an alternative approach to the partitioning of binding free energies see ref. 274).

In those cases where ligand and receptor show good complementarity and there is little strain in the complex, eq. **R-25** can be simplified[264] to:

$$\Delta G = \Delta G_{t+r} + \Delta G_r + \Sigma\Delta G_p + \Delta G_{VdW} + \Delta G_h \qquad \textbf{R-26}$$

Furthermore, when dealing with the binding of small ligands, it can be assumed[264] that $\Delta G_{VdW} = 0$ since the packing forces developed are likely to be very small and eq. **R-26** can be simplified to:

$$\Delta G = \Delta G_{t+r} + \Delta G_r + \Sigma\Delta G_p + \Delta G_h \qquad \textbf{R-27}$$

For the purpose of this analysis, eq. **R-27** can be writen as:

$$\Delta G = \Delta G_{t+r} + \Delta G_r + \Delta G_{q1} + \Delta G_{q2} + \Delta G_{q3} + \Delta G_h \qquad \textbf{R-28}$$

where ΔG_{q1}, ΔG_{q2} and ΔG_{q3} are the intrinsic binding energies of the first, second and third quinolinium groups in the molecules of the dequalinium analogues and ΔG_h is the energy gain from the hydrophobic interaction due to the putative binding of the alkyl chain. However, we will assume that $\Delta G_h = 0$ for the dequalinium analogues for the following reason: Compound **64**, a conformationally constrained analogue of **18** (**Table 4.14**), binds to the SK_{Ca} channel with a more negative free energy of 0.9 Kcal/mol than **18** (**Table 4.15**). However, **18** has 11 rotatable bonds in its alkyl chain, whereas in **64** the same bonds are constrained. Therefore, if the alkyl chain were binding, **64** should have had a ΔG at least 11 x 1.2 = 13.2 Kcal/mol more negative than **18** (where 1.2 Kcal/mol is the free energy change associated with the entropy loss upon restraining one

rotatable bond, as mentioned above). This is serious evidence that the alkyl chain does not contribute to the binding of the compounds. Hence, eq. **R-28** can be simplified to:

$$\Delta G = \Delta G_{t+r} + \Delta G_r + \Delta G_{q1} + \Delta G_{q2} + \Delta G_{q3} \qquad \textbf{R-29}$$

For the **monoquinolinium** compounds **45** and **46**, eq. **R-29** becomes:

$$\Delta G = \Delta G_{t+r} + \Delta G_r + \Delta G_{q1} \qquad \textbf{R-30}$$

Since the alkyl chain is presumed not to contribute to binding $\Delta G_r = 0$. Note that bonds leading to terminal methyl groups are generally regarded as freely rotating in the drug receptor complex since they have small barriers to rotation even in the crystalline state.[268] On the other hand, the NH_2 group is rotationally restricted even in the uncomplexed compound since the C—N bond has considerable double bond character as supported by theoretical calculations (AM1 semiempirical, not shown) and by ^1H NMR data (the hydrogens of the NH_2 group resonate as two singlets which collapse to one singlet upon raising the temperature). In the case of **45**, setting ΔG = -6.0 Kcal/mol and ΔG_{t+r} = 14.5 Kcal/mol[269] gives ΔG_q = 20.5 Kcal/mol. Similarly, for **46** setting ΔG = -5.7 Kcal/mol and ΔG_{t+r} = 13.7 Kcal/mol[269] gives ΔG_q = 19.4 Kcal/mol. Averaging the two ΔG_q values gives an *intrinsic binding energy* for the quinolinium group of 20 Kcal/mol.

The **bisquinolinium** compounds **32 - 35** (**Table 1**) and dequalinium in which the alkyl chain is varied can then provide useful insight into the mode of binding of the second quinoline present in these molecules. Although binding data is not available for **32 - 35**, it is reasonable to assume that, since their EMRs are very similar to the EMR of dequalinium, their K_is will be similar to the K_i of dequalinium. Three models are then possible depending on the mode of binding of the quinolinium groups: **i.** Only one of the two quinolinium groups binds to the channel. **ii.** Both quinolinium groups bind at similar sites. **iii.** Both quinolinium groups bind at dissimilar sites. These models are examined below.

i. Only one quinoline binds.

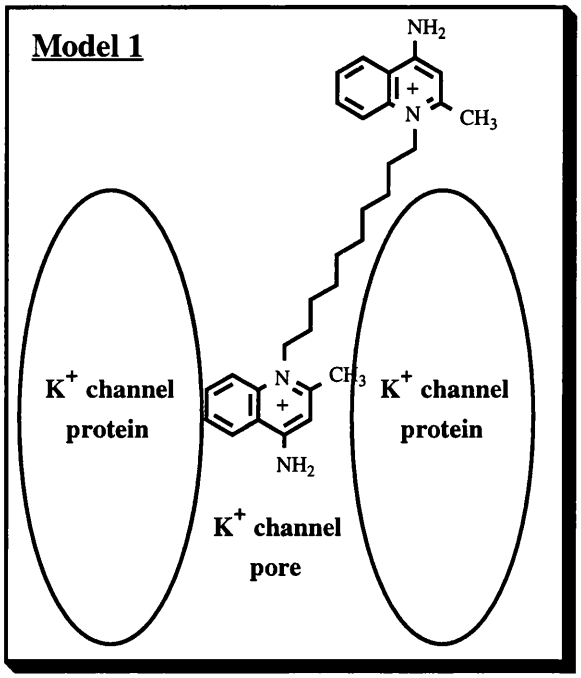

Eq. **R-29** becomes:

$$\Delta G = \Delta G_{t+r} + \Delta G_r + \Delta G_{q1} + \Delta G_{q2} \qquad \textbf{R-31}$$

where ΔG_{q2} is the free energy associated with the contribution of the 2nd quinolinium group in the molecule and is entropic in nature. Working in like manner as above for **45** and **46** and using the value of 20 Kcal/mol for ΔG_{q1}, the following values for the statistical contribution of the 2nd group are obtained:

Compd No	ΔG_{q2} (Kcal/mol)
35	-3.1
8	-3.2
34	-2.9
33	-2.9
32	-2.7

ii. Both quinolinium groups bind at similar sites.

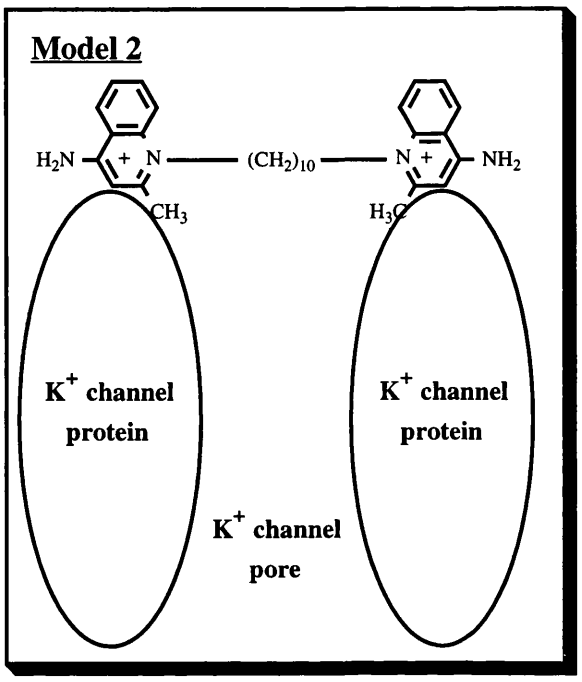

Since the quinolinium groups bind at similar sites, their contributions to the binding energy (*intrinsic binding energies*) must be similar. Therefore, $\Delta G_{q1} = \Delta G_{q2}$ and eq. **R-29** becomes:

$$\Delta G = \Delta G_{t+r} + \Delta G_r + 2\Delta G_{q1} \qquad \textbf{R-32}$$

However, this time, although the aliphatic chain is still considered not to contribute to binding enthalpically, constraints imposed by the binding of the two quinolinium groups on either end of the chain have to be taken into account. Therefore, the value n x 1.2 Kcal/mol is used for ΔG_r, where n is the number of rotatable bonds in the chain. All terms are then known in eq. **R-32** and hence the binding free energy can be calculated and the values compared with the experimentally found ones:

Compd No	ΔG_{calc} (Kcal/mol)	ΔG_{obs} (Kcal/mol)
35	-9.0	-7.8
8	-11.6	-8.1
34	-14.0	-7.7
33	-16.6	-7.9
32	-18.1	-8.1

iii. Both quinolines bind at dissimilar sites.

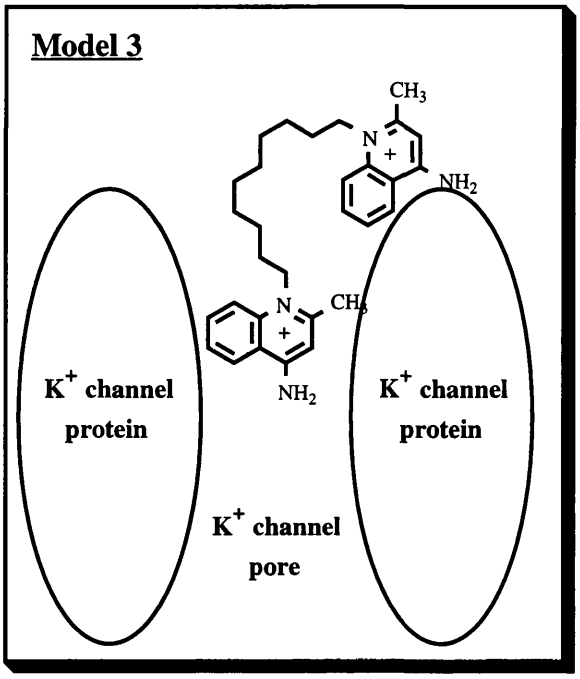

In this case, $\Delta G_{q1} \neq \Delta G_{q2}$ and eq. **R-29** becomes:

$$\Delta G = \Delta G_{t+r} + \Delta G_r + \Delta G_{q1} + \Delta G_{q2} \qquad \textbf{R-33}$$

In eq. **R-33** ΔG_{q2} is the only unknown and can be calculated, making the same provisions for the constraining of the aliphatic chain as in model 2. The results are:

Compd No	ΔG_{q2} (Kcal/mol)
35	-18.7
8	-16.4
34	-13.7
33	-11.3
32	-9.9

From a critical evaluation of the results for the three potential modes of binding of the bisquinolinium compounds it is evident that:

- *Model 1* gives consistent free energy values for the statistical contribution of the 2nd quinolinium group.
- *Model 2* provides calculated binding free energies which are variabe and too large

compared with the experimentally determined ones.

- *Model 3* yields intrinsic binding energies for the 2nd quinolinium group which are very variable. The implication of this is that the model is not in agreement with the 2nd quinolinium group binding at a site which is the same for all compounds. On the contrary, it suggests that this group binds at a site which is different for each compound.

As far as the **trisquinolinium** analogue **47** is concerned, eq. **R-29** has too many unknowns and cannot be solved. However, for the simplest of cases corresponding to *model 1* discussed above in which only one quinolinium group binds to the channel, eq. **R-32** yields $\Delta G_{q2} + \Delta G_{q3} = -5.1$ Kcal/mol. If the statistical contributions of the 2nd and 3rd quinolinium groups are assumed to be equal then each one is approximately -2.6 Kcal/mol, a value which is in good aggreement with the contribution of the 2nd quinolinium group in *model 1* discussed above.

By way of conclusion, although the analysis presented is limited by the quality of the values for the entropy terms ΔG_{t+r} and ΔG_r and by the assumptions used, it does show that the suggestion that only one quinolinium group binds to the channel and that the 2nd and 3rd quinolinium groups contribute entropically is a valid one. *Model 3* however cannot be ruled out. Nevertheless, *model 1* is much simpler and uses less explanatory variables than *model 3*, a fact which should credit additional validity to it.

4.5 REPLACEMENT OF THE QUINOLINIUM GROUP BY OTHER CHARGED GROUPS

It has previously been shown that replacement of one quinolinium group of dequalinium by the triethyl ammonium group to give analogue **65** resulted in a 20 - fold drop in potency (relative to dequalinium).[209]

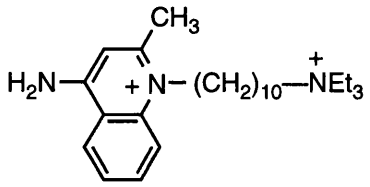

65

Focussing on those differences between the triethylammonium and quinolinium groups which might account for the superiority of the latter, it is evident that the charge distribution is very different, and that enhanced delocalisation via the resonance effect of the amino group in the case of dequalinium may be of significance (**Figure 4.1**). The flatness of the ring could also contribute through, for example, π - stacking if there were appropriately situated side chains of aromatic amino acids in the channel. Indeed, quinolinium cations have been shown to bind more strongly than alkylammonium cations to artificial receptors containing aromatic rings.[275] Although the structure of the SK_{Ca} channel is not known, there appears to be remarkable conservation of aromatic amino acids close to or in the pore - forming areas of the proteins of the structures which have been proposed for the ATP - regulated,[39] inward rectifier,[38] voltage - dependent[276] and high conductance Ca^{2+} - activated[99] K^+ channels. Further evidence on the importance of aromatic amino acids in the binding of K^+ channel blockers is provided by the finding that TEA blocks tetrameric voltage - dependent K^+ channels by binding at a site consisting of four aromatic amino acids, one being contributed from each of the four subunits.[277,278]

On the other hand, the preference for the quinolinium over the triethylammonium group could arise from a more favourable electrostatic interaction with anionic sites on the channel and this in turn may be due to a more favourable charge distribution. Although, conventionally, the positive charge is shown localised on the quaternary nitrogen in the structure of the quinolinium and triethylammonium groups, it is actually mainly distributed

over the hydrogen atoms. To identify any differences in charge distribution between the two groups, the partial charges for two model compounds, namely 4-amino-1,2-dimethylquinolinium and methyltriethyl-ammonium, were examined (**Figure 4.20**). The choice of the two model compounds was based on the assumption that the two charged groups in the bis - quaternary blockers, which are separated by ten carbons and cannot therefore interact inductively or mesomerically, do not interact through space i.e. the two charged groups are treated as being isolated. To simplify the problem, the aliphatic chain was replaced by methyl. Although the former has slightly different electronic properties in terms of its inductive and hyperconjugation effects compared with the latter, the errors introduced are expected to be largely the same in the case of the quinolinium and triethylammonium groups so that the results should be comparable. The charges were obtained by a semiempirical molecular orbital calculation using the MOPAC package, with the AM1 Hamiltonian[232] and performing Mulliken population analysis.

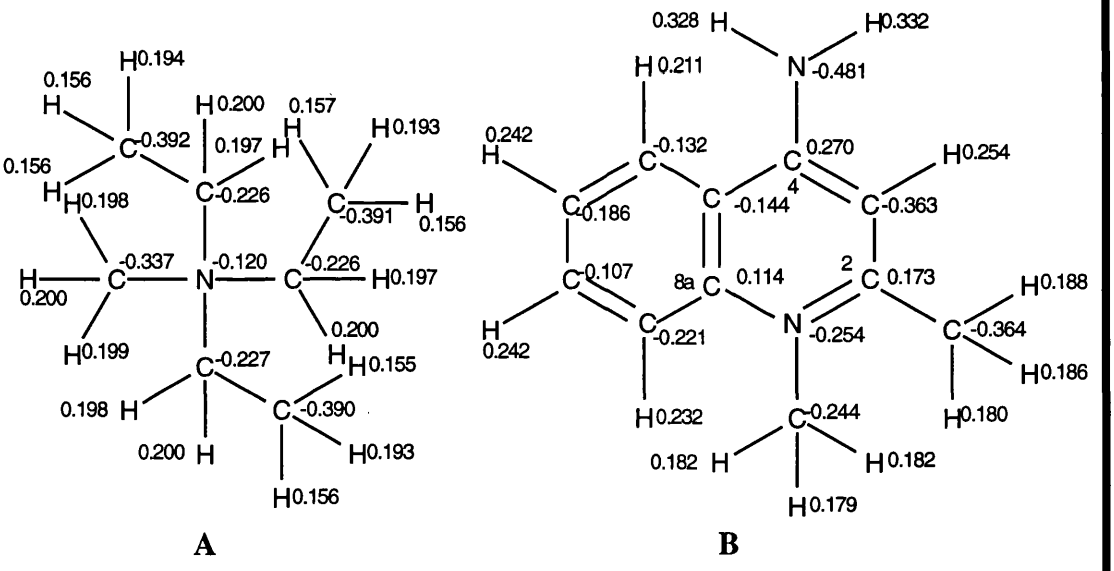

Figure 4.20 Partial charges on the atoms of two model compounds: methyltriethyl-ammonium (**A**) and 4-amino-1,2-dimethylquinolinium (**B**)

It can be seen in **Figure 4.20** that in the quinolinium group the positive charge is mainly distributed over carbon atoms 2, 4 and 8a, and the hydrogen atoms of the two methyl and of the amino groups, with all aromatic hydrogen atoms carrying substantial positive charges. The fact that the carbon atoms of positions 2, 4 and 8a are positively charged is in qualitative agreement with the conventional depiction of delocalisation that

results from resonance structures for the quinolinium group. On the other hand, the positive charge of the triethylammonium group is distributed over its hydrogen atoms, with the methylene groups directly attached to the quaternary nitrogen atom being more positively charged than the three terminal methyl groups. The charge distribution differences observed between the two groups may account for the difference in the potencies of dequalinium and **65** but it is not clear that this is necessarily so.

Alternatively, the electrostatic interaction may involve matching parts of the electric fields of the two interacting species, which have opposite signs, rather than matching point charges. It is likely that the interaction with the receptor is at an anionic site, in which case the electrostatic potential maps of the molecules should provide a better representation of what the receptor actually "sees" of the molecule. These are shown in **Figure 4.21**. The electrostatic potential energy map of the triethylammonium group corresponds to one of the low energy conformations of the group. Clearly, there are considerable differences in the two maps. The field around the methyltriethylammonium is more spherical in shape, while the one around the quinolinium group is more ring shaped and arises from the positively charged hydrogen atoms of the heterocycle. There is no build up of positive charge above and below the plane of the quinolinium ring. It should also be noted that the shape of the positive field around the quinolinium group is "fixed" since all atoms that give rise to the field occupy strictly defined positions relative to each other. This is not the case with the field of the triethylammonium group because of the conformational mobility of the three ethyl groups.

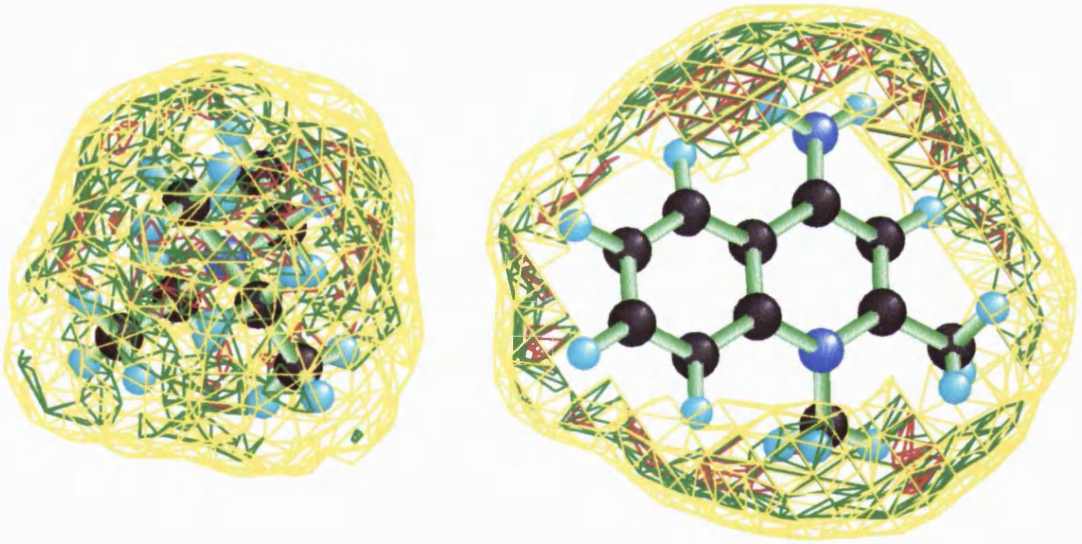

A B

Figure 4.21 Electrostatic potential energy maps of the two model compounds **A** and **B** of Figure 4.20. Contours were calculated at 30 (yellow), 40 (green) and 50 (red) Kcal/mol using Sybyl 6.0. The molecules were minimized with AM1. Atoms are coloured black (carbon), blue (nitrogen) and turquoise (hydrogen).

The advantageous interaction resulting from a ring - shaped charge distribution might be related to the existence of rings of negative charge in the pore region of many ion channels.[279] These result from the negatively charged side chains of amino acids, one being contributed from each subunit of the channel, arranged in a circular fashion, pointing towards the center of the pore, thus forming a negative "wall" at that point. One can envisage the positive ring of the quinolinium group complementing the negative ring of the channel. In this way, the plane of the quinoline would be perpendicular to the longitudal axis of the channel pore and the compound would obstruct the flow of K^+ through the channel thus acting as a blocker. On the other hand, the spherical (and smaller) field of the triethyl ammonium group would be a poor match to the ring shaped field of the channel, yielding an interaction of lower strength. The conformational mobility of the ethyl groups could further weaken the interaction either directly, by varying the electrostatic field of the molecule, or indirectly, by introducing unfavorable entropic factors. Although, as mentioned in the introductory section, the structure of the SK_{Ca} channel is not known, this represents a resonable hypothesis explaining the observed more favourable binding of the quinolinium compared with the triethylammonium groups, particularly since all K^+ channel types that have been cloned so far have negatively charged amino acids in the sequence of the putative pore - forming region of the protein.[38,39,99,276]

It has previously been demonstrated[209] that removal of the fused benzene ring of compound **10** (**Table 1**) to provide a pyridinium compound (**53**, **Table 4.16**) results in substantial loss of potency, and this may be due to reduction in the area of the flat π - electron system and/or altered charge distribution. As far as the latter is concerned, the size of the positively charged ring in the electrostatic potential energy map of the compound is smaller than in the case of the quinoline.

As mentioned in the introductory section, it is believed that the arginine residues of apamin and in particular the guanidinium groups are crucial for activity. To bridge apamin with the dequalinium - like compounds, **48** (**Table 4.16**) was synthesised in which a guanidinium - type group is partially incorporated into a heterocyclic ring to provide an amino - pyrimidinium structure. This compound was less potent than **53**.

Table 4.16 Structure and biological results for the compounds of **series V**.

Compd No	UCL No	Notebook No	Structure	EMR (±SD)
48	1468	DG-251A	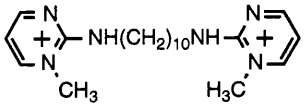	>>10
49	1553	DG-637A	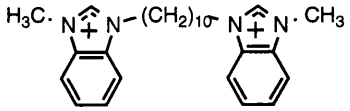	77 ± 23
50	1562	DG-649C	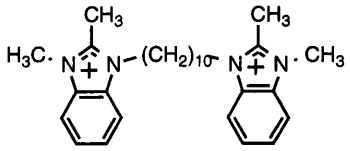	>10
51	1586	DG-735B	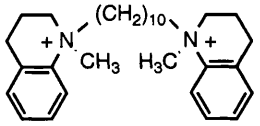	36 ± 20
52	1622	DG-831B	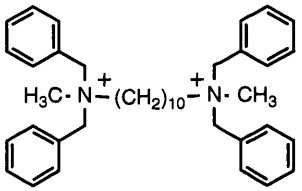	~50
53	1054	CD-1	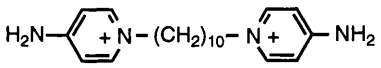	33 ± 13
54	1119	CD-39A	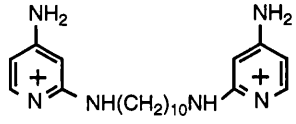	5.0 ± 1.8
55	1143	CD-52	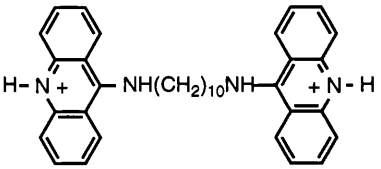	12 ± 4.9
56	1461	BR-103B	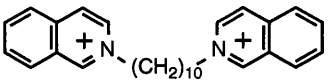	80 ± 42

It has also been demonstrated[209] that replacement of the quinoline ring of **9** (**Table 1**) by the isoquinoline ring results in **56** (**Table 4.16**) which is 5 times less potent than **9**.[209]

Furthermore, earlier results from our laboratory show that compounds having tricyclic heterocycles such as **11** (**Table 1**) and **55** (**Table 4.16**) are effective blockers of the SK_{Ca} channel, suggesting that the binding site can accommodate a tricyclic structure.[209]

Assuming that the nitrogen of the amino group of dequalinium serves to delocalise the positive charge, it seemed appropriate to examine the importance of it being exocyclic. Hence, the benzimidazole compound (**49**, **Table 4.16**) was synthesised, in which the exocyclic nitrogen of dequalinium has been incorporated into the ring, while keeping its ability to delocalise the charge. This compound is considerably less potent than dequalinium. It is even 5 times less potent than **9** (**Table 1**) and half as potent as **53**. Adding a methyl group at position 2 of the benzimidazole (**50**, **Table 4.16**) did not alter potency significantly.

On the other hand, partial "saturation" of the quinolinium groups of **9** (**Table 1**) to provide a 1,2,3,4-tetrahydroquinolinium analogue (**51**, **Table 4.16**) resulted in a two fold drop in potency compared with **9**, suggesting that the π - system and the flatness that its presence induces in the pyridine rings of **9** is not a critical feature of the molecule for SK_{Ca} channel blockade.

Moreover, the simple quaternary ammonium analogue **52** (**Table 4.16**) which features two phenyl rings not fused but independently attached on the charged nitrogen via a methylene group is three times less potent than **9** but an order of magnitude more potent than decamethonium which possesses trimethylammonium groups. Although too many structural changes have been effected in the transition from **9** to **52** for the loss in biological activity to be attributed with certainty to any of them, it may be appropriate to suggest that the presence of the heterocycle in itself is not the most critical feature for SK_{Ca} channel blockade but rather some properties (such as charge distribution and/or MO energies discussed above) associated with its presence may be the determinant factors. Consequently, once these factors have been identified, it is possible to select other, non -

heterocyclic groups which incorporate them, to design structurally novel series of SK_{Ca} channel blockers.

From the above it is evident that the quinolinium ring of dequalinium can be replaced by other charged heterocyclic and non - heterocyclic cations to give active compounds. The binding site must therefore possess steric tolerance since compounds having monocyclic, bicyclic or tricyclic heterocycles can be accommodated.

CHAPTER 5

DESIGN AND SYNTHESIS OF AN AFFINITY MATRIX FOR THE PURIFICATION OF THE SK_{Ca} CHANNEL PROTEIN

As mentioned in the introductory section, structural information on K^+ channels is only recently becoming available and is limited. No crystal structure of any K^+ channel has been reported and one would expect that crystallisation of K^+ channel (and ion channel in general) proteins would be a difficult task since these are highly associated with the membrane and, perhaps, their structure is stabilised by membrane components. In view of this, two general approaches for obtaining structural evidence for K^+ channels have been employed. The first and most widely used involves sequencing of the gene responsible for the expression of a particular channel and therefore, obtaining information on the primary structure of the protein(s) involved. Then, hydropathy plots can identify hydrophobic regions in the sequence of the protein(s) which are likely to form either membrane spanning or membrane embedded parts of the protein. Molecular modelling can then provide suggestions on the tertiary (and possibly quaternary) structure of the channel. This approach has been successfully applied to the voltage - activated K^+ channels,[11] an inward rectifier[38] and an ATP - regulated[39] K^+ channel. For Ca^{2+} - activated K^+ channels, a gene encoding for high conductance Ca^{2+} - activated K^+ (BK_{Ca}) channels has been cloned, sequenced and expressed in Xenopus oocytes.[99] Such molecular biological techniques have failed to provide any information on the gene encoding for the SK_{Ca} channel.

The second approach involves obtaining structural information directly at the protein level in two ways. Either by covalently cosslinking a radioligand to the channel and purifying the modified protein or by purifying the intact protein using a combination

of gradient centrifugations, conventional chromatography and/or affinity chromatography. Electrophoresis studies can yield information on the MW and number of different proteins (subunits) that form the channel, while sequencing of the purified protein can reveal its amino acid composition. This approach has been applied to Ca^{2+} - activated K^+ channels and the BK_{Ca} channel from tracheal smooth muscle has been purified by a combination of sucrose gradient centrifugation and conventional chromatography and reconstituted into artificial bilayers.[100]

The application of these methods to the SK_{Ca} channel has led to a much more complicated situation. The purification of the SK_{Ca} channel has been hampered so far by the low density of its expression[163] and its instability after solubilisation from the membrane[153,146]. As a result, structural investigations on the SK_{Ca} channel have been limited to crosslinking studies. In particular, ^{125}I-apamin (or in some cases ^{125}I-leiurotoxin I) has been covalently linked to the channel via a number of crosslinking molecules in a variety of tissues and the labelled proteins identified by electrophoresis studies. Initially, comparable but not identical ~30 KDa polypeptides were identified in rat brain synaptic plasma membranes[152,153] and rat pheochromocytoma (PC12) cells.[154,155] However, additional polypeptides of ~86, 59 and 44 KDa have been reported from rat brain synaptic plasma membranes, PC12 cells,[154] cultured neurones[148,147] and astrocytes.[149] This complex situation has somewhat been simplified by the suggestion that the 59 and 44 KDa polypeptides may be stable fragments of the 86 KDa protein. This combined with the finding of a ~30 KDa polypeptide in rabbit, guinea-pig and bovine brain,[156] strengthen the view that the SK_{Ca} channel may be composed of two subunits of ~86 and ~30 KDa. Furthermore, it has been suggested[156] that there may exist isoforms of the SK_{Ca} channel in brain and liver, following the finding of analogous but not identical apamin binding polypeptides that resemble the ~30 KDa brain polypeptide in rabbit, guinea-pig and bovine liver plasma membranes. These polypeptides were similar to the PC12 30 KDa peptide. However, no structural information is available on these peptides. In view of the clear need for larger scale purification of the SK_{Ca} channel, the task of employing affinity chromatography for this purpose has been undertaken in collaboration with Drs P.N. Strong and J.D.F. Wadsworth of the Neuromuscular Unit of

Hammersmith Hospital. The success of such an effort is dependent upon a number of factors, the most important of which are obtaining conditions that will allow a stable, solubilized form of the SK_{Ca} channel to exist and the synthesis of an affinity matrix that will bind the solubilized channel selectively and efficiently to allow its purification. Our efforts have concentrated on the latter factor.

A number of points that influence the design of an affinity matrix merit discussion. In general, an affinity support consists of a ligand (for the macromolecule to be purified) attached to a matrix via a spacer:

The procedure is in principle simple: A column is packed with the affinity support and a preparation containing the solubilized macromolecule is passed down the column. The macromolecule attaches to the ligand and stays on the solid phase while all other impurities are eluted. Then, the macromolecule is recovered by washing the column with a solution of another (or the same) ligand.

The properties of the ligand and of the spacer are critical. The ligand must have specific and reversible affinity for the macromolecule to be purified of the order of 10^{-4} - 10^{-8} M. It must also possess a reactive group that will allow the immobilisation onto the matrix with retention of affinity for the macromolecule. The length of the spacer is also critical. If it is too short, the matrix can sterically interfere with the binding process of the ligand to the macromolecule. On the other hand, if it is too long undesirable binding of macromolecules to the spacer can occur via non - specific hydrophobic effects.

Turning now to the design of an affinity matrix for the purification of the SK_{Ca} channel, dequalinium is a good candidate for a ligand. It has been shown that in rat sympathetic neurones dequalinium is a specific blocker of the SK_{Ca} channel[191] and its action is reversible.[190,191] Its binding affinity for the channel is approximately 0.3 μM as measured in our binding assay (see binding studies section) which falls somewhere in the middle of the above mentioned desired range. Concerning the incorporation of a spacer into the molecule of dequalinium, SAR indicated (see results and discussion section) that there is considerable steric tolerance in the direction of the NH_2 group and since the latter

provides a convenient handle, it was decided to attach an alkyl chain of three methylenes to the NH_2 group. Three methylene groups have been used succesfully in other cases (see for example ref 280) and provides a starting point.

Finally, a reactive group had to be incorporated at the end of the spacer to effect immobilization of the derivative to the matrix. Obviously, the nature of this group will be largely determined by the matrix to be used. It was decided to use epoxy - activated Sepharose 6B the terminal epoxide of which can be conveniently opened by an amino group, and so one was attached to the end of the spacer. The molecule that results from these structural modifications on dequalinium is **66**.

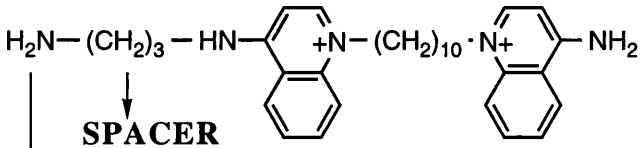

66

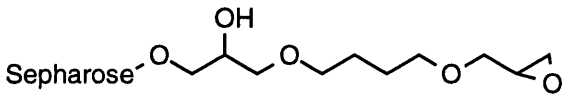

EPOXY - ACTIVATED SEPHAROSE - 6B

Retrosynthetic analysis for such a molecule is shown in **Scheme 5.1**: a disconnection of the type shown and synthesis of the two parts **A** and **B** separately provides an appropriate, convergent approach.

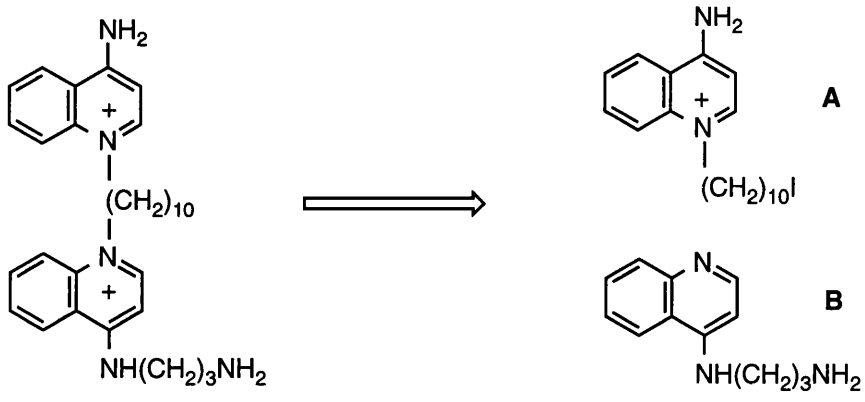

66

Scheme 5.1 Retrosynthetic analysis of compound **66**.

The synthesis of molecule **A** involved amination of 4-chloroquinoline using dry NH_3 gas in phenol and quaternisation of the resulting 4-aminoquinoline with an excess of 1,10-diiododecane to yield the desired compound (**Scheme 5.2**). In the synthesis of **B** one of the two groups of 1,3-diaminopropane was protected with the tert-butoxycarbonyl (BOC) group and the product was reacted with 4-chloroquinoline in pentanol in the presence of N-ethylmorpholine as a base; the latter is required to trap the HCl produced in the course of the reaction in order to avoid deprotection of the primary amino group. This yielded compound **B** which was coupled with **A** in butanone to yield the protected ligand in 84% yield. This was deprotected with HCl/MeOH and the product purified by preparative HPLC as described in the experimental section.

A ligand for the histamine H_1 receptor based on mepyramine and featuring a spacer identical to the one present in **66** has been coupled to epoxy - activated Sepharose 6B in carbonate buffers at pH = 11.[280] However, several attempts to immobilize **66** onto epoxy - activated Sepharose 6B using these literature conditions failed. Therefore, the conditions had to be modified and it was found that coupling of **66** to the Sepharose can be effected in 68% yield using aqueous NaOH at pH = 13 as the coupling medium (as described in the experimental section). No biochemical results are available at present since Dr J.D.F. Wadsworth is in the process of using it for the purification of the SK_{Ca} channel. Nevertheless, compound **66** has been tested on the rat sympathetic neurone assay and its EMR was 0.78 ± 0.26. This is encouraging since it demonstrates that the aminopropyl spacer can be accommodated at the binding site, as its presence in **66** does not result in loss of potency compared with the parent compound **10** (EMR = 1.3 ± 0.5, **Table 1**). This finding is in line with our predictions relating to the presence of steric tolerance in the direction of the 4-NH_2 group of dequalinium, as mentioned above.

It should be noted that very recently (after the synthesis of **67** had been completed), Sokol et al[158] claim to have cloned an apamin - binding protein from smooth muscle. The early stages of the experimental procedure (see section **1.4**) involved affinity chromatography using an apamin - based affinity matrix. The matrix used was prepared through coupling of the only free carboxyl group of apamin (Glu_7) to the terminal NH_2 group of EAH - Sepharose 4B via a carbodiimide reaction.

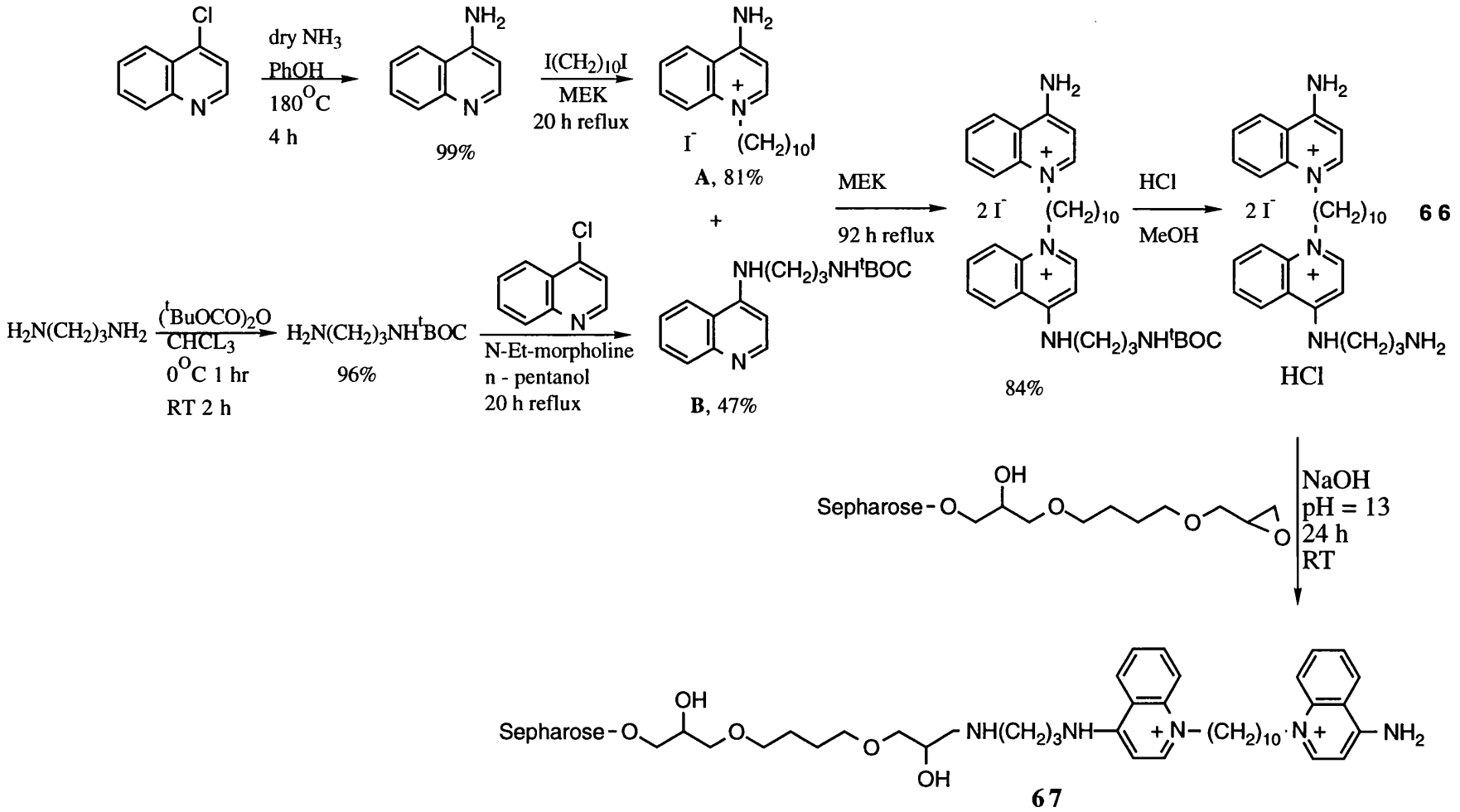

Scheme 5.2 Synthesis of affinity matrix for the purification of the SK_{Ca} channel protein

CHAPTER 6

BIOLOGICAL TESTING*

Electrophysiological testing on neurones was carried out in the Department of Pharmacology of UCL by Dr. P.M. Dunn in Professor D.H. Jenkinson's group. The SK_{Ca} blocking action of the compounds was assessed from their ability to inhibit the after - hyperpolarisation (AHP) in cultured rat sympathetic neurones as described previously.[191] Each compound was tested at 2 to 4 concentrations on at least three cells. Between 3 and 8 compounds were examined at a time, and in each such series of experiments, dequalinium was also included as a reference compound. The Hill equation was fitted to the data to obtain estimates of the IC_{50}. However, because there was some variation in the potency of dequalinium during the course of the study, equi - effective molar ratios (EMR: relative to dequalinium) were obtained by simultaneous non linear least squares fitting of the data with the Hill equation. It is these values which have been used for the comparison between compounds. It should be noted that the compounds were applied in a continuously flowing solution to isolated cells, so that differences in depletion as a consequence of variation in lipophilicity are unlikely to have been a complicating factor.

Although relatively simple, this assay relies on Ca^{2+} influx during the action potential to activate the SK_{Ca} channels, and the potency of any compound interfering with this influx may be overestimated. Dequalinium itself is a highly selective blocker of the SK_{Ca} channel, with no detectable effect on Ca^{2+} current even at the relatively high

---

* Radioligand binding studies are described in the experimental section (**7.3**)

concentration of 10 μM.[191] As most of the compounds tested in the present work have a similar bis-cationic structure to dequalinium, an action on Ca^{2+} channels seems unlikely. Nevertheless, because of the indirectness of the assay, test concentrations of more than 10 - 30 μM were generally avoided. The time course of the onset of the blocking action provided an additional criterion since dequalinium and all but two of the compounds tested acted rapidly, within 90 sec. The two exceptions were the amphipathic monocations **45** and **46** which were clearly less selective in their actions on sympathetic neurones.

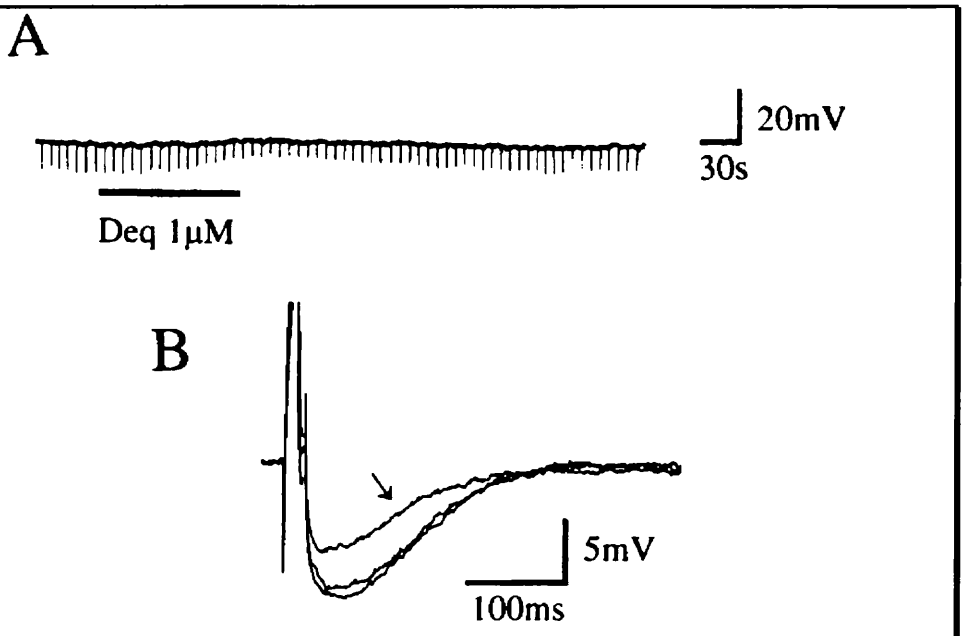

Figure 6.1 Reduction of the AHP measured on rat sympathetic neurones by dequalinium. (**A**) Continuous recording of AHPs (downward deflections) showing the effect of the application of 1 μM dequalinium. (**B**) Individual AHPs recorded before, in the presence of (arrow) and after washout of 1 μM dequalinium.

Table 6.1 Biological results for the compounds

Compd No	UCL No	Notebook No	IC_{50} ± SD (μM)	EMR ± SD
1	1463	DG-155A	2.7 ± 1.6	6.5 ± 1.9
2	1491	DG-367B	2.4 ± 0.5	3.4 ± 1.8
3	1504	DG-459A	4.5 ± 0.3	5.5 ± 1.0
4	1560	DG-589B	0.5 ± 0.15	0.9 ± 0.5
5	1580	DG-703C	0.59 ± 0.09	1.0 ± 0.6
6	1598	DG-739B	1	1.8 ± 0.8
7	1507	DG-467A	>>10	>>10
8	Deq	—	1.0 ± 0.2 0.82 ± 0.23 0.66 ± 0.16	1
9	1072	CD-9A	21 ± 5	15 ± 7.9
10	1127	CD-45	1.4 ± 0.3	1.3 ± 0.5
11	1130	CD-43B	1.0 ± 0.2	0.9 ± 0.7
12	1173	CD-74	1.4 ± 0.3	1.4 ± 0.6
13	1359	CO-199B	0.52 ± 0.07	0.7 ± 0.3
14	1431	BR-19A	15 ± 3.8	26 ± 14
15	1417	DG-13C	2.5	3.6 ± 1.2
16	1436	DG-81D	4.3 ± 1.3	6.2 ± 3.2
17	1438	DG-115C	1.7 ± 0.3	2.1 ± 0.9
18	1439	DG-127C	0.4 ± 0.05	0.6 ± 0.3
19	1440	DG-115B	0.75 ± 0.05	1.2 ± 0.8
20	1445	DG-167A	3.9 ± 0.5	5.9 ± 3.9
21	1454	DG-127B	1.3 ± 1.17	2.4 ± 0.5
22	1467	DG-223A	3.7 ± 0.6	6.2 ± 1.7
23	1601	DG-219B	>10	>10
24	1602	DG-159B	>>10	>>10
25	1091	SB-10A	4.4 ± 1.1	3.5 ± 1.2

Table 6.1 (continued)

Compd No	UCL No	Notebook No	IC_{50} ± SD (μM)	EMR ± SD
26	1118	CD-40	2.1 ± 0.2	1.9 ± 1.0
27	1144	CD-59	18 ± 7.0	16 ± 21
28	1156	CD-62	6.8 ± 1.7	7.2 ± 3.4
29	1360	CO-141A	0.7 ± 0.1	1.0 ± 0.4
30	1449	BR-67C	1.3 ± 0.18	1.5 ± 0.6
31	1437	DG-109A	1.6 ± 0.3	2.4 ± 0.9
32	1635	SM-114B	1.1	1.0 ± 0.2
33	1636	SM-109A	≈1	≈1
34	1637	SM-104A	≈1	≈1
35	1638	SM-106A	1.7	1.8 ± 0.5
36	1407	DG-23B	3.8	7.1 ± 2.8
37	1426	DG-33C	4.4 ± 0.6	8.0 ± 5.9
38	1427	DG-33D	2.4 ± 0.08	4.0 ± 2.0
39	1450	DG-199A	40 ± 39	26 ± 9.8
40	1172	CD-71	2.7 ± 0.25	3.1 ± 1.4
41	1455	DG-183B	9.5 ± 3.5	27 ± 9.2
42	1460	DG-207D	72 ± 15	130 ± 34
43	1480	DG-287B	21 ± 15	33 ± 10
44	1129	CD-42	6 ± 0.8	4.7 ± 1.6
45	1092	CD-29	5.5 ± 1.6	4.7 ± 1.7
46	1171	CD-69	12.4 ± 2	11.9 ± 5.9
47	1605	DG-723B	0.084 ±0.02	0.24 ± 0.11
48	1468	DG-251A	61	>>10
49	1553	DG-637A	16 ± 5.6	77 ± 23
50	1562	DG-649C	>10	>10
51	1586	DG-735B	41 ± 14	36 ± 20

Table 6.1 (continued)

Compd No	UCL No	Notebook No	IC_{50} ± SD (μM)	EMR ± SD
52	1622	DG-831B	≈40	≈40
53	1054	CD-1	35 ± 6	33 ± 13
54	1119	CD-39A	5.5 ± 0.7	5.0 ± 0.7
55	1143	CD-52	6.7 ± 0.4	12 ± 4.9
56	1461	BR-103B	25 ± 5	80 ± 42
66	1469	DG-267B	0.49 ± 0.03	0.78 ± 0.26

CHAPTER 7

EXPERIMENTAL

7.1 CHEMISTRY

Commercially available compounds were obtained either from Aldrich Chemical Company or from Lancaster Synthesis. Melting points (mp) were obtained on an Electrothermal melting point apparatus and are uncorrected. Infrared (IR) spectra were run on a Perkin - Elmer 983 spectrophotometer. Nuclear magnetic resonance (NMR) spectra were recorded on a Varian XL-200 (200 MHz) or VXR-400 (400 MHz) spectrometer, and chemical shifts (ppm) are reported relative to the solvent peak ($CHCl_3$ in $CDCl_3$ at 7.24 ppm and DMSO in DMSO-d_6 at 2.49 ppm) or relative to TMS. Signals are designated as follows: s, singlet; s_{br}, broad singlet; d, doublet; dd, doublet of doublets; t, triplet; q, quadruplet; quint, quintet; m, multiplet. Mass spectra were run on a ZAB SE or VG 7070H spectrometer. Analytical reverse phase high performance liquid chromatography (HPLC) was performed either on a Gilson or Shimadzu HPLC apparatus with a UV detector at 215 or 254 nm and a Kromasil C18 7μm (**K**) or Lichrosorb RP SELECT B 7 μm (**L**) column. Isocratic elutions using solvent mixtures of **A** = water + 0.1% TFA and **B** = MeOH + 0.1% TFA or **C** = water + 0.5% sodium salt of hexanesulphonic acid + 0.5% orthophosphoric acid and **D** = MeOH + 0.5% sodium salt of hexanesulphonic acid + 0.5% orthophosphoric acid were performed unless otherwise stated. The ratio of A : B or C : D is indicated for each individual compound. The flow rate was 1 ml / min. For preparative HPLC a Gilson apparatus was used with a UV detector at 215 nm and a Kromasil C18 7μm column. The solvent mixtures were as above and the flow rate was 15 ml / min.

4-chloroquinoline[281]

(1a, DG-131A, DG-139A, DG-359A)

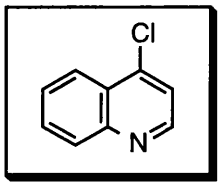

4-hydroxyquinoline (1.3 g, 8.96 mmol) and phosphorous oxychloride (2.5 g, 16.33 mmol) were heated without solvent in an oil bath at 110°-120°C for 1 hr. More $POCl_3$ (2.5 g, 16.33 mmol) was then added and the solution was heated for a further 1 hr. After cooling to room temperature, the excess of $POCl_3$ was removed by vacuum distillation (using a water pump). Ice was added to the redish, oily residue and the resultant solution was basified with conc. NH_4OH and extracted with dichloromethane. The extracts were combined, dried with K_2CO_3 and the solvent was removed in vacuo to yield a yellowish oil (1.296 g, 88%) which solidified after 1 hr in the freezer. The reaction was repeated to obtain more material (7.518 g, 95%).

^1H NMR (200 MHz, $CDCl_3$) δ 7.49 (d, 1 H, quin-H_3), 7.64 (t, 1 H, quin-H_6 or quin-H_7), 7.77 (t, 1 H, quin-H_7 or quin-H_6), 8.12 (d, 1 H, quin-H_5), 8.24 (d, 1 H, quin-H_8), 8.78 (d, 1 H, quin-H_2).

4-Phenoxyquinoline[282]

(1b, DG-151A)

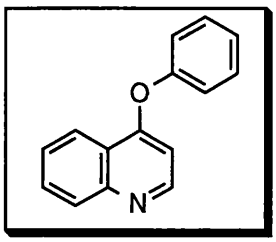

4-Chloroquinoline (**1a**) (0.778 g, 4.76 mmol), phenol (3.892 g, 41.36 mmol) and KOH (0.296 g, 5.28 mmol) were heated in an oil bath at 125° - 130°C for 1 h. The reaction

mixture was cooled to room temperature, basified with a concentrated solution of KOH and extracted with ether. The extracts were dried (K_2CO_3) and the ether was removed on a rotary evaporator to dryness. Some phenol was present in the resulting oil, therefore, the later was adsorbed onto silica and chromatographed using CH_2Cl_2 until all phenol had been eluted and then with EtOAc until all the product had been eluted. The compound was isolated as a colourless, viscous oil (1.05 g, 100%).

^{1}H NMR (200 MHz, $CDCl_3$) δ 6.55 (d, J = 5.3 Hz, 1 H, quin-H_3), 7.25 (m, 3 H, Ph), 7.48 (m, 3 H, Ph + quinoline), 7.76 (td, J_1 = 1.5 Hz, J_2 = 7.7 Hz, 1 H, quin-H_6 or H_7), 8.09 (dd, J_1 = 1.2 Hz, J_2 = 8.5 Hz, 1 H, quin-H_5 or H_8), 8.37 (dd, J_1 = 1.6 Hz, J_2 = 8.3 Hz, 1 H, quin-H_8 or H_5), 8.67 (d, J = 5.2 Hz, 1 H, quin-H_2).

1,1'-(Decane-1,10-diyl)-bis-(4-phenoxyquinolinium) diiodide hydrate (1, DG-155A, UCL 1463-C_2)

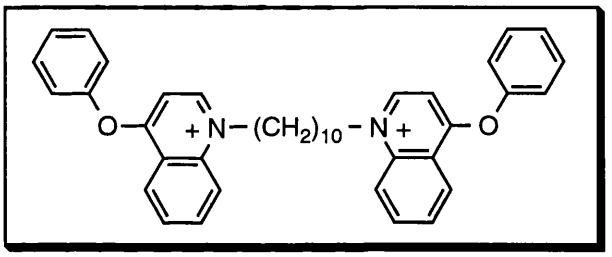

4-Phenoxyquinoline (**1b**, 0.806 g, 3.64 mmol) and 1,10-diiododecane (0.718 g, 1.82 mmol) were dissolved in 40 ml butanone and heated under reflux for 96 h. On cooling a wellow oil came out of solution. The supernatant was decanted and the oil washed extensively with butanone. On drying in vacuo the oil solidified to a yellow powder (0.24 g, 15.7%).

mp = 100° - 102°C.

IR (KBr disc) ν_{max} 3439, 3012, 2919, 2845, 1618, 1571, 1525, 1477, 1461, 1405, 1304, 1194 cm^{-1}.

^{1}H NMR (400 MHz, DMSO-d_6, TMS) δ 1.23 - 1.35 (m, 12 H, -CH_2-), 1.87 (m, 4 H,

-CH_2-), 4.89 (t, 4 H, N^+-CH_2), 7.06 (d, 2 H, quinoline-H_3), 7.46 - 7.53 (m, 6 H, Ph), 7.66 (t, 4 H, Ph), 8.06 (t, 2 H, quinoline-H_6 or H_7), 8.31 (t, 2 H, quinoline-H_7 or H_6), 8.54 (d, 2 H, quinoline-H_5), 8.72 (d, 2 H, quinoline-H_6), 9.21 (d, 2 H, quinoline-H_2).

MS (FAB, matrix MNOBA) $[M+I]^+$ 709, $[M]^+$ 582, fragments at m/z 505, 488, 360.

HPLC: column (K), A : B = 35 : 65, major peak at 6.21 min representing 96.2% of the absorption at 215 nm.

Anal. ($C_{40}H_{42}N_2O_2I_2 \cdot H_2O$) calc: C = 56.22, H = 5.19, N = 3.28
found: C = 55.90, H = 4.82, N = 2.96

4-Anilinoquinoline[283]

(2a, DG-363B)

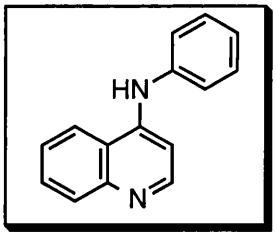

4-Chloroquinoline (**1a**, 0.5 g, 3.06 mmol) and freshly distilled aniline (0.356 g, 3.82 mmol) were dissolved in 10 ml of glacial AcOH and the solution was heated under reflux for 3 h under Ar. The solvent was removed in vacuo at 40°C, the residue was dissolved in MeOH, excess of Et_2O was added and a yellow precipitate formed. The mixture was placed in the 4°C fridge for 2 h, then the precipitate was collected by filtration and washed with Et_2O. This was dispersed in water, MeOH was added until the solution was clear and it was basified with a conc. solution of KOH in water. A white precipitate immediately formed, which was collected by filtration, washed well with water and dried in vacuo at 25°C over P_2O_5 for 6 h (0.581 g, 86%).

mp = 206° - 207°C.

^{1}H NMR (400 MHz, $CDCl_3$, TMS, ppm) δ 6.80 (s_{br}, 1 H, NH), 7.00 (d, J = 5.2 Hz, 1 H, quinoline-H_3), 7.20 (dt, J_1 = 1.2 Hz, J_2 = 7.4 Hz, 1 H, Ph-H_4'), 7.32 (td, J_1 = 1.2 Hz, J_2 = 7.4 Hz, 2 H, Ph-H_2' + H_6'), 7.43 (tt, J_1 = 1.1 Hz, J_2 = 2 Hz, J_3 = 7.7 Hz, 2 H, Ph-H_3' + H_5'), 7.52 (td, J_1 = 1.3 Hz, J_2 = 7.7 Hz, 1 H, quinoline-H_6 or H_7), 7.70 (td, J_1 = 1.4 Hz, J_2 = 7.7 Hz, 1 H, quinoline-H_7 or H_6), 7.96 (dd, J_1 = 0.9 Hz, J_2 = 8.4 Hz, 1 H, quinoline-H_5 or H_8), 8.06 (d, J = 8.5 Hz, 1 H, quinoline-H_8 or H_5), 8.57 (d, J = 5.1 Hz, 1 H, quinoline-H_2).

MS (EI) $[M]^+$ 220, fragments at m/z 128, 77.

1,1'-(Decane-1,10-diyl)-bis-(4-anilinoquinolinium) diiodide (2, DG-367B, UCL 1491-C_2)

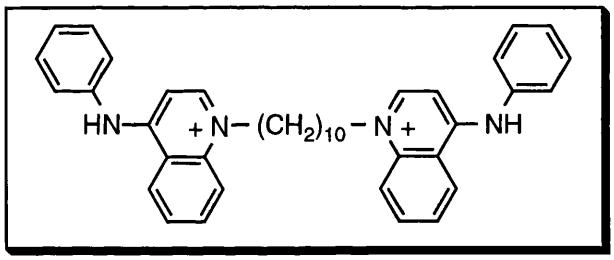

4-Anilinoquinoline (**2a**, 0.5 g, 2.27 mmol) and 1,10-diiododecane (0.447 g, 1.13 mmol) were dissolved in 50 ml butanone and the solution was heated under reflux for 96 h under Ar. The yellow precipitate formed was collected by filtration, washed with butanone and Et_2O and dried. This was dispersed in approximately 25 ml abs. EtOH, heated to boiling and MeOH was added dropwise until the solution became clear. It was then allowed to concentrate by boiling to approximately 20 ml, cooled to room temperature and placed at 4°C overnight. The yellow crystals formed were collected and dried in vacuo at 45°C over P_2O_5 (0.777 g, 82%).

mp = 241°C - 243°C.

IR (KBr disc) ν_{max} 3446, 3386, 3159, 3039, 2919, 2845, 1611, 1588, 1545, 1525 cm^{-1}.

^{1}H NMR (400 MHz, DMSO-d_6, TMS, ppm) δ 1.21 - 1.27 (m, 12 H, CH_2), 1.78 (m, 4

H, CH_2), 4.60 (t, J = 7.3 Hz, 4 H, N^+-CH_2), 6.79 (d, J = 7.3 Hz, 2 H, quinoline-H_3), 7.43 - 7.49 (m, 6 H, Ph-H_2' + H_6' + H_4'), 7.59 (t, J = 7.8 Hz, 4 H, Ph-H_3' + H_5'), 7.88 (t, J = 7.6 Hz, 2 H, quinoline-H_6 or H_7), 8.11 (td, J_1 = 1.3 Hz, J_2 = 7.7 Hz, 2 H, quinoline-H_7 or H_6), 8.25 (d, J = 9 Hz, 2 H, quinoline-H_5 or H_8), 8.61 (d, J = 7.5 Hz, 2 H, quinoline-H_2), 8.74 (dd, J_1 = 0.9 Hz, J_2 = 8 Hz, 2 H, quinoline-H_8 or H_5).

MS (FAB, MNOBA matrix) $[M-H]^+$ 579, fragments at m/z 290, 221, 54.

HPLC: column (L), C : D = 35 : 65, major peak at 9.25 min representing 99.2% of the absorption at 215 nm.

Anal. ($C_{40}H_{44}N_4I_2 \cdot 0.7H_2O$) calc: C = 56.71, H = 5.40, N = 6.61

found: C = 56.72, H = 5.48, N = 6.43

4-Aminoquinoline[281]

(3a, DG-231A, DG-891A, UCL 1541)

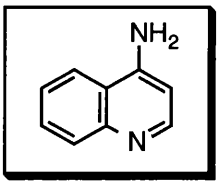

4-Chloroquinoline (**1a**, 0.811 g, 4.96 mmol) and phenol (1.866 g, 19.83 mmol) were heated together without solvent at 180°C and NH_3 (gas) was bubbled through the melt for 4 h. The NH_3 was dried by passage through a column loosely packed with soda lime. The reaction mixture was cooled to room temperature and diluted with 10 ml of a 50% solution of KOH in water. This was extracted with 5 x 50 ml of Et_2O. The extracts were combined, dried with Na_2SO_4 and the Et_2O removed in vacuo to yield a yellow oil which solidified on standing to a yellowish solid (0.709 g, 99%).

mp = 151° - 152°C (dec).

^1H NMR (400 MHz, $CDCl_3$, TMS) δ 4.84 (s_{br}, 2 H, NH_2), 6.60 (d, 1 H, quinoline-H_3),

7.45 (td, 1 H, quinoline-H_6 or H_7), 7.65 (td, 1 H, quinoline-H_7 or H_6), 7.78 (dd, 1 H, quinoline-H_5 or H_8), 8.01 (d, 1 H, quinoline-H_8 or H_5), 8.53 (d, 1 H, quinoline-H_2).

4-Acetamidoquinoline[284]

(3b, DG-389A, DG-447D)

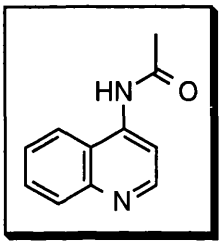

4-Aminoquinoline (**3a**, 0.2 g, 1.39 mmol) was dissolved in 4 ml pyridine and Ac_2O (0.3 ml, 3.18 mmol) was added. The solution was heated in an oil bath at 80°C for 24 h under Ar. The solution was cooled to room temperature, the solvent removed in vacuo and the residue basified with approximately 5 ml of 2 N NaOH and extracted with 8 x 20 ml $CHCl_3$. The extracts were combined, dried (Na_2SO_4) and the solvent removed in vacuo to yield a yellowish solid (0.259 g, 100%).

mp = 172° - 174°C.

^1H NMR (200 MHz, $CDCl_3$, TMS, ppm) δ 2.37 (s, 3 H, CH_3), 7.58 (td, J_1 = 1.4 Hz, J_2 = 7.6 Hz, 1 H, quinoline-H_6 or H_7), 7.74 (td, J_1 = 1.4 Hz, J_2 = 7.7 Hz, 1 H, quinoline-H_7 or H_6), 7.86 (dd, J_1 = 1 Hz, J_2 = 8.1 Hz, 1 H, quinoline-H_5 or H_8), 8.03 (s_{br}, 1 H, NH, disappears on D_2O treatment), 8.14 (dd, J_1 = 1.1 Hz, J_2 = 8.1 Hz, 1 H, quinoline-H_8 or H_5), 8.28 (s_{br}, 1 H, quinoline-H_3), 8.87 (d, J = 5.1 Hz, 1 H, quinoline-H_2).

1,1'-(Decane-1,10-diyl)-bis-(4-acetamidoquinolinium) diiodide hemihydrate

(3, DG-459A, UCL 1504-C_2)

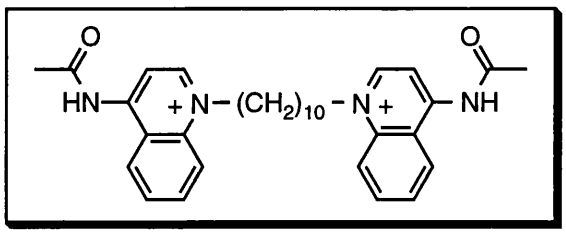

4-Acetamidoquinoline (**3b**, 0.09 g, 0.48 mmol) and 1,10-diiododecane (0.095 g, 0.24 mmol) were dissolved in 10 ml 4-methyl-2-pentanol and the solution was heated under reflux for 30 h under N_2. The yellow solid formed was collected by filtration, washed extensively with the solvent and Et_2O and dried in vacuo (0.13 g, 71%).

mp = 202° - 203°C.

IR (KBr disc) ν_{max} 3426, 3000, 2918, 2839, 1718, 1618, 1601, 1531, 1505, 1408 cm^{-1}.

^1H NMR (400 MHz, DMSO-d_6, TMS, ppm) δ 1.25 - 1.35 (m, 12 H, CH_2), 1.89 (m, 4 H, CH_2), 2.43 (s, overlaps with DMSO signal, $COCH_3$), 4.87 (t, J = 7.4 Hz, 4 H, N^+-CH_2), 8.04 (t, J = 7.9 Hz, 2 H, quinoline-H_6 or H_7), 8.24 (t, J = 8.1 Hz, 2 H, quinoline-H_7 or H_6), 8.51 (d, J = 9 Hz, 2 H, quinoline-H_5 or H_8), 8.70 (d, J = 7 Hz, 2 H, quinoline-H_3), 8.88 (d, J = 8.7 Hz, 2 H, quinoline-H_8 or H_5), 9.26 (d, J = 7 Hz, 2 H, quinoline-H_2), 11.08 (s, 2 H, NH).

MS (FAB, MNOBA matrix) $[M-H]^+$ 511, fragments at m/z 469, 427, 325, 283, 269, 256, 241, 227, 213, 200, 187.

HPLC: column (L), C : D = 40 : 60, major peak at 5.86 min representing 98.2% of the absorption at 215 nm.

Anal. ($C_{32}H_{40}N_4O_2I_2 \cdot 0.5H_2O$) calc: C = 49.56, H = 5.33, N = 7.22

found: C = 49.61, H = 5.23, N = 6.97

2-Ethoxycarbonyl-3-[(3-nitrophenyl)amino]acrylate[217,285]

(4a, DG-503A)

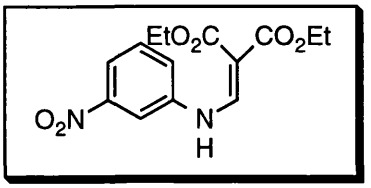

3-Nitroaniline (13.813 g, 100 mmol) and diethyl ethoxymethylene malonate (21.623 g, 100 mmol) were heated together without solvent at 100°C under Ar for 5.5 h (until the evolution of EtOH had ceased). The resultant brown oil solidified on standing at room temperature to a yellow solid (30.8 g, 100%).

^{1}H NMR (200 MHz, $CDCl_3$, TMS, ppm) δ 1.39 (m, 6 H, CH_3), 4.30 (m, 4 H, CH_2), 7.45 (m, 1 H, Ph-H), 7.58 (m, 1 H, Ph-H), 7.99 (m, 1 H, Ph-H), 8.53 (d, J = 13.3 Hz, 1 H, =CH).

7-Nitro-3-ethoxycarbonyl-4-1H-quinolone[217,285]

(4b, DG-507A)

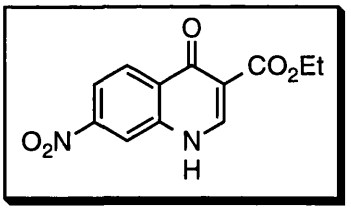

Molten 2-ethoxycarbonyl-3-[(3-nitrophenyl)amino]acrylate (**4a**, 30.57 g, 99.15 mmol) was added slowly through an air condenser into boiling diphenyl ether (100 g) and the resultant solution was boiled under reflux for 45 min. A creamy - yellow precipitate started to form after 15 min. The reaction mixture was cooled to room temperature and 50 ml of petroleum spirit (80° - 100°C range) were added and the creamy solid was collected by filtration. It was then washed with 2 x 50 ml petroleum spirit. The solid was transfered into a 250 ml flask and triturated well with 3 x 50 ml of petroleum spirit to remove any

diphenyl ether. Finally, it was dried in vacuo at 70°C overnight (23.64 g, 91%).

mp = 330°C (dec).

MS (FAB, MNOBA matrix) $[M+H]^+$ 263 fragment at m/z 217.

^1H NMR: The poor solubility of the compound prevented the recording of a good quality NMR spectrum.

7-Nitro-3-carboxy-4-1H-quinolone[217]

(4c, DG-511A, DG-535A)

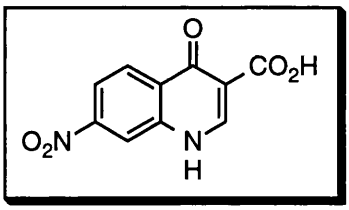

7-Nitro-3-ethoxycarbonyl-4-1H-quinolone (**4b**, 4 g, 15.25 mmol) was dispersed in 30 ml of 10% NaOH and the mixture was heated under reflux in an oil bath for 1 h. After cooling to room temperature the resultant dark solution was acidified to pH 2 with 10% HCl and the brown solid formed was collected on a Buchner funnel, washed with water and dried in vacuo at 70°C (3.203 g, 90%). This was shown by ^1H NMR to be a mixture of 7-nitro-3-carboxy-4-1H-quinolone : 5-nitro-3-carboxy-4-1H-quinolone ≅ 3 : 1.

mp = 255° - 257°C.

^{1} H NMR (200 MHz, DMSO-d_6, ppm) δ *7-Nitro-3-carboxy-4-quinolone* : 8.24 (dd, J_1 = 2.2 Hz, J_2 = 9 Hz, 1 H, quinolone-H_6), 8.45 (d, J = 8.9 Hz, 1 H, quinolone-H_5), 8.69 (d, J = 1.9 Hz, 1 H, quinolone-H_8), 9.02 (s, 1 H, quinolone-H_2), *5-nitro-3-carboxy-4-quinolone* : 7.85 (d, J = 7.3 Hz, 1 H, quinolone-H_6 or H_8), 7.96 (d, J = 8.3 Hz, 1 H, quinolone-H_8 or H_6), 8.05 (t, J = 7 Hz, 1 H, quinolone-H_7), 8.92 (s, 1 H, quinolone-H_2).

MS (EI) $[M]^+$ 234 fragments at m/z 190, 174, 160, 144, 116, 43.

Mixture of **7-nitro-4-1H-quinolone**[217] and **5-nitro-4-1H-quinolone**

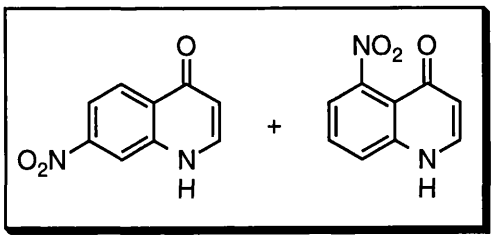

i. From 7-nitro-3-carboxy-4-1H-quinolone and 5-nitro-3-carboxy-4-1H-quinolone

(4d, DG-515A, DG-519A, DG-551A)

The above prepared mixture of 7-nitro-3-carboxy-4-1H-quinolone and 5-nitro-3-carboxy-4-1H-quinolone (**4c**, 2 g, 8.54 mmol) was dispersed in 10 ml Dowtherm A and the mixture was placed in an oil bath preheated to 250°C. The reaction mixture was heated under reflux with stirring for 30 min. After cooling to room temperature, 20 ml of petroleum spirit (80° - 100°C range) were added and the dark solid formed was collected by filtration. This was washed extensively with petroleum spirit and dried (1.624 g, 100%).

ii. From 7-nitro-3-ethoxycarbonyl-4-1H-quinolone and 5-nitro-3-ethoxycarbonyl-4-1H-quinolone

(4e, DG-543A)

A suspension of a mixture of 7-nitro-3-ethoxycarbonyl-4-1H-quinolone and 5-nitro-3-ethoxycarbonyl-4-1H-quinolone (**4b**, 1 g, 3.81 mmol) in 5 ml Dowtherm A containing p-toluenesolfonic acid (0.024 g, 0.13 mmol) was added to 10 ml Dowtherm A heated to 255° - 260°C. More Dowtherm A (5 ml) was used to assist the complete transfer of **4b**. To the heated reaction mixture, 10 drops of water were added **CAUSIOUSLY** and the mixture was heated for a further 30 min. After cooling to room temperature, 20 ml of petroleum spirit (80° - 100°C) were added and the green solid was collected by filtration, washed with 150 ml petroleum spirit and dried in vacuo at 70°C (0.709 g, 98%).

mp = 310°C (dec).

^{1}H NMR (200 MHz, DMSO-d_6, ppm) δ *7-nitro-4-1H-quinolone* : 6.16 (d, J = 7.4 Hz, 1 H, quinolone-H_3), 8.02 (dd, J_1 = 2.1 Hz, J_2 = 8.9 Hz, 1 H, quinolone-H_7), 8.10 (d, J = 7.3 Hz, 1 H, quinolone-H_2), 8.27 (d, J = 8.9 Hz, 1 H, quinolone-H_5), 8.41 (d, J = 2.1 Hz, 1 H, quinolone-H_8), 9.11 (s, 1 H, NH), *5-nitro-4-1H-quinolone* : most peaks overlaping with 7-nitro isomer signals.

7-Nitro-4-chloroquinoline[217]

(4f, DG-523B, DG-547A)

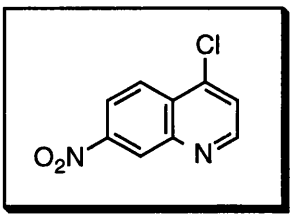

A mixture of 7-nitro-4-1H-quinolone and 5-nitro-4-1H-quinolone (**4d**, 0.692 g, 3.64 mmol) and phosphorous oxychloride (3 ml, 32.72 mmol) were heated together at 110° - 120°C under Ar for 2 h. The excess of $POCl_3$ was removed by vacuum distillation (using a water pump) and the residue was basified with conc. NH_4OH and extracted with CH_2Cl_2. After drying (Na_2SO_4) of the extracts, the solvent was removed in vacuo to yield a brown solid. This was purified by column chromatography on silica gel using petroleum spirit (40° - 60°C) : EtOAc = 4 : 1. The first product to be eluted was 7-nitro-4-chloroquinoline (0.468 g, 62%,white cottony crystals) and the second was 5-nitro-4-chloroquinoline (0.2 g, 26%, yellow solid).

mp = 177° - 179°C.

^{1}H NMR (200 MHz, $CDCl_3$, TMS, ppm) δ 7.70 (d, J = 4.7 Hz, 1 H, quinoline-H_3), 8.44 (d, J = 1.3 Hz, 2 H, quinoline-H_5 + H_8), 8.98 (d, J = 4.7 Hz, 1 H, quinoline-H_2), 9.05 (t, J = 1.4 Hz, 1 H, quinoline-H_6).

MS (EI) $[M]^+$ 208 fragments at m/z 162, 135, 126, 99.

5-Nitro-4-chloroquinoline

(4g, DG-523C)

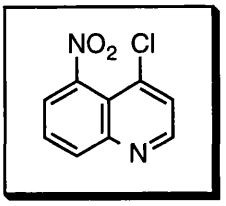

The synthesis is described under 7-nitro-4-chloroquinoline (**4f**).

^{1}H NMR (200 MHz, $CDCl_3$, TMS, ppm) δ 7.65 (d, J = 4.6 Hz, 1 H, quinoline-H_3), 7.81 (d, J = 3.5 Hz, 1 H, quinoline-H_6 or H_8), 7.82 (d, J = 6.6 Hz, 1 H, quinoline-H_8 or H_6), 8.34 (dd, J_1 = 3.4 Hz, J_2 = 6.4 Hz, 1 H, quinoline-H_7), 8.90 (d, J = 4.7 Hz, 1 H, quinoline-H_2).

MS (EI) $[M]^+$ 208 fragments at m/z 192, 173, 162, 135, 126, 99.

7-Nitro-4-(N-benzyl)aminoquinoline

(4h, DG-555B)

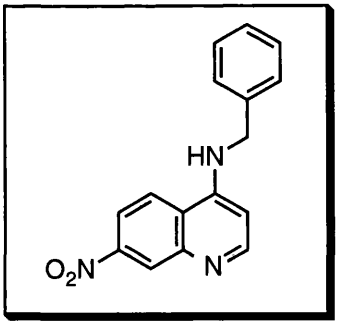

7-Nitro-4-chloroquinoline (**4f**, 0.2 g, 0.959 mmol) and benzylamine (0.103 g, 0.959 mmol) were heated under reflux in EtOH containing N,N,N',N'-tetramethylethylenediamine (0.123 g, 1.055 mmol) under Ar overnight. No reaction was observed by TLC, therefore, the solvent was removed in vacuo, the residue was dispersed in n-pentanol (10 ml), 4 equivalents of benzylamine were added and the solution was

heated under reflux under Ar for 18 h. After cooling to room temperature, excess of petroleum ether (40° - 60°C) was added and the solid was collected by filtration. The filtrate was concentrated to dryness in vacuo and the residue was purified by column chromatography on silica gel using petroleum ether : EtOAc = 1 : 2. The product (Rf = 0.3) was isolated as a yellow powder (0.13 g, 49%).

mp = 140° - 141°C.

^{1}H NMR (200 MHz, $CDCl_3$TMS, ppm) δ 4.57 (d, J = 5.1 Hz, 2 H, CH_2), 5.50 (s_{br}, 1 H, NH), 6.60 (d, J = 5.4 Hz, 1 H, quinoline-H_3), 7.42 (m, 5 H, Ph), 7.92 (d, J = 9.1 Hz, 1 H, quinoline-H_5), 8.20 (dd, J_1 = 2.4 Hz, J_2 = 9.2 Hz, 1 H, quinoline-H_6), 8.69 (d, J = 5.4 Hz, 1 H, quinoline-H_2), 8.88 (d, 2.3 Hz, 1 H, quinoline-H_8).

MS (FAB, MNOBA matrix) $[M+H]^+$ 280 fragments at m/z 264, 234, 91.

Anal. ($C_{16}H_{13}N_3O_2 \cdot 1.5H_2O$) calc: C = 62.74, H = 5.26, N = 13.72

found: C = 62.75, H = 4.96, N = 13.33

7-Amino-4-(N-benzyl)aminoquinoline

(4i, DG-563A)

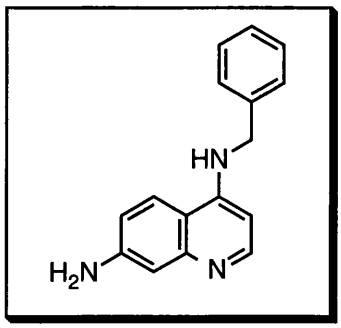

To a solution of 7-nitro-4-[(N-benzyl)amino]quinoline (**4h**, 0.1 g, 0.358 mmol) in 1 ml AcOH at room temperature, a suspension of $SnCl_2$ (0.296 g, 1.313 mmol) in conc. HCl (2 ml) / water (0.2 ml) was added and the mixture was heated at 65°C for 30 min. The solid dissolved on heating. On cooling to room temperature a precipitate formed. The reaction mixture was basified with 20% NaOH and extracted with 10 x 15 ml $CHCl_3$. The

extracts were combined, dried (Na_2SO_4) and the solvent removed in vacuo to yield a gum (0.089 g, 100%).

^1H NMR (200 MHz, $CDCl_3$, TMS, ppm) δ 3.99 (s_{br}, 2 H, NH_2), 4.51 (d, J = 5.3 Hz, 2 H, CH_2), 5.30 (s_{br}, 1 H, NH), 6.28 (d, J = 5.5 Hz, 1 H, quinoline-H_3), 6.86 (dd, J_1 = 2.3 Hz, J_2 = 8.9 Hz, 1 H, quinoline-H_6), 7.14 (d, J = 2.3 Hz, 1 H, quinoline-H_8), 7.39 (m, 5 H, Ph), 7.59 (d, J = 8.9 Hz, 1 H, quinoline-H_5), 7.41 (d, J = 5.3 Hz, 1 H, quinoline-H_2).

MS (FAB, MNOBA matrix) $[M+H]^+$ 250 fragment at m/z 144.

1,1'-(Decane-1,10-diyl)-bis-[7-amino-4-[(N-benzyl)amino]quinolinium] ditrifluoroacetate

(4, DG-589B, UCL 1560-F_2)

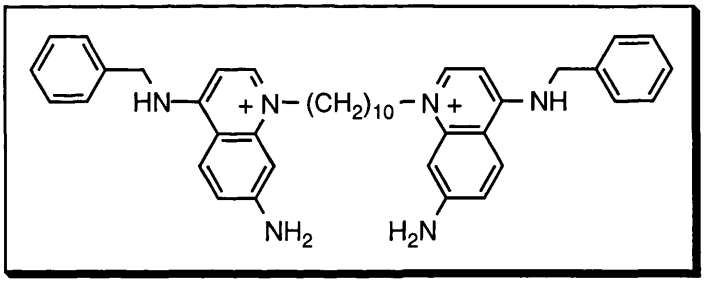

7-Amino-4-[(N-benzyl)amino]quinoline (**4i**, 0.08 g, 0.321 mmol) and 1,10-diiododecane (0.063 g, 0.16 mmol) were dissolved in 5 ml butanone and the solution heated under reflux for 60 h under Ar. A gum came out of solution which, after decanting of the solvent, was dried in vacuo to yield a foam (0.083 g, 58%). This was purified by preparative HPLC using a Lichrosorb RP SELECT B 7 μM column and **A** : **B** = 35 : 65 to yield a yellow - brown crystalline material.

mp = 113° - 115°C.

IR (KBr disc) ν_{max} 3359, 3200, 2919, 2852, 1685, 1621, 1558 cm^{-1}.

^1H NMR (400 MHz, DMSO-d_6, TMS, ppm) δ 1.29 (m, 12 H, CH_2), 1.73 (m, 4 H,

CH_2), 4.22 (t, J = 7.1 Hz, 4 H, N^+-CH_2), 4.70 (d, J = 5.9 Hz, 4 H, NH-$\underline{CH_2}$), 6.49 (d, J = 7.5 Hz, 2 H, quinoline-H_3), 6.65 (s, 4 H, NH_2), 6.83 (d, J = 1.8 Hz, 2 H, quinoline-H_8), 7.00 (dd, J_1 = 1.7 Hz, J_2 = 9 Hz, 2 H, quinoline-H_6), 7.28 (t, J = 6.6 Hz, 2 H, Ph-H_4'), 7.37 (m, 8 H, Ph), 8.25 (m, 4 H, quinoline-H_2 + H_5), 9.39 (t, 2 H, NH).

MS (FAB, MNOBA matrix) $[M-H]^+$ 637, fragment at m/z 311.

HPLC: column (L), A : B = 35 : 65, major peak at 4.88 min representing 94.8% of the absorption at 215 nm.

Anal. ($C_{42}H_{50}N_6^{2+}\cdot 2CF_3CO_2^-\cdot CF_3CO_2H\cdot 1.5CH_3CH_2OH\cdot 2H_2O$)

calc: C = 56.50, H = 5.95, N = 7.75

found: C = 56.20, H = 5.61, N = 7.49

4-[[N-(2,4,6-Trimethoxybenzyl)]amino]quinoline

(5a, DG-653A, DG-677B)

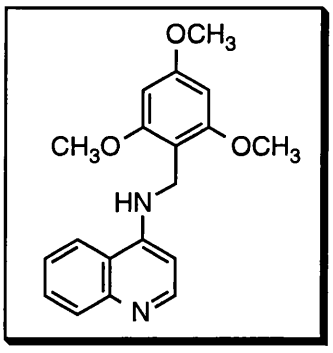

4-Chloroquinoline (**1a**, 0.7 g, 4.28 mmol), 2,4,6-trimethoxybenzylamine hydrochloride (2 g, 8.56 mmol) and DBU (1.95 g, 12.84 mmol) were dissolved in 15 ml dry DMSO and the solution was heated to 120°C for 30 h under Ar. The solvent was removed by vacuum distillation and the residue was partitioned between 50 ml 10% NaOH and 50 ml $CHCl_3$. The aqueous phase was extracted with another 50 ml of $CHCl_3$. The extracts were combined, dried (Na_2SO_4) and the solvent removed in vacuo to yield a gum. This was purified by column chromatography on silica gel using EtOAc : MeOH = 10 : 1. The

product (Rf = 0.3) was isolated as a creamy solid (0.72 g, 52%).

mp = 204° - 205°C.

^{1}H NMR (400 MHz, $CDCl_3$, ppm) δ 3.80 (s, 3 H, OCH_3), 3.85 (s, 6 H, OCH_3), 4.49 (d, J = 5.6 Hz, 2 H, N-CH_2), 5.54 (s_{br}, 1 H, NH), 6.14 (s, 2 H, Ph), 6.71 (d, J = 5.6 Hz, 1 H, quinoline-H_3), 7.37 (t, J = 7.1 Hz, 1 H, quinoline-H_6 or H_7), 7.58 (t, J = 7 Hz, 1 H, quinoline-H_7 or H_6), 7.66 (d, J = 8 Hz, 1 H, quinoline-H_5 or H_8), 7.94 (d, J = 8.1 Hz, 1 H, quinoline-H_8 or H_5), 8.52 (d, J = 5.6 Hz, 1 H, quinoline-H_2).

^{13}C NMR (100 MHz, $CDCl_3$, ppm) δ 36.0, 55.4, 55.8, 90.6, 99.1, 106.2, 118.9, 119.5, 124.4, 129.0, 129.3, 150.4, 150.5, 159.3, 161.1.

Anal. ($C_{19}H_{20}N_2O_3 \cdot 0.2CHCl_3$) calc: C = 66.22, H = 5.85, N = 8.04
found: C = 66.45, H = 5.98, N = 7.84

1,1'-(Decane-1,10-diyl)-bis-[4-[[N-(2,4,6-trimethoxybenzyl)]amino]-quinolinium] dibromide dihydrate
(5, DG-703C, UCL 1580-B_2)

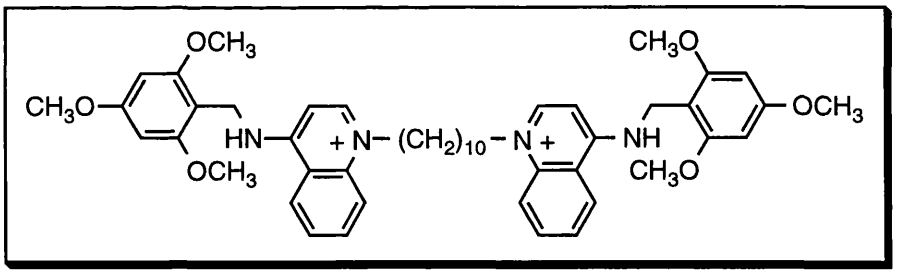

4-[[N-(2,4,6-Trimethoxybenzyl)]amino]quinoline (**5a**, 0.3 g, 0.92 mmol) and 1,10-dibromodecane (0.139 g, 0.46 mmol) were dissolved in 10 ml butanone and the solution was heated under reflux for 240 h. The white precipitate formed was collected by filtration and washed extensively with butanone. This was recrystallised from MeOH : EtOH = 2 : 1 to give a white solid. This was not sufficiently pure (by HPLC), therefore, it was recrystallised from MeOH to yield pure product (0.207 g, 47%).

mp = 163° - 164°C.

IR (KBr disc) ν_{max} 3412, 3199, 3092, 2930, 1611, 1451, 1224, 1200, 1151, 1131 cm^{-1}.

^1H NMR (400 MHz, DMSO-d_6, ppm) δ 1.19 - 1.25 (m, 12 H, CH_2), 1.75 (m, 4 H, CH_2), 3.78 (s, 6 H, OCH_3), 3.80 (s, 12 H, OCH_3), 4.47 - 4.53 (m, 8 H, NH-$\underline{CH_2}$ + N^+-CH_2), 6.29 (s, 4 H, Ph), 6.93 (d, J = 7.6 Hz, 2 H, quinoline-H_3), 7.69 (t, J = 7.6 Hz, 2 H, quinoline-H_6 or H_7), 7.98 (t, J = 7.9 Hz, 2 H, quinoline-H_7 or H_6), 8.10 (d, J = 8.7 Hz, 2 H, quinoline-H_5 or H_8), 8.65 (m, 4 H, quinoline -H_8 or H_5 + H_2), 9.30 (t_{br}, 2 H, NH).

^{13}C NMR (100 MHz, DMSO-d_6, ppm) δ 25.9, 28.6, 28.8, 28.9, 36.8, 53.8, 55.4, 56.0, 90.9, 98.3, 103.2, 117.6, 118.3, 124.3, 126.5, 133.8, 137.3, 146.5, 154.7, 159.3, 161.3.

MS (FAB, MNOBA matrix) $[M+^{81}Br]^+$ 569, $[M+^{79}Br]$ 867, $[M-H]^+$ 787, fragment at m/z 607.

HPLC: column (K), A : B = 35 : 65, major peak at 16.72 min representing 99.5% of the absorption at 215 nm.

Anal. ($C_{48}H_{60}N_4O_6Br_2 \cdot 2.6H_2O$) calc: C = 57.90, H = 6.60, N = 5.63
found: C = 57.88, H = 6.79, N = 5.49

4-(N-Phenyl-N-methyl)aminoquinoline hydrochloride

(6a, DG-711D)

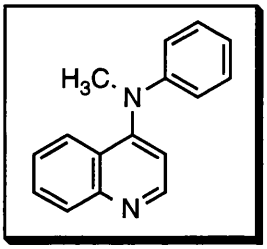

4-Chloroquinoline (**1a**, 0.77 g, 4.71 mmol) and freshly distilled N-methylaniline (0.63 g,

5.88 mmol) were dissolved in 10 ml glacial AcOH and the solution was heated under reflux for 3 h under Ar. The solvent was removed in vacuo, the residue basified with conc. NH_4OH and extracted with 3 x 40 ml $CHCl_3$. The extracts were combined, dried (Na_2SO_4) and the solvent removed in vacuo to yield an oil. This was purified by column chromatography on silica gel using EtOAc : petroleum ether = 1 : 1 until all the N-methylaniline had been eluted and then using EtOAc until all the product had been eluted. This was isolated as a yellow oil. This was still impure, therefore, it was converted to the hydrochloride salt using HCl/MeOH. Evaporation of the solvents gave an oil which upon trituration with toluene solidified. This was dissolved in MeOH (10 ml) and Et_2O was added until the solution became slightly cloudy. It was then placed at -20°C for 2 h. A dark solid precipitated. The supernatant was decanted into another flask, Et_2O was added until the solution became cloudy and placed at -20°C. The yellow crystals formed were collected, washed with Et_2O and dried (0.65 g, 51%). This was dissolved in water, basified with conc. NH_4OH and extracted with 4 x 20 ml CH_2Cl_2. The extracts were combined, dried ($MgSO_4$) and the solvent removed in vacuo to yield an oil (0.395 g).

mp = 216° - 218°C.

^1H NMR (400 MHz, $CDCl_3$, ppm) δ 3.69 (s, 3 H, CH_3), 7.01 (d, J = 6.7 Hz, 1 H, quinoline-H_3), 7.16 (m, 3 H, Ph), 7.22 (d, J = 8.8 Hz, 1 H, quinoline-H_5 or H_8), 7.36 (t, J = 7.1 Hz, 1 H, quinoline-H_6 or H_7), 7.44 (t, J = 7.9 Hz, 2 H, Ph), 7.66 (td, J_1 = 1.3 Hz, J_2 = 6.8 Hz, 1 H, quinoline-H_7 or H_6), 8.51 (d, J = 8.4 Hz, 1 H, quinoline-H_8 or H_5), 8.56 (d, J = 6.8 Hz, 1 H, quinoline-H_2).

Anal. ($C_{16}H_{14}N_2 \cdot HCl \cdot 0.1H_2O$) calc: C = 70.51, H = 5.62, N = 10.28

found: C = 70.34, H = 5.92, N = 10.11

1,1'-(Decane-1,10-diyl)-bis-[4-(N-phenyl-N-methyl)aminoquinolinium] diiodide hydrate

(6, DG-739B, UCL 1598-C_2)

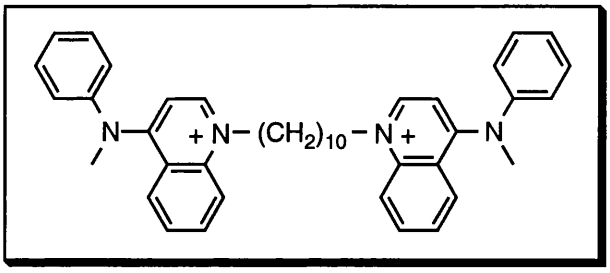

4-(N-Phenyl-N-methyl)aminoquinoline (**6a**, 0.395 g, 1.68 mmol) and 1,10-diiododecane (0.332 g, 0.84 mmol) were dissolved in butanone and heated under reflux for 168 h under Ar. The yellow solid formed was collected by filtration and washed with the solvent. It was recrystallised from a mixture of iPrOH : MeOH = 1 : 1 to yield yellow crystals (0.34 g, 47%).

mp = 208° - 209°C (dec).

IR (KBr disc) ν_{max} 3423, 3017, 2920, 2853, 1614, 1557, 1489 cm^{-1}.

^1H NMR (400 MHz, DMSO-d_6, ppm) δ 1.26 - 1.35 (m, 12 H, CH_2), 1.84 (m, 4 H, CH_2), 3.70 (s, 6 H, CH_3), 4.70 (t, J = 7.3 Hz, 4 H, N^+-CH_2), 7.37 (m, 10 H, Ar), 7.47 (m, 6 H, Ar), 7.89 (t, J = 7.2 Hz, 2 H, quinoline-H_6 or H_7), 8.22 (d, J = 9 Hz, 2 H, quinoline-H_8), 8.95 (d, J = 7.4 Hz, 2 H, quinoline-H_2).

^{13}C NMR (100 MHz, DMSO-d_6, ppm) δ 25.9, 28.6, 28.9, 29.0, 45.0, 54.7, 106.6, 118.8, 119.7, 125.4, 125.8, 127.4, 127.6, 130.5, 133.4, 138.6, 146.7, 147.9, 157.6.

MS (FAB, thioglycerol + glycerol + TFA matrix) $[M+I]^+$ 735, $[M-H]^+$ 607, fragments at m/z 721, 643, 593, 501, 359, 345, 331, 317, 303, 289, 275, 261, 247, 234, 219.

HPLC: column (K), A : B = 40 : 60, major peak at 12.15 min representing 100% of the absorption at 215 nm.

Anal. ($C_{42}H_{48}N_4I_2 \cdot H_2O$) calc: C = 57.28, H = 5.72, N = 6.36

found: C = 57.56, H = 5.63, N = 6.14

1,1'-(Decane-1,10-diyl)-bis-(4-quinolone)

(7, DG-467A, UCL1507)

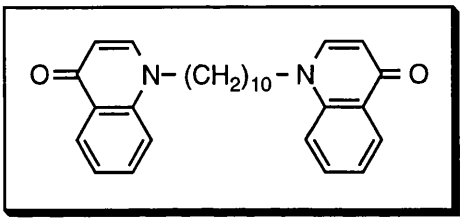

1,1'-(Decane-1,10-diyl)-bis-(4-aminoquinolinium) diiodide (**10**, 0.28 g, 0.446 mmol) was dispersed in 10 ml of a 50% solution of NaOH in water and MeOH was added to help dissolution. The mixture was heated under reflux for 48 h. After cooling to room temperature, it was extracted with 8 x 30 ml CH_2Cl_2. After drying and evaporation of the solvent a yellowish solid was obtained. This was recrystallised from CH_2Cl_2/EtOAc to yield a yellowish solid (0.15 g, 79%).

mp = 155° - 157°C.

IR (KBr disc) ν_{max} 3439, 3039, 2919, 2845, 1621, 1604, 1581, 1478 cm^{-1}.

^1H NMR (400 MHz, $CDCl_3$, TMS, ppm) δ 1.26 - 1.34 (m, 12 H, CH_2), 1.84 (quint, 4 H, CH_2), 4.11 (t, J = 7.2 Hz, 4 H, N-CH_2), 6.28 (d, J = 7.7 Hz, 2 H, quinoline-H_3), 7.38 (t, J = 7.5 Hz, 2 H, quinoline-H_6 or H_7), 7.42 (d, J = 8.6 Hz, 2 H, quinoline-H_5 or H_8), 7.53 (d, J = 7.7 Hz, 2 H, quinoline-H_2), 7.66 (td, J_1 = 1.6 Hz, J_2 = 7.8 Hz, 2 H, quinoline-H_7 or H_6), 8.47 (dd, J_1 = 1.6 Hz, J_2 = 8.1 Hz, 2 H, quinoline-H_8 or H_5).

MS (EI) $[M]^+$ 428, fragments at m/z 284, 270, 256, 242, 228, 214, 200, 186, 172, 158, 145.

HPLC: column (L), C : D = 35 : 65, major peak at 12.19 min representing 98.7% of the

absorption at 215 nm.

Anal. ($C_{28}H_{32}N_2O_2 \cdot 0.2H_2O$) calc: C = 77.82, H = 7.56, N = 6.48

found: C = 77.66, H = 7.66, N = 6.33

Genaral procedure for the preparation of 1,10-bis-(2-methylquinolin-4-yl)-diaminodecane[287,288] (15, DG-13C, 43B, UCL 1417) and 1,12-bis-(2-methylquinolin-4-yl)-diaminododecane[287,288] (36, DG-23B, UCL 1407)

4-chloroquinaldine (2 g, 11.26 mmol) and the corresponding diamine (1,8-diaminooctane, 1,10-diaminodecane or 1,12-diaminododecane, 5.68 mmol) were disolved with heating in 30 ml of n-pentanol. The solution was heated under reflux for 30 h. On cooling a creamy precipitate formed, which was collected by vacuum filtration and dried under vacuum at 50°C. This was dissolved in methanol, the solution was made alkaline by addition of NaOH (10% in water), excess of water was added and the mixture was kept at 4°C overnight. The precipitate formed was collected by vacuum filtration, washed well with water and dried under high vacuum over P_2O_5.

1,10-bis-(2-methylquinolin-4-yl)-diaminodecane[287,288] (84%)

(15, DG-13C, DG-43B, UCL 1417)

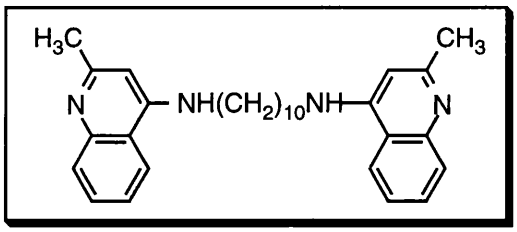

mp = 188°-190°C.

IR (nujol mul) ν_{max} 3230 (N-H_{ar} str), 1585,1560 (C=C_{ar} str) cm^{-1}.

^1H NMR (400 MHz, $CDCl_3$) δ 1.35, 1.48 (m, 12 H, -CH_2-), 1.75 (quin, 4 H, -CH_2-), 2.61 (s, 6 H, -CH_3), 3.29 (q, 4 H, -CH_2-), 4.93 (s_{br}, 2 H, N-H), 6.32 (s, 2 H, quin-

H_3), 7.36 (t, 2 H, quin-H_6 or quin-H_7), 7.59 (t, 2 H, quin-H_7 or quin-H_6), 7.67 (d, 2 H, quin-H_5), 7.90 (d, 2 H, quin-H_8).

MS (EI) $[M]^+$ 454, fragments at m/z 297, 283, 269, 255, 241.

Anal. ($C_{30}H_{38}N_4 \cdot 0.55$ MeOH) calc: C = 77.69, H = 8.58, N = 11.86

found: C = 77.71, H = 8.66, N = 11.83

1,1'-(3-iodopropylidene)-bis-benzene

(16a, DG-77A)

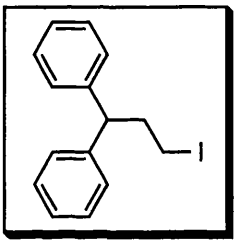

To a stirred and cooled to 0°C solution of 3,3-diphenyl-1-propanol (2.5 g, 11.78 mmol) in dry dichloromethane triphenylphosphine (3.243 g, 12.36 mmol) and iodine (3.048 g, 12.01 mmol) were successively added. The work was carried out under an atmosphere of argon. The orange solution was stirred for 15 min and an orange precipitate formed. Imidazole (1.042 g, 15.31 mmol) was added, the color dissapeared and a white precipitate formed. The reaction mixture was stirred at 0°C for 30 min and then was heated under reflux for 2 h. After cooling to RT, the reaction mixture was washed with 20 ml of water and the water layer extracted with 20 ml dichloromethane. The dichloromethane extracts were combined, dried with Na_2SO_4 and rotary evaporated to dryness to yield a white solid. The iodide was purified by column chromatography (silica, Pet. spirit 30°-40°C : CH_2Cl_2 = 5 : 1) and was isolated as a white solid (2.910 g, 76.7%).

mp = 54°-55°C.

^{1}H NMR (200 MHz, $CDCl_3$) δ 2.49 (q, 2 H, -CH_2-), 3.02 (t, 2 H, -CH_2-I), 4.04 (t, 1 H, Ph_2-CH), 7.09-7.28 (m, 10 H, Ph).

MS (EI) $[M]^+$ 322, fragments at m/z 245, 168, 167, 155, 141, 127.

1,10-bis-{N,N'-[1-(3,3-diphenylprop-1-yl)-2-methylquinolinium-4-yl]}diaminodecane ditrifluoroacetate

(16, DG-81D, UCL 1436-F_2)

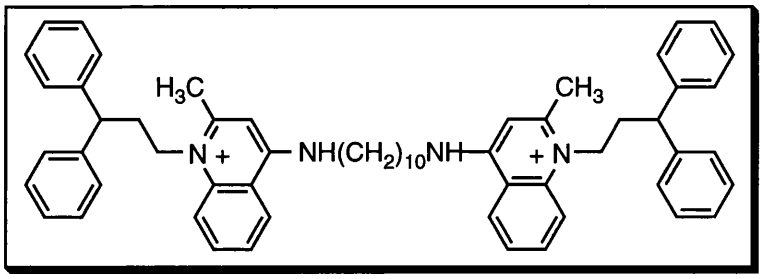

15 (0.3 g, 0.66 mmol) and **16a** (0.5 g, 1.552 mmol) were dissolved with heating in 10 ml of 4-methylpentan-2-ol and the solution was heated under reflux for 120 h under argon, more iodide being added after 36 h (0.2 g, 0.621 mmol) and 60 h (0.2 g, 0.621 mmol). On cooling, a red solid came out of solution, which was collected by filtration, washed with the solvent and dried. This was shown (MS, HPLC) to contain mainly the desired product together with some of the monoquaternary compound. Attempts to purify it by crystallisation failed, therefore, it was purified by preparetive HPLC. The product was isolated as a pink oil which was disolved in the minimum amount of cold isopropanol, filtered and the solvent removed in vacuo to yield a pink oil. This solidified after drying in vacuo over P_2O_5 (0.22 g, 30.3%).

mp = 77°-78°C.

IR (nujol mul) 3280 (N-H_{ar} str), 1610, 1570 (C=C_{ar} str) cm^{-1}.

^1H NMR (400 MHz, DMSO-d_6) δ 1.28 (m, 12 H, -CH_2-), 1.64 (q, 4 H, -CH_2-), 2.56 (m, 10 H, -CH_2-,-CH_3), 3.46 (q, 4 H, NH-CH_2-), 4.29 (t, 6 H, Ph_2CH,-CH_2-N^+), 6.87 (s, 2 H, quin-H_3), 7.20 (t, 4 H, Ph-H_p), 7.30 (t, 8 H, Ph-H_m), 7.39 (d, 8 H, Ph-H_o), 7.70 (t, 2 H, quin-H_6 or quin-H_7), 7.93 (t, 2 H, quin-H_7 or quin-H_6), 7.98 (d, 2 H, quin-H_5), 8.48 (d, 2 H, quin-H_8), 9.10 (t, 2 H, N-H).

MS (FAB, matrix GLYCEROL + THIOGLYCEROL + TFA) $[M]^+$ 844, fragments at m/z 649, 422, 380, 365, 200, 185.

HPLC: column (K), A : B = 25 : 75, major peak at 18.35 min representing 99.6% of the absorption at 215 nm.

Anal. ($C_{64}H_{68}F_6N_4O_4 \cdot 0.4HI \cdot 0.4CF_3COOH \cdot H_2O$)

calc: C = 65.62, H = 6.02, N = 4.72, I = 4.28

found: C = 65.55, H = 5.96, N = 4.97, I = 4.64

3,5-dimethoxybenzyl iodide

(17a, DG-105B)

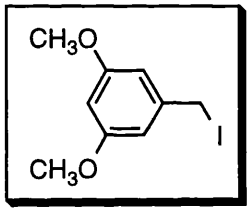

3,5-Dimethoxybenzyl chloride (0.5 g, 2.68 mmol) and dry sodium iodide (0.44 g, 2.94 mmol) were dissolved in 10 ml of dry (K_2CO_3) acetone and the solution heated to 50°C for 3 h. The solvent was removed in vacuo and the residue treated with dichloromethane and filtered in order to remove the NaCl formed and the excess of NaI. The filtrate was concentrated to dryness and the last traces of solvents removed under vacuum to yield a yelowish solid.

mp = 84°-85°C.

^1H NMR (200 MHz, $CDCl_3$) δ 3.77 (s, 6 H, $-CH_3$), 4.37 (s, 2 H, $-CH_2-$), 6.31 (m, 1 H, Ph-H_4), 6.51 (d, J=2.25 Hz, 2 H, Ph-H_2, Ph-H_6).

1,10-N,N-bis-[1-(3,5-dimethoxybenzyl)-2-methylquinolinium-4-yl]diaminodecane ditrifluoroacetate

(17, DG-115C, UCL 1438-F_2)

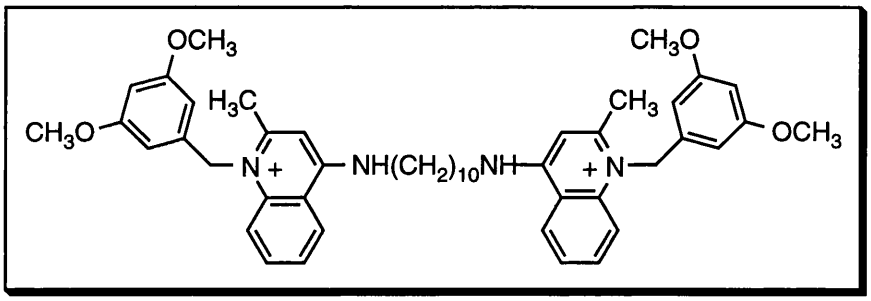

15 (0.3 g, 0.66 mmol) and **17a** (0.367 g, 1.32 mmol) were dissolved with heating in 10 ml of previously dried (molecular sieves 4Å) nitrobenzene and the solution was heated under argon in an oil bath at 100°-120°C for 144 h. The reaction mixture was cooled to RT and dry ether was added until the solution became cloudy. The creamy precipitate formed was collected by filtration, washed three times with EtOH and dried under vacuum at 60°C over P_2O_5. The later was a mixture of the mono- and diquaternary compounds, which were separated by preparative HPLC. The product was isolated as a creamy oil which solidified after drying in vacuo.

mp = 96°-98°C melts, 115°-119°C solidifies, 213°-215°C melts.

IR (nujol mull) ν_{max} 3200 (N-H_{ar} str), 1685,1605 (C=C_{ar} str), 1200 (C_{ar}-O-C_{al} str, asymetric), 1015 (C_{ar}-O-C_{al} str, symetric) cm^{-1}.

^1H NMR (400 MHz, DMSO-d_6) δ 1.30-1.45 (m, 12 H, -CH_2-), 1.71 (quint, 4 H, -CH_2-), 2.72 (s, 6 H, -CH_3), 3.54 (q, overlaps with water signal, N-CH_2-), 3.67 (s, 12 H, O-CH_3), 5.74 (s, 4 H, -CH_2-N^+), 6.14 (d, 4 H, Ph-H_o), 6.44 (t, 2 H, Ph-H_p), 7.04 (s, 2 H, quin-H_3), 7.69 (m, 2 H, quin-H_6 or quin-H_7), 7.90 (d, 4 H, quin-H_5, quin-H_7 or quin-H_5, quin-H_6), 8.58 (d, 2 H, quin-H_8), 9.30 (t, 2 H, N-H).

MS (FAB, matrix glycerol + thioglycerol + TFA) $[M]^+$ 756, fragments at m/z 605, 335, 185, 151.

HPLC: column (K), A : B = 35 : 65, major peak at 34.83 min representing 99.6% of the absorption at 215 nm.

Anal. ($C_{52}H_{60}N_4F_6O_8 \cdot 0.5CF_3CO_2H$) calc: C = 61.21, H = 5.86, N = 5.39
found: C = 61.12, H = 6.03, N = 5.30

1,10-[N,N'-[bis-(1-benzyl-2-methylquinolinium-4-yl)]]diaminodecane ditrifluoroacetate

(18, DG-127C, UCL 1439-F_2)

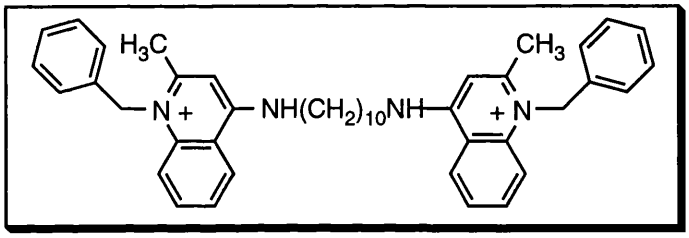

15 (0.3 g, 0.66 mmol) was dissolved with heating in 10 ml of previously dried (molecular sieves 4A) nitrobenzene and benzylbromide (0.288 g, 1.68 mmol) was added. The solution was heated in an oil bath under argon at 100°-120°C for 96 h and then at 120°-140°C for 12 h. More benzylbromide was added after 48 h (0.144 g, 0.84 mmol) and 72 h (0.144 g, 0.84 mmol). The reaction mixture was cooled to RT, excess of ether was added and a gum came out of solution. The supernatant solution was decanted and the gum washed several times with ether. This consisted mainly of the mono- and the diquaternary products which were separated by preparative HPLC. The product was isolated as a green oil which solidified after drying under vacuum.

mp = 58°-60°C.

IR (nujol mul) ν_{max} 3252 (N-H_{ar} str), 1688, 1608 (C=C_{ar} str) cm^{-1}.

^1H NMR (400 MHz, DMSO-d_6) δ 1.31-1.40 (m, 12 H, -CH_2-), 1.71 (quint, 4 H, -CH_2-), 2.73 (s, 6 H, -CH_3), 3.54 (q, 4 H, N-CH_2-), 5.84 (s, 4 H, -CH_2-N^+), 7.05 (d, 6 H, C_3-H, Ph-H_o), 7.29 (t, 2 H, Ph-H_p), 7.35 (t, 4 H, Ph-H_m), 7.69 (t, 4 H, quin-H_6 or

quin-H_7), 7.88 (t, 2 H, quin-H_7 or quin-H_6), 7.93 (d, 2 H, quin-H_5), 8.56 (d, 2 H, quin-H_8), 9.31 (t, 2 H, N-H).

MS (FAB, matrix MNOBA) $[M-H]^+$ 635.

HPLC: column (K), A : B = 35 : 65, major peak at 19.42 min representing 100% of the absorption at 215 nm.

Anal. ($C_{48}H_{52}N_4F_6O_8 \cdot 1.2CF_3CO_2H$) calc: C = 60.55, H = 5.36, N = 5.60

found: C = 60.53, H = 5.34, N = 5.57

1-N-[1-(3,5-dimethoxybenzyl)-2-methylquinolinium-4-yl]-10-N-(2-methylquinolinium-4-yl)diaminodecane ditrifluoroacetate (19, DG-115B, UCL 1440-F_2)

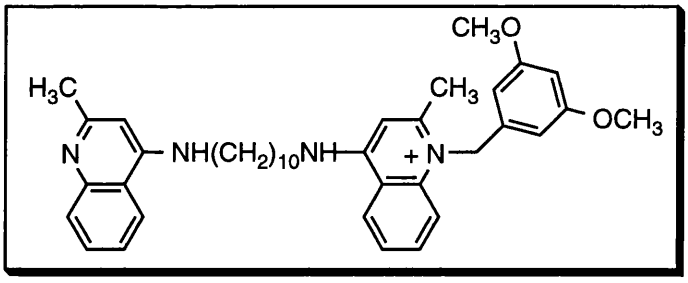

The preparation is described under **17**. The product was isolated as a creamy oil which solidified after drying at high vacuum.

mp = 77°-78°C.

IR (nujol mul) ν_{max} 3270 (N-H_{ar} str), 1685,1605 (C=C_{ar} str), 1200 (C_{ar}-O-C_{al} str, asymetric), 1070 (C_{ar}-O-C_{al} str, symetric) cm^{-1}.

^1H NMR (400 MHz, DMSO-d_6) δ 1.34-1.38 (m, 12 H, -CH_2-), 1.72 (m, 4 H, -CH_2-), 2.62 (s, 3 H, -CH_3´), 2.72 (s, 3 H, -CH_3´), 3.53 (m, 4 H, N-CH_2-), 3.67 (s, 6 H, O-CH_3), 5.74 (s, 2 H, -CH_2-N^+), 6.15 (s, 2 H, Ph-H_o), 6.44 (s, 1 H, Ph-H_p), 6.78 (s, 1 H, quin-H_3´), 7.04 (s, 1 H, quin-H_3), 7.64-7.70 (m, 2 H, quin-H_6, quin-H_6´ or quin-

H_7, quin-H_7'), 7.81 (d, 1 H, quin-H_5'), 7.90 (m, 3 H, quin-H_5, quin-H_7, quin-H_7' or quin-H_5, quin-H_6, quin-H_6'), 8.45 (d, 1 H, quin-H_8'), 8.55 (d, 1 H, quin-H_8), 9.04 (t, 1 H, N-H'), 9.30 (t, 1 H, N-H).

MS (FAB, matrix glycerol + thioglycerol + TFA) $[M]^+$ 605, fragments at m/z 455, 185, 171, 151.

HPLC: column (K), A : B = 35 : 65, major peak at 14.71 min representing 99.5% of the absorption at 215 nm.

Anal. ($C_{41}H_{50}N_4F_6O_8 \cdot 0.5CF_3CO_2H$) calc: C = 59.39, H = 5.72, N = 6.30
found: C = 59.31, H = 5.60, N = 6.20

1,1'-dimethyl-4,4'-(dodecan-1,12-diyl)-bis-quinolinium diiodide (20, DG-167A, UCL 1445-C_2)

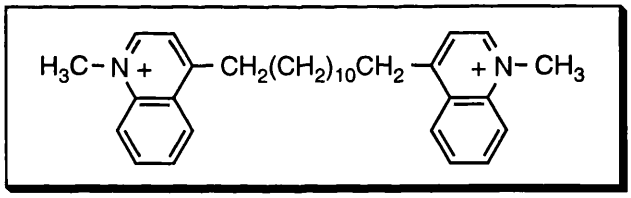

24 (0.2 g, 0.47 mmol) and MeI (2 ml, 32.13 mmol) were dissolved in 40 ml MEK and the solution was heated under reflux for 4 h under argon. The reaction mixture was cooled to RT, the yellow solid collected by filtration, washed with the solvent and dried under vacuum (0.284 g, 85%).

mp = 156°-158°C.

IR (KBr disc) ν_{max} 3040 (C-H_{ar} str), 3000 (C-H_{ar} str), 2910 (C-H_{al} str), 2840 (C-H_{al} str), 1605 (C=C_{ar} str), 1600 (C=C_{ar} str), 1580 (C-H_{al} bend), 1440 (C-H_{al} bend) cm^{-1}.

^1H NMR (400 MHz, DMSO-d_6) δ 1.25 (m, 8 H, -CH_2-), 1.32 (m, 4 H, -CH_2-), 1.41 (m, 4 H, -CH_2-), 1.73 (m, 4 H, -CH_2-), 3.34-3.38 (m, Ar-CH_2-, water), 4.57 (s, 6 H, N^+-CH_3), 8.03-8.07 (m, 4 H, quin-H_3, quin-H_6 or quin-H_7), 8.27 (t, 2 H, quin-H_7 or

quin-H_6), 8.49 (d, 2 H, quin-H_5), 8.60 (d, 2 H, quin-H_8), 9.36 (d, 2 H, quin-H_2).

MS (FAB, matrix MNOBA + Li + Na) $[M-H]^+$ 453, fragments at m/z 438, 412, 170.

HPLC: column (K), A : B = 35 : 65, major peak at 5.23 min representing 99.2% of the absorption at 215 nm.

Anal. ($C_{32}H_{42}N_2I_2$) calc: C = 54.25, H = 5.98, N = 3.95
found: C = 54.38, H = 6.00, N = 3.88

1-[N-(1-benzyl-2-methylquinolinium-4-yl)]-10-(N'-2-methylquinolinium-4-yl)-diaminodecane ditrifluoroacetate

(21, DG-127B, UCL 1454-F_2)

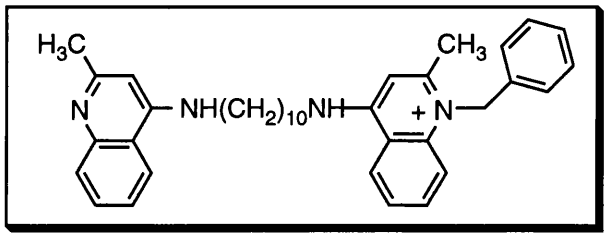

The preparation is described under **18**. The compound was isolated as a greenish oil which solidified after drying under vacuum.

mp = 72°-74°C.

IR (KBr disc) ν_{max} 3252 (N-H_{ar} str), 1684, 1604 (C=C_{ar} str) cm^{-1}.

^1H NMR (400 MHz, DMSO-d_6) δ 1.30 (m, 12 H, -CH_2-), 1.70 (quint, 4 H, -CH_2-), 2.64 (s, 3 H, -CH_3'), 2.74 (s, 3 H, -CH_3), 2.48 (q, 2 H, N-CH_2-'), 2.55 (q, 2 H, N-CH_2-), 5.85 (s, 2 H, -CH_2-N^+), 6.79 (s, 1 H, quin-H_3'), 7.06 (d, 3 H, quin-H_3, Ph-H_o), 7.30 (t, 1 H, Ph-H_p), 7.36 (t, 2 H, Ph-H_m), 7.67 (m, 2 H, quin-H_6, quin-H_6', or quin-H_7, quin-H_7'), 7.83 (d, 1 H, quin-H_5'), 7.89 (t, 2 H, quin-H_7, quin-H_7', or quin-H_6, quin-H_6'), 7.94 (d, 1 H, quin-H_5), 8.46 (d, 1 H, quin-H_8'), 8.56 (d, 1 H, quin-H_8), 9.06 (t, 1 H, N-H'), 9.32 (t, 1 H, N-H).

MS (FAB, matrix MNOBA) $[M-H]^+$ 544.

HPLC: column (K), A : B = 35 : 65, major peak at 9.52 min representing 96.8% of the absorption at 215 nm.

Anal. ($C_{41}H_{46}N_4F_6O_8 \cdot 0.5CF_3CO_2H$) calc: C = 60.52, H = 5.62, N = 6.71

found: C = 60.52, H = 5.75, N = 6.35

S,S'-(Decane-1,10-diyl)-bis-(1-methyl-4-mercaptoquinolinium) diiodide hydrate

(22, DG-223A, UCL 1467-C_2)

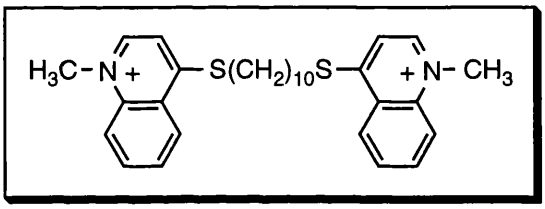

S,S'-(Decane-1,10-diyl)-bis-(4-mercaptoquinoline) (**23**, 0.124 g, 0.27 mmol) and methyl iodide (2 ml, 32.13 mmol) were dissolved in 20 ml of butanone and the solution was heated under reflux for 4 h under Ar. A yellow precipitate formed which, after cooling to room temperature, was collected by vacuum filtration, washed with butanone and dried in vacuo (0.172 g, 86%).

mp = 196° - 198°C.

^1H NMR (400 MHz, DMSO-d_6, TMS) δ 1.32 (m, 8 H, -CH_2-), 1.51 (quint, 4 H, -CH_2-), 1.79 (quint, 4 H, -CH_2-), 3.46 (t, 4 H, S-CH_2), 4.48 (s, 6 H, N^+-CH_3), 7.96 - 8.03 (m, 4 H, quinoline), 8.25 (t, 2 H, quinoline-H_7 or H_6), 8.43 (d,d, 4 H, quinoline-H_5 + H_8), 9.14 (d, 2 H, quinoline-H_2).

MS (FAB, matrix MNOBA) $[M-H]^+$ 489, fragments at m/z 475, 315, 300, 286, 272, 258, 245, 230, 216, 202, 189, 175, 143.

HPLC: column (K), A : B = 40 : 60, major peak at 14.13 min representing 100% of the absorption at 215 nm.

Anal. ($C_{30}H_{38}N_2S_2I_2 \cdot H_2O$) calc: C = 47.25, H = 5.29, N = 3.67
found: C = 47.29, H = 5.23, N = 3.41

1,1'-(Decane-1,10-diyl)-bis-isothiuronium dihydrochloride[289]
(23a, DG-215A)

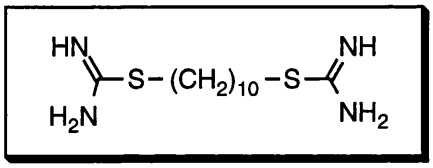

1,10-Dichlorodecane (3 g, 14.21 mmol) and thiourea (2.163 g, 28.41 mmol) were dissolved in 20 ml absolute EtOH and the solution was heated under reflux for 13 h. The mixture was cooled to room temperature and then in an ice bath. Et_2O was added and the white precipitate was collected by vacuum filtration, washed with Et_2O and dried in vacuo at 40°C for 2 h.

^1H NMR (200 MHz, DMSO-d_6, TMS) δ 1.27 (m, 12 H, -CH_2-), 1.59 (m, 4 H, -CH_2-), 3.17 (t, 4 H, S-CH_2-), 9.25 (s_{br}, 2 H, NH, exchanges on D_2O treatment).

S,S'-(Decane-1,10-diyl)-bis-(4-mercaptoquinoline)
(23, DG-219B, UCL 1601)

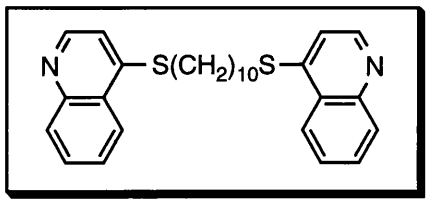

1,1'-(Decane-1,10-diyl)-bis-isothiuronium dihydrochloride (**23a**, 0.788 g, 2.17 mmol), 4-chloroquinoline (**1a**, 0.71 g, 4.34 mmol) and KOH (0.789 g, 14.06 mmol) were

dissolved with heating in 30 ml abs. EtOH and the solution was heated under reflux for 3 h. The white precipitate formed was removed by vacuum filtration while the solution was still warm. The filtrate was concentrated to dryness in vacuo, dispersed in water and extracted with 5 x 50 ml CH_2Cl_2. The extracts were combined, dried with K_2CO_3 and the solvent removed in vacuo to yield a yellow oil. This was dissolved in the minimum amount of EtOAc, excess of petroleum spirit was added and the white solid formed was collected by filtration and washed with EtOAc. This was recrystallised from EtOAc to yield a white hygroscopic powder (0.518 g, 52%).

mp = 96° - 97°C.

IR (KBr disc) ν_{max} 2924, 2852, 1562, 1498, 1379 cm^{-1}.

^1H NMR (400 MHz, $CDCl_3$, TMS) δ 1.34 (m, 8 H, $-CH_2-$), 1.52 (quint, 4 H, $-CH_2-$), 1.82 (quint, 4 H, $-CH_2-$), 3.10 (t, 4 H, $S-CH_2$), 7.17 (d, 2 H, quinoline-H_3), 7.54 (t, 2 H, quinoline-H_6 or H_7), 7.71 (t, 2 H, quinoline-H_7 or H_6), 8.06 (d, 2 H, quinoline-H_5), 8.13 (d, 2 H, quinoline-H_8), 8.71 (d, 2 H, quinoline-H_2).

MS (FAB, matrix MNOBA) $[M+H]^+$ 461, fragments at m/z 332, 300, 286, 272, 258, 244, 230, 216, 188, 175, 162, 129.

TLC : Silica plates, EtOAc, Rf = 0.38

HPLC: column (K), A : B = 30 : 70, major peak at 7.06 min representing 98.2% of the absorption at 215 nm.

Anal. ($C_{28}H_{32}N_2S_2 \cdot 0.7H_2O$) calc: C = 71.06, H = 7.11, N = 5.92

found: C = 71.13, H = 7.29, N = 5.64

4,4´-(dodecan-1,12-diyl)-bis-quinoline

(24, DG-159B, UCL 1602)

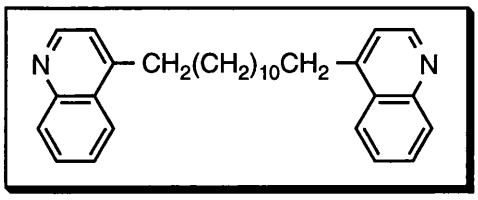

Na (0.482 g, 20.96 mmol) was dispersed in liquid ammonia containing a catalytic amount of $Fe(NO_3)_3$ under argon. When the dark blue colour of the suspension turned grey, lepidine (3 g, 20.95 mmol) was added and the reaction mixture was stirred for 1 h. 1,10-dibromodecane (2.075 g, 6.91 mmol) was then gradualy added and the ammonia was allowed to evaporate overnight. Water was added to the residue and the aqueous phase extracted with ether. The extracts were combined, dried (Na_2SO_4) and concentrated to dryness in vacuo to yield an oil which contained mainly lepidine and the title compound. The later was purified by column chromatography and was isolated as a yellow oil. This was dissolved in the minimum amount of hot MeOH and placed at -20°C. White crystalls separated which were collected by filtration, washed with cold MeOH and dried under vacuum (1.275 g, 43.4%).

mp = 50°-51°C.

IR (KBr disc) ν_{max} 2924, 2850, 1593, 1570, 1467 cm^{-1}.

^1H NMR (400 MHz, $CDCl_3$) δ 1.27-1.36 (m, 12 H, $-CH_2-$), 1.43 (quin, 4 H, $-CH_2-$), 1.76 (quin, 4 H, $-CH_2-$), 3.08 (t, 4 H, Ar-CH_2-), 7.27 (d, 2 H, quin-H_3), 7.58 (t, 2 H, quin-H_6 or quin-H_7), 7.73 (t, 2 H, quin-H_7 or quin-H_6), 8.06 (d, 2 H, quin-H_5), 8.18 (d, 2 H, quin-H_8), 8.80 (d, 2 H, quin-H_2).

MS (FAB, matrix MNOBA) $[M+H]^+$ 425.

TLC : Silica plates, EtOAc, Rf = 0.52.

HPLC: column (K), A : B = 35 : 65, major peak at 10.16 min representing 97.3% of the

absorption at 215 nm.

Anal. ($C_{30}H_{36}N_2$) calc: C = 84.86, H = 8.55, N = 6.60

found: C = 84.59, H = 8.62, N = 6.43

5-Iodo-1-pentyne

(31a, DG-95A)

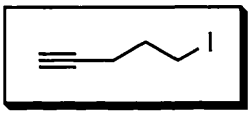

5-Chloro-1-pentyne (0.5 g, 48.7 mmol) and dry sodium iodide (0.731 g, 48.7 mmol) were dissolved in 10 ml of MEK previously dried with anhydrous K_2CO_3. The solution was heated under reflux overnight under argon and then cooled to 20°C. NaCl was removed by filtration and the filtrate was evaporated to dryness to yield an oil. This was used directly for the next reaction.

1-(4-Pentyn-1-yl)-2-methyl-4-aminoquinolinium iodide

(31b, DG-99B)

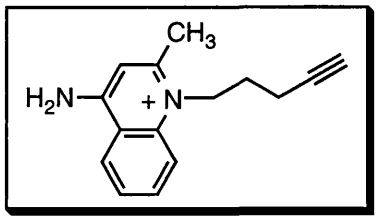

4-Aminoquinaldine (0.7 g, 4.42 mmol) and the previously prepared 5-iodo-1-pentyne (**31a**) were dissolved in 25 ml of hot diisobutyl ketone and the solution heated to 120°-140°C under argon for 96 h. The reaction mixture was cooled to RT and the dark solid collected by filtration and dried under vacuum. This was dissolved in MeOH, adsorbed

onto silica and chromatographed using 10% MeOH in EtOAc. The fractions containing the product were combined, the solvents removed in vacuo to yield a dark red oil (1.1 g, 70.6%) which was recrystallised form MeOH - Et_2O to yield a pink solid.

mp = 193°-195°C.

IR (nujol mul) ν_{max} 3305, 3260, 1640, 1600 cm^{-1}

^1H NMR (400 MHz, DMSO-d_6) δ 1.92 (quin, 2 H, $-CH_2-$), 2.42 (t_{br}, 2 H, $-CH_2-$), 2.73 (s, 3 H, $-CH_3$), 2.97 (s, 1 H, ≡C-H), 4.52 (t, J = 8.2 Hz, 2 H, N^+-CH_2-), 6.71 (s, 1 H, quinoline-H_3), 7.72 (t, J = 7.6 Hz, 1 H, quinoline-H_6 or H_7), 8.02 (t, J = 7.6 Hz, 1 H, quinoline-H_7 or H_6), 8.19 (d, J = 8.9 Hz, 1 H, quinoline-H_5 or H_8), 8.43 (d, J = 8.1 Hz, 1 H, quinoline-H_8 or H_5), 8.84 (d_{br}, 2 H, NH_2).

MS (chemical ionization using NH_3) M^+ 225, fragment at m/z 159.

Anal. ($C_{15}H_{17}N_2I \cdot 0.25\ H_2O$) calc: C = 50.51, H = 4.94, N = 7.85, I = 35.57
found: C = 50.57, H = 4.75, N = 7.83, I = 34.98

1,1´-(Deca-4,6-diyn-1,10-diyl)-bis-(4-amino-2-methylquinolinium) diiodide hydrate

(31, DG-109A, UCL 1437)

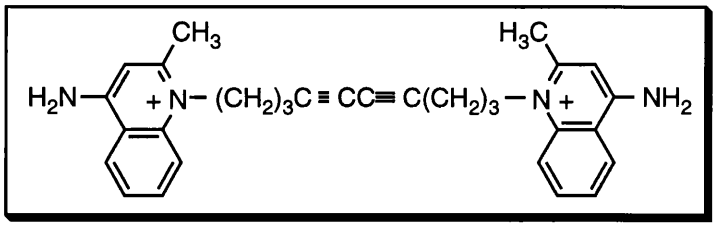

N,N,N',N'-Tetramethylethylenediamine (0.5 g, 4.3 mmol) and CuCl (0.42 g, 4.25 mmol) were dispersed with vigorous stirring in 100 ml of isopropanol. The solution turned deep blue and some solid remained undissolved. After allowing the solid to precipitate, 2 ml of the supernatant solution were added to a solution of 1-(4-pentyn-1-yl)-2-methyl-4-amino-quinolinium iodide (**31b**, 0.1 g, 0.284 mmol) in a mixture of

isopropanol : MeOH = 4 : 1. The solution was rapidly decolourised. Oxygen was bubbled through with vigorous stirring for 2 h, while the reaction mixture was kept in a water bath of 40°C. The bubbling of oxygen was stopped and the solution was stirred vigorously for another 48 h. The reaction mixture was concentrated to a small volume, the creamy precipitate formed was collected, washed with MeOH and dried in vacuo (0.07 g, 70%).

mp = 295°-297°C (dec).

IR (nujol mul) ν_{max} 3320, 3295, 1640, 1600 cm^{-1}.

^1H NMR (400 MHz, DMSO-d_6) δ 1.95 (q, 4 H, $-CH_2-$), 2.58 (t, J = 6.9 Hz, 4 H, $-CH_2-$), 2.73 (s, 6 H, $-CH_3$), 4.50 (t, J = 8.1 Hz, 4 H, N^+-CH_2-), 6.71 (s, 2 H, quinoline-H_3), 7.72 (t, J = 7.6 Hz, 2 H, quinoline-H_6 or H_7), 8.01 (t, J = 8.5 Hz, 2 H, quinoline-H_7 or H_6), 8.18 (d, J = 9.0 Hz, 2 H, quinoline-H_5 or H_8), 8.43 (d, J = 8.4 Hz, 2 H, quinoline-H_8 or H_5), 8.85 (d, 2 H, NH_2).

MS (FAB, matrix glycerol + thioglycerol + TFA) $[M-H]^+$ 447, fragments at m/z 262, 225, 201, 185.

HPLC: column (K), A : B = 55 : 45, major peak at 13.67 min representing 95% of the absorption at 215 nm.

Anal. ($C_{30}H_{32}N_4I_2 \cdot 1.25\ H_2O$) calc: C = 49.71, H = 4.80, N = 7.73, I = 35.01
found: C = 49.64, H = 4.50, N = 7.52, I = 33.44

General proceedure for the preparation of 1,1'-(pentane-1,5-diyl)-bis-(4-aminoquinolinium) diiodide (32, SM-114B, UCL 1635-C_2), 1,1'-(hexane-1,6-diyl)-bis-(4-aminoquinolinium) diiodide (33, SM-109A, UCL 1636-C_2), 1,1'-(octane-1,8-diyl)-bis-(4-aminoquinolinium) diiodide (34, SM-104A, UCL 1637-C_2) and 1,1'-(dodecane-1,12-diyl)-bis-(4-amino-quinolinium) dibromide hemihydrate (35, SM-106A, UCL 1638-B_2)

4-Aminoquinoline (**3a**, 0.2 g, 1.4 mmol) and 0.5 molar ratio of the corresponding

dihalide (1,5-diiodopentane, 1,6-diiodohexane, 1,8-diiodooctane or 1,12-dibromododecane) were dissolved in 10 ml MEK and the solution was heated under reflux for 96 h, using a silica gel tube to prevent moisture from getting into the reaction mixture. After cooling to room temperature, the solid was collected by filtration, washed with MEK and recrystallised from the solvent mentioned in each individual case.

1,1'-(Pentane-1,5-diyl)-bis-(4-aminoquinolinium) diiodide (32, SM-114B, UCL 1635-C_2)

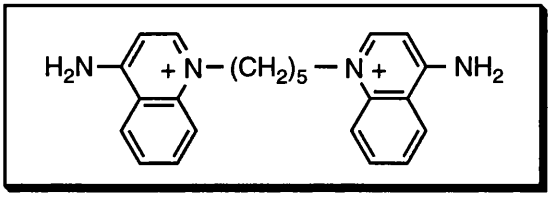

Recrystallised from water (49% yield).

mp = 291°-292°C.

IR (KBr disc) 3305 (N-H_{ar} str), 3060 (C-H_{al} str), 1695, 1616 (C=C_{ar} str) cm^{-1}.

^1H NMR (400 MHz, DMSO-d_6) δ 1.37 (m, 2 H, -CH_2-), 1.80 (m, 4 H, -CH_2-), 4.50 (t, 4 H, N^+-CH_2), 6.76 (d, 2 H, quin-H_3), 7.73 (t, 2 H, quin-H_6 or quin-H_7), 8.01 (t, 2 H, quin-H_7 or quin-H_6), 8.12 (d, 2 H, quin-H_5 or quin-H_8), 8.45 (d, 2 H, quin-H_8 or quin-H_5), 8.50 (d, 2 H, quin-H_2), 9.00 (s, 1 H, NH), 9.02 (s, 1 H, NH).

MS (FAB, matrix MNOBA) $[M-H]^+$ 357, minimal fragmentation.

HPLC: column (K), A : B = 65 : 35, major peak at 6.91 min representing 100% of the absorption at 340 nm.

Anal. ($C_{23}H_{26}N_4I_2 \cdot 0.8\ H_2O$) calc: C = 44.08, H = 4.44, N = 8.94

found: C = 44.19, H = 4.05, N = 8.55

1,1'-(Hexane-1,6-diyl)-bis-(4-aminoquinolinium) diiodide

(33, SM-109A, UCL 1636-C_2)

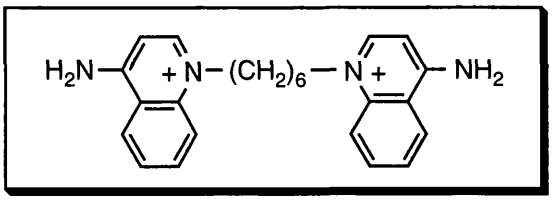

Recrystallised from MeOH - EtOH (58% yield).

mp = 275°-276°C.

IR (KBr disc) 3312 (N-H_{ar} str), 3060 (C-H_{al} str), 1646, 1619 (C=C_{ar} str) cm^{-1}.

^1H NMR (400 MHz, DMSO-d_6) δ 1.33 (m, 4 H, -CH_2-), 1.74 (m, 4 H, -CH_2-), 4.51 (t, 4 H, N^+-CH_2), 6.76 (d, 2 H, quin-H_3), 7.74 (t, 2 H, quin-H_6 or quin-H_7), 8.01 (t, 2 H, quin-H_7 or quin-H_6), 8.12 (d, 2 H, quin-H_5 or quin-H_8), 8.45 (d, 2 H, quin-H_8 or quin-H_5), 8.51 (d, 2 H, quin-H_2), 9.01 (s, 2 H, NH_2).

MS (FAB, matrix MNOBA) $[M-H]^+$ 371, fragments at m/e 227, 213, 199, 186, 43.

HPLC: column (K), 0 min, A : B = 60 : 40; 30 min, A : B = 40 : 60; 35 min A : B = 60 : 40, major peak at 5.44 min representing 97.19% of the absorption at 320 nm.

Anal. ($C_{24}H_{28}N_4I_2 \cdot 0.8\ CH_3OH$) calc: C = 45.69, H = 4.82, N = 8.59

found: C = 45.83, H = 4.42, N = 8.18

1,1'-(Octane-1,8-diyl)-bis-(4-aminoquinolinium) diiodide

(34, SM-104A, UCL 1637-C_2)

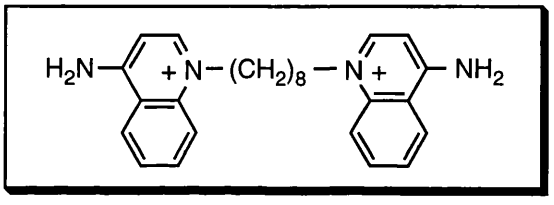

Recrystallised from MeOH - EtOH (57% yield).

mp = 278°-279°C.

IR (KBr disc) 3253 (N-H_{ar} str), 3025 (C-H_{al} str), 1653, 1618 (C=C_{ar} str) cm^{-1}.

^1H NMR (400 MHz, DMSO-d_6) δ 1.26 (m, 8 H, -CH_2-), 1.74 (m, 4 H, -CH_2-), 4.51 (t, 4 H, N^+-CH_2), 6.77 (d, 2 H, quin-H_3), 7.75 (t, 2 H, quin-H_6 or quin-H_7), 8.00 (t, 2 H, quin-H_7 or quin-H_6), 8.14 (d, 2 H, quin-H_5 or quin-H_8), 8.46 (d, 2 H, quin-H_8 or quin-H_5), 8.52 (d, 2 H, quin-H_2), 9.01 (s, 2 H, NH_2).

MS (FAB, matrix MNOBA) $[M-H]^+$ 399, fragments at m/e 255, 241, 227, 213, 55.

HPLC: column (K), 0 min, A : B = 60 : 40; 30 min, A : B = 40 : 60; 35 min A : B = 60 : 40, major peak at 12.41 min representing 98.48% of the absorption at 320 nm.

Anal. ($C_{26}H_{32}N_4I_2 \cdot 0.8\ CH_3OH$) calc: C = 47.34, H = 5.22, N = 8.24
found: C = 47.69, H = 5.25, N = 7.83

1,1'-(Dodecane-1,12-diyl)-bis-(4-aminoquinolinium) dibromide hemi-hydrate

(35, SM-106A, UCL 1638-B_2)

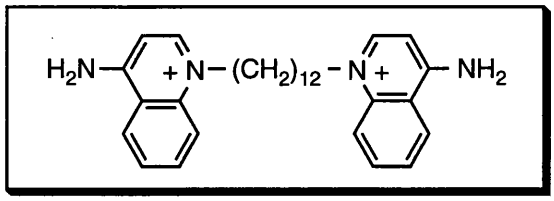

Recrystallised from MeOH - EtOH (36% yield).

mp = 267°-268°C.

IR (KBr disc) 3283 (N-H_{ar} str), 3050 (C-H_{al} str), 1653, 1618 (C=C_{ar} str) cm^{-1}.

^1H NMR (400 MHz, DMSO-d_6) δ 1.18 (m, 16 H, -CH_2-), 1.73 (m, 4 H, -CH_2-), 4.52

(t, 4 H, N^+-CH_2), 6.81 (d, 2 H, quin-H_3), 7.74 (t, 2 H, quin-H_6 or quin-H_7), 8.03 (t, 2 H, quin-H_7 or quin-H_6), 8.13 (d, 2 H, quin-H_5 or quin-H_8), 8.50 (d, 2 H, quin-H_8 or quin-H_5), 8.55 (d, 2 H, quin-H_2), 9.04 (s, 1 H, NH), 9.09 (s, 1 H, NH).

MS (FAB, matrix MNOBA) $[M-H]^+$ 455, fragments at m/e 311, 297, 283, 269, 255, 241.

HPLC: column (K), 0 min, A : B = 45 : 55; 15 min, A : B = 45 : 55; 30 min A : B = 20 : 80; 31 min, A : B = 45 : 55, major peak at 16.98 min representing 97.5% of the absorption at 320 nm.

Anal. ($C_{30}H_{40}N_4Br_2 \cdot 0.5\ H_2O$) calc: C = 57.61, H = 6.61, N = 8.96
found: C = 57.82, H = 6.68, N = 8.76

1,12-bis-(2-methylquinolin-4-yl)-diaminododecane[287,288] (79%)
(36, DG-23B, UCL 1407)

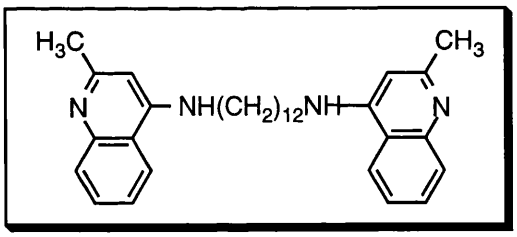

For experimental details see compound **15**.

mp = 153°-155°C.

IR (nujol mul) 3282 (N-H_{ar} str), 1587, 1560 (C=C_{ar} str) cm^{-1}.

^1H NMR (400 MHz, $CDCl_3$) δ 1.31, 1.47 (m, 16 H, -CH_2-), 1.75, (quin, 4 H, -CH_2-), 2.61 (s, 6 H, -CH_3), 3.29 (q, 4 H, -CH_2-), 4.90 (s_{br}, 2 H, N-H), 6.32 (s, 2 H, quin-H_3), 7.36 (t, 2 H, quin-H_6 or quin-H_6), 7.59 (t, 2 H, quin-H_7 or quin-H_6), 7.67 (d, 2 H, quin-H_4), 7.91 (d, 2 H, quin-H_8).

MS (FAB, matrix MNOBA + NaI) $[M+H]^+$ 483, fragments at m/z 325, 311, 297, 283, 269.

Anal. ($C_{32}H_{42}N_4 \cdot 1.5$ MeOH) calc: C = 76.39, H = 9.19, N = 10.63
found: C = 76.84, H = 9.66, N = 10.62

1-[N-(1-benzyl-2-methylquinolinium-4-yl)]-12-(N'-2-methylquinolinium-4-yl)-diaminododecane ditrifluoroacetate

(37, DG-33C, UCL 1426-F_2)

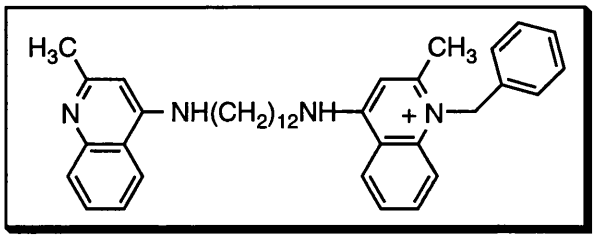

The experimental procedure is described under **38**. The compound was isolated as a greenish oil which solidified after thorough drying in vacuo over P_2O_5 (greenish, hygroscopic crystals).

mp = 77°-79°C melts, 104°-106°C liquifies.

IR (nujol mul, cm^{-1}) ν_{max} 3245 (N-H_{ar} str), 1581, 1561 (C=C_{ar} str) cm^{-1}.

^1H NMR (400 MHz, DMSO-d_6) δ 1.27 (m, 16 H, -CH_2-), 1.70 (m, 4 H, -CH_2-), 2.64 (s, 3 H, -CH_3'), 2.74 (s, 3 H, -CH_3), 3.48 (q, 2 H, -CH_2-), 3.52 (q, 2 H, -CH_2-), 5.85 (s, 2 H, Ph-CH_2-N^+), 6.78 (s, 1 H, quin-H_3'), 7.06 (d, 3 H, Ph-H_o and quin-H_3), 7.32 (t, 1 H, Ph-H_p), 7.36 (t, 2 H, Ph-H_m), 7,67 (dt, 2 H, quin-H_6 or quin-H_7, quin-H_6' or quin-H_7'), 7.82-7.95 (m, 4 H, quin-H_5, quin-H_5', quin-H_7 or quin-H_6, quin-H_7' or quin-H_6'), 8.46 (d, 1 H, quin-H_8'), 8.56 (d, 1 H, quin-H_8), 9.03 (t_{br}, 1 H, N-H'), 9.30 (t_{br}, 1 H, N-H).

MS (FAB, matrix MNOBA + NaI) $[M+H]^+$ 574, fragment at m/z 482.

HPLC: column (K), A : B = 35 : 65, major peak at 13.48 min representing 97.5% of the absorption at 215 nm.

Anal. ($C_{43}H_{50}F_6N_4O_4 \cdot 0.6\ CF_3COOH$) calc: C = 61.07, H = 5.87, N = 6.44
found: C = 60.95, H = 5.64, N = 6.36

1,12-bis-[N,N'-(1-benzyl-2-methylquinolinium-4-yl)]-diaminododecane ditrifluoroacetate

(38, DG-33D, UCL 1427-F_2)

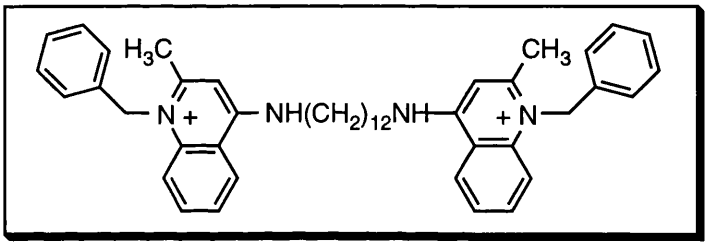

36 (0.3 g, 0.621 mmol) and benzyl bromide (0.319 g, 1.865 mmol) were dissolved with heating in 10 ml of distilled diisobutyl ketone and the solution was heated under reflux for 24 hrs. On cooling a dark gum came out of solution which crystallised on standing. This was collected by filtration and dried overnight in vacuo over P_2O_5. It was shown (MS, HPLC) that this was a mixture of three compounds, namely **36**, the monobenzylated (**37**) and the dibenzylated (**38**) products. These were separated by preparative RP HPLC. The compound was isolated as a greenish oil which solidified after thorough drying in vacuo over P_2O_5 (greenish, hygroscopic crystals).

mp = 133°-134°C.

IR (nujol mul) ν_{max} 3400 (N-H_{ar} str), 1610, 1570 (C=C_{ar} str) cm^{-1}.

^1H NMR (400 MHz, DMSO-d_6) δ 1.26-1.41 (m, 16 H, -CH_2-), 1.72 (quint, 4 H, -CH_2-), 2.74 (s, 6 H, -CH_3), 3.55 (q, 4 H, -CH_2-), 5.85 (s, 4 H, Ph-CH_2-N^+), 7.06 (d and s, 6 H, Ph-H_o and quin-H_3), 7.30 (t, 2 H, Ph-H_p), 7.36 (t, 4 H, Ph-H_m), 7.69 (t, 2 H, quin-H_6 or quin-H_7), 7.89 (t, 2 H, quin-H_7 or quin-H_6), 7.94 (d, 2 H, quin-H_5), 8.57

(d, 2 H, quin-H_8), 9.30 (t_{br}, 2 H, N-H).

MS (FAB, matrix MNOBA + NaI) $[M]^+$ 664, fragments at m/z 547, 482, 431, 415, 401, 387.

HPLC: column (K), A : B = 35 : 65, major peak at 27.28 min representing 98.1% of the absorption at 215 nm.

Anal. ($C_{50}H_{56}F_6N_4O_4 \cdot 2CF_3COOH \cdot 4H_2O$)

calc: C = 48.89, H = 5.09, N = 4.22, ASH = 10.14

found: C = 48.63, H = 4.94, N = 4.25, ASH = 10.14

4,4'-(decan-1,10-diyl)-bis-quinoline

(39a, DG-187A)

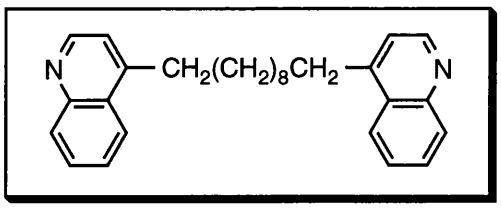

Lepidine (2.762 g, 19.28 mmol), Na (0.52 g, 22.6 mmol) and 1,8-diiodooctane (3.53 g, 9.64 mmol) were reacted in a manner similar to the one described under **24**. The product was isolated as a yellow oil which solidified after drying under vacuum to yield a creamy solid (1.28 g, 33.5%).

mp = 61°-62°C.

^1H NMR (400 MHz, $CDCl_3$, TMS) δ 1.31-1.45 (m, 12 H, -CH_2-), 1.76 (quint, 4 H, -CH_2-), 3.06 (t, 4 H, Ar-CH_3), 7.23 (d, 2 H, quin-H_3), 7.55 (t, 2 H, quin-H_6 or quin-H_7), 7.70 (t, 2 H, quin-H_7 or quin-H_6), 8.04 (d, 2 H, quin-H_5), 8.12 (d, 2 H, quin-H_8), 8.80 (d, 2 H, quin-H_2).

Anal. ($C_{28}H_{32}N_2 \cdot 0.3H_2O$) calc: C = 83.66, H = 8.17, N = 6.97

found: C = 83.55, H = 8.39, N = 6.86

1,1′-Dimethyl-4,4′-(decan-1,10-diyl)-bis-quinolinium diiodide (39, DG-199A, UCL 1450-C_2)

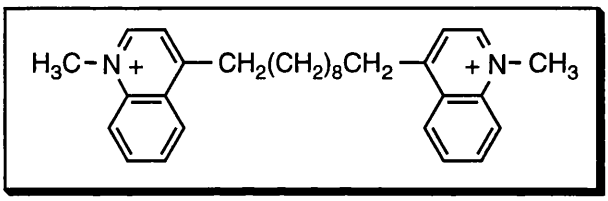

39a Was methylated as described in the preparation of **20** in 88.5% yield.

mp = 198°-200°C.

IR (KBr disc) ν_{max} 3499 (H-OH), 3045 (C-H_{ar} str), 3005 (C-H_{ar} str), 2918 (C-H_{al} str), 2845 (C-H_{ar} str), 1601 (C=C_{ar} str), 1581 (C=C_{ar} str), 1528 (C=C_{ar} str), 1434 (C-H_{al} bend), 1400 (C-H_{al} bend) cm^{-1}.

^1H NMR (400 MHz, DMSO-d_6 + 10 drops TFA, TMS) δ 1.27-1.44 (m, 12 H, -CH_2-), 1.75 (quint, 4 H, -CH_2-), 3.38 (t, 4 H, Ar-CH_2-), 4.59 (s, 6 H, N^+-CH_3), 8.03-8.08 (m, 4 H, quin-H_3, quin-H_6 or quin-H_7), 8.27 (t, 2 H, quin-H_7 or quin-H_6), 8.51 (d, 2 H, quin-H_5), 8.60 (d, 2 H, quin-H_8), 9.38 (d, 2H, quin-H_2).

MS (FAB, matrix MNOBA + Li + Na) $[(M+I)-H]^+$ 552, 426 $[M]^+$, fragments at m/z 412, 282, 268, 254.

HPLC: column (K), A : B = 50 : 50, major peak at 13.30 min representing 100% of the absorption at 215 nm.

Anal. ($C_{30}H_{38}N_2I_2 \cdot H_2O$) calc: C = 51.59, H = 5.77, N = 4.01

found: C = 51.50, H = 5.78, N = 3.66

4-Methoxy-2-methylquinoline[290]

(41a, DG-119A)

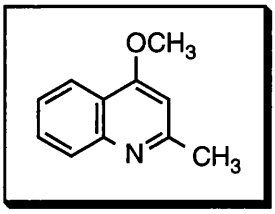

Na (0.517 g, 22.49 mmol) was added to 30 ml of MeOH under argon. When the Na had completely dissolved, 4-chloroquinaldine (3.3 ml, 16.37 mmol) was added and the solution was heated under reflux for 48 h, more NaOMe (0.3 g of Na dissolved in 20 ml MeOH) being added after 24 h. The solvent was removed in vacuo and the residue was dispersed in water and extracted with CH_2Cl_2. After drying (K_2CO_3) the CH_2Cl_2 was removed in vacuo to yield a white - creamy solid (2.76 g, 97%).

mp = 81 - 82°C; [lit[290] mp = 81°C].

^1H NMR (200 MHz, $CDCl_3$) δ 2.68 (s, 3 H, quinoline-CH_3), 4.00 (s, 3 H, OCH_3), 6.61 (s, 1 H, quinoline-H_3), 7.42 (td, J_1 = 1.2 Hz, J_2 = 7.6 Hz, 1 H, quinoline-H_6 or H_7), 7.64 (td, J_1 = 1.6 Hz, J_2 = 7.7 Hz, 1 H, quinoline-H_7 or H_6), 7.93 (dd, J_1 = 0.6 Hz, J_2 = 8.4 Hz, 1 H, quinoline-H_5 or H_8), 8.12 (dd, J_1 = 1 Hz, J_2 = 7.3 Hz, 1 H, quinoline-H_8 or H_5).

2,2'-(Decan-1,10-diyl)-bis-(4-methoxyquinoline)

(41b, DG-179F)

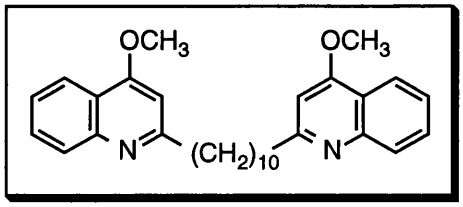

Na (0.42 g, 18.27 mmol) was dispersed in approximately 150 ml of liquid ammonia, under argon, containing a catalytic ammount of ferric nitrate. When the initialy dark blue suspension had turned grey, 4-methoxyquinoline (**41a**, 3 g, 17.32 mmol) was added and the dark red reaction mixture was stirred for 1 h. Then, 1,8 diiodooctane (3.128 g, 8.54 mmol) was added slowly. After 1 h of stirring, no reaction had taken place (TLC), therefore, 90 ml of dry DMF were added and the solution was stirred overnight. The reaction mixture was quenched by adding water and the solvents were removed in vacuo at 35°C. Water was added to the residue and it was extracted with ether. The extracts were combined, dried (Na_2SO_4) and the solvent removed in vacuo. The residue consisted mainly of product and 4-methoxyquinaldine, which were separated by column chromatography on silica gel using CH_2Cl_2 : AcOEt = 2 : 1. The product was recrystallised from MeOH to yield small, white - greyish crystalls (1.1 g, 28%).

mp = 88°-89°C.

^1H NMR (200 MHz, $CDCl_3$) δ 1.29 - 1.42 (m, 12 H, -CH_2-), 1.80 (quint, J = 7.4 Hz, 4 H, -CH_2-), 2.94 (t, J = 7.9 Hz, 4 H, quinoline-CH_2-), 4.04 (s, 6 H, OCH_3), 6.64 (s, 2 H, quinoline-H_3), 7.44 (t, J = 7.1 Hz, 2 H, quinoline-H_6 or H_7), 7.66 (t, J = 7.1 Hz, 2 H, quinoline-H_7 or H_6), 7.99 (d, J = 8.5 Hz, 2 H, quinoline-H_5 or H_8), 8.14 (dd, J_1 = 1.5 Hz, J_2 = 8.3 Hz, 2 H, quinoline-H_8 or H_5).

MS (FAB, matrix MNOBA + Li + Na) $[M+H]^+$ 457, fragments at m/z 443, 427, 298, 284, 256, 242, 228, 200.

HPLC: column (K), A : B = 45 : 55, major peak at 18.02 min representing 98.8% of the absorption at 215 nm.

Anal. ($C_{30}H_{36}N_2O_2.0.4H_2O$) calc: C = 77.69, H = 8.00, N = 6.04
found: C = 77.70, H = 8.10, N = 5.98

2,2'-(Decan-1,10-diyl)-bis-(1-methyl-4-methoxyquinolinium) diiodide (41, DG-183B, UCL 1455)

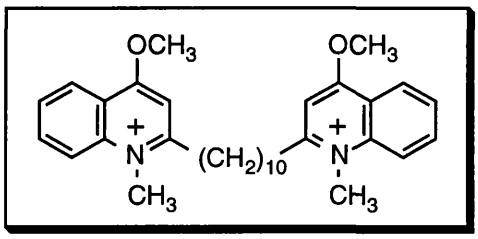

2,2'-(Decan-1,10-diyl)-bis-(4-methoxyquinoline) (**41b**, 0.2 g, 0.44 mmol) and MeI (2 ml, 32.13 mmol) were dissolved in 20 ml of methyl ethyl ketone and the solution was heated under reflux for 12 h under argon. The white precipitate formed was collected by filtration, washed with the solvent and dried in vacuo. A single recrystallisation from dichloromethane afforded pure material (0.167 g, 51.5%).

mp = 186°-188°C.

IR (KBr disc) ν_{max} 3012, 2918, 2838, 1598, 1517, 1464, 1401, 1371, 1257, 1130 cm^{-1}.

^1H NMR (400 MHz, DMSO-d_6, TMS) δ 1.33 (m, 8 H, -CH_2-), 1.47 (m, 4 H, -CH_2-), 1.74 (m, 4 H, -CH_2-), 3.28 (t, J = 8.1 Hz, 4 H, quinoline-CH_2), 4.30 (s, 12 H, OCH_3 and NCH_3), 7.62 (s, 2 H, quinoline-H_3), 7.91 (t, J = 7.2 Hz, 2 H, quinoline-H_6 or H_7), 8.17 (t, J = 7.1 Hz, 2 H, quinoline-H_7 or H_6), 8.38-8.45 (d, d, 4 H, quinoline-H_5, quinoline-H_8).

MS (FAB, matrix MNOBA + Li + Na) $[M]^+$ 486, fragments at m/z 471, 457, 298, 284.

HPLC: column (K), A : B = 45 : 55, major peak at 8.16 min representing 100% of the absorption at 215 nm.

Anal. ($C_{32}H_{42}N_2O_2I_2$) calc: C = 51.90, H = 5.72, N = 3.78

found: C = 51.44, H = 5.55, N = 3.57

2,2´-(Decan-1,10-diyl)-bisquinoline

(42a, DG-203D)

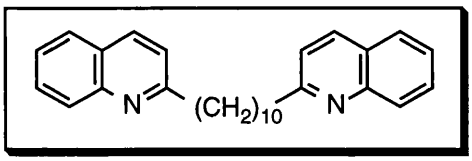

Na (1.966 g, 85.52 mmol) was dispersed in liquid ammonia containing a catalytic amount of $Fe(NO_3)_3$ under argon. When the dark blue colour of the suspension turned grey, quinaldine (11.638 g, 81.28 mmol) was added and the reaction mixture was stirred for 1 h. 1,8-diiodooctane (14.87 g, 40.63 mmol) was then gradually added and the ammonia was allowed to evaporate overnight. Water was added to the residue and the aqueous phase extracted with Et_2O. The extracts were combined, dried (Na_2SO_4) and concentrated to dryness in vacuo to yield an oil which was dissolved in the minimum amount of pet. spirit 40°-60°C and placed in the freezer overnight. The solid mass that had formed was allowed to warm to RT, filtered and the yellow solid obtained was washed with the solvent and dried (1.984 g, 12.3%). This contained some quinaldine (TLC), hence it was recrystallised from MeOH. Large, orange crystalls came out of solution, which were collected and dried. However, the compound was still impure, therefore, it was purified by collumn chromatography on silica gel using petroleum spirit : ethyl acetate = 3 : 1. It was isolated as yellow crystalls which were dried in vacuo (1.03 g).

mp = 96°-97°C.

^1H NMR (400 MHz, $CDCl_3$, TMS) δ 1.27-1.42 (m, 12 H, $-CH_2-$), 1.80 (quint, 4 H, $-CH_2-$), 2.96 (t, J = 7.9 Hz, 4 H, quinoline-CH_2-), 7.29 (d, J = 8.4 Hz, 2 H, quinoline-H_3), 7.48 (t, J = 6.9 Hz, 2 H, quinoline-H_6 or H_7), 7.68 (t, J = 7.0 Hz, 2 H, quinoline-H_7 or H_6), 7.77 (d, J = 8.1 Hz, 2 H, quinoline-H_5 or H_8), 8.03-8.07 (d, d, 4 H, quinoline-H_8 or H_5, quinoline-H_4).

HPLC: column (K), A : B = 50 : 50, major peak at 14.76 min representing 100% of the

absorption at 215 nm.

Anal. ($C_{28}H_{32}N_2 \cdot 0.1H_2O$) calc: C = 84.42, H = 8.15, N = 7.03

found: C = 84.26, H = 8.34, N = 6.98

2,2'-(Decan-1,10-diyl)-bis-(1-methylquinolinium) diiodide hydrate (42, DG-207D, UCL 1460)

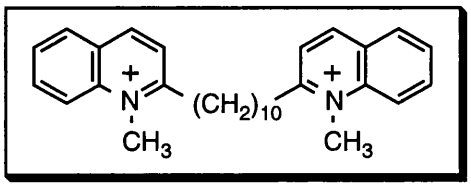

2,2´-(Decan-1,10-diyl)-bis-quinoline (**42a**, 0.3 g, 0.757 mmol) and MeI (2 ml, 32.13 mmol) were dissolved in MEK and the solution was heated under reflux for 33 h. More MeI was added after 6 h (1 ml, 16.07 mmol) and after 16 h (2 ml, 32.13 mmol). The reaction mixture was filtered hot and the yellow solid collected was dried. Four recrystallisations from MeOH were needed to get an analyticaly pure sample for testing. At the last two, care was taken to allow the material to crystallise only for 30 min at room temperature. The crystals collected were washed with hot MeOH (0.119 g, 23%).

mp = 234°C (dec).

IR (KBr disc) ν_{max} 3412, 3038, 2911, 2845, 1614, 1598, 1568, 1514 cm^{-1}.

^1H NMR (400 MHz, DMSO-d_6, TMS) δ 1.31 (m, 8 H, -CH_2-), 1.45 (m, 4 H, -CH_2-), 1.76 (quint, 4 H, -CH_2-), 3.36 (t, J = 7.9 Hz, 4 H, quinoline-CH_2-), 4.48 (s, 6 H, N^+-CH_3), 8.00 (t, J = 7.5 Hz, 2 H, quinoline-H_6 or H_7), 8.11 (d, J = 8.7 Hz, 2 H, quinoline-H_3), 8.23 (td, J_1 = 1.5 Hz, J_2 = 8.1 Hz, 2 H, quinoline-H_7 or H_6), 8.40 (d, J = 8.1 Hz, 2 H, quinoline-H_5 or H_8), 8.57 (d, J = 9.1 Hz, 2 H, quinoline-H_8 or H_5), 9.11 (d, J = 8.7 Hz, 2 H, quinoline-H_4).

MS (FAB, matrix MNOBA + Li + Na) $[M-H]^+$ 425, fragments at m/z 411, 397, 284,

268.

HPLC: column (K), A : B = 50 : 50, major peak at 4.92 min representing 97.3% of the absorption at 215 nm.

Anal. ($C_{30}H_{38}N_2I_2 \cdot H_2O$) calc: C = 51.59, H = 5.77, N = 4.01

found: C = 51.46, H = 5.52, N = 3.84

2,2´-(Dodecane-1,12-diyl)-bis-quinoline hemihydrate

(43a, DG-275B)

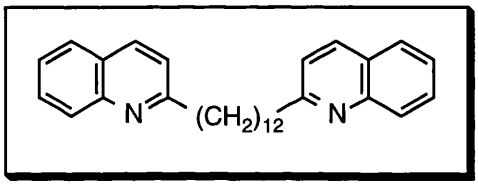

To a solution of LDA (23.05 mmol) in THF at -78°C, quinaldine (3 g, 20.95 mmol) was added over a period of 15 min. The solution was stirred at -78°C for 1 h. 1,10-Diiododecane (3.144 g, 10.47 mmol) was then added and the solution was allowed to warm gradually to room temperature and stirred for 18 h. The reaction mixture was quenched with MeOH, concentrated to dryness, diluted with water and extracted with $CHCl_3$. The extracts were dried (Na_2SO_4) and concentrated to dryness in vacuo to yield a yellow solid. This was recrystallised from MeOH to give pale yellow crystalls (3.46 g, 78%).

mp = 98° - 100°C.

^1H NMR (400 MHz, $CDCl_3$) δ 1.25 (m, 16 H, $-CH_2-$), 1.80 (quint, 4 H, $-CH_2-$), 2.96 (t, 4 H, quinoline-CH_2), 7.30 (d, J = 8.5 Hz, 2 H, quinoline-H_3), 7.47 (t, J = 7.5 Hz, 2 H, quinoline-H_6 or H_7), 7.66 (t, J = 7.6 Hz, 2 H, quinoline-H_7 or H_6), 7.77 (d, J = 8.1 Hz, 2 H, quinoline-H_5 or H_8), 8.05 (d, d, 4 H, quinoline-H_4, H_8 or H_5).

MS (FAB, MNOBA matrix) $[M+H]^+$ 425, fragments at m/z 296, 282, 268, 254, 240,

226, 212, 198, 184, 170, 156, 143, 128.

HPLC: column (K), A : B = 35 : 65, major peak at 6.32 min representing 100% of the absorption at 215 nm.

Anal. ($C_{30}H_{36}N_2 \cdot 0.5H_2O$) calc: C = 83.09, H = 8.60, N = 6.46
found: C = 83.14, H = 8.29, N = 6.33

2,2'-(Dodecan-1,12-diyl)-bis-(1-methylquinolinium) diiodide (43, DG-287B, UCL 1480)

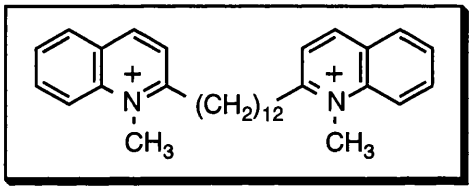

2,2′-(Dodecane-1,12-diyl)-bis-quinoline (**43a**, 0.5 g, 1.18 mmol) and MeI (2 ml, 32.13 mmol) were dissolved in MEK and the solution was heated under reflux for 72 h under argon, more portions of MeI (2 ml) being added after 12, 24, 36, 48 and 60 h. The yellow solid formed was collected by filtration and washed with the solvent and Et_2O. This was recrystallised twice from abs. EtOH to yield yellow crystals (0.7 g, 84%).

mp = 172° - 174°C.

IR (KBr disc) ν_{max} 3039, 3005, 2912, 2845, 1611, 1595, 1578, 1514 cm^{-1}.

^1H NMR (400 MHz, DMSO-d_6) δ 1.28 (m, 12 H, -CH_2-), 1.46 (m, 4 H, -CH_2-), 1.77 (quint, 4 H, -CH_2-), 3.38 (t, J = 8 Hz, 4 H, quinoline-CH_2), 4.52 (s, 6 H, -CH_3), 8.01 (td, J_1 = 7.6 Hz, J_2 = 0.7 Hz, 2 H, quinoline-H_6 or H_7), 8.12 (d, J = 8.6 Hz, 2 H, quinoline-H_3), 8.24 (td, J_1 = 7.7 Hz, J_2 = 1.4 Hz, 2 H, quinoline-H_7 or H_6), 8.41 (d, J = 8.1 Hz, 2 H, quinoline-H_5 or H_8), 8.59 (d, J = 9 Hz, 2 H, quinoline-H_8 or H_5), 9.13 (d, J = 8.6 Hz, 2 H, quinoline-H_4).

MS (FAB, MNOBA matrix) $[M+I-H]^+$ 582, $[M-H]^+$ 453, fragments at m/z 439, 425,

296, 282, 268, 254, 240, 227, 212, 198, 184, 170, 157, 143, 129.

HPLC: column (L), A : B = 50 : 50, major peak at 17.42 min representing 100% of the absorption at 215 nm.

Anal. ($C_{32}H_{42}N_2I_2$) calc: C = 54.25, H = 5.98, N = 3.95

found: C = 53.95, H = 6.35, N = 3.72

5-(4-Bromobut-1-yl)-1,9-dibromononan-5-ol[219]

(47a, DG-715D)

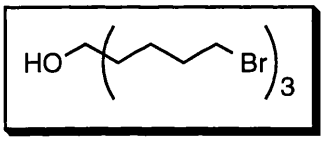

4-Bromo-1-butene (20 g, 148.14 mmol) was dissolved in 30 ml dry THF and BH_3·THF (49.4 ml, 49.38 mmol) was added at 0°C over 10 min. The solution was stirred at 0°C for 1 h. Then, dry KCN (3.216 g, 49.38 mmol) was added and the mixture was stirred at room temperature for 4 h. Then, TFAA (20.9 ml, 148.14 mmol) was added at 0°C and the mixture was placed in the fridge overnight. The excess of TFAA was removed at room temperature in vacuo, 59 ml (177.77 mmol) of 3 N NaOH were added to the residue at 0°C and then slowly and carefully 30% H_2O_2 (65.8 ml, 580.9 mmol) was added at -5° - 0°C. The reaction mixture was allowed to warm to room temperature and was stirred for 2 h. Acidification was effected with glacial AcOH, followed by extraction with 4 x 50 ml CH_2Cl_2. The extracts were combined, dried (Na_2SO_4), and the solvent removed in vacuo to yield a yellowish oil. This was chromatographed on silica gel using petroleum ether : EtOAc = 5 : 1 and the product (Rf = 0.25) was isolated as a colourless oil (7.34 g, 34% overall).

^{1}H NMR (400 MHz, $CDCl_3$, ppm) δ 1.46 (m, 13 H, CH_2 + OH), 1.87 (m, 6 H, CH_2), 3.43 (t, 6 H, CH_2Br).

^{13}C NMR (100 MHz, $CDCl_3$, ppm) δ 22.0, 33.0, 33.7, 38.1, 74.0.

5-(4-Bromobut-1-yl)-1,9-dibromonon-4-ene

(47b, DG-719A)

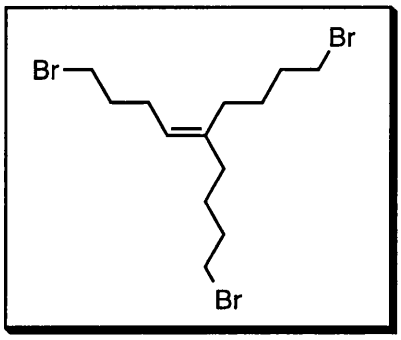

To a solution of 5-(4-Bromobut-1-yl)-1,9-dibromononan-5-ol (**47a**, 1.6 g, 3.66 mmol) and triethylsilane (0.58 ml, 3.66 mmol) in 15 ml CH_2Cl_2, TFA (1.83 ml, 23.77 mmol) was added and the solution was stirred at room temperature for 48 h. The solvents were evaporated in vacuo and the residue chromatographed on silica gel using petroleum ether : EtOAc = 50 : 1. The product (Rf = 0.3) was isolated as a colourless oil (0.843 g, 55%, **47b**). Further elution of the column with petroleum spirit : EtOAc = 20 : 1 afforded a second compound (Rf = 0.3) which was 5-(4-bromobut-1-yl)-1,9-dibromononane (**47c** 0.2 g, 13%).

^{1}H NMR (400 MHz, $CDCl_3$, ppm) δ 1.54 (m, 4 H, CH_2), 1.90 (m, 6 H, CH_2), 2.05 (m, 4 H, CH_2), 2.17 (q, J = 7.3 Hz, 2H, $\underline{CH_2}CH=C$), 3.42 (m, 6 H, CH_2Br), 5.11 (t, J = 7.2 Hz, 1 H, CH=C).

^{13}C NMR (100 MHz, $CDCl_3$, ppm) δ 26.1, 26.5, 26.8, 28.9, 32.3, 32.6, 32.9, 33.6, 33.7, 33.8, 35.7, 123.8, 139.7.

MS (FAB, MNOBA matrix) $[M+H]^+$ 417, fragment at m/z 337.

Anal. ($C_{13}H_{23}Br_3$) calc: C = 37.26, H = 5.53

found: C = 37.03, H = 5.33

5-(4-Bromobut-1-yl)-1,9-dibromononane

(47c, DG-719B)

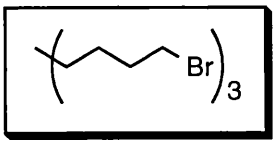

The synthesis is described under 5-(4-bromobut-1-yl)-1,9-dibromonon-4-ene (**47b**).

^{1}H NMR (400 MHz, $CDCl_3$, ppm) δ 1.43 (m, 6 H, CH_2), 1.58 (m, 1 H, CH), 1.87 (m, 12 H, CH_2), 3.41 (t, J = 6.5 Hz, 6 H, CH_2Br).

^{13}C NMR (100 MHz, $CDCl_3$, ppm) δ 21.6, 32.3, 33.1, 33.9, 93.4.

MS (FAB, MNOBA matrix) $[M+H]^+$ 419, fragments at m/z 149, 69.

1,1'-[5-[4-(4-Aminoquinolinium-1-yl)but-1-yl]non-4-en-1,9-diyl]-bis-(4-aminoquinolinium) tetratrifluoroacetate

(47, DG-723B, UCL 1605-F_3)

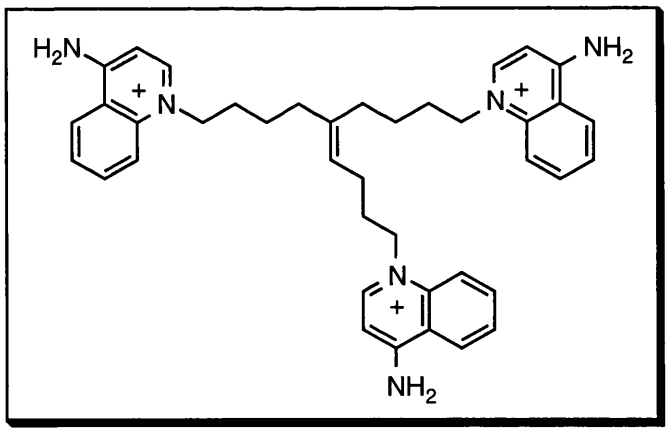

5-(4-Bromobut-1-yl)-1,9-dibromonon-4-ene (**47b**, 0.4 g, 0.955 mmol) and 4-aminoquinoline (**3a**, 0.413 g, 2.863 mmol) were dissolved in 15 ml abs. EtOH and heated under reflux for 204 h under Ar. The solvent was removed in vacuo and the residue dried in vacuo to yield a foam (63% based on HPLC). A portion of this was purified by preparative HPLC.

IR (KBr disc) ν_{max} 3370, 3150, 2950, 1775, 1685, 1625 cm^{-1}.

^1H NMR (400 MHz, $CDCl_3$, ppm) δ 1.32 (m, 4 H, CH_2), 1.70 (m, 6 H, CH_2), 1.91 (m, 6 H, CH_2), 4.42 (t, J = 7.3 Hz, 2 H, N^+-CH_2), 4.49 (t, J = 7.6 Hz, 4 H, N^+-CH_2), 5.05 (t, J = 7.2 Hz, 1 H, CH=C), 6.79 (m, 3 H, quinoline-H_3), 7.70 (m, 3 H, quinoline), 8.01 (m, 6 H, quinoine), 8.48 (m, 6 H, quinoline), 9.07 (m, 6 H, NH_2).

^{13}C NMR (100 MHz, $CDCl_3$, ppm) δ 21.0, 24.1, 24.5, 28.4, 28.6, 28.7, 29.1, 35.2, 38.5, 38.7, 45.7, 53.4, 53.7, 102.05, 102.08, 117.08, 117.11, 118.1, 118.2, 118.24, 118.29, 118.5, 123.8, 126.58, 124.62, 124.72, 126.23, 126.27, 126.35, 126.39, 134.33, 134.45, 137.91, 137.93, 137.98, 139.06, 146.11, 157.78, 157.91, 157.95, 158.09, 158.41.

MS (FAB, MNOBA matrix) $[M-2H]^+$ 609, fragments at m/z 465, 451.

HPLC: column (K), A : B = 55 : 45, major peak at 8.98 min representing 98.3% of the absorption at 215 nm.

Anal. ($C_{46}H_{47}N_6^{3+}\cdot 3CF_3CO_2^-\cdot 1.2CF_3CO_2H$)

calc: C = 53.44, H = 4.47, N = 7.73

found: C = 53.21, H = 4.82, N = 7.49

2,2′-[N,N′-(Decane-1,10-diyl)]-bis-(2-aminopyrimidine)

(48a, DG-243A)

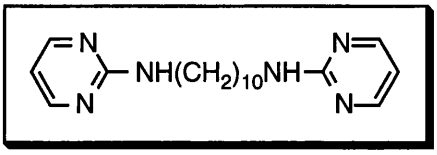

2-Chloropyrimidine (1 g, 8.73 mmol), 1,10-diaminodecane (0.752 g, 4.37 mmol) and Et_3N (2 ml, 14.35 mmol) were dissolved in 40 ml absolute EtOH and heated under reflux for 30 h. After cooling to room temperature, MeOH was added to the solution and the white precipitate formed was collected by vacuum filtration and washed with MeOH to

yield pure product. The filtrate was concentrated to dryness, the solid formed was basified with dilute KOH solution until the solution was strongly alkaline and extracted with 5 x 50 ml CH_2Cl_2. After drying (Na_2SO_4) the CH_2Cl_2 was removed in vacuo to give a redish oil which was recrystallized from MeOH to yield white crystalls (total: 0.973 g, 68%).

mp = 107 - 108°C.

^1H NMR (400 MHz, $CDCl_3$, TMS) δ 1.29 (m, 12 H, $-CH_2-$), 1.62 (quin, 4 H, $-CH_2-$), 3.39 (td, J_1 = 5.8 Hz, J_2 = 7.2 Hz, 4 H, $N-CH_2-$), 5.18 (s_{br}, 2 H, NH), 6.50 (t, J = 4.8 Hz, 2 H, pyrimidine-H_5), 8.27 (d, J = 4.7 Hz, 4 H, pyrimidine-H_4 and H_6).

MS (FAB, MNOBA matrix) $[M+H]^+$ 329, fragments at m/z 220, 206, 192, 178, 164, 150, 136, 122, 108.

HPLC: column (K), A : B = 50 : 50, major peak at 12.12 min representing 97.7% of the absorption at 215 nm.

Anal. ($C_{18}H_{28}N_6 \cdot 0.2CH_3OH$) calc: C = 65.28, H = 8.67, N = 25.01

found: C = 65.66, H = 8.84, N = 24.81

2,2´-[N,N´-(Decane-1,10-diyl)]-bis-(1-methyl-2-aminopyrimidinium) diiodide

(48, DG-251A, UCL 1468-C_2)

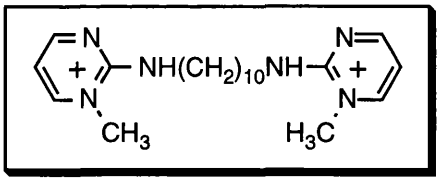

2,2´-[N,N´-(Decane-1,10-diyl)]-bis-(2-amino-pyrimidine) (**48a**, 0.2 g, 0.61 mmol) and MeI (3 ml, 48.2 mmol) were dissolved in MEK and heated under reflux under argon for 14 h. A creamy precipitate formed which was collected by vacuum filtration and washed extensively with MEK (0.328 g, 88%).

mp = 182° - 184°C (dec).

IR (KBr disc) ν_{max} 3218, 3052, 2999, 2918, 2845, 1635, 1598, 1541, 1465, 1408 cm^{-1}.

^1H NMR (400 MHz, DMSO-d_6, TMS) δ 1.26 (m, 12 H, -CH_2-), 1.58 (m, 4 H, -CH_2-), 3.50 (q, 4 H, N-CH_2-), 3.72 (s, 6 H, -CH_3), 7.08 (dd, J_1 = 4.4 Hz, J_2 = 6.5 Hz, 2 H, pyrimidine-H_5), 8.61 (dd, J_1 = 2.1 Hz, J_2 = 6.5 Hz, 2 H, pyrimidine-H_4), 8.74 (t_{br}, 2 H, NH), 8.88 (dd, J_1 = 4.4 Hz, J_2 = 2.1 Hz, 2 H, pyrimidine-H_6).

MS (FAB, MNOBA matrix) $[M+I]^+$ 485, $[M-H]^+$ 357, fragments at m/z 343, 248, 234, 220, 206, 192, 178, 164, 150, 136, 122, 108.

HPLC: column (K), gradient elution with A : B = 45 : 55 at 0 min to A : B = 10 : 90 at 15 min, major peak at 4.46 min representing 100% of the absorption at 254 nm.

Anal. ($C_{20}H_{34}N_6I_2$) calc: C = 39.23, H = 5.60, N = 13.72
found: C = 39.15, H = 5.65, N = 13.40

1,1′-(Decane-1,10-diyl)-bis-(1H-benzimidazole)

(49a, DG-629C)

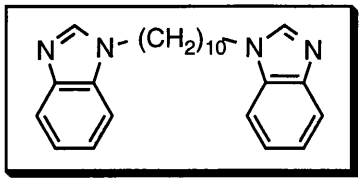

To a suspension of benzimidazole (1 g, 8.47 mmol) in THF at -78°C, 5.3 ml (8.48 mmol) of a 1.6 M solution of BuLi in hexanes was added. The resultant solution was strirred for 30 min and then allowed to warm to room temperature. 1,10-Diiododecane (1.668 g, 4.23 mmol) was added and the solution was heated under reflux for 36 h under argon. MeOH was then added and the solvents were removed in vacuo to yield an oil. This was purified by column chromatography on silica gel using EtOAc : MeOH = 10 : 1. The product (Rf = 0.3) was obtained as a yellow solid. This was dispersed in 50 ml hot water and EtOH was

added until the solution was clear. On cooling to room temperature, a yellow oil came out of solution. The supernatant was decanted into another flask and excess of water was added dropwise to it while scratching the walls of the flask and the suspension was placed at 4°C for 5 h. The white precipitate was collected by filtration, washed well with water and dried in vacuo at 40°C (60% yield).

mp = 87°C.

^{1}H NMR (400 MHz, $CDCl_3$) δ 1.22 - 1.29 (m, 12 H, $-CH_2-$), 1.86 (m, 4 H, $-CH_2-$), 4.16 (t, J = 7 Hz, 4 H, NCH_2), 7.26 - 7.31 (m, 4 H, benzimidazole-H_5, H_6), 7.40 (dd, J_1 = 6.9 Hz, J_2 = 2.5 Hz, 2 H, benzimidazole-H_4 or H_7), 7.81 (dd, J_1 = 6.8 Hz, J_2 = 2 Hz, 2 H, benzimidazole-H_7 or H_4), 7.89 (s, 2 H, benzimidazole-H_2).

^{13}C NMR (100 MHz, $CDCl_3$) δ 26.7, 29.0, 29.2, 29.7, 45.1, 109.6, 120.3, 122.0, 122.8, 133.7, 142.9, 143.8.

MS (FAB, MNOBA matrix) $[M+H]^+$ 375, fragments at m/z 257, 243, 229, 215, 201, 187, 173, 159, 145, 131, 119.

HPLC: column (K), A : B = 55 : 45, major peak at 10.44 min representing 99.9% of the absorption at 215 nm.

Anal. ($C_{24}H_{30}N_4 \cdot 0.2H_2O$) calc: C = 76.23, H = 8.10, N = 14.82
found: C = 76.19, H = 7.87, N = 14.56

1,1′-(Decane-1,10-diyl)-bis-(3-methylbenzimidazolium) diiodide hemihydrate

(49, DG-637A, UCL 1553)

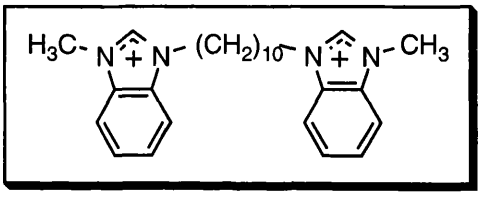

1,1´-(Decane-1,10-diyl)-bis-(1H-benzimidazole) (**49a**, 0.2 g, 0.53 mmol) and MeI (1 ml, 16.06 mmol) were dissolved in 15 ml MEK and heated under reflux for 36 h, more MeI (1 ml) being added after 12 h. The white solid that had formed was collected by filtration, washed extensively with the solvent and dried (0.332 g, 95%).

mp = 204 - 205°C.

IR (KBr disc) ν_{max} 3516, 3454, 2921, 2853, 1571, 1462 cm^{-1}.

^1H NMR (400 MHz, DMSO-d_6) δ 1.24 - 1.30 (m, 12 H, -CH_2-), 1.88 (m, 4 H, -CH_2-), 4.08 (s, 6 H, CH_3), 4.47 (t, J = 7.1 Hz, 4 H, N-CH_2), 7.69 - 7.73 (m, 4 H, benzimidazole-H), 8.02 - 8.04 (m, 2 H, benzimidazole-H), 8.08 - 8.10 (m, 2 H, benzimidazole-H), 9.72 (s, 2 H, benzimidazole-H_2).

MS (FAB, MNOBA matrix) $[M+I]^+$ 531, $[M-H]^+$ 403, fragments at m/z 389, 272, 257, 243, 229, 215, 202, 187, 173, 159, 145, 133.

HPLC: column (K), A : B = 55 : 45, major peak at 11.91 min representing 99.2% of the absorption at 215 nm.

Anal. ($C_{26}H_{36}N_4I_2 \cdot 0.5H_2O$) calc: C = 46.79, H = 5.59, N = 8.39
found: C = 46.83, H = 5.42, N = 8.37

1,1'-(Decane-1,10-diyl)-bis-(2-methylbenzimidazole)

(50a, DG-645A)

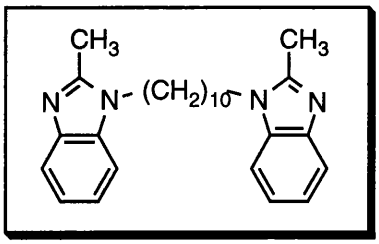

To a suspension of 2-methylbenzimidazole (1 g, 7.57 mmol) in THF (70 ml) at -78°C a 1.6 M solution of BuLi in hexanes (5 ml, 7.95 mmol) was added dropwise and the

mixture was stirred at -78°C for 30 min. Then, a solution of 1,10-diiododecane (1.49 g, 3.78 mmol) in THF was added and the mixture was warmed to room temperature and then heated under reflux for 36 h under Ar. After cooling to room temperature, MeOH was added and the solvents were removed in vacuo to yield an oil. This was partitioned between water (50 ml) and $CHCl_3$ (40 ml) and the water phase was further extracted with 40 ml $CHCl_3$. The extracts were combined, dried (Na_2SO_4) and the solvent removed in vacuo to yield an oil. This was purified by column chromatography on silica gel using petroleum ether : EtOAc = 10 : 1. The product (Rf = 0.25) was isolated as a white solid which was dissolved in $CHCl_3$, filtered to remove any silica and the solvent removed in vacuo to yield a white solid (1.444 g, 95%).

mp = 101° - 102°C.

^1H NMR (200 MHz, $CDCl_3$, TMS, ppm) δ 1.23 - 1.31 (m, 12 H, CH_2), 1.78 (m, 4 H, CH_2), 2.60 (s, 6 H, CH_3), 4.09 (t, J = 7.1 Hz, 4 H, N-CH_2), 7.20 - 7.30 (m, 6 H, Ar), 7.67 - 7.72 (m, 2 H, Ar).

MS (FAB, MNOBA matrix) $[M+H]^+$ 403, fragments at m/z 387, 271, 257, 243, 229, 215, 201, 187, 173, 159, 145, 132.

Anal. ($C_{26}H_{34}N_4 \cdot 0.2H_2O$) calc: C = 76.88, H = 8.54, N = 13.79
found: C = 76.72, H = 8.62, N = 13.54

1,1'-(Decane-1,10-diyl)-bis-(2,3-dimethylbenzimidazolium) diiodide (50, DG-649C, UCL 1562-C_2)

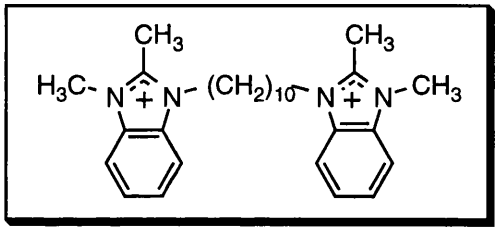

1,1'-(Decane-1,10-diyl)-bis-(2-methylbenzimidazole) (**50a**, 0.2 g, 0.497 mmol) and MeI

(1 ml, 16.06 mmol) were dissolved in butanone and heated under reflux for 36 h under Ar, more MeI (1 ml) being added after 24 h. After cooling to room temperature, the solid formed was collected by filtration and washed extensively with butanone. This was recrystallised from MeOH but the sample obtained was less pure (by HPLC). It was suspected that it decomposed on heating, therefore, it was recrystallised again from approximately 25 ml MeOH with gentle heating (0.2 g, 59%).

mp = 274° - 276°C.

IR (KBr disc) ν_{max} 3573, 3446, 3025, 2919, 2812, 1528, 1471, 1417 cm^{-1}.

^1H NMR (400 MHz, DMSO-d_6, ppm) δ 1.23 - 1.32 (m, 12 H, CH_2), 1.74 (quint, 4 H, CH_2), 2.88 (s, 6 H, CH_3), 3.98 (s, 6 H, N-CH_3), 4.47 (t, J = 7.4 Hz, 4 H, N-CH_2), 7.62 - 7.64 (m, 4 H, Ar), 7.98 - 8.02 (m, 4 H, Ar).

MS (FAB, MNOBA matrix) $[M+I]^+$ 559, $[M-H]^+$ 431, fragments at m/z 417, 285, 271, 257, 243, 229, 216, 201, 187, 173, 160, 146.

HPLC: column (K), A : B = 50 : 50, major peak at 4.62 min representing 97.8% of the absorption at 215 nm.

Anal. ($C_{28}H_{40}N_4I_2 \cdot 0.2H_2O$) calc: C = 48.74, H = 5.90, N = 8.12
found: C = 48.43, H = 5.62, N = 7.86

1,1'-(Decane-1,10-diyl)-bis-(1,2,3,4-tetrahydroquinoline)[286]
(51a, DG-731A)

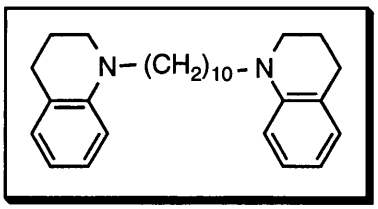

To a stirred and cooled to -78°C solution of 1,2,3,4-tetrahydroquinoline (5 g, 37.54 mmol) in 100 ml THF a 1.6 M solution of BuLi (25.8 ml, 41.3 mmol) in hexanes was

added slowly. The resultant suspension was stirred at -78°C for 3 h. Then a solution of 1,10-diiododecane (7.397 g, 18.77 mmol) in THF was added and the mixture was allowed to warm to room temperature and stirred for 48 h. MeOH was added to this and the solvents were removed in vacuo. The residue was purified by column chromatography on silica gel using petroleun ether : EtOAc = 30 : 1. The product (Rf = 0.3) was isolated as a yellow oil (6.4 g, 84%).

^{1}H NMR (400 MHz, $CDCl_3$, ppm) δ 1.32 (m, 12 H, CH_2), 1.58 (m, 4 H, CH_2), 1.94 (quint, J = 6 Hz, 4 H, quinoline-H_3), 2.75 (t, J = 6.2 Hz, 4 H, quinoline-H_4), 3.22 (t, J = 7.8 Hz, 4 H, N-CH_2), 3.27 (t, J = 5.6 Hz, 4 H, quinoline-H_2), 6.57 (m, 4 H, quinoline-H_6 + H_8), 6.93 (dd, J_1 = 0.9 Hz, J_2 = 7.5 Hz, 2 H, quinoline-H_5), 7.04 (td, J_1 = 1.6 Hz, J_2 = 7.6 Hz, 2 H, quinoline-H_7).

^{13}C NMR (100 MHz, $CDCl_3$, ppm) δ 22.3, 26.2, 27.3, 28.3, 29.6, 29.7, 49.5, 51.6, 110.5, 115.2, 122.2, 127.1, 129.2, 145.4.

MS (FAB, MNOBA matrix) $[M-H]^+$ 403, fragment at m/z 146.

1,1'-(Decane-1,10-diyl)-bis-(1-methyl-1,2,3,4-tetrahydroquinoli-nium) ditrifluoroacetate hydrate[286]

(51, DG-735B, UCL1586-F_3)

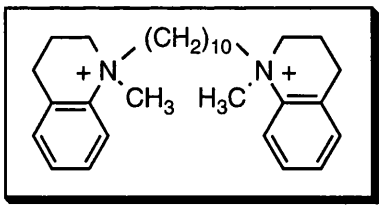

1,1'-(Decane-1,10-diyl)-bis-(1,2,3,4-tetrahydroquinoline) (**51a**, 1 g, 2.74 mmol) and MeI (1 ml, 16.06 mmol) were dissolved in 30 ml butanone and the solution heated under reflux for 48 h under Ar. A yellow gum formed. After cooling to room temperature, the solvent was removed in vacuo and the residue dried in vacuo to produce a foam. This was triturated with sodium dried Et_2O to yield a hygroscopic solid. A portion of this was

purified by preparative HPLC using A : B = 50 : 50 to yield a greenish oil (0.16 g, 60%).

IR (nujol) ν_{max} 2932, 2845, 1685, 1458, 1375, 1198, 1174 cm^{-1}.

^1H NMR (400 MHz, DMSO-d_6, ppm) δ 1.21 (m, 14 H, CH_2), 1.64 (m, 2 H, CH), 2.10 - 2.22 (m, 4 H, CH_2), 2.92 (m, 4 H, CH_2), 3.51 (s, 6 H, CH_3), 3.69 (m, 4 H, N-CH_2), 3.88 (td, J_1 = 2.7 Hz, J_2 = 9.6 Hz, 2 H, N-CH_{ring}), 3.97 (td, J_1 = 4.2 Hz, J_2 = 12.4 Hz, 2 H, N-CH_{ring}), 7.38 (m, 2 H, Ph), 7.44 (m, 4 H, Ph), 7.87 (m, 2 H, Ph).

^{13}C NMR (100 MHz, DMSO-d_6, ppm) δ 16.7, 22.6, 25.3, 25.6, 28.4, 28.7, 55.5, 59.7, 66.8, 121.8, 128.0, 129.5, 131.1, 131.6, 141.1.

MS (FAB, T.G.T matrix) $[M+CF_3CO_2^-]^+$ 547, $[M+H]^+$ 435, fragments at m/z 419, 147.

HPLC: column (K), A : B = 50 : 50, major peak at 7.75 min representing 100% of the absorption at 215 nm.

Anal. ($C_{30}H_{46}N_4^{2+}\cdot 2CF_3CO_2^-\cdot CF_3CO_2H\cdot H_2O$)

calc: C = 54.54, H = 6.23, N = 3.53

found: C = 54.76, H = 6.51, N = 3.36

1,10-(N,N,N',N'-Tetrabenzyl)diaminodecane

(52a, DG-799A)

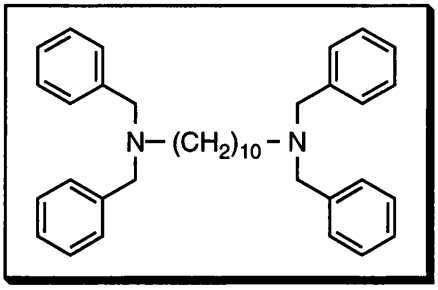

To a solution of dibenzylamine (5 ml, 26 mmol) in 50 ml THF at -78°C, a 2 M solution of BuLi (14.3 ml, 28.6 mmol) in cyclohexane was added dropwise. The resultant red solution was stirred at -78°C for 40 min under Ar. Then a solution of 1,10-diiododecane

(5.123 g, 13 mmol) in THF was added with vigorous stirring at -78°C. The resultant suspension was allowed to warm to room temperature and stirred overnight. MeOH was then added, the solvents removed in vacuo and the residue partitioned between a saturated solution of Na_2CO_3 in water and CH_2Cl_2 (50 ml). The aqueous phase was further extracted with 4 x 50 ml CH_2Cl_2. The extracts were combined, dried ($MgSO_4$) and the solvent evaporated in vacuo to yield an oil. Trituration of this with MeOH effected solidification. The white solid was collected, washed with MeOH and dried (5 g, 72%).

^1H NMR (400 MHz, $CDCl_3$, ppm) δ 1.18 (m, 12 H, CH_2), 1.49 (quint, J = 7 Hz, 4 H, CH_2), 2.39 (t, J = 7.1 Hz, 4 H, N-CH_2), 3.54 (s, 8 H, Ph-$\underline{CH_2}$-N), 7.21 (t, J = 7.1 Hz, 4 H, Ph), 7.30 (dt, J_1 = 1.4 Hz, J_2 = 7.1 Hz, 8 H, Ph), 7.36 (d, J = 6.9 Hz, 8 H, Ph).

^{13}C NMR (100 MHz, $CDCl_3$, ppm) δ 27.0, 27.2, 29.5, 29.6, 53.4, 58.2, 126.7, 128.1, 128.7, 140.0.

1,10-[(N,N,N',N'-Tetrabenzyl)-(N,N'-dimethyl)]diammoniumdecane ditrifluoroacetate

(52, DG-831B, UCL 1622-F_2)

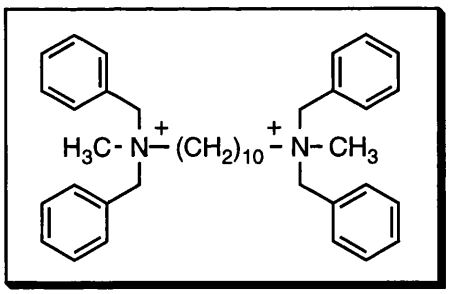

1,10-(N,N,N',N'-Tetrabenzyl)diaminodecane (**52a**, 0.5 g, 0.94 mmol) and MeI (2 ml, 32.12 mmol) were dissolved in 10 ml DMSO containing enough $CHCl_3$ to clear the solution and set aside overnight at room temperature. The solvents were removed by vacuum distillation to yield an oil. This failed to solidify or crystallise from a variety of solvents, therefore, 0.2 g were purified by preparative HPLC (0.1 g, 49%).

IR (neat) ν_{max} 3421, 3038, 2933, 2861, 1779, 1738, 1687, 1477, 1459, 1387, 1374 cm^{-}

1.

^{1}H NMR (400 MHz, $CDCl_3$, ppm) δ 1.28 (m, 12 H, CH_2), 1.87 (m, 4 H, CH_2), 2.85 (s, 6 H, CH_3), 3.04 (m, 4 H, N^+-CH_2), 4.47 (d, J = 12.8 Hz, 4 H, N^+-$\underline{CH_2}$-Ph), 4.61 (d, J = 12.7 Hz, 4 H, N^+-$\underline{CH_2}$-Ph), 7.52 (m, 20 H, Ph).

MS (FAB, MNOBA matrix) $[M-H]^+$ 561, fragments at m/z 547, 471, 379, 366, 350, 91.

HPLC: column (K), A : B = 40 : 60, major peak at 6.87 min representing 100% of the absorption at 215 nm.

Anal. ($C_{40}H_{54}N_2^{2+}\cdot 2CF_3CO_2^-\cdot 1.9CF_3CO_2H$)

calc: C = 57.10, H = 5.60, N = 2.79

found: C = 57.17, H = 5.73, N = 2.66

1-(10-iododecan-1-yl)-4-aminoquinolinium iodide

(66a, DG-239D)

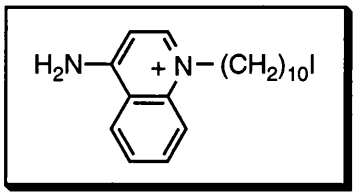

4-Aminoquinoline (**3a**, 0.659 g, 4.57 mmol) and 1,10-diiododecane (9.6 g, 24.36 mmol) were dissolved in 400 ml of butanone and the solution was heated under reflux for 20 h. Then the solvent was removed in vacuo to yield a yellow solid. This was dispersed in 10 ml CH_2Cl_2 and the precipitate collected by filtration. The yellow solid contained 1,10-diiododecane, therefore, it was dispersed in boiling petroleum spirit (40° - 60°C range) and filtered. The pale yellow solid on the funnel was washed with boiling petroleum spirit and dried in vacuo (**DG-239A**). The filtrate was concentrated to dryness and the residue was treated with boiling petroleum spirit. The pale yellow solid was collected by vacuum filtration, washed with boiling petroleum spirit and dried (**DG-239B**). **DG-239A** and **DG-239B** were combined, dispersed in boiling petroleum spirit and the pale yellow solid

collected by filtration, washed several times with boiling petroleum spirit and dried. This was recrystallised from MeOH. The crystallisation was not allowed to go to completion but the first fraction of crystals appeared after 30 min at -20°C was collected and washed with cold MeOH. The filtrate was concentrated to dryness and the residue triturated with sodium dried Et_2O to yield a pale yellow powder which was collected, washed with Et_2O and dried (2 g, 81%). Subsequently, an improved preparation was found. This is as follows: 4-Aminoquinoline (**3a**, 1 g, 6.94 mmol) and 1,10-diiododecane (14.58 g, 36.99 mmol) were dissolved in 600 ml butanone and the solution was heated under reflux for 20 h. After cooling to room temperature, the white precipitate that had formed was collected by filtration and was shown by NMR to be the bis-alkylated product. The filtrate was concentrated to a small volume and placed at 4°C for 2 h. The yellow crystals formed were collected by filtration and washed with butanone (**DG-895B**). The filtrate was further concentrated and placed at 4°C for 2 h. The white solid formed was collected by filtration and washed with butanone (**DG-895C**). **DG-895B** and **DG-895C** were shown by NMR to be the correct products.

mp = 143° - 145°C.

^1H NMR (400 MHz, DMSO-d_6, ppm) δ 1.21 (m, 12 H, CH_2), 1.70 (m, 4H, CH_2), 3.24 (t, J = 6.9 Hz, 2 H, I-CH_2), 4.52 (t, J = 7.3 Hz, 2 H, N^+-CH_2), 6.78 (d, J = 7.2 Hz, 1 H, quinoline-H_3), 7.75 (t, J = 7.3 Hz, 1 H, quinoline-H_6 or H_7), 8.03 (td, J_1 = 1.4 Hz, J_2 = 7.8 Hz, 1 H, quinoline-H_7 or H_6), 8.14 (d, J = 8.7 Hz, 1 H, quinoline-H_5 or H_8), 8.46 (dd, J_1 = 1.3 Hz, J_2 = 8.4 Hz, 1 H, quinoline-H_8 or H_5), 8.53 (d, J = 7.3 Hz, 1 H, quinoline-H_2), 9.00 (s, s, 2 H, NH_2).

MS (FAB, MNOBA matrix) $[M]^+$ 411, fragments at m/z 283, 269, 255, 185, 171, 158, 144.

3-[N-(tert-Butoxycarbonyl)amino]propylamine[179]

(66b, DG-227A)

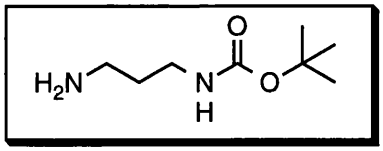

1,3-Diaminopropane (9.2 ml, 110 mmol) was dissolved in 500 ml $CHCl_3$ and the solution cooled to 0°C. To this, a solution of di-tert-butyl-dicarbonate (5 ml, 22 mmol) in 250 ml $CHCl_3$ was added dropwise over a period of 1 h. The reaction mixture was stirred at room temperature for a further 2 h, filtered and the solvent removed in vacuo. The remaining oil was treated with a saturated solution of NaCl in water, the di-protected byproduct removed by filtration and the filtrate extracted with 5 x 50 ml Et_2O. The extracts were combined, dried with $MgSO_4$ and the solvent removed in vacuo to yield a colourless oil (3.683 g, 96%).

^1H NMR (400 MHz, $CDCl_3$, TMS, ppm) δ 1.44 (s, 11 H, t-Bu + NH_2), 1.61 (quint, 2 H, CH_2), 2.76 (t, 2 H, $\underline{CH_2}$-NH_2), 3.21 ($quint_{br}$, 2 H, $\underline{CH_2}$-NHCO), 5.06 (s_{br}, 1 H, NHCO).

1-[N-(4-Quinolinyl)]-3-[N-(tert-butoxycarbonyl)amino]propanamine

(66c, DG-135B)

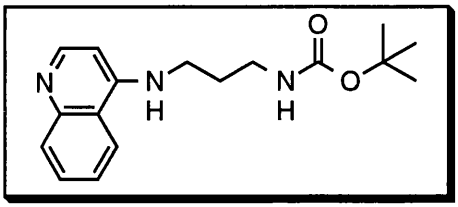

4-Chloroquinoline (**1a**, 0.779 g, 3.06 mmol), 3-[N-(tert-Butoxycarbonyl)amino]-propylamine (**66b**, 0.83 g, 4.76 mmol) and N-ethylmorpholine (0.72 ml, 6.12 mmol) were dissolved in 20 ml of n-pentanol and the solution heated under reflux for 20 h. The solvent was removed in vacuo at 70°C and the oily residue placed under vacuun overnight.

To this, 10 ml of conc. NH_4OH were added and the mixture extracted with 3 x 50 ml CH_2Cl_2. The extracts were combined, dried (Na_2SO_4) and the solvent removed in vacuo. The yellow oil was dried under high vacuum and solidified to a creamy solid. This contained **66b** (by NMR) therefore, it was chromatographed on silica gel using EtOAc : MeOH = 2 : 1. The product (Rf ≈ 0.3) was isolated as a creamy solid. This was dissolved in cold iPrOH, filtered and the solvent removed in vacuo to yield a creamy solid (0.68 g, 47%).

^1H NMR (400 MHz, $CDCl_3$, TMS, ppm) δ 1.49 (s, 9 H, CH_3), 1.85 (m, 2 H, CH_2), 3.30 (q, 2 H, $\underline{CH_2}$-NHCO), 3.42 (q, 2 H, $\underline{CH_2}$-NHquinoline), 4.80 (s_{br}, 1 H, NHCO), 6.09 (s_{br}, 1 H, quinoline-NH), 6.41 (d, 1 H, quinoline-H_3), 7.44 (td, 1 H, quinoline-H_6 or H_7), 7.63 (td, 1 H, quinoline-H_7 or H_6), 7.91 (d, 1 H, quinoline-H_5 or H_8), 7.97 (d, 1 H, quinoline-H_8 or H_5), 8.53 (d, 1 H, quinoline-H_2).

MS (FAB, MNOBA matrix) $[M+H]^+$ 302, fragments at m/z 246, 228, 171, 157.

1-[10-(4-Aminoquinolinium-1-yl)decan-1-yl]-4-[N-[3-[N-(tert-butoxy-carbonyl)]amino]prop-1-yl]aminoquinolinium diiodide (66d, DG-259A)

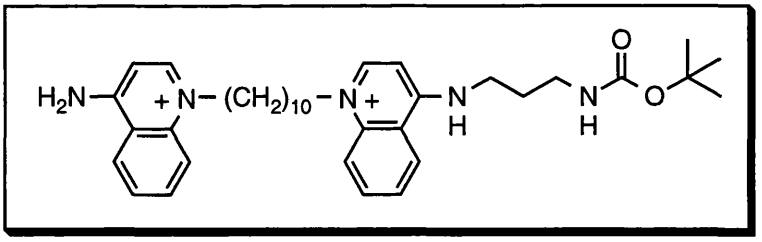

1-[N-(4-Quinolinyl)]-3-[N-(tert-butoxycarbonyl)amino]propanamine (**66c**, 0.6 g, 1.99 mmol) and 1-(10-iododecan-1-yl)-4-aminoquinolinium iodide (**66a**, 1.07 g, 1.99 mmol) were dissolved with heating in 50 ml butanone and the solution was heated under reflux for 92 h under Ar. More **66b** was added in two portions of 0.2 g each after 36 and 60 h respectively. The yellow gum that had come out of solution was collected by decanting the supernatant solution. It was then triturated with sodium dried Et_2O to give a hygroscopic

pale yellow powder which was collected by filtration and dried quickly in vacuo (1.4 g, 84%).

^{1}H NMR (400 MHz, DMSO-d_6, TMS, ppm) δ 1.27 (m, 21 H, CH_2 + tBu), 1.79 (m, 6 H, CH_2), 3.06 (q, 2 H, $\underline{CH_2}$-$NHCO_2$), 3.54 (q, 2 H, $\underline{CH_2}$-NHquinoline), 4.53 (m, 4 H, N^+-CH_2), 6.79 (d, 1 H, quinoline-H_3), 6.94 (m, 2 H, quinoline-H_3' + $NHCO_2$), 7.77 (m, 2 H, quinoline-H_6 + H_6' or H_7 + H_7'), 8.04 (m, 2 H, quinoline-H_7 + H_7' or H_6 + H_6'), 8.16 (m, 2 H, quinoline-H_5 + H_5' or H_8 + H_8'), 8.48 (d, 1 H, quinoline-H_5), 8.54 (m, 2 H, quinoline-H_5' + H_2), 8.65 (d, 1 H, quinoline-H_2'), 9.02 (s, s, 2 H, NH_2), 9.24 (t_{br}, 1 H, quinoline-$\underline{NH}$).

1-[10-(4-Aminoquinolinium-1-yl)decan-1-yl]-4-[N-(3-aminoprop-1-yl)]-aminoquinolinium tritrifluoroacetate

(66, DG-267B, UCL 1469-F_3)

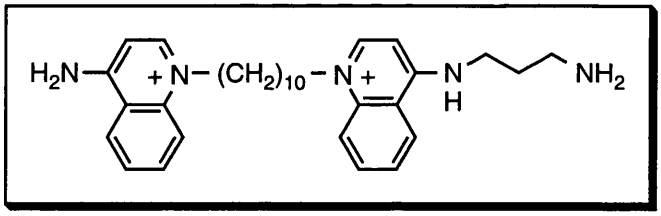

1-[10-(4-Aminoquinolinium-1-yl)decan-1-yl]-4-[N-[3-[N-(tert-butoxycarbonyl)]amino]-prop-1-yl]aminoquinolinium diiodide (**66d**, 0.5 g, 0.595 mmol) was dissolved in a 4 M solution of HCl in MeOH and the solution was set aside for 3 h. The solvent was removed in vacuo, the residue was dissolved in fresh MeOH and concentrated to dryness several times and finally it was dissolved in the minimum amount of MeOH and purified by preparative HPLC using **A** : **B** = 45 : 55. The product was isolated as a colourless oil which after thorough drying and treatment with sodium dried Et_2O solidified to a white solid (0.43 g, 75%).

mp = 55° - 57°C.

IR (KBr disc) ν_{max} 3387, 2958, 2930, 1675, 1616, 1574 cm^{-1}.

^{1}H NMR (400 MHz, CD_3OD, TMS) δ 1.31 - 1.36 (m, 12 H, CH_2), 1.89 (m, 4 H, CH_2), 2.15 (quint, J = 7.5 Hz, 2 H, CH_2), 3.11 (t, J = 7.7 Hz, 2 H, $\underline{CH_2}$-NH_2), 3.71 (t, J = 7.2 Hz, 2 H, $\underline{CH_2}$-NH), 4.55 (m, 4 H, N^+-CH_2), 6.81 (d, J = 7.3 Hz, 1 H, quinoline-H_3 or H_3'), 6.91 (d, J = 7.3 Hz, 1 H, quinoline-H_3' or H_3), 7.74 (m, 2 H, quinoline), 8.06 (m, 4 H, quinoline), 8.39 (m, 2 H, quinoline), 8.47 (d, J = 7.6 Hz, 1 H, quinoline), 8.54 (d, J = 7.4 Hz, 1 H, quinoline).

MS (FAB, MNOBA matrix) $[M-H]^+$ 484, fragments at m/z 284, 256, 242, 228, 215.

HPLC: column (K), A : B = 45 : 55, major peak at 5.38 min representing 100% of the absorption at 215 nm.

Anal. ($C_{31}H_{43}N_5^{2+}\cdot 2CF_3CO_2^-\cdot 2.2CF_3CO_2H$)

calc: C = 49.16, H = 4.73, N = 7.28

found: C = 49.13, H = 4.89, N = 7.28

Immobilized 1-[10-(4-Aminoquinolinium-1-yl)decan-1-yl]-4-[N-(3-aminoprop-1-yl)]aminoquinolinium tritrifluoroacetate (40, DG-267B, UCL 1469-F_3) onto epoxy - activated Sepharose 6B (67, DG-539A, UCL 1533)

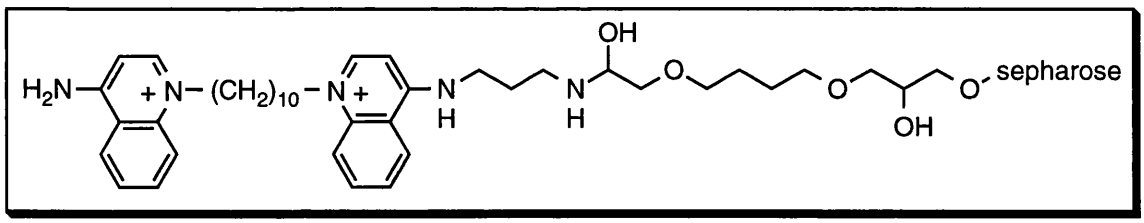

1 g of epoxy - activated Sepharose 6B (Pharmacia) was suspended in distilled water and allowed to hydrate for 45 min using a shaker. It was then transfered onto a sintered - glass funnel and washed extensively with water (150 ml) and finally with 15 ml 0.1 M NaOH (freshly made). 34 mg (0.0353 mmol) of **66** were dispersed in 1 ml 0.1 M NaOH, 0.5 ml dioxane was added to help dissolution and the solution was made up to 6 ml with 0.1 M NaOH. This coupling solution was then mixed with the above prepared gel of Sepharose

and UV assayed as follows: 0.5 ml of the mixture were centrifugated at 10,000 rpm for 3 min and 0.2 ml of the supernatant were diluted to 25 ml with 0.1 M NaOH. The UV spectrum of this solution was recorded. The rest of the mixture was shaken for 24 h at room temperature and UV assayed as above. The gel was then filtered off and washed successively with 60 ml 0.1 M NaOH, 60 ml 0.1 M AcOH containing 1 M NaCl and 60 ml 0.1 M $NaHCO_3$ containing 0.5 M NaCl. To block the remaining free amino groups, the gel was suspended in 6 ml 1 M ethanolamine and shaken overnight at room temperature. It was then filtered off and washed successively with 60 ml 0.1 M AcOH containing 1 M NaCl, 60 ml 0.1 M $NaHCO_3$ containing 0.5 M NaCl, 150 ml 0.01 M Tris-HCl buffer (pH = 8) and 150 ml Tris-HCl buffer (pH = 8) containing 20% EtOH as a preservative. The gel was air - dried on the funnel and stored at 4°C. The yield of the coupling based on the difference in the absorption of the coupling solution at 334.8 nm was 70%.

4-methoxyquinoline[283]

(68, DG-135A)

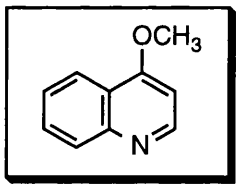

1a (1.296 g, 8.45 mmol) was added to a solution of Na (0.25 g, 10.87 mmol) in 40 ml of freshly distilled from Mg MeOH and the resultant solution was heated under reflux for 54 h, more Na (0.15 g, 6.52 mmol) being added after 24 h. The solvent was removed in vacuo, water was added to the residue and the solution was extracted with CH_2Cl_2. The extracts were combined, dried with K_2CO_3 and the solvent removed in vacuo to yield a yellow oil. This was coevaporated three times with dry ether and dried under high vacuum overnight to yield a yellow solid (1.118 g, 83%) which was purified by column chromatography. The product was isolated as a yelowish oil which solidified in the freezer.

mp = 35°-36°C (reported mp = 41°C).

NMR (^{1}H, 200 MHz, $CDCl_3$, ppm) δ 4.00 (s, 3H, OCH_3), 6.72 (d, 1H, quin-H_3), 7.25 ($CHCl_3$), 7.49 (t, 1H, quin-H_6 or quin-H_7), 7.68 (t, 1H, quin-H_7 or quin-H_6), 8.02 (d, 1H, quin-H_5), 8.19 (d, 1H, quin-H_8), 8.74 (d, 1H, quin-H_2).

Attempted preparation of **1,1′-decan-1,10-diyl-4,4'-dimethoxy-bis-quinolinium diiodide**

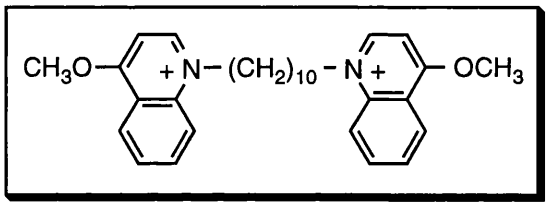

68 (0.9 g, 5.65 mmol) and 1,10-diiododecane (1.1 g, 2.79 mmol) were dissolved in MEK and the solution was heated under reflux for 60 hrs under argon. The solvent was removed in vacuo and the residue was shown to be a mixture of three compounds which were separated by column chromatography. The first fraction obtained was unreacted 1,10-diiododecane, the second N-methyl-4-quinolone [mp = 151°-152°C, reported (in Beilstein) mp = 152°C] and the third probably being 1-(10-iodo-1-decanyl)-4-hydroxyquinolinium iodide (MS, NMR).

7.2 MOLECULAR MODELLING

Molecular orbital calculations. These were performed on the model compounds of **Tables 4.4** and **4.7**. The structures were initially built in Sybyl 5.5[291] running on a Silicon Graphics IRIS 4D workstation. In view of the absence of an atom type corresponding to the quaternary ring nitrogen of the quinoline, an alternative atom type had to be used and the trigonal planar (Npl3) was found to give the best results. To minimize the computational time of the MO calculations the compounds were first subjected to energy minimization using the Tripos forcefield.[292] The minimization method of Powell was employed, which uses the conjugate - gradient minimizer.[293] The minimization was terminated when the energy gradient difference between two consecutive iterations was lower than 0.05 Kcal/mol·Å. The number of iterations between the reevaluation of the non - bonded interaction list (*non - bonded reset*) was set to 10 and atoms separated by at least 8 Å were not included in the non - bonded interactions calculation (*non - bonded cutoff*). For the calculation of the electrostatic component of the total energy, charges were assigned to the atoms using the Gasteiger - Hückel method. This is a combination of two charge computation methods: The Gasteiger - Marsili method[294-296] to calculate the σ component of the atomic charge and the Hückel method[297] to calculate the π component of the atomic charge. The total charge is the sum of the charges calculated by the two methods. Finally, a distance - dependent dielectric function r (i.e., the interatomic distance) was used.

The minimized structures were then submitted for semiemperical MO calculations using the MOPAC 5.0 MO package and usually the AM1[232] Hamiltonian, although MINDO/3, MNDO or PM3 were used in some cases as described in the discussion part (chapter 4). The normal self - consistent field (SCF) convergence procedure (default setting) was used and full geometry optimization of the structure was carried out. The charge on the system was set to 1. In the keyword section, *nointer* was routinely entered to exclude the interatomic distances from the output file, thus reducing its size. Since all four semi - empirical methods underestimate the barrier to rotation of a peptide bond, a molecular mechanics correction was applied (using *MMOK*), which increases the barrier

to rotation in N-methyl acetamide to 14 Kcal/mol, when calculations were performed on structures containing such a bond. It should also be noted that the AM1 Hamiltonian in MOPAC 5.0 does not have parameters for the S atom. Therefore, in the calculations on compounds **22** and **23** *PARASOK* was utilised to allow the use of the parameters of MNDO for the S atom in the AM1 calculation. Since this is not usual practice and to assess its validity, two series of calculations were performed on compounds **20** (X = CH_2), **22** (X = S), **26** (X = NH) and **28** (X = O), one using MNDO and the other using AM1. Although there was variance in the *absolute* values of the MO energies when comparing the results from the two methods, the *differences* in MO energies calculated by the two methods were similar. Finally, bond orders, localised orbitals and molecular orbitals were included in the output file. A Mulliken population analysis was also performed and the results included in the output file. A MO plotfile was created as this is required by SYBYL for creating MO contour plots.

7.3 RADIOLIGAND BINDING STUDIES

7.3.1 Saturation experiment to obtain the K_D of ^{125}I-apamin

The experiment was performed using a filtration assay as described previously.[298,299,156] Rat brain synaptic plasma membranes were prepared and kindly provided by Miss K. Doorty. The protein content of the membrane preparation was determined using the method of Lowry et al[300] using bovine serum albumin (BSA) as standard.

A standard curve of UV absorption at 750 nm vs the amount of BSA in μg was created as follows: A series of solutions was prepared in duplicate containing increasing concentrations of BSA as shown in **Table 7.1**. 2 ml of Lowry solution were then added and the resultant solutions were allowed to stand for 10 min (to prepare the Lowry solution, mix 50 ml of 2% w/v Na_2CO_3 in 0.1 N NaOH with 1 ml 0.5% w/v $CuSO_4 \cdot 5H_2O$ in 1% w/v sodium or potassium tartrate). Finally, 100 μl of diluted Folin reagent[300] were added and the UV absorption of each solution measured at 750 nM. The UV absorption of a solution of 5 μl of the membrane preparation in 395 μl of water and 2 ml of Lowry solution containing 100 μl of diluted Folin reagent prepared in triplicate was then measured and found to be 0.365. From the standard curve this corresponds to a protein content of 7.86 mg/ml for the rat brain synaptic plasma membrane preparation.

Table 7.1 Solutions of BSA for standard curve of protein content determination

BSA (μg)	2 mg/ml BSA (μl)	water (μl)	UV abs (750 nM)
0	—	400	0
10	5	395	0.114
20	10	390	0.216
30	15	385	0.311
40	20	380	0.370
50	25	375	0.411
60	30	370	0.466

In the saturation experiment to determine the K_D of ^{125}I-apamin, aliquots of the

membrane preparation containing 100 μg of protein were incubated on ice for 1 h with increasing concentrations of ^{125}I-apamin. The incubation medium (1 ml) consisted of 10 mM KCl, 25 mM Tris at pH = 8.4, containing 0.1% w/v BSA. The non specific binding was determined in the presence of 0.1 μM cold apamin. After rapid filtration through Whatman GF/B FP-100 filters presoaked for 1 h in 0.5% (v/v) polyethyleneimine, filters were counted at 84% efficiency in a calibrated γ counter.

The results from the saturation experiment were analysed using the EBDA (Biosoft) computer program. The amounts of ^{125}I-apamin bound specifically and non - specifically as a function of the concentration of the radioligand is shown in **Figure 7.3.1**. The semilogarithmic plot of the percentage of saturably bound ^{125}I-apamin vs the total concentration of ^{125}I-apamin is shown in **Figure 7.3.2**. The K_D of ^{125}I-apamin was found to be 4.8 pM. Furthermore, the plot of the ratio of the concentrations of bound over free ^{125}I-apamin vs the concentration of free ^{125}I-apamin (Scatchard plot) is shown in **Figure 7.3.3**. It is consistent with a single class of binding sites and the maximum receptor concentration (B_{max}) was found to be 41 fmol/mg of protein. The Hill plot is shown in **Figure 7.3.4** and the Hill coefficient was found to be 1.001.

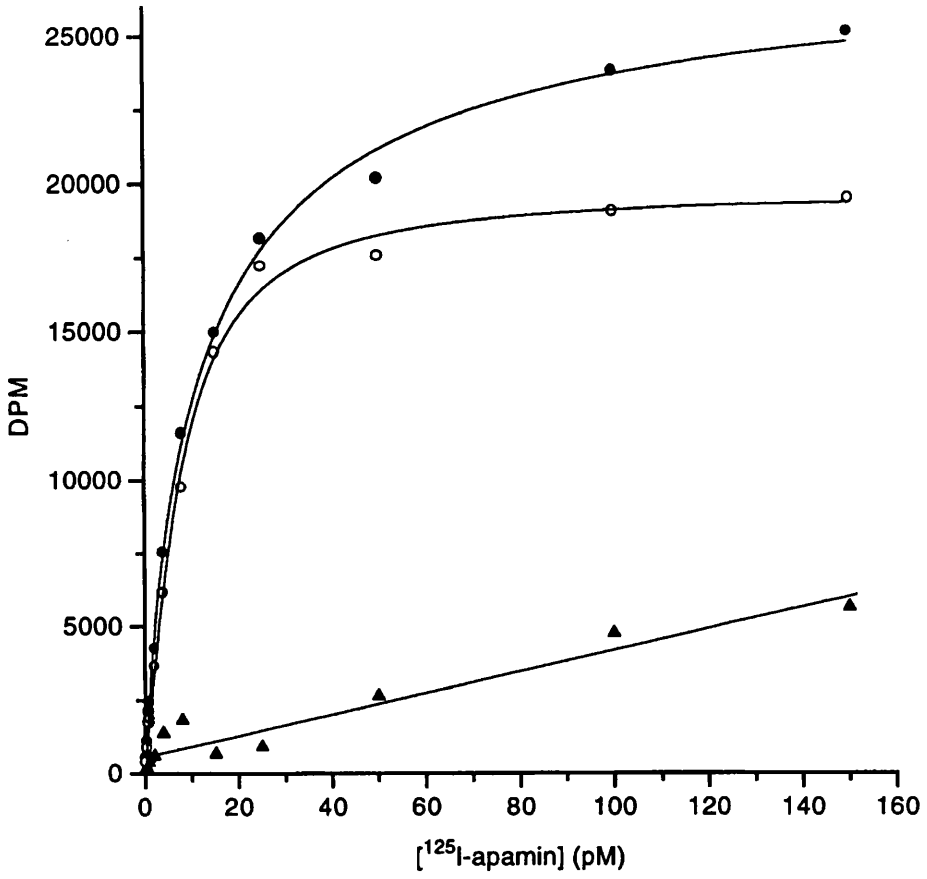

Figure 7.3.1 Plot of DPM of total ^{125}I-apamin bound (●), DPM of non - specifically bound ^{125}I-apamin (▲) and DPM of specifically bound ^{125}I-apamin (○) to rat synaptic plasma membranes vs the concentration of the radioligand. DPM: disintegrations per min.

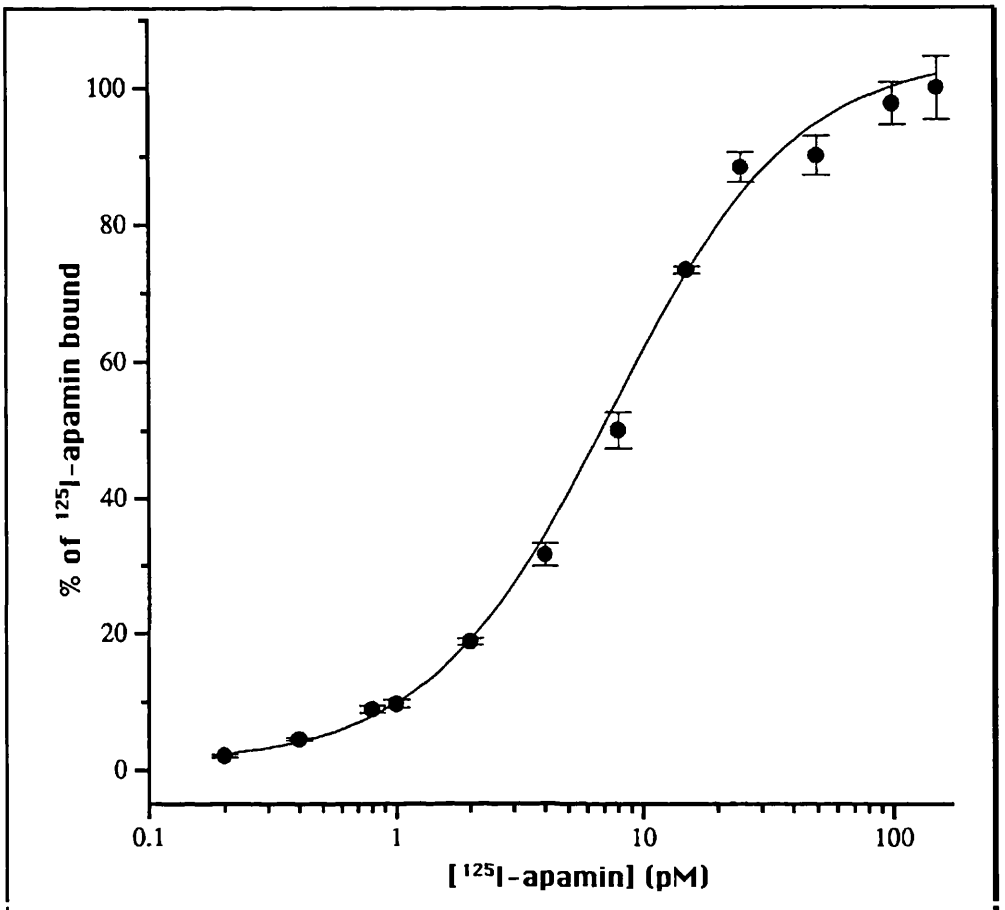

Figure 7.3.2 Plot of the % of saturably bound ^{125}I-apamin vs the total concentration of ^{125}I-apamin with data from the saturation experiment.

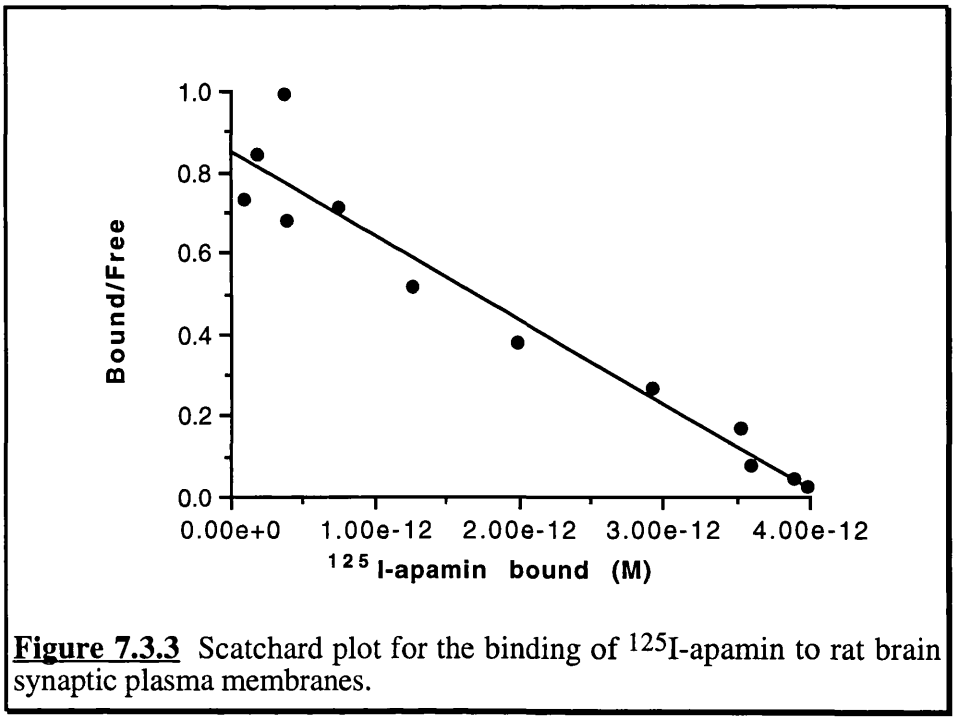

Figure 7.3.3 Scatchard plot for the binding of ^{125}I-apamin to rat brain synaptic plasma membranes.

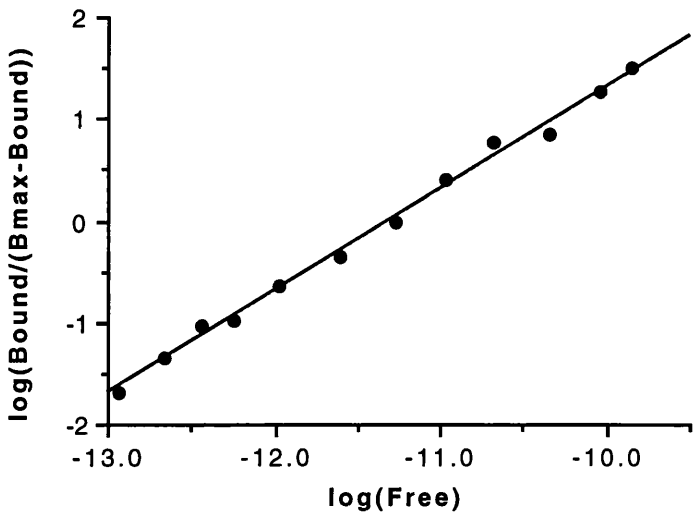

Figure 7.3.4 Hill plot for the binding of ^{125}I-apamin to rat brain synaptic plasma membranes.

7.3.2 Competition experiments to determine the K_i values of blockers

In these experiments, rat synaptic plasma membranes were incubated with a fixed concentration of 10 pM ^{125}I-apamin in the presence or absence of increasing concentrations of the blocker. The incubation medium, time, filtration and counting were as above. ORIGIN was then used to obtain estimates for the IC_{50} (the concentration causing 50% inhibition of ^{125}I-apamin binding) values of the blockers by non - linear least squares fitting of the data to the equation:

$$B = \frac{B_{max} - BG}{1 + \left[\frac{[I]}{IC_{50}}\right]^P} + BG \qquad \textbf{eq. 1}$$

or to the Hill equation:

$$B = B_{max} - \frac{B_{max} \cdot [I]^P}{[I]^P + [IC_{50}]^P} \qquad \textbf{eq. 2}$$

where B is the amount of ^{125}I-apamin bound in the presence of $[I]$ concentration of the inhibitor,

B_{max} is the maximum amount of ^{125}I-apamin bound in the absence of any inhibitor,

BG is the non - specific binding,

[*I*] is the concentration of the inhibitor,

IC_{50} is the concentration of the inhibitor that causes 50% inhibition of ^{125}I-apamin binding and

P is the slope factor (Hill coefficient)

The IC_{50} values estimated in this way were then used to determine the dissociation constants (K_i) of the compounds using the Cheng - Prusoff equation:[301]

$$K_i = \frac{IC_{50}}{1 + \frac{[R]}{K_D}}$$

where K_i is the dissociation constant of the inhibitor,

IC_{50} is the concentration of the inhibitor that causes 50% inhibition of the binding of the radioligand *R*,

[*R*] is the concentration of the radioligand and

K_D is the dissociation constant of the radioligand.

It is important to note that the use of the Cheng - Prusoff equation to convert the IC_{50} to K_i values is only valid when the law of mass action is observed in the reaction of the ligands with the receptor, ie. when the slope factor takes values not significantly different from unity. Initial analysis of the binding data using EBDA yielded slope factors which were significantly higher than unity except for compound **47** for which the slope factor was close to 1 (**Table 7.2**). To gain insight into the potential problem, different software was used to analyse the data and also two different fitting functions were employed as shown in **Table 7.2**. Furthermore, the effect of weighting in the fitting process was investigated. Note that weighting is a procedure by which more significance is granted to points with low standard error of the mean (SEM) and, as a result, the curve is "forced" by the non - linear least squares fitting routine to pass as close to those points as possible. This is based on the reasoning that data points with low SEMs are more reliable.

However, as can be seen from **Table 7.2**, the application of weighting in the fitting process always yielded either very high or very low slope factors. Visual inspection of the semilogarithmic plots of the amount of ^{125}I-apamin bound vs the concentration of the inhibitor provided an explanation for this fact. Hence, in all cases, the data points at the low end of the curve (ie. at high inhibitor concentrations, at which little ^{125}I-apamin binds) have particularly low SEMs and the curve is "forced" to pass through these points. As a result of this and because of symmetry restrictions (arising from the symmetrical nature of the sigmoidal curves produced by the two fitting functions), points at the upper end of the curve are virtually ignored in some cases (such as that of compound **45**, **Figure 7.3.5**) and either steep (**eq. 1**) or shallow (**eq. 2**) curves are produced. It is therefore evident that slope factors produced from weighted fitting are not reliable.

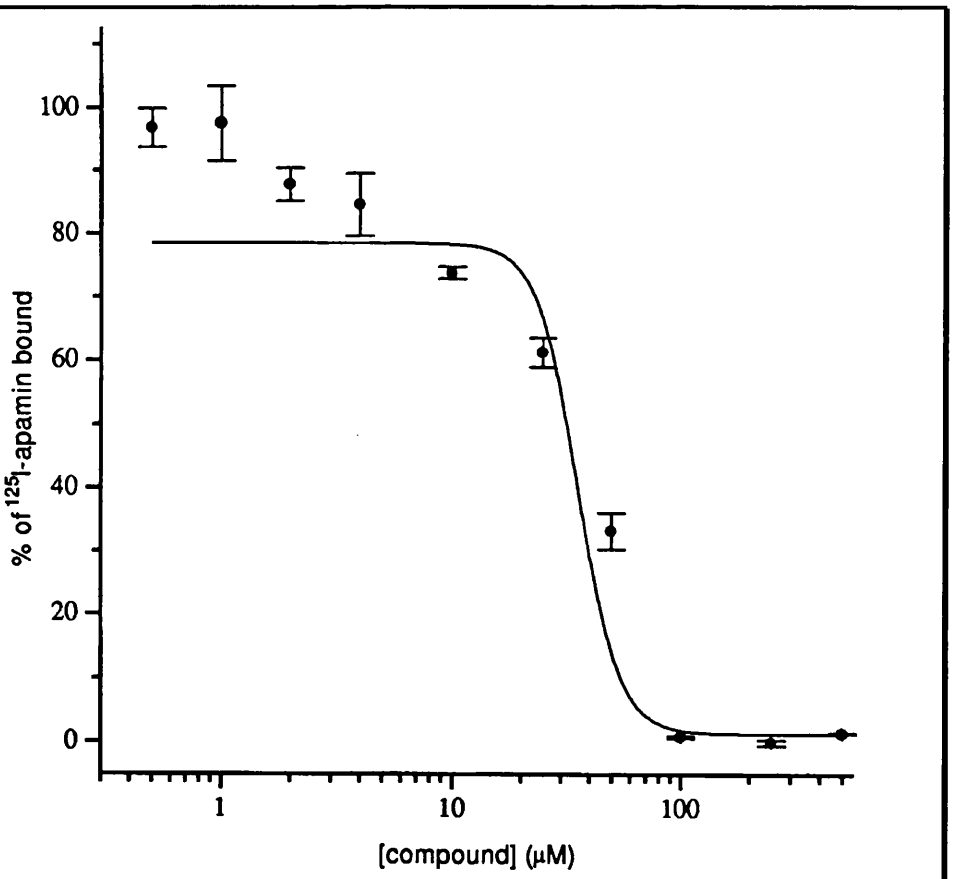

Figure 7.3.5 ^{125}I-apamin binding to rat brain synaptic plasma membranes in the presence of compound **45**. The curve was produced with ORIGIN, using a weighted least squares fitting of the data to **eq. 1**. Note the steepness of the descending part of the curve (slope factor = 4.27) and also the fact that the curve is "forced" by the weighting process to pass through the bottom 3 points which have low SEMs.

Table 7.2 Dependence of slope factors on the method and program used for the analysis

Compd No	P					
	eq 1: $B = \frac{B_{max} - BG}{1 + \left[\frac{[I]}{IC_{50}}\right]^P} + BG$			**eq 2:** $B = B_{max} - \frac{B_{max} \cdot [I]^P}{[I]^P + [IC_{50}]^P}$		
	EBDA	ORIGIN		ORIGIN		MINIM
	Weighted	Weighted	Unweighted*	Unweighted	Weighted	Unweighted
Deq (**8**)	1.60	1.56	1.18	1.15	1.14	1.08
45	5.67	4.27	1.43	1.39	0.57	1.21
46	1.51	1.52	1.43	1.15	1.00	1.42
18	2.11	1.14	1.33	1.20	1.08	1.67
64	1.66	1.58	1.45	1.31	0.90	1.70
47	1.14	1.08	1.00	0.93	0.78	1.04

* This column of data was used for the generation of the plots in **Figures 4.19, 7.3.6** and **7.3.7**.

On the other hand, no unusual features were observed on visual inspection of the sigmoidal curves resulting from unweighted fitting and the slope factors take more reasonable values. Nevertheless, there appears to be some variation in the slope factor values calculated using different programs or fitting functions. The only compounds that give slope factors consistently close to unity are dequalinium and the trisquinolinium **47**. The two monoquaternary compounds **45** and **46** as well as the two bisquaternary analogues **18** and **64** have slope factors noticeably higher than unity. Hill coefficients greater than 1 have generally been associated with positive cooperativity. In such cases, two or more molecules of the ligand bind to the receptor, the binding of the second molecule being more facile since the first molecule has already displaced the radioligand. The significance of the slope factors for the compounds **45**, **46**, **18** and **64** being generally between 1 and 1.5 is not clear, since a slope factor of close to 2 is required if two molecules of the compound bind to the receptor. Further work is needed to elucidate the implications of these observations. It is interesting to note, however, that the

compounds with slope factors greater than 1 probably have higher lipophilicity than dequalinium or **47** due either to the presence of additional hydrophobic groups (**18** and **64**) or to the lack of a second positive charge (**45** and **46**). The ^{125}I-apamin displacement curves in the presence of compounds **8**, **45**, **46** and **47** are shown in **Figure 4.19**, while the curves for compounds **18** and **64** are shown in **Figures 7.3.6** and **7.3.7** respectively. The curves in these figures were fitted to **eq. 1** (**Table 7.2**) using the unweighted routine of ORIGIN. This method was used to calculate the K_i values for the blockers.

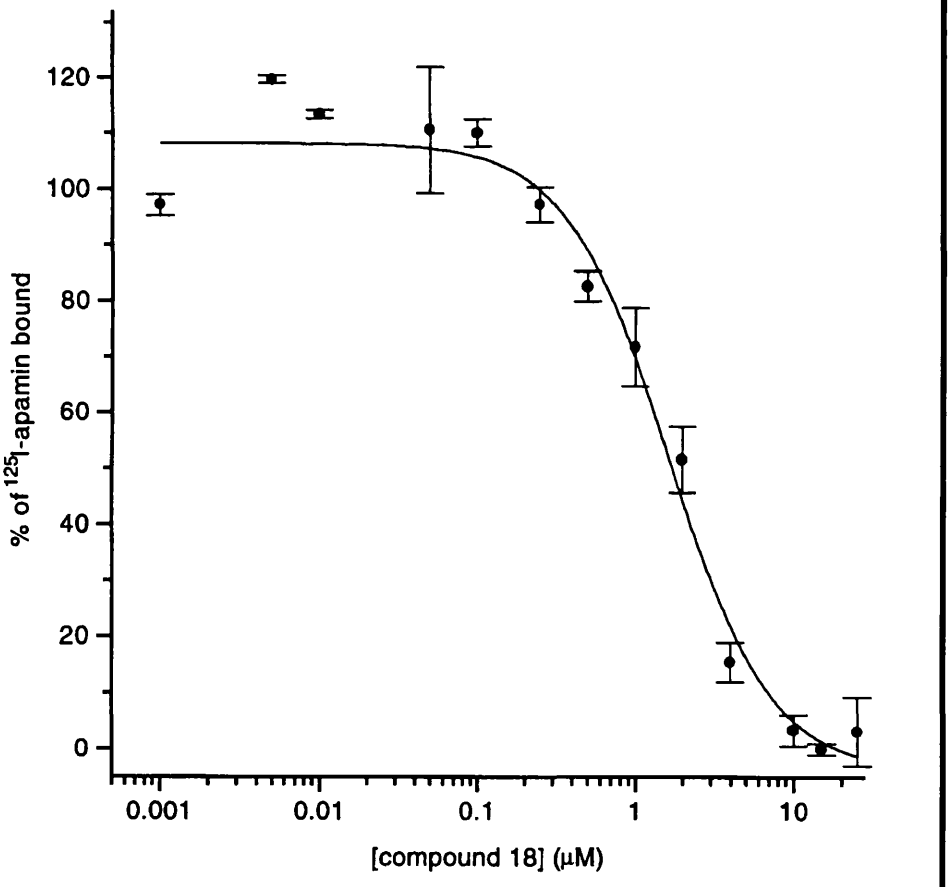

Figure 7.3.6 ^{125}I-apamin binding to rat brain synaptic plasma membranes in the presence of compound **18**. The curve was produced with ORIGIN, using an unweighted least squares fitting of the data to **eq. 1**.

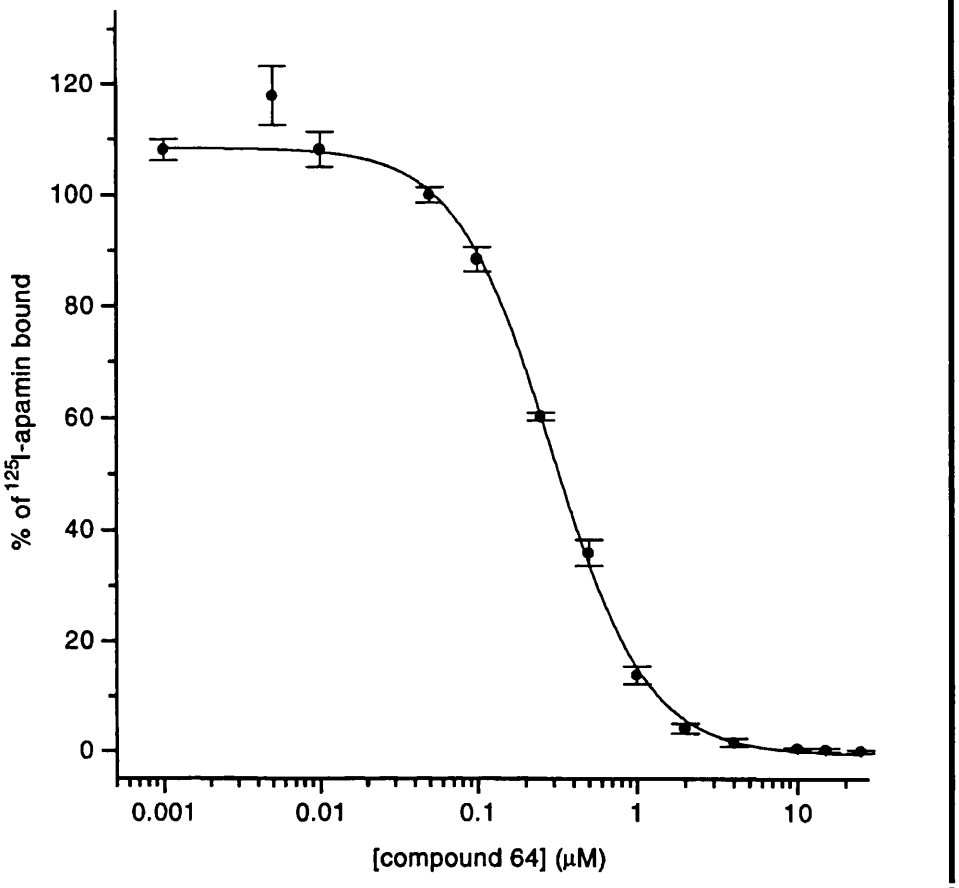

Figure 7.3.7 ^{125}I-apamin binding to rat brain synaptic plasma membranes in the presence of compound **64**. The curve was produced with ORIGIN, using an unweighted least squares fitting of the data to **eq. 1**.

These slight abnormalities in the values for the slope factors, on the whole, do not question the validity of the analysis of the binding data in terms of free energies, presented in section **4.3**. Although the absolute value for the intrinsic binding energy of the quinolinium group, which is calculated from the K_is of **45** and **46**, should be treated in the context of the reservations created by the high slope factors, the arguments presented remain valid because they are mainly *qualitative* in nature.

REFERENCES

(1) Cook, N. S. The pharmacology of potassium channels and their therapeutic potential. *Trends Pharm. Sci.* **1988**, *9*, 21 - 28.

(2) Robertson, D. W.; Steinberg, M. I. Potassium Channel Modulators: Scientific Applications and Therapeutic Promise. *J. Med. Chem.* **1990**, *33*, 1529 - 1541.

(3) Hodgkin, A. L.; Huxley, A. F. A quantitative description of membrane current and its application to conduction and excitation in nerve. *J. Physiol.* **1952**, *117*, 500 - 544.

(4) Rudy, B. Diversity and ubiquity of K channels. *Neuroscience* **1988**, *25*, 729 - 749.

(5) Dubois, J. M. Potassium currents in the frog node of ranvier. *Prog. Biophys. Molec. Biol.* **1983**, *42*, 1 - 20.

(6) Adams, P. R.; Brown, D. A.; Constanti, A. M-currents and other currents in bulfrog sympathetic neurones. *J. Physiol.* **1982**, *330*, 537 - 572.

(7) Belluzzi, O.; Sacchi, O.; Wanke, E. Identification of delayed potassium and calcium currents in the rat sympathetic neurone under voltage clamp. *J. Physiol.* **1985**, *358*, 109 - 130.

(8) Segal, M.; Barker, J. L. Potassium conductancies in rat sympathetic neurones in culture. *J. Neurophysiol.* **1984**, *51*, 1409 - 1433.

(9) Giles, W. R.; Shibata, E. F. Voltage clamp of bullfrog cardiac pacemaker cells: A quantitative analysis of potassium currents. *J. Physiol.* **1985**, *368*, 265 - 292.

(10) Dural, A.; Lesty, C. Comparison between the delayed outward current in slow and fast skeletal muscle in the rat. *J. Physiol.* **1980**, *307*, 43 - 57.

(11) Pongs, O. Structural basis of voltage - gated K^+ channel pharmacology. *Trends Pharm. Sci.* **1992**, *13*, 359 - 365.

(12) Kirsch, G. E.; Narahashi, T. 3,4-Diaminopyridine. A potent new potassium channel blocker. *Biophys. J.* **1978**, *22*, 507 - 512.

(13) Albuquerque, E. X.; Aguayo, L. G.; Warnick, J. E.; Weinstein, H.; Glick, S. D.;

Maayani, S.; Ickowitz, R. K.; Blaustein, M. P. The behavioural effects of phencyclidines may be due to their blockade of potassium channels. *Proc. Natl. Acad. Sci. USA* **1981**, *78*, 7792 - 7796.

(14) Almers, W. Differential effects of tetracaine on delayed potassium channels and displacement currents in frog skeletal muscle. *J. Physiol.* **1976**, *262*, 1613 - 1637.

(15) Blaustein, M. P.; Rogowski, R. S.; Schneider, M. J.; Krueger, B. K. Polypeptide toxins from the venoms of old-world and new-world scorpions preferentially block different potassium channels. *Mol. Pharmacol.* **1991**, *40*, 932 - 942.

(16) Sands, S. B.; Lewis, R. S.; Cahalan, M. D. Charybdotoxin blocks voltage - gated K^+ channels in human and murine lymphocytes-T. *J. Gen. Physiol.* **1989**, *93*, 1061 - 1074.

(17) Garcia-Calvo, M.; Leonard, R. J.; Norick, J.; Stevens, S. P.; Schmalhofer, W.; Kaczorowski, G. J.; Garcia, M. L. Purification, characterization and biosynthesis of margatoxin, a component of *Centruroides - margaritatus* venom that selectively inhibits voltage - dependent potassium channels. *J. Biol. Chem.* **1993**, *268*, 18866 - 18874.

(18) Carbon, E.; Wanke, E.; Prestipino, G.; Possani, L. D.; Maelicke, A. Selective blockage of voltage - dependent K^+ channels by a novel scorpion toxin. *Nature* **1982**, *296*, 90 - 91.

(19) Harvey, A. L.; Anderson, A. J. Dendrotoxins: snake toxins that block potassium channels and facilitate transmitter release. *Pharmac. Ther.* **1985**, *31*, 33 - 55.

(20) Sanguinetti, C. M.; Jurkiewicz, N. K. Two components of cardiac delayed rectifier K^+ current. *J. Gen. Physiol.* **1990**, *96*, 195 - 215.

(21) Convar, J. A.; Stevens, C. F. Voltage clamp studies of a transient outward membrane current in gastropod neural somata. *J. Physiol.* **1971**, *213*, 21 - 30.

(22) Pongs, O. Molecular basis of potassium channel diversity. *Pflügers Arch.* **1989**, *414*, 71 - 75.

(23) Catterall, W. A. Structure and function of voltage - gated ion channels. *Trends Neurosci.* **1993**, *16*, 500 - 506.

(24) Scott, V. E. S.; Retting, J.; Parcej, D. N.; Keen, J. N.; Findlay, J. B. C.; Pongs, O.; Dolly, J. O. Primary structure of a beta - subunit of alpha - dendrotoxin - sensitive K^+ channels from bovine brain. *Proc. Natl. Acad. Sci. USA* **1994**, *91*, 1637 - 1641.

(25) Rogawski, M. A. The A-current: how ubiquitous a feature of excitable cells is it? *Trends Neurosci.* **1985**, *8*, 214 - 219.

(26) Rogawski, M. A. Tetrahydroaminoacridine blocks voltage - dependent ion channels in hippocampal neurons. *Eur. J. Pharmacol.* **1987**, *142*, 169 - 172.

(27) Aguayo, L. G.; Alburquerque, E. X. Phencyclidine blocks two potassium currents in spinal neurones in cell culture. *Brain Res.* **1987**, *436*, 9 - 17.

(28) Thompson, S. H.; Aldrich, R. W. In *The cell surface and neuronal funcion*; G. Poste and G. L. Nicholson, Ed.; Elsevier / North Holland Biomedical Press: Amsterdam, 1980; pp 49 - 58.

(29) Halliwell, J. V.; Othman, I. B.; Pelden-Matheus, A.; Dolly, J. O. Central action of dendrotoxin: selective reduction of a transient K conductance in hippocampus and binding to localized acceptors. *Proc. Natl. Acad. Sci. USA* **1986**, *83*, 493 - 497.

(30) Stansfeld, C. E.; March, S. J.; Parcej, D. N.; Dolly, J. O.; Brown, D. A. Mast cell degranulating peptide and dendrotoxin selectively inhibit a fast - activating potassium current and bind to common neuronal proteins. *Neuroscience* **1987**, *23*, 893 - 902.

(31) MacKinnon, R.; Reinhart, P. H.; White, M. M. Charybdotoxin block of Shaker K^+ channels suggests that different types of K^+ channels share common structural features. *Neuron* **1988**, *1*, 997 - 1001.

(32) Goldstein, S. A. N.; Miller, C. Mechanism of charybdotoxin block of a voltage - gated K^+ channel. *Biophys. J.* **1993**, *65*, 1613 - 1619.

(33) Goldstein, S. A. N.; Miller, C. A point mutation in a shaker K^+ channel changes its charybdotoxin binding site from low to high affinity. *Biophys. J.* **1992**, *62*, 5 - 7.

(34) MacKinnon, R.; Miller, C. Mutant potassium channels with altered binding of charybdotoxin, a pore - blocking peptide inhibitor. *Science* **1989**, *245*, 1382 -

1385.

(35) MacKinnon, R.; Heginbotham, L.; Abramson, T. Mapping the receptor site for charybdotoxin, a pore - blocking potassium channel inhibitor. *Neuron* **1990**, *5*, 676 - 771.

(36) Reuter, H. Ion channels in cardiac membranes. *Ann. Rev. Physiol.* **1984**, *46*, 473 - 484.

(37) Adrian, R. H. Rectification in muscle membrane. *Prog. Biophys. Mol. Biol.* **1969**, *19*, 340 - 369.

(38) Kubo, Y.; Baldwin, T. J.; Jan, Y. N.; Jan, L. Y. Primary structure and functional expression of a mouse inward rectifier potassium channel. *Nature* **1993**, *362*, 127 - 133.

(39) Ho, K.; Nichols, C. G.; Lederer, W. J.; Lytton, J.; Vassilev, P. M.; Kanazirska, M. V.; Hebert, S. C. Cloning and expression of an inwardly rectifying ATP - regulated potassium channel. *Nature* **1993**, *362*, 31 - 38.

(40) Stanfield, P. R. Tetraethylammonium ions and the potassium permeability of excitable cells. *Rev. Physiol. Biochem. Pharmacol.* **1983**, *97*, 1 - 67.

(41) Busso, C.; Camino, E.; Cedrini, L.; Lovisolo, D. The effects of gaboon viper (*Bitis gabonica*) venom on voltage - clamped single heart cells. *Toxicon* **1988**, *26*, 559 - 570.

(42) Young, R. C.; Allen, R. J.; Meissner, G. Permeability of reconstituted sarcoplasmic reticulum vesicles. Reconstitution of the potassium ion, sodium ion channel. *Biochim. Biophys. Acta* **1981**, *640*, 409 - 418.

(43) Moutin, M. J.; Dupont, Y. Rapid filtration studies of calcium - induced calcium release from skeletal sarcoplasmic reticulum. Role of monovalent ions. *J. Biol. Chem.* **1988**, *269*, 4228 - 4235.

(44) Gray, M. A.; Tomlis, B.; Montgomery, R. A. P.; Williams, A. J. Structural aspects of the sarcoplasmic reticulum potassium channel revealed by gallium block. *Biophys. J.* **1988**, *54*, 233 - 239.

(45) Coronado, R.; Miller, C. Conductance and block by organic cations in a K^+ selective channel from sarcoplasmic reticulum incorporated into planar

phospholipid bilayers. *J. Gen. Physiol.* **1982**, *79*, 529 - 547.

(46) Brown, D. A.; Adams, P. R. Muscarinic suppression of a novel voltage - sensitive K^+ current in a vertebrate neurone. *Nature* **1980**, *283*, 673 - 676.

(47) Adams, P. R.; Brown, D. A.; Constanti, A. Pharmacological inhibition of the M-current. *J. Physiol.* **1982**, *332*, 223 - 262.

(48) Adams, P. R.; Galvan, M. In *Advances in Neurology*; A. Delgado-Escueta, A. A. Ward, D. M. Woodbury and R. Porter, Ed.; Raven Press: New York, 1986; Vol. 44; pp 137 - 170.

(49) Sakmann, B.; Noma, A.; Trautwein, W. Acetylcholine activation of single muscarinic K^+ channels in isolated pacemaker cells of mammalian heart. *Nature* **1983**, *303*, 250 - 253.

(50) Soejima, M.; Noma, A. Mode of regulation of the ACh-sensitive K-channel by the muscarinic receptor in rabbit atrial cells. *Pflügers Arch.* **1984**, *400*, 424 - 431.

(51) Kubo, Y.; Reuveny, E.; Slesinger, P. A.; Jan, Y. N.; Jan, L. Y. Primary structure and functional expression of a rat G-protein - coupled muscarinic potassium channel. *Nature* **1993**, *364*, 802 - 806.

(52) Kurachi, Y.; Nakajima, T.; Sugimoto, T. On the mechanism of activation of muscarinic K^+ channels by adenosin in isolated atrial cells: involvement of GTP-binding proteins. *Pflügers Arch.* **1986**, *407*, 264 - 274.

(53) Klein, M.; Camardo, J. S.; Kandel, E. R. Serotonin modulates a specific potassium current in the sensory neurons that show presynaptic facilitation in *Aplysia*. *Proc. Natl. Acad. Sci. USA* **1982**, *79*, 5713 - 5717.

(54) Shuster, M. J.; Carmardo, J. S.; Siegelbaum, S. A.; Kandel, E. R. Cyclic-AMP-dependent protein kinase closes the serotonin sensitive K^+ channels of *Aplysia* sensory neurons in cell - free membrane patches. *Nature* **1985**, *313*, 392 - 395.

(55) Brezine, V.; Eckert, R.; Erxleben, C. Modulation of potassium conductances by an endogenous neuropeptide in neurones of *Aplysia californica*. *J. Physiol.* **1987**, *382*, 267 - 290.

(56) Ashcroft, F. M.; Harrison, D. E.; Ashcroft, J. H. Glucose induces closure of single potassium channels in isolated pancreatic β-cells. *Nature* **1984**, *312*, 446 -

448.

(57) Cook, D. L.; Hales, C. N. Intracellular ATP directly blocks K^+ channels in pancreatic β-cells. *Nature* **1984**, *311*, 271 - 273.

(58) Noma, A. ATP - regulated K^+ channels in cardiac muscle. *Nature* **1983**, *305*, 147 - 148.

(59) Trube, G.; Hescheler, J. Inward - rectifying channels in isolated patches of the heart cell membrane: ATP - dependence and comparison with cell - attached patches. *Pflügers Arch.* **1984**, *401*, 178 - 184.

(60) Spruce, A. E.; Standen, N. B.; Stanfield, P. R. Voltage - dependent ATP - sensitive potassium channels of skeletal muscle membrane. *Nature* **1985**, *316*, 736 - 738.

(61) Ashford, M. L. J.; Sturgess, N. C.; Trout, N. J.; Gardner, N. J.; Hales, C. N. Adenosine-5´-triphosphate - sensitive ion channels in neonatal rat cultured central neurones. *Pflügers Arch.* **1988**, *412*, 297 - 304.

(62) Ashcroft, F. M. Adenosine-5´-triphosphate - sensitive potassium channels. *Ann. Rev. Neurosci.* **1988**, *11*, 97 - 118.

(63) Findlay, I. Effects of ADP upon the ATP - sensitive K^+ channel in rat ventricular myocytes. *J. Membr. Biol.* **1988**, *101*, 83 - 92.

(64) Bokvist, K.; Berggre, P.-O.; Rorsman, P. Evidence that ADP and ATP binds at different sites at the G-channel. *Diabetologia* **1988**, *30*, 473A.

(65) Corkey, B. E.; Deeney, J. T.; Glennon, M. C.; Matschinsky, F. M.; Prentki, M. Regulation of steady - state Ca^{2+} levels by the ATP/ADP ratio and orthophosphate in permeabilized RINm5f insulinoma cells. *J. Biol. Chem.* **1988**, *263*, 4247 - 4253.

(66) Corkey, B. E.; Tornheim, K.; Deeney, J. T.; Glennon, M. C.; Parker, J. C.; Matschinsky, F. M.; Ruderman, N. B.; Prentki, M. Linked oscillations of free Ca^{2+} and the ATP/ADP ratio in permeabilized RINm5f insulinoma cells supplemented with a glycolyzing cell - free muscle extract. *J. Biol. Chem.* **1988**, *263*, 4254 - 4258.

(67) Noma, A.; Shibasaki, T. Membrane current through adenosine - triphosphate -

regulated potassium channels in guinea - pig ventricular cells. *J. physiol.* **1985**, *363*, 463 - 80.

(68) Wilde, A. A. M.; Escande, D.; Schumacher, C. A.; Thuringer, D.; Mestre, M.; Fiolet, J. W. T.; Janse, M. J. Potassium accumulation in the globally ischemic mammalian heart. A role for the ATP - sensitive potassium channel. *Circulation Res.* **1990**, *67*, 835 - 43.

(69) Lederer, W. J.; Nichols, C. G.; Smith, G. L. The mechanism of early contractile failure of isolated rat ventricular myocytes subjected to complete metabolic inhibition. *J. Physiol.* **1989**, *413*, 329 - 49.

(70) Fink, R.; Hase, S.; Lüttgau, H. C.; Wettwer, E. The effects of cellular energy reserves and internal calcium ions on the potassium conductance in skeletal muscle of the frog. *J. Physiol.* **1983**, *336*, 211 - 218.

(71) Wall, K. H.; Lönnendonker, V.; Neumcke, B. ATP - sensitive K^+ channels in adult mouse skeletal muscle: different modes of blockage by internal cations, ATP and tolbutamide. *Pflügers Arch.* **1988**, *414*, 622 - 628.

(72) Spruce, A. E.; Standen, N. B.; Stanfield, P. R. Studies of the unitary properties of adenosine-5′-triphosphate - regulated potassium channels of frog skeletal muscle. *J. Physiol.* **1987**, *382*, 213 - 36.

(73) Ben Ari, Y.; Krnjevic, K. The ATP - sensitive K^+ channel opener diazoxide reduces anoxic depolarization in rat CA3 hippocampal neurones in isolated slices. *J. Physiol.* **1989**, *418*, 192P.

(74) Ben Ari, Y.; Lazdunski, M. Galanin protects hippocampal neurones from the functional effects of anoxia. *Eur. J. Pharmacol.* **1989**, *165*, 331 - 332.

(75) Ben Ari, Y.; Krnjevic, K.; Crepel, V. Activators of ATP - sensitive K^+ channels reduce anoxic depolarization in CA3 hippocampal neurones. *Neuroscience* **1990**, *37*, 55 - 60.

(76) Abele, A. E.; Miller, R. J. Potassium channel activators abolish cytotoxicity in cultured hippocampal pyramidal neurones. *Neuroscience* **1990**, *115*, 195 - 200.

(77) Amoroso, S.; Schmid - Antomarchi, H.; Fosset, M.; Lazdunski, M. Glucose, sulfonylureas and neurotransmitter release: a role of ATP - sensitive K^+ channels.

Science **1990**, *247*, 852 - 854.

(78) Schmid - Antomarchi, H.; Ambroso, S.; Fosset, M.; Lazdunski, M. K^+ channel openers activate brain sulfonylurea - sensitive K^+ channels and block neurosecretion. *Proc. Natl. Acad. Sci. USA* **1990**, *87*, 3489 - 3492.

(79) Sturgess, N. C.; Ashford, M. L. J.; Cook, D. L.; Hales, C. N. The sulphonylurea receptor may be an ATP - sensitive potassium channel. *Lancet* **1985**, *II*, 474 - 475.

(80) Trube, G.; Rorsman, P.; Ohno - Shosaku, T. Opposite effects of tulbutamide and diazoxide on the ATP - dependent K^+ channel in mouse pancreatic β - cells. *Pflügers Arch.* **1986**, *407*, 493 - 499.

(81) Schmid - Antomarchi, H.; DeWille, J.; Fosset, M.; Lazdunski, M. The receptor for antidiabetic sulphonylureas controls the activity of the ATP - modulated K^+ channel in insulin - secreting cells. *J. Biol. Chem.* **1987**, *262*, 15840 - 15844.

(82) Sturgess, N. C.; Kozlowski, R. Z.; Carrington, C. A.; Hales, C. N.; Ashford, M. L. J. Effects of sulphonylureas and diazoxide on insulin secretion and nucleotide - sensitive channels in an insulin - secreting cell line. *Br. J. Pharmacol.* **1988**, *95*, 83 - 94.

(83) Zlunkler, B. K.; Lenzen, S.; Monner, K.; Panten, U.; Trube, G. Concentration - dependent effects of tolbutamide, meglitinide, glipizide, glibenclamide and diazoxide on ATP - regulated K^+ currents in pancreatic β - cells. *Naunyn - Schmiedeberg`s Arch. Pharmacol.* **1988**, *337*, 225 - 230.

(84) Kantor, P. F.; Coatzee, W. A.; Dennis, S. C.; Opie, L. H. Effects of glibenclamide on ischemic arrythmias. *Circulation* **1987**, *76*, 65.

(85) Kameyama, M.; Kakei, M.; Sato, R.; Shibasaki, T.; Matsuda, H.; Ivisawa, H. Intracellular Na^+ activates a K^+ channel in mammalian cardiac cells. *Nature* **1984**, *309*, 354 - 356.

(86) Bader, C. R.; Bernheim, L.; Bertrand, D. Sodium - activated potassium current in cultured avian neurones. *Nature* **1985**, *317*, 540 - 542.

(87) Dryer, S. E.; Fujii, J. T.; Martin, A. R. A Na^+ - activated K^+ current in cultured brainstem neurones from chicks. *J. Physiol.* **1989**, *410*, 283 - 296.

(88) Bader, C. R.; Bernheim, L.; Bertrand, D.; Haimann, C. In *Potassium channels*; N. S. Cook, Ed.; Ellis Horwood: Chichester, 1990; pp 154 - 166.

(89) Sandford, C. A.; Sweiry, J. H.; Jenkinson, D. H. Properties of a cell volume - sensitive potassium conductance in isolated guinea - pig and rat hepatocytes. *J. Physiol.* **1992**, *447*, 133 - 148.

(90) Haylett, D. G.; Jenkinson, D. H. In *Potassium Channels*; N. S. Cook, Ed.; Ellis Horwood Limited: Chichester, 1990; pp pp 70 - 95.

(91) Morty, A. Ca - dependent K channels with large unitary conductance in chromaffin cell membranes. *Nature* **1981**, *291*, 497 - 500.

(92) Pallotta, B. S.; Magleby, K. L.; Barrett, J. N. Single channel recordings of Ca^{2+} - activated K^+ currents in rat nuscle cell culture. *Nature* **1981**, *293*, 471 - 474.

(93) Wong, B. S.; Lecar, H.; Alder, M. Single calcium - dependent potassium channels in clonar anterior pituitary cells. *Biophys. J.* **1982**, *39*, 313 - 317.

(94) Adams, P. R.; Constanti, A.; Brown, D. A.; Clark, R. B. Intracellular Ca^{2+} activates a fast voltage - sensitive K^+ current in vertebrate sympathetic neurones. *Nature* **1982**, *296*, 746 - 749.

(95) Petersen, O. H. Calcium - activated potassium channels and fluid secretion by exocrine glands. *Am. J. Physiol.* **1986**, *251*, G1 - G13.

(96) Chay, T. R. On the effect of the intracellular calcium - sensitive K^+ channel in the bursting pancraetic β - cell. *Biophys. J.* **1986**, *50*, 765 - 777.

(97) Sherman, A.; Rinzel, J.; Keizer, J. Emergence of organized bursting in clusters of pancreatic β - cells by channel sharing. *Biophys. J.* **1988**, *54*, 411 - 425.

(98) Barrett, J. N.; Magleby, K. L.; Pallotta, B. S. Properties of single calcium - activated potassium channels in cultured rat muscle. *J. Physiol.* **1982**, *331*, 211 - 230.

(99) Butler, A.; Tsunoda, S.; McCobb, D. P.; Wei, A.; Salkoff, L. *mSlo*, a Complex Mouse Gene Encoding "Maxi" Calcium - Activated Potassium Channels. *Science* **1993**, *261*, 221 - 224.

(100) Garcia - Calvo, M.; Knaus, H.-G.; McNaus, O. B.; Giangiacomo, K. M.; Kaczarowski, G. J.; Garcia, M. L. Purification and reconstitution of the high -

conductance, calcium activated potassium channel from tracheal smooth muscle. *J. Biol. Chem.* **1994**, *269*, 676 - 682.

(101) Knaus, H.-G.; Folander, K.; Garcia - Calvo, M.; Garcia, M. L.; Kaczorowski, G. J.; Smith, M.; Swanson, R. Primary sequence and immunological characterization of β - subunit of high conductance Ca^{2+} - activated K^+ channel from smooth muscle. *J. Biol. Chem.* **1994**, *269*, 17274 - 17278.

(102) McCann, J. D.; Welsh, M. J. Neuroleptics antagonize a calcium - activated potassium channel in airway smooth muscle. *J. Gen. Physiol.* **1987**, *89*, 339 - 352.

(103) Smith, C. D.; Phillips, M.; Miller, C. Purification of charubdotoxin, a specific inhibitor of the high conductance Ca^{2+} - activated K^+ channel. *J. Biol. Chem.* **1986**, *261*, 14607 - 14613.

(104) Anderson, C. A.; MacKinnon, R.; Smith, C.; Miller, C. Charybdotoxin block of single Ca^{2+} - activated K^+ channels. *J. Gen. Physiol.* **1988**, *91*, 317 - 333.

(105) Vita, C.; Bontems, F.; Bouet, F.; Tauc, M.; Poujeol, P.; Vatanpour, H.; Harrey, A. L.; Menez, A.; Toma, F. Synthesis of charybdotoxin and two N-terminal truncated analogues. Structural and functional characterization. *Eur. J. Biochem.* **1993**, *217*, 157 - 169.

(106) Bontems, F.; Roumestrand, C.; Boyot, P.; Gilquin, B.; Doljansky, Y.; Menez, A.; Toma, F. Three - dimensional structure of natural charybdotoxin in aqueous solution by ^{1}H-NMR. *Eur. J. Biochem.* **1991**, *196*, 19 - 28.

(107) Bontems, F.; Roumestrand, C.; Gilquin, B.; Ménez, A.; Toma, F. Refined structure of charybdotoxin: Common motifs in scorpion toxins and insect defensins. *Science* **1991**, *254*, 1521 - 1523.

(108) Bontems, F.; Gilquin, B.; Roumestrand, C.; Ménez, A.; Toma, F. Analysis of side - chain organization on a refined model of charybdotoxin:structural and functional implications. *Biochemistry* **1992**, *31*, 7756 - 7764.

(109) MacKinnon, R.; Miller, C. Mechanism of charybdotoxin block of the high conductance, Ca^{2+} - activated K^+ channel. *J. Gen. Physiol.* **1988**, *91*, 335 - 349.

(110) Park, C.-S.; Miller, C. Interaction of charybdotoxin with permeant ions inside the pore of a K^+ channel. *Neuron* **1992**, *9*, 307 - 313.

(111) Park, C.-S.; Miller, C. Mapping function to structure in a channel - blocking peptide: Electrostatic mutants of charybdotoxin. *Biochemistry* **1992**, *31*, 7749 - 7755.

(112) Stampe, P.; Kolmakova-Partensky, L.; Miller, C. Mapping hydrophobic residues of the interaction surface of charybdotoxin. *Biophys. J.* **1992**, *62*, 8 - 9.

(113) Stampe, P.; Kolmakova-Partensky, L.; Miller, C. Intimations of K^+ channel structure from a complete functional map of the molecular surface of charybdotoxin. *Biochemistry* **1994**, *33*, 443 - 450.

(114) Wolff, D.; Cecchi, X.; Spalvins, A.; Canessa, M. Charybdotoxin blocks with high affinity the Ca^{2+} - activated K^+ channel of HbA and HbS red cells: individual differences in the number of channels. *J. Membr. Biol.* **1988**, *106*, 243 - 252.

(115) Galvez, A.; Gimenez-Gallego, G.; Reuben, J. P.; Roy-Contancin, L.; Feigenbaum, P.; Kaczorowski, G. J.; Garcia, M. L. Purification and characterization of a unique, potent, peptidyl probe for the high conductance calcium - activated potessium channel from venom of the scorpion *Buthus tamulus*. *J. Biol. Chem.* **1990**, *265*, 11083 - 11090.

(116) Giangiacomo, K. M.; Sugg, E. E.; Garcia-Calvo, M.; Leonard, R. J.; McManus, O. B.; Kaczorowski, G. J.; Garcia, M. L. Synthetic charybdotoxin - iberiotoxin chimeric peptides define toxin binding sites on calcium - activated and voltage - dependent potassium channels. *Biochemistry* **1993**, *32*, 2363 - 2370.

(117) Johnson, B. A.; Sugg, E. E. Determination of the three - dimensional structure of iberiotoxin in solution by ^1H nuclear magnetic resonance spectroscopy. *Biochemistry* **1992**, *31*, 8151 - 8159.

(118) Valdivia, H. H.; Smith, J. S.; Martin, B. M.; Coronado, R.; Possani, L. D. Charybdotoxin and noxiustoxin, two homologous peptidic inhibitors of the K^+ (Ca^{2+}) channel. *FEBS Lett.* **1988**, *226*, 280 - 284.

(119) Olesen, S.-P.; Wätjen, F.; Hayes, A. G. A novel benzimidazolone, NS004, activates large - conductance Ca^{2+} - dependent K^+ channels in aortic smooth

muscle. *Br. J. Pharmacol.* **1993**, *110*, 25P.

(120) McManus, O. B.; Harris, G. H.; Giangiacomo, K. M.; Feigenbaum, P.; Reuben, J. P.; Addy, M. E.; Burka, J. F.; Kaczorowski, G. J.; Garcia, M. L. An activator of calcium - dependent potassiun channels isolated from a medicinal herb. *Biochemistry* **1993**, *32*, 6128 - 6133.

(121) Bolotina, V. M.; Najibi, S.; Palacino, J. J.; Pagano, P. J.; Cohen, R. A. Nitric oxide directly activates calcium - dependent potassium channels in vascular smooth muscle. *Nature* **1994**, *368*, 850 - 853.

(122) Sarkadi, B.; Gárdos, G. In *The enzymes of biological membranes*; 2nd ed.; A. N. Martonosi, Ed.; Plenum Press: New York, 1985; Vol. 3; pp 193 - 234.

(123) Armando-Hardy, M.; Ellory, J. C.; Ferreira, H. G.; Fleminger, S.; Lew, V. L. Inhibition of the calcium - induced increase in the potassium permeability of human red blood cells by quinine. *J. Physiol.* **1975**, *250*, 32 - 33P.

(124) Simons, T. J. B. Actions of carbocyanine dye on calcium - dependent potassium transport in human red cell ghosts. *J. Physiol.* **1979**, *288*, 481 - 507.

(125) Berkowitz, L. R.; Orringer, E. P. Effect of cetiedil, an in vitro antisickling agent, on erythrocyte membrane cation permeability. *J. Clin. Invest.* **1981**, *68*, 1215 - 1220.

(126) Meech, R. W.; Strumwasser, F. Intracellular calcium injection activates potassium conductance in Aplysia nerve cells. *Fed. Proc.* **1970**, *29*, 834.

(127) Meech, R. W. The sensitivity of Helix aspersa neurones to injected calcium ions. *J. Physiol.* **1974**, *237*, 259 - 277.

(128) Hermann, A.; Hartung, K. Ca^{2+} - activated K^+ conductance in molluscan neurones. *Cell Calcium* **1983**, *4*, 387 - 405.

(129) Hermann, A.; Erxleben, C. Charybdotoxin selectively blocks small Ca - activated K channels in Aplysia neurons. *J. Gen. Physiol.* **1987**, *90*, 27 - 47.

(130) Ferrero, J. D.; Cocks, T.; Burnstock, G. A comparison between ATP and bradykinin as possible mediators of the responces of smooth muscle to non - adrenergic non - cholinergic nerves. *Eur. J. Pharmacol.* **1980**, *63*, 295 - 302.

(131) Brown, C. M.; Burnstock, G. Evidence in support of the P_1/P_2 purinoceptor

hypothesis in the guinea - pig taenia coli. *Br. J. Pharmacol.* **1981**, *73*, 617 - 624.

(132) Gater, P. R.; Haylett, D. G.; Jenkinson, D. H. Neuromuscular blocking agents inhibit receptor - mediated increases in the potassium permeability of intestinal smooth muscle. *Br. J. Pharmacol.* **1985**, *86*, 861 - 868.

(133) Nohmi, M.; Kuba, K. (+) - Tubocurarine blocks Ca^{2+} - dependent K^+ channel of the bullfrog sympathetic ganglion cell. *Brain Res.* **1984**, *301*, 146 - 148.

(134) Pennefather, P.; Lancaster, B.; Adams, P. R.; Nicoll, R. A. Two distinct Ca - activated K currents in bullfrog sympathetic ganglion cells. *Proc. Natl. Acad. Sci. USA* **1985**, *82*, 3040 - 3044.

(135) Mourre, C.; Hugues, M.; Lazdunski, M. Quantitative autoradiographic mapping in rat brain of the receptor of apamin, a polypeptide toxin specific for one class of Ca^{2+} - dependent K^+ channels. *Brain Res.* **1986**, *382*, 239 - 249.

(136) Fosset, M.; Schmid - Antomarchi, H.; Hugues, M.; Romey, G.; Lazdunski, M. The presence in pig brain of an endogenous equivalent of apamin, the bee venom peptide that specifically blocks Ca^{2+} - dependent K^+ channels. *Proc. Natl. Acad. Sci. USA* **1984**, *81*, 7228 - 7232.

(137) Auguste, P.; Hugues, M.; Borsotto, M.; Thibault, J.; Romey, G.; Coppola, T.; Lazdunski, M. Characterization and partial purification from pheochromocytoma cells of an endogenous equivalent of scyllatoxin, a scorpion toxin which blocks small conductance Ca^{2+} - activated K^+ channels. *Brain Res.* **1992**, *599*, 230 - 236.

(138) Coats, R. A. Effects of apamin on α-adrenoceptor - mediated changes in plasma potassium in guinea - pigs. *Br. J. Pharmacol.* **1983**, *80*, 573 - 580.

(139) Coats, R. A. The effects of adrenoceptor agonists and antagonists on plasma potassium concentration in anaesthetized guinea - pigs, rabbits and rats. *Br. J. Pharmacol.* **1985**, *86*, 827 - 836.

(140) Nånberg, E.; Connolly, E.; Nedergaard, J. Presence of Ca^{2+} - dependent K^+ channel in brown adipocytes: possible role in maintenance of α_1-adrenergic stimulation. *Biochim. Biophys. Acta* **1985**, *844*, 42 - 49.

(141) Hugues, M.; Romey, G.; Duval, D.; Vincent, J.-P.; Lazdunski, M. Apamin as a

selective blocker of the calcium - dependent potassium channel in neuroblastoma cells: voltage clamp and biochemical characterization of the toxin receptor. *Proc. Natl. Acad. Sci. USA* **1982**, *79*, 1308 - 1312.

(142) Traoré, F.; Cognard, C.; Potreau, D.; Raymond, G. The apamin - sensitive potassium current in frog skeletal muscle: its dependence on the extracellular calcium and sensitivity to calciul channel blockers. *Pflügers Arch.* **1986**, *407*, 199 - 203.

(143) Blatz, A. L.; Magleby, K. L. Single apamin - blocked Ca - activated K^+ channels of small conductance in rat cultured skeletal muscle. *Nature* **1986**, *323*, 718 - 720.

(144) Capiod, T.; Ogden, D. C. The properties of single apamin - sensitive potassium ion channels in guinea - pig hepatocytes. *J. Physiol.* **1987**, *394*, 46P.

(145) Capiod, T.; Ogden, D. C. In *Gastrointestinal and hepatic secretions: mechanism and control*; J. S. Davison and E. A. Shaffer, Ed.; University of Calgary Press: Calgary, 1988; pp 74 - 79.

(146) Seagar, M. J.; Marqueze, B.; Gouraud, F. Solubilization of the apamin receptor associated with a calcium - activated potassium channel from rat brain. *J. Neurosci.* **1987**, *7*, 565 - 570.

(147) Seagar, M. J.; Labbé - Jullié, C.; Granier, C.; Van Rietschloten, J.; Couraud, F. Photoaffinity labeling of components of the apamin - sensitive K^+ channel in neuronal membranes. *J. Biol. Chem.* **1985**, *260*, 3895 - 3898.

(148) Seagar, M. J.; Labbé - Jullié, C.; Granier, C.; Gall, A.; Glossmann, H.; Van Rietschloten, J.; Couraud, F. Molecular structure of rat brain apamin receptor: Differential photoaffinity labeling of putative K^+ channel subunits and target size analysis. *Biochemistry* **1986**, *25*, 4051 - 4057.

(149) Seagar, M. J.; Deprez, P.; Moutot, M.; Couraud, F. Detection and photoaffinity labeling of the Ca^{2+} - activated K^+ channel - associated apamin receptor in cultured astrocytes from rat brain. *Brain Res.* **1987**, *411*, 226 - 230.

(150) Marqueze, B.; Seagar, M.; Couraud, C. Photoaffinity labeling of the K^+ - channel - associated apamin - binding molecule in smooth muscle, liver and heart

membranes. *Eur. J. Biochem.* **1987**, *169*, 295 - 298.

(151) Lereque, C.; Marqueze, B.; Couraud, F.; Seagar, M. Polypeptide components of the apamin receptor associated with a calcium - activated potassium channel. *FEBS Lett.* **1990**, *275*, 185 - 189.

(152) Hugues, M.; Schmid, H.; Lazdunski, M. Identification of a protein component of the Ca^{2+} - dependent K^+ channel by affinity labeling with apamin. *Biochem. Biophys. Res. Commun.* **1982**, *107*, 1577 - 1582.

(153) Schmid - Antomarchi, H.; Hugues, M.; Norman, R.; Ellony, C.; Borsotto, M.; Lazdunski, M. Molecular properties of the apamin - binding component of the Ca^{2+} - dependent K^+ channel. *Eur. J. Biochem.* **1984**, *142*, 1 - 6.

(154) Auguste, P.; Hugues, M.; Lazdunski, M. Polypeptide constitution of receptors for apamin, a neurotoxin which blocks a class of Ca^{2+} - activated K^+ channels. *FEBS Lett.* **1989**, *248*, 150 - 154.

(155) Auguste, P.; Hugues, M.; Grave, B.; Gesquiere, J.-C.; Maes, P.; Tartar, A.; Romey, G.; Schweitz, H.; Lazdunski, M. Leiurotoxin I (Scyllatoxin), a peptide ligand for Ca^{2+} - activated K^+ channels. *J. Biol. Chem.* **1990**, *265*, 4753 - 4759.

(156) Wadsworth, J. D. F.; Doorty, K. B.; Strong, P. N. Comparable 30 KDa apamin binding polypeptides may fulfil equivalent roles within putative subtypes of small conductance Ca^{2+} - activated K^+ channels. *J. Biol. Chem.* **1994**, *269*, 18053 - 18061.

(157) Burgess, G. M.; Claret, M.; Jenkinson, D. H. Effects of quinine and apamin on the calcium - dependent potassium permeability of mammalian hepatocytes and red cells. *J. Physiol. (Lond)* **1981**, *317*, 67 - 90.

(158) Sokol, P. T.; Hu, W.; Yi, L.; Torol, J.; Chandra, M.; Ziai, M. R. Cloning of an apamin - binding protein of smooth muscle. *J. Protein Chem.* **1994**, *13*, 117 - 128.

(159) Banks, B. E. C.; Brown, C.; Burgess, G. M.; Burnstock, G.; Claret, M.; Cocks, T. M.; Jenkinson, D. H. Apamin blocks certain neurotransmitter - induced increases in potassium permeability. *Nature* **1979**, *282*, 415 - 417.

(160) Lazdunski, M. Apamin, a neurotoxin specific for one class of Ca^{2+} - dependent

K^+ channels. *Cell Calcium* **1983**, *4*, 421 - 428.

(161) Habermann, E. Apamin. *Pharmac. Ther.* **1984**, *25*, 255 - 270.

(162) Castle, N. A.; Haylett, D. G.; Jenkinson, D. H. Toxins in the characterization of potassium channels. *Trends Neurosci.* **1989**, *12*, 59 - 65.

(163) Strong, P. N. Potassium channel toxins. *Pharmac. Ther.* **1990**, *46*, 137 - 162.

(164) Bystrov, V. F.; Okhanov, V. V.; Miroshnikov, A. I.; Ovchinnikov, Y. A. Solution spatial structure of apamin as derived from NMR study. *FEBS Lett.* **1980**, *119*, 113 - 117.

(165) Hider, R. C.; Ragnarsson, U. A proposal for the structure of apamin. *FEBS Lett.* **1980**, *111*, 189 - 193.

(166) Busetta, B. Conformational analysis of apamin using the residual representation. *FEBS Lett.* **1980**, *112*, 138 - 142.

(167) Wemmer, D.; Kallenbach, N. R. Structure of apamin in solution: A two dimensional nuclear magnetic resonance study. *Biochemistry* **1983**, *22*, 1901 - 1906.

(168) Freeman, C. M.; Catlow, C. R. A.; Hemmings, A. M.; Hider, R. C. The conformation of apamin. *FEBS Lett.* **1986**, *197*, 289 - 296.

(169) Pease, J. H. B.; Wemmer, D. E. Solution structure of apamin determined by nuclear magnetic resonance and distance geometry. *Biochemistry* **1988**, *27*, 8491 - 8498.

(170) Van Rietschoten, J.; Granier, C.; Rochat, H.; Lissitzky, S.; Miranda, F. Synthesis of apamin, a neurotoxic peptide from bee venom. *Eur. J. Biochem.* **1975**, *56*, 35 - 40.

(171) Sandberg, B. E. B.; Ragnarsson, U. Solid phase synthesis of apamin, the principal neurotoxin in bee venom. *Int. J. Peptide Protein Res.* **1978**, *11*, 238 - 245.

(172) Sandberg, B. E. B. Solid phase synthesis of 13-lysine-apamin, 14-lysine-apamin and the corresponding guanidinated derivatives. *Int. J. Peptide Protein Res.* **1979**, *13*, 327 - 333.

(173) Vincent, J.-P.; Schweitz, H.; Lazdunski, M. Structure - function relationships and

site of action of apamin, a neurotoxic peptide of bee venom with an action on the central nervous system. *Biochemistry* **1975**, *14*, 2521 - 2525.

(174) Granier, C.; Pedroso Muller, E.; Van Rietschoten, J. Use of synthetic analogues for a study on the structure - activity relationship of apamin. *Eur. J. Biochem.* **1978**, *82*, 293 - 299.

(175) Labbé-Jullié, C.; Granier, C.; Albericio, F.; Defendini, M.-L.; Ceard, B.; Rochat, H.; Van Rietschoten, J. Binding and toxicity of apamin. Characterization of the active site. *Eur. J. Biochem.* **1991**, *196*, 639 - 645.

(176) Cheng-Raude, D.; Treloar, M.; Habermann, E. Preparation and pharmacokinetics of labeled derivatives of apamin. *Toxicon* **1976**, *19*, 467 - 476.

(177) Auguste, P.; Hugues, M.; Mourre, C.; Moinier, D.; Tartar, A.; Lazdunski, M. Scyllatoxin, a blocker of Ca^{2+} - activated K^+ channels: Structure - function relationships and brain localization of the binding sites. *Biochemistry* **1992**, *31*, 648 - 654.

(178) Sabatier, J.-M.; Zerrouk, H.; Darbon, H.; Mabrouk, K.; Benslimare, A.; Rochat, H.; Martin-Eauclaire, M.-F.; Van Rietschoten, J. PO_5, a new leiurotoxin I - like scorpion toxin: Synthesis and structure - activity ralationships of the α-amidated analog, a ligand of Ca^{2+} - activated K^+ channels with increased affinity. *Biochemistry* **1993**, *32*, 2763 - 2770.

(179) Demonchaux, P.; Ganellin, C. R.; Dunn, P. M.; Haylett, D. G.; Jenkinson, D. H. Search for the pharmacophore of the K^+ channel blocker, apamin. *Eur. J. Med. Chem.* **1991**, *26*, 915 - 920.

(180) Bkaily, G.; Jacques, D.; Sculptoreanu, A.; Yamamoto, T.; Carrier, D.; Vigneault, D.; Sperelakis, N. Apamin, a highly potent blocker of the TTX - and Mn^{2+} - insensitive fast transient Na^+ current in young embryonic heart. *J. Mol. Cell Cardiol.* **1991**, *23*, 25 - 29.

(181) Bkaily, G.; Sculptoreanu, A.; Jacques, D.; Economos, D.; Ménard, D. Apamin, a highly potent fetal L-type Ca^{2+} - current blocker in single heart cells. *Am. J. Physiol.* **1992**, *262*, H463 - H471.

(182) Chicchi, G. G.; Gimenez-Gallego, G.; Ber, E.; Garcia, M. L.; Winquist, R.;

Cascieri, M. A. Purification and characterization of a unique, potent inhibitor of apamin binding from *Leiurus quinquestriatus hebraeus* venom. *J. Biol. Chem.* **1988**, *263*, 10192 - 10197.

(183) Martins, J. C.; Zhang, W.; Tartar, A.; Lazdunski, M.; Borremans, F. A. M. Solution conformation of leiurotoxin I (scyllatoxin) by ^1H nuclear magnetic resonance. Resonance assignment and secondary structure. *FEBS Lett.* **1990**, *260*, 249 - 253.

(184) Zerrouk, H.; Mansuelle, P.; Benslimane, A.; Rochat, H.; Martin-Eauclaire, M. F. Characterization of a new leiurotoxin I - like scorpion toxin PO5 from *Androctonus mauretanicus mauretanicus*. *FEBS Lett.* **1993**, *320*, 189 - 192.

(185) Meunier, S.; Bernassau, J.-M.; Sabatier, J.-M.; Martin-Eauclaire, M. F.; Van Rietschoten, J.; Cambillau, C.; Darbon, H. Solution structure of PO_5-NH_2, a scorpion toxin analog with high affinity for the apamin - sensitive potassium channel. *Biochemistry* **1993**, *32*, 11969 - 11976.

(186) Kobayashi, Y.; Takashima, H.; Tamaoki, H.; Kyogoku, Y.; Lambert, P.; Kuroda, H.; Chino, N.; Watanabe, T. X.; Kimura, T.; Sakakibara, S.; Moroder, L. The cystine - stabilized α-helix: a common structural motif of ion channel blocking neurotoxic peptides. *Biopolymers* **1991**, *31*, 1213 - 1220.

(187) Jenkinson, D. H.; Haylett, D. G.; Cook, N. S. Calcium - activated potassium channels in liver cells. *Cell Calcium* **1983**, *4*, 429 - 437.

(188) Cook, N. S.; Haylett, D. G. Effects of apamin, quinine and neuromuscular blockers on calcium - activated potassium channels in guinea pig hepatocytes. *J. Physiol.* **1985**, *358*, 373 - 394.

(189) Babbs, M.; Collier, H. O. J.; Austin, W. C.; Potter, M. D.; Taylor, E. P. Salts of decamethylene-bis-4-aminoquinaldinium ("Dequadin"), a new antimicrobial agent. *J. Pharm. Pharmacol.* **1956**, *8*, 110 - 119.

(190) Castle, N. A.; Haylett, D. G.; Morgan, J. M.; Jenkinson, D. H. Dequalinium; a potent inhibitor of apamin - sensitive K^+ channels in hepatocytes and of nicotinic responses in skeletal muscle. *Eur. J. Pharmacol.* **1993**, *236*, 201 - 207.

(191) Dunn, P. M. Dequalinium, a selective blocker of the slow afterhyperpolarization in

rat sympathetic neurones in culture. *Eur. J. Pharmacol.* **1994**, *252*, 189 - 194.

(192) Dunn, P. M. Ganglion - blocking activity of dequalinium in frog and rat sympathetic ganglia in vitro. *Eur. J. Pharmacol.* **1993**, *230*, 335 - 339.

(193) Renaud, J. F.; Desnuelle, C.; Schmid - Antomarchi, H.; Hugues, M.; Serratrice, G.; Lazdunski, M. Expression of apamin receptor in muscles of patients with myotonic muscular dystrophy. *Nature* **1986**, *319*, 678 - 680.

(194) Behrens, M. I.; Vergara, C. Increase of apamin receptors in sceletal muscle induced by colchicine: possible role in myotonia. *Am. J. Physiol.* **1992**, *263*, C974 - C802.

(195) Dinan, T. G.; Crunelli, V.; Kelly, J. S. Neuroleptics decrease calcium - activated potassium conductance in hippocampal pyramidal cells. *Brain Res.* **1987**, *407*, 159 - 162.

(196) Madison, D. V.; Nicoll, R. A. Control of negative discharge of rat CA1 pyramidal neurones in vitro. *J. Physiol.* **1984**, *354*, 319 - 331.

(197) Lancaster, B.; Adams, P. R. Calcium - dependent current generating the afterhyperpolarization of hippocampal neurones. *J. Neurophysiol.* **1986**, *55*, 1268 - 1282.

(198) Cook, N. S.; Quast, U. In *Potassium channels*; N. S. Cook, Ed.; Ellis Horwood Ltd: Chichester, 1990; pp 181 - 255.

(199) Dinan, T. G. Calcium - activated potassium conductance; an alternative to the dopamine hypothesis of neuroleptic action. *Br. J. Psychiatry* **1987**, *151*, 455 - 459.

(200) Kunze, W. A. A.; Bornstein, J. C.; Furness, J. B.; Hendriks, R.; Stephenson, D. S. H. Charybdotoxin and iberiotoxin but not apamin abolish the slow after - hyperpolarisation in myenteric plexus neurons. *Eur. J. Physiol.* **1994**, *428*, 300 - 306.

(201) Benishin, C. G.; Krueger, B. K.; Blaustein, M. P. Phenothiazines and haloperidol block Ca - activated K channels in rat forebrain synaptosomes. *Am. Soc. Pharmacol. Exp. Ther.* **1988**, *33*, 195 - 201.

(202) Ikeda, M.; Dewar, D.; McCulloch, J. Selective reduction of [^{125}I]apamin binding

sites in Alzheimer hippocampus: a quantitative autoradigraphic study. *Brain Res.* **1991**, *567*, 51 - 56.

(203) Ikeda, M.; Dewar, D.; McCulloch, J. Differential alterations of ion channel binding sites in temporal and occipital regions of the cerebral cortex in Alzheimer's disease. *Brain Res.* **1993**, *630*, 50 - 56.

(204) Messier, C.; Mourre, C.; Bontempi, B.; Sif, J.; Lazdunski, M.; Destrade, C. Effect of apamin, a toxin that inhibits Ca^{2+} - dependent K^+ channels, on learning and memory processes. *Brain Res.* **1991**, *551*, 322 - 326.

(205) Steketee, J. D.; Kalivas, P. W. Affect of microinjections of apamin into the A10 dopamine region of rats: A behavioral and neurochemical analysis. *J. Pharmacol. Exp. Ther.* **1990**, *254*, 711 - 719.

(206) Carlen, P. L.; Gurevich, N.; Durand, D. Ethanol in low doses augments calcium - mediated mechanisms measured intracellularly in hippocampal neurons. *Science* **1982**, *215*, 306 - 309.

(207) Yamamoto, H.-A.; Harris, R. A. Calcium - dependent ^{86}Rb efflux and ethanol intoxication: Studies of human red blood cells and rodent brain synaptosomes. *Eur. J. Pharmacol.* **1983**, *88*, 357 - 363.

(208) Dunn, P. M.; Davis, C. A.; Ganellin, C. R.; Haylett, D. G.; Morgan, J. M.; Jenkinson, D. H. Potassium channel blocking activity of dequalinium analogues in guinea - pig hepatocytes and rat sympathetic neurones. *Br. J. Pharmacol.* **1991**, *104*, 165P.

(209) Galanakis, D.; Davis, C. A.; Del Rey Herrero, B.; Ganellin, C. R.; Dunn, P. M.; Jenkinson, D. H. Synthesis and structure - activity relationships of dequalinium analogues as K^+ channel blockers. Investigations on the role of the charged heterocycle. *J. Med. Chem.* **1995**, *38*, 595 - 606.

(210) Galanakis, D.; Davis, C. A.; Del Rey Herrero, B.; Ganellin, C. R.; Dunn, P. M.; Jenkinson, D. H. Synthesis and QSAR of dequalinium analogues as K^+ channel blockers. Investigations on the role of the 4-NH_2 group. *Bioorg. Med. Chem. Lett.* **1995**, *5*, 559 - 562.

(211) Surrey, A. R.; Cutler, R. K. The role of phenol in the reaction of 4,7-

dichloroquinoline with novol diamine. *J. Am. Chem. Soc.* **1951**, *73*, 2623 - 2626.

(212) Perrin, D. D. *Dissociation constants of organic bases in aqueous solution*; Butterworths: London, 1965.

(213) Hay, A. S. Oxidative Coupling of Acetylenes. *J. Org. Chem.* **1962**, *27*, 3320 - 3321.

(214) Campbell, I. O.; Englinton, G. Diphenyl acetylene. *Organic Synthesis Col. Vol. V* **1973**, 517 - 520.

(215) Persico, F.; Wuest, J. D. Use of Hydrogen Bonds to Control Molecular Aggregation. Behavior of a Self - Complementary Dipyridone Designed to Self - Replicate. *J. Org. Chem.* **1993**, *58*, 95 - 99.

(216) Eglinton, G.; McCrae, W. The coupling of acetylenic compounds. *Adv. Org. Chem.* **1963**, *4*, 225 - 328.

(217) Ellis, J.; Gellert, E.; Robson, J. Synthesis of some new iodoquinolines. *Aust. J. Chem.* **1973**, *26*, 907 - 911.

(218) Keneford, J. R.; Lourie, E. M.; Morley, J. S.; Simpson, J. C. E.; Williamson, J.; Wright, P. H. Cinnolines and other heterocyclic types in relation to the chemotherapy of trypanosomiasis. Part I. General introduction. Part II. Quaternary salts of amino-cinnolines, -quinazolines and -quinolines. *J. Chem. Soc.* **1952**, 2595 - 2602.

(219) Hallgren, J. E.; Lucas, G. M. A tripod hexaketone as a ligand for manganese. *Tetrahedron Lett.* **1980**, *21*, 3951 - 3954.

(220) Pelter, A.; Smith, K.; Hutchings, M. G.; Rowe, K. The chemistry of organoborates. Part I. New, high yield ketone syntheses by reaction of trialkylcyanoborates with acylating agents or N-phenylbenzimidoyl chloride. *J. Chem. Soc. Perkin I* **1975**, 129 - 138.

(221) Pelter, A.; Hutchings, M. G.; Rowe, K.; Smith, K. The chemistry of organoborates. Part II. High yield syntheses of trialkylmethanols by the cyanoborate process. *J. Chem. Soc. Perkin I* **1975**, 138 - 142.

(222) Carey, F. A.; Tremper, H. S. Carbonium ion - silane hydride transfer reactions.

V. tert-Alkyl cations. *J. Org. Chem.* **1971**, *36*, 758 - 761.

(223) Van de Waterbeemd, H.; Testa, B. The parameterization of lipophilicity and other structural properties in drug design. *Adv. Drug Res.* **1987**, *16*, 85 - 225.

(224) Exner, O. Correlation analysis of chemical data. **1988**,

(225) Hansch, C.; Leo, A. *Substituent constants for correlation analysis in chemistry and biology*; Wiley: New York, 1979, pp 1-8.

(226) Sjöström, M.; Wold, S. Statistical analysis of the Hammett equation. IV. An expanded sigma zero scale. *Chem. Script.* **1976**, *9*, 200 - 210.

(227) Mager, P. P. Masca model of pharmacochemistry. Part 7. Statistical analysis of inductive and resonance contributions to electronic substituent effects. *Sci. Pharm.* **1980**, *48*, 117 - 126.

(228) Exner, O. In: Correlation analysis in chemistry. **1978**, 439 - 540.

(229) Charton, M. Electrical effect substituent constants for correlation analysis. *Prog. Phys. Org. Chem.* **1981**, *13*, 119 - 251.

(230) Hansch, C.; A., L.; Unger, S. H.; Kim, K. H.; Nikaitani, D.; Lien, E. J. "Aromatic" substituent constants for structure - activity correlations. *J. Med. Chem.* **1973**, *16*, 1207 - 1216.

(231) Swain, C. G.; Unger, S. H.; Rosenquist, N. R.; Swain, M. S. Substituent effects on chemical reactivity. Improved evaluation of field and resonance components. *J. Am. Chem. Soc.* **1983**, *105*, 492 - 502.

(232) Dewar, M. J. S.; Zoebisch, E. G.; Healy, E. F.; Stewart, J. J. P. AM1: A New General Purpose Quantum Mechanical Molecular Model. *J. Am. Chem. Soc.* **1985**, *107*, 3902 - 3909.

(233) Mulliken, R. S. Molecular complexes and their spectra. VI. Some problems and new developments. *Recl. Trav. Chim. Pays-Bas* **1956**, *75*, 845 - 852.

(234) Cheney, B. V.; Tolly, T. Electronic factors affecting receptor binding of dibenzo-*p*-dioxins and dibenzofurans. *Int. J. Quant. Chem.* **1979**, *16*, 87 - 110.

(235) Jensen, W. B. The Lewis acid - base definitions: A status report. *Chem. Rev.* **1978**, *78*, 1 - 22.

(236) Debnath, A. K.; R.L., L. d. C.; Debnath, G.; Shusterman, A. J.; Hansch, C.

Structure - activity relationship of mutagenic aromatic and heteroaromatic compounds. Correlation with molecular orbital energies and hydrophobicity. *J. Med. Chem.* **1991**, *34*, 786 - 797.

(237) Tuppurainen, K.; Lötjönen, S.; Laatikainen, R.; Vartiainen, T.; Maran, U.; Strandberg, M.; Tamm, T. About the mutagenicity of chlorine - substituted furanones and halopropenals. A QSAR study using molecular orbital indices. *Mutation Res.* **1991**, *247*, 97 - 102.

(238) Benigni, R.; Cotta-Ramusino, M.; Andreoli, C.; Giuliani, A. Electrophilicity as measured by K_e: molecular determinants, relationship with other physical - chemical and quantum mechanical parameters, and ability to predict rodent carcinogenicity. *Carcinogenesis* **1992**, *13*, 547 - 553.

(239) Tuppurainen, K.; Lötjönen, S.; Laatikainen, R.; Vartiainen, T. Structural and electronic properties of MX compounds related to TA100 mutagenicity. A semi-empirical molecular orbital QSAR study. *Mutat. Res.* **1992**, *266*, 181 - 188.

(240) Gomez-Jeria, J. S.; Sotomayor, P. Quantum chemical study of electronic structure and receptor binding in opiates. *J. Mol. Structure (Theochem)* **1988**, *166*, 493 - 498.

(241) Mehler, E. L.; Gerhards, J. Electronic determinants of the anti-inflammatory action of benzoic and salicylic acids. *Mol. Pharmacol.* **1987**, *31*, 284 - 293.

(242) Cheney, B. V.; Wright, J. B.; Hall, C. M.; Johnson, H. G. Structure - activity correlations for a series of antiallergy agents. Oxanilic, Quinaldic and Benzopyran-2-carboxylic acids. *J. Med. Chem.* **1978**, *21*, 936 - 940.

(243) Szymoniak, J.; Boudon, A.; Cherétien, J. R.; Dubois, J.-E. Drug design: Le contrôle LUMO du pharmacophore neuroleptique. *Eur. J. Med. Chem.* **1987**, *22*, 101-107.

(244) Paulino-Blumenfeld, M.; Hansz, M.; Hikichi, N. Electronic properties and free radical production by nitrofuran compounds. *Free Rad. Res. Commun.* **1992**, *16*, 207 - 215.

(245) Esaki, T. Quantitative drug design studies. VI. Quantitative structure - activity relationships of ionisable substances: Antibacterial activities of phenols. *Chem.*

Pharm. Bull. **1987**, *35*, 3105 - 3111.

(246) Kawakami, Y.; Hopfinger, A. J. Prediction of initial reduction potentials of compounds related to anthracyclines and implications for estimating cardiotoxicity. *Chem. Res. Toxicol.* **1990**, *3*, 244 - 247.

(247) Itokawa, H.; Totshuka, N.; Nakahara, K.; Maezuru, M.; Takeya, K.; Kondo, M.; Inamatsu, M.; Morita, H. A quantitative structure - activity relationsip for antitumor activity of long chain phenols from *Ginkgo biloba* L. *Chem. Pharm. Bull.* **1989**, *37*, 1619 - 1621.

(248) Türker, L.; Sener, E.; Yalçin, I.; Akbulut, U.; Kayalidere, I. QSAR of some antifungal - active benzoxazoles using the quantum chemical parameters. *Sci. Pharm.* **1990**, *58*, 107 - 113.

(249) Greco, G.; Novellino, E.; Silipo, C.; Vittoria, A. Study of benzodiazepines receptor sites using a combined QSAR - CoMFA approach. *Quant. Struct.-Act. Relat.* **1992**, *11*, 461 - 477.

(250) Santos, L.; Cornago, M. P.; Izquierdo, M. C.; Lopez-Zumel, M. C.; Smeyers, Y. G. Electron affinity/radiosensitizing activity relationship for quaternary 5-nitroimidazole derivatives. Quantum chemical QSAR. *Quant. Struct.-Act. Relat.* **1989**, *8*, 214 - 217.

(251) Clare, B. W. Structure - activity correlations for psychotomimetics. 1. Phenylalkylamines: Electronic, volume and hydrophobicity parameters. *J. Med. Chem.* **1990**, *33*, 687 - 702.

(252) Pearson, R. G. Recent advances in the concept of hard and soft acids and bases. *J. Chem. Educ.* **1987**, *64*, 561 - 567.

(253) Pearson, R. G. The principle of maximum hardness. *Acc. Chem. Res.* **1993**, *26*, 150 - 255.

(254) Parr, R. G.; Chattaraj, P. K. Principle of maximum hardness. *J. Am. Chem. Soc.* **1991**, *113*, 1854 - 1856.

(255) Klopman, G. Chemical reactivity and the concept of charge- and frontier-controlled reactions. *J. Am. Chem. Soc.* **1968**, *90*, 223 - 234.

(256) Mulliken, R. S.; Person, W. R. *Molecular complexes*; Wiley: New York, 1969.

(257) Still, W. C.; Tempczyk, A.; Hawley, R. C.; Hendrikson, T. Semianalytical treatment of solvation for molecular mechanics and dynamics. *J. Am. Chem. Soc.* **1990**, *112*, 6127 - 6129.

(258) Columbia University: New York, 1990.

(259) Jean-Charles, A.; Nicholls, A.; Sharp, K.; Honig, B.; Tempczyk, A.; Hendrickson, T. F.; Still, W. C. Electrostatic contributions to solvation energies: comparison of free energy perturbation and continuum calculations. *J. Am. Chem. Soc.* **1991**, *113*, 1454 - 1455.

(260) Allinger, N. L. Conformational analysis. 130. MM2. A hydrocarbon force field utilizing V_1 and V_2 torsional terms. *J. Am. Chem. Soc.* **1977**, *99*, 8127 - 8134.

(261) Weiner, S. J.; Kollman, P. A.; Case, D. A.; Singh, U. C.; Ghio, C.; Alagone, G.; Profeta, S.; Weiner, P. A new force field for molecular mechanical simulation of nucleic acids and proteins. *J. Am. Chem. Soc.* **1984**, *106*, 765 - 784.

(262) Jencks, W. P. On the attribution and additivity of binding energies. *Proc. Natl. Acad. Sci. USA* **1981**, *78*, 4046 - 4050.

(263) Williams, D. H. The molecular basis of biological order. *Aldrichim. Acta* **1991**, *24*, 71 - 80.

(264) Williams, D. H.; Cox, J. P. L.; Doig, A. J.; Gardner, M.; Gerhard, U.; Kaye, P. T.; Lal, A. R.; Nicholls, I. A.; Salter, C. J.; Mitchell, R. C. Toward the semiquantitative estimation of binding constants. Guides for peptide - peptide binding in aqueous solution. *J. Am. Chem. Soc.* **1991**, *113*, 7020 - 7030.

(265) Williams, D. H. The molecular basis of biological order and amide - amide hydrogen bonds - An addendum. *Aldrichim. Acta* **1992**, *25*, 9.

(266) Williams, D. H.; Searle, M. S.; Westwell, M. S.; Gerhard, U.; Holroyd, S. E. Towards a semi-quantitative description of a bimolecular association involving weak interactions in aqueous solution. *Phil. Trans. R. Soc. Lond. A* **1993**, 11 - 21.

(267) Williams, D. H.; Searle, M. S.; Mackay, J. P.; Gerhard, U.; Maplestone, R. A. Toward an estimation of binding constants in aqueous solution: Studies of associations of vancomycin group of antibiotics. *Proc. Natl. Acad. Sci. USA*

1993, *90*, 1172 - 1178.

(268) Searle, M. S.; Williams, D. H. The cost of conformational order: Entropy changes in molecular associations. *J. Am. Chem. Soc.* **1992**, *114*, 10690 - 10697.

(269) Searle, M. S.; Williams, D. H.; Gerhard, U. Partitioning of free energy contributions in the estimation of binding constants: Residual motions and concequences for amide - amide hydrogen bond strengths. *J. Am. Chem. Soc.* **1992**, *114*, 10697 - 10704.

(270) Searle, M. S.; Williams, D. H. On the stability of nucleic acid structure in solution: enthalpy - entropy compensations, internal rotations and reversibility. *Nucl. Acids Res.* **1993**, *21*, 2051 - 2056.

(271) Cox, J. P. L.; Nicholls, I. A.; Williams, D. H. Molecular recognition in aqueous solution: An estimate of the intrinsic binding energy of an amide - hydroxy hydrogen bond. *J. Chem. Soc. Chem. Commun.* **1991**, 1295 - 1297.

(272) Doig, A. J.; Williams, D. H. Binding energy of an amide - amide hydrogen bond in aqueous and nonpolar solvents. *J. Am. Chem. Soc.* **1992**, *114*, 338 - 343.

(273) Page, M. I.; Jencks, W. P. Entropic contributions to rate accelerations in enzymic and intramolecular reactions and the chelate effect. *Proc. Natl. Acad. Sci USA* **1971**, *68*, 1678 - 1683.

(274) Andrews, P. R.; Craik, D. J.; Martin, J. L. Functional group contributions to drug - receptor interactions. *J. Med. Chem.* **1984**, *27*, 1648 - 1657.

(275) Kearney, P. C.; Mizoue, L. S.; Kumpf, R. A.; Forman, J. E.; McCurdy, A.; Dougherty, D. A. Molecular recognition in aqueous media. New binding studies provide further insight into the cation - π interaction and related phenomena. *J. Am. Chem. Soc.* **1993**, *115*, 9907 - 9919.

(276) Kavanaugh, M. P.; Varnum, M. D.; Osborne, P. B.; Christie, M. J.; Busch, A. E.; Adelman, J. P.; North, R. A. Interaction between Tetraethylammonium and Amino Acid Residues in the Pore of Cloned Voltage - dependent Potassium Channels. *J. Biol. Chem.* **1991**, *266*, 7583 - 7587.

(277) Heginbotham, L.; MacKinnon, R. The aromatic binding site for tetraethylammonium ion on potassium channels. *Neuron* **1992**, *8*, 483 - 491.

(278) Kavanaugh, M. P.; Hurst, R. S.; Yakel, J.; Varnum, M. D.; Adelman, J. P.; North, R. A. Multiple subunits of a voltage - dependent potassium channel contribute to the binding site for tetraethylammonium. *Neuron* **1992**, *8*, 493 - 497.

(279) Imoto, K.; Busch, C.; Sakmann, B.; Mishina, M.; Konno, T.; Nakai, J.; Bujo, H.; Mori, Y.; Fukuda, K.; Numa, S. Rings of negatively charged amino acids determine the acetylcholine receptor channel conductance. *Nature* **1988**, *335*, 645 - 648.

(280) Ruat, M.; Traiffort, E.; Garbarg, M.; Schwartz, J. C.; Demonchaux, P.; Ife, R. J.; Tertiuk, W.; Ganellin, C. R. Design of an affinity matrix for purification of the histamine H_1 receptor from guinea pig cerebellum. *J. Neurochem.* **1992**, *58*, 350 - 356.

(281) Hauser, C. R.; Reynolds, G. A. Relative ease of cyclization of 2-, 3- and 4-aminopyridine derivatives. Synthesis of naphthyridines. *J. Org. Chem.* **1950**, *15*, 1224 - 1232.

(282) Keneford, J. R.; Morley, J. S.; Simpson, J. C. E.; Wright, P. H. The Chemistry of Simple Heterocyclic Systems. Part V. A Comparative Study of Some 4-Substituted Cinnolines, Quinazolines and Quinolines. *J. Chem. Soc.* **1950**, 1104 - 1111.

(283) Backeberg, O. G. The Action of Phosphoryl Chloride on the Toluene-p-sulphonyl Derivative of β-Anilinopropionic Acid. *J. Chem. Soc.* **1933**, 618 - 619.

(284) Feller, C.; Renault, J. Recherche sur les aminoquinoléines. VII. - Alkylation en milieu basique des acylamino-4 quinoléines: influence des effects stériques et électroniques. *Bull. Soc. Chim. Fr.* **1972**, 4757 - 4762.

(285) Price, C. C.; Roberts, R. M. The Synthesis of 4-Hydroxyquinolines. I. Through Ethoxymethylenemalonic Ester. *J. Am. Chem. Soc.* **1946**, *68*, 1204 - 1208.

(286) Taylor, E. P. Synthetic Neuromuscular Blocking Agents. Part I. Heterocyclic Decamethylenebis(quaternary Ammonium Salts). *J. Chem. Soc.* **1951**, 1150 - 1157.

(287) Austin, W. C.; Potter, M. D.; Taylor, E. P. Potential Trypanocides. The Action of

Polymethylene Dihalides on 4-aminoquinaldine. *J. Chem. Soc.* **1958**, 1489 - 1498.

(288) Deshpande, S. M.; Singh, A. K. Preparation of some N,N´-bis-(4-quinaldino)/(4-quinazolino)-α,ω-diaminialkanes(HCl) as potential antibacterial and antitubercular compounds. *Agric. Biol. Chem.* **1971**, *35*, 119 - 121.

(289) Grogan, C. H.; Rice, L. M.; Sullivan, M. X. Diisothiuronium dihydrohalide salts. *J. Org. Chem.* **1953**, *18*, 728 - 735.

(290) Conrad, M.; Limpach, L. Ueber das c - Oxychinaldin und dessen Derivate. *Chem. Ber.* **1887**, *20*, 948 - 959.

(291) Tripos Associates: St Louis, MO, U.S.A..

(292) Clark, M.; Cramer III, R. D.; Van Opdenbosch, N. Validation of the general - purpose TRIPOS 5.2 force - field. *J. Comp. Chem.* **1989**, *10*, 982 - 1012.

(293) Powell, M. J. D. Restart procedures for the conjugate - gradient method. *Mathematical Programming* **1977**, *12*, 241 - 254.

(294) Gasteiger, J.; Marsili, M. Iterative partial equalization of orbital electronegativity - A rapid access to atomic charges. *Tetrahedron* **1980**, *36*, 3219 - 3228.

(295) Marsili, M.; Gasteiger, J. pi charge distribution from molecular topology and pi orbital electronegativity. *Croat. Chem. Acta* **1980**, *53*, 601 - 614.

(296) Gasteiger, J.; Marsili, M. Prediction of proton magnetic resonance shifts: The dependence on hydrogen charges obtained by iterative partial equalization of orbital electronegativity. *Org. Magn. Reson.* **1981**, *15*, 353 - 360.

(297) Streitwieser, A. *Molecular orbital theory for organic chemists*; Wiley: New York, 1961.

(298) Hugues, M.; Duval, D.; Kitabgi, P.; Lazdunski, M.; Vincent, J. P. Preparation of a pure monoiodo derivative of the bee venom neurotoxin apamin and its binding properties to rat brain synaptosomes. *J. Biol. Chem.* **1982**, *257*, 2762 - 2769.

(299) Strong, P. N.; Brewster, B. S. Apamin: a probe for small - conductance, calcium - activated potassium channels. *Methods Neurosci.* **1992**, *8*, 15 - 24.

(300) Lowry, O. H.; Rosebrough, N. J.; Farr, A. L.; Randall, R. J. Protein measurement with the folin phenol reagent. *J. Biol. Chem.* **1951**, *193*, 265 - 275.

(301) Cheng, Y.; Prusoff, W. H. Relationship between the inhibition constant (K_I) and the concentration of inhibitor which causes 50 per cent inhibition (I_{50}) of an enzymatic reaction. *Biochem. Pharmacol.* **1973**, *22*, 3099 - 3108.

PUBLICATIONS

Synthesis and Structure–Activity Relationships of Dequalinium Analogues as K^+ Channel Blockers. Investigations on the Role of the Charged Heterocycle

Dimitrios Galanakis,[†] Carole A. Davis,[†] Benedicto Del Rey Herrero,[†] C. Robin Ganellin,*[,†] Philip M. Dunn,[‡] and Donald H. Jenkinson[‡]

Departments of Chemistry and Pharmacology, University College London, Gower Street, London WC1E 6BT, U. K.

Received August 31, 1994[⊗]

Small conductance Ca^{2+}-activated K^+ (SK_{Ca}) channels occur in many cells but have been relatively little studied. Dequalinium, a bis-quinolinium compound, has recently been shown to be the most potent nonpeptidic blocker of this K^+ channel subtype. This paper examines the importance of the quinolinium rings for blocking activity. Analogues of dequalinium were synthesised in which one quinolinium group was removed (**1** and **2**) or replaced by a triethylammonium group (**3**). They have been assayed in vitro for their ability to block the after-hyperpolarization (mediated by the opening of SK_{Ca} channels) that follows the action potential in rat sympathetic neurones. The compound having one quinolinium and one triethylammonium group (**3**) showed reduced activity, and it is suggested that the stronger binding to the channel of the quinolinium relative to the triethylammonium group may be related to differences in their electrostatic potential energy maps. Two monoquaternary compounds (**1** and **2**) were tested, but they exhibited a different pharmacological profile that did not allow definite conclusions to be drawn concerning their potency as blockers of the SK_{Ca} channel. Replacement of both quinolinium groups by pyridinium, acridinium, isoquinolinium, or benzimidazolium reduced but did not abolish activity. These results show that compounds having a number of different heterocyclic cations are capable of blocking the SK_{Ca} channel. However, among the heterocycles studied, quinoline is optimal. Furthermore, charge delocalization seems to be important: the higher the degree of delocalization the more potent the compound.

Introduction

K^+ channels comprise the most diverse family of ion channels so far described with at least 20 subtypes.[1] The characterization of these subtypes has been based mainly on their electrophysiology and pharmacology. Despite the wealth of information that has emerged in recent years, the physiological role of many of the subtypes as well as their tissue distribution has still to be established. Furthermore, the structure of most K^+ channels (including the one which is the subject of the present work) is still unknown. The bulk of the structural information available concerns voltage-activated K^+ channels.[2] The latter are thought to have a tetrameric structure consisting of four identical subunits. Each subunit contains six (S1–S6) transmembrane domains and a hydrophobic part (H5), located between S5 and S6 in the primary sequence of the protein, which is tucked into the lipid bilayer forming a hairpin structure. It has been suggested that the pore of the channel is formed by four H5 segments, one being contributed from each of the four subunits, arranged in a cylindrical fashion. Recently, the structures of an inward rectifier[3] and an ATP-regulated[4] K^+ channel have been proposed, a gene encoding for high conductance Ca^{2+}-activated K^+ (BK_{Ca}) channels has been cloned, sequenced, and expressed in *Xenopus* oocytes,[5] and a BK_{Ca} channel from smooth muscle has been characterized.[6,7]

The difficulties in studying K^+ channels are due in part to the lack of potent and selective blockers of the various subtypes. The existing K^+ channel blockers can be categorized into inorganic ions (e.g., Ba^{2+}), small organic compounds (e.g., tetraethylammonium, TEA), and peptide toxins. Of the second group, TEA has been used extensively for the characterization of K^+ channels. The mechanism of block of voltage-gated K^+ channels by TEA has been studied in some detail, and it has been suggested that the latter binds at a site formed by the side chains of four aromatic amino acids.[8,9] The binding site is situated inside the pore of the channel, and as a result, TEA physically obstructs the flow of K^+ ions through the pore. The usefulness of TEA is limited however by its lack of selectivity. On the other hand, some natural peptidic toxins that block K^+ channel subtypes[10] have been very helpful, but their use is also associated with problems arising from their limited supply and, in some instances (e.g., charybdotoxin), lack of selectivity. Since K^+ channels are involved in a variety of physiological and pathophysiological processes and since most of them are open to pharmacological exploration,[11,12] the discovery of novel, small, nonpeptidic blockers is of particular interest, as such compounds may lead to the development of novel therapeutically useful agents.

One of the least well-studied class of K^+ channels is that of small conductance Ca^{2+}-activated K^+ (SK_{Ca}) channels.[13,14] Apamin, an 18-amino acid neurotoxin isolated from the venom of the honey bee (*Apis mellifera*), has been shown to block SK_{Ca} channels potently ($IC_{50} \approx 1$ nM) and selectively.[15–17] Some efforts to elucidate its pharmacophore have been undertaken.[18] These channels are present in intestinal smooth muscle

* Address for correspondence: University College London, Department of Chemistry, Christopher Ingold Laboratories, 20 Gordon Str., London WC1H 0AJ, U.K.
† Department of Chemistry.
‡ Department of Pharmacology.
⊗ Abstract published in *Advance ACS Abstracts*, January 15, 1995.

0022-2623/95/1838-0595$09.00/0

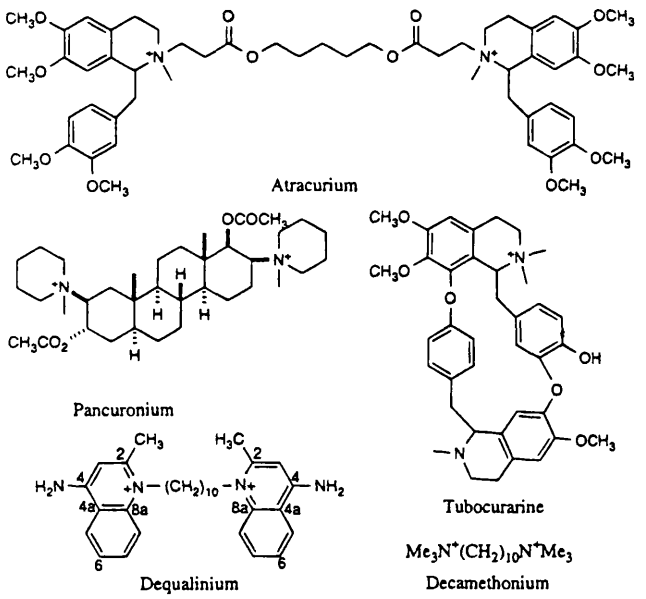

Figure 1. Structures of some SK_{Ca} channel blockers.

where their activation mediates the inhibitory action of α_1-adrenoceptors and the receptors for neurotensin and ATP.[19-21] In many neurones, including those of the sympathetic ganglia,[22,23] opening of SK_{Ca} channels mediates long hyperpolarizations that follow the action potential. That SK_{Ca} channels have a physiological role in the central nervous system is supported by the isolation of an endogenous ligand with apamin-like activity (see below) from pig brain.[24] Furthermore, SK_{Ca} channels have been implicated in myotonic muscular dystrophy, since the binding site for apamin is expressed in muscles of patients with this disease while it is completely absent in normal human muscle.[25] In addition, it has been suggested that a neurotrophic factor is involved in the regulation of the expression of apamin binding sites in skeletal muscle membranes.[26]

Apamin contains two contiguous arginine residues at positions 13 and 14. These positively charged amino acids are believed to be part of the pharmacophore, although alone they cannot account for the potency of apamin.[18] The presence of the bis-charged pharmacophore of apamin prompted tests of a number of bis-quaternary neuromuscular blockers, some of which were found to be effective blockers of the SK_{Ca} channel.[27-29] The three most potent are atracurium, tubocurarine, and pancuronium (Figure 1) having IC_{50}'s of 4.5, 7.5, and 6.8 μM, respectively. Furthermore, dequalinium (Figure 1), another bis-quaternary compound that has been used as an antiseptic,[30] is the most potent non-peptidic blocker of the SK_{Ca} channel so far described.[31,32] As nothing is known about the structure–activity relationships (SAR) of dequalinium, we have initiated studies toward identifying the pharmacophore of dequalinium for SK_{Ca} channel blockade.[33] Two of the structural features of dequalinium merit investigation, and these are the two quinolinium groups and the alkyl chain. The aim of the present work was to examine the role of the two quinolinium groups in an effort to gain some understanding of the interaction between the blocker and the channel, the ultimate objective being the design of more potent and selective nonpeptidic blockers. The investigation of the alkyl chain is currently under way in our laboratory.

Scheme 1[a]

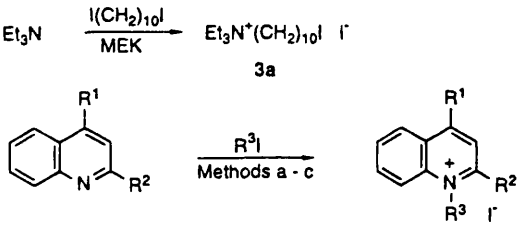

compd	R^1	R^2	R^3	method
1	NH_2	CH_3	$(CH_2)_9CH_3$	a
2	NH_2	CH_3	$(CH_2)_3CH_3$	b
3	NH_2	CH_3	$(CH_2)_{10}N^+Et_3$	c

[a] Methods: (a) 4-methylpentan-2-ol, reflux, 80 h; (b) MEK, reflux, 70 h; (c) 4-methylpentan-2-ol, 80 °C, 36 h.

Scheme 2[a]

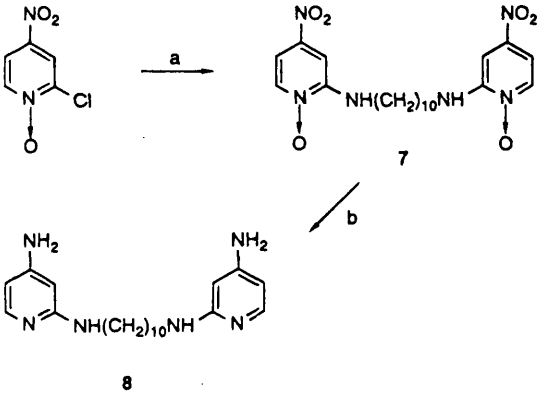

[a] Methods: (a) $H_2N(CH_2)_{10}NH_2$, EtOH, reflux, 4 h; (b) H_2, Pd/C, MeOH.

Chemistry

Compounds **1–3** were prepared by quaternization of the ring nitrogen of 4-amino-2-methylquinoline by the appropriate halide in 4-methylpentan-2-ol or methyl ethyl ketone (MEK) as described in Scheme 1. The (iododecanyl)ammonium salt **3a** was synthesized by quaternization of Et_3N with excess of 1,10-diiododecane. Scheme 2 shows the synthesis of compounds **7** and **8**. Displacement of the highly reactive chlorine atom of 2-chloro-4-nitropyridine *N*-oxide with 1,10-diaminodecane afforded **7**, hydrogenation of which reduced both the nitro group and the *N*-oxide to give **8**.

For the synthesis of the diacetylenes **6** and **10** (Scheme 3), we chose to make the quaternary ammonium monoacetylenes first and then couple these oxidatively to form the desired products. In the case of **6**, the method of Campbell and Eglinton[34] was employed. However, difficulties in the purification of the product were encountered, and the compound had to be treated with H_2S to remove Cu that was present in the sample. Therefore, it was decided to alter the method in the preparation of **10**, and in this case, the monoacetylene intermediate was efficiently coupled using the modification of Hay.[35] This method has the advantage of using milder conditions, while the CuCl·TMEDA (*N,N,N′,N′*-tetramethylethylenediamine) catalyst is capable of functioning in a variety of solvents (for a recent application, see ref 36). Indeed, no difficulties in the purification of **10** were encountered.

Compounds **13–15** were synthesized as shown in Scheme 4. The procedure using LDA to deprotonate the

Scheme 3[a]

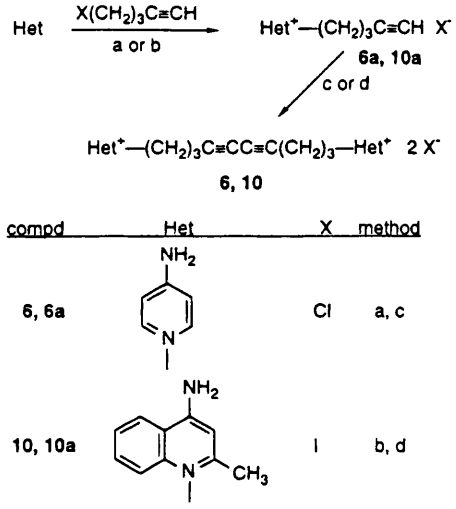

[a] Methods: (a) MEK, reflux, 28 h; (b) iBu_2CO, 120–140 °C, 96 h; (c) i. MeOH/Py, $(AcO)_2Cu$, reflux, 24 h; ii. H^+, H_2S; (d) iPrOH:MeOH (4:1), CuCl, TMEDA, O_2.

Scheme 4[a]

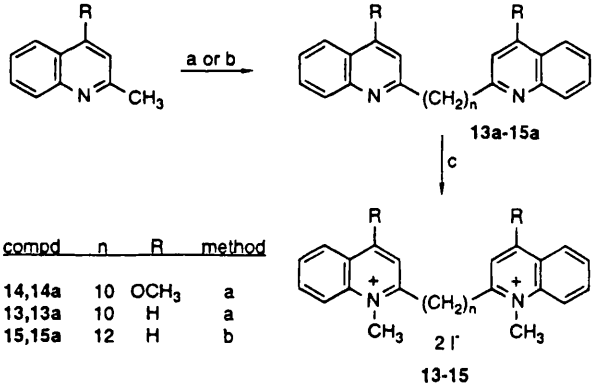

[a] Methods: (a) i. Na/liq NH_3; ii. $I(CH_2)_8I$; (b) i. LDA/THF; ii. $Br(CH_2)_{10}Br$ −78 °C → room temperature; (c) MeI, MEK.

methyl of the quinoline was found to be advantageous both in terms of yield and ease of purification over the procedure using $NaNH_2$/liquid NH_3.

Quaternization of 4-aminopyridine, quinoline, isoquinoline, and 4-bromoisoquinoline with 1,10-diiododecane afforded compounds **5**, **11**, **16**, and **17**, respectively, as shown in Scheme 5.

The two benzimidazolium compounds **18** and **19** were synthesized by deprotonation of benzimidazole or 2-methylbenzimidazole with nBuLi in THF, alkylation with 1,10-diiododecane to yield the bis-benzimidazole compounds, and quaternization of these with MeI (Scheme 6). It should be noted that the anions of both benzimidazole and 2-methylbenzimidazole failed to attack 1,10-diiododecane at room temperature and reflux temperatures were required.

Reaction of 2-chloropyrimidine with 1,10-diaminodecane in ethanol afforded the corresponding bis-(pyrimidinylamino)decane, quaternization of which with MeI as usual gave compound **9** (Scheme 7). Similarly, displacement of the chlorine atom of 9-chloroacridine by 1,10-diaminodecane in phenol gave **20**. This, however, failed to react with MeI in a quaternization reaction and was, therefore, tested as the base (Scheme 7). The acridine groups of **20**, however, are basic enough to be protonated at physiological pH (cf. pK_a of 9-(methylamino)acridine[37] = 10.43). We were unable to quaternize 9-aminoacridine with 1,10-diiododecane to obtain a direct analogue of dequalinium, and this led to the decision of joining the two rings from the exocyclic rather than the endocyclic nitrogens. The other tricyclic compound, **12**, was synthesized by quaternization of

Scheme 5[a]

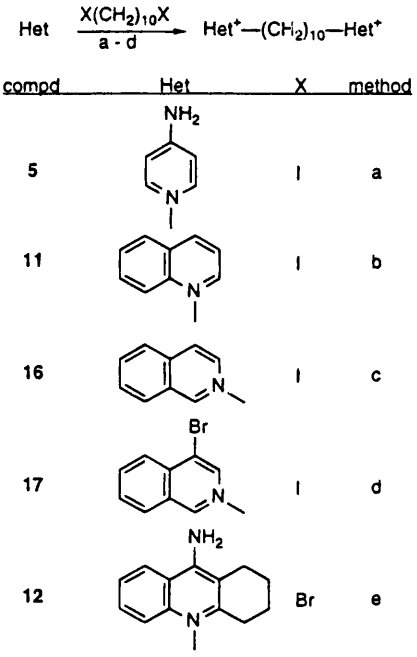

[a] Methods: (a) 4-methylpentan-2-ol, reflux, 1 h; (b) MEK, reflux, 99 h; (c) MEK, reflux, 23 h; (d) MEK, reflux, 96 h; (e) 155 °C, 1 h, no solvent.

Scheme 6[a]

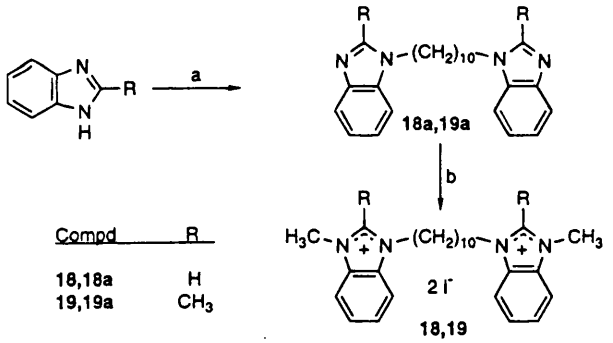

[a] Methods: (a) i. nBuLi/THF, −78 °C; ii. $I(CH_2)_{10}I$, reflux, 36 h; (b) MeI, MEK, 36 h.

Scheme 7[a]

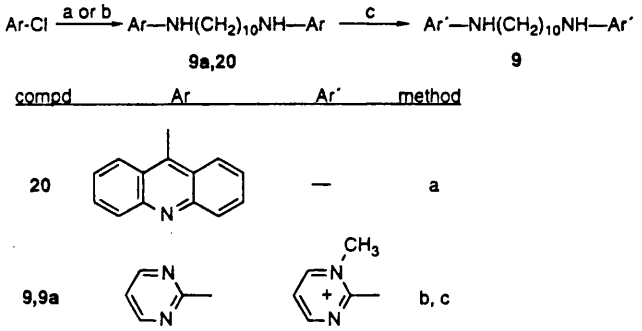

[a] Methods: (a) $H_2N(CH_2)_{10}NH_2$, PhOH, 130–135 °C, overnight; (b) $H_2N(CH_2)_{10}NH_2$, Et_3N, EtOH, reflux, 30 h; (c) MeI, MEK, reflux, 14 h.

Table 1.

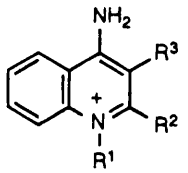

compd	R^1	R^2	R^3	$IC_{50} \pm SD$ (μM)	EMR[a] ± SD	n^b
1	$(CH_2)_9CH_3$	CH_3	H	5.5 ± 1.6	4.7 ± 1.7	3
2	$(CH_2)_3CH_3$	CH_3	H	12 ± 2	12 ± 5.9	3
3	$(CH_2)_{10}N^+Et_3$	CH_3	H	18 ± 3	17 ± 7.7	3
4	H	CH_2CH_2—CH_2CH_2		30[c]	30[c]	3

[a] Equieffective molar ratio: the ratio of the concentrations of the test compound and dequalinium that cause 50% inhibition, as determined in the same experiment. [b] Number of neurones tested. [c] Insufficient activity at this concentration to determine IC_{50}.

9-amino-1,2,3,4-tetrahydroacridine with 1,10-diiododecane. All compounds gave satisfactory analytical data, although in many cases the compounds tenaciously retained some water even after prolonged and thorough drying.

Biological Testing

The SK_{Ca} blocking action of the compounds was assessed from their ability to inhibit the after-hyperpolarization (AHP) in cultured rat sympathetic neurones as described previously.[32] Each compound was tested at two to four concentrations on at least three cells. Between three and eight compounds were examined at a time, and in each such series of experiments, dequalinium was also included as a reference compound. The Hill equation was fitted to the data to obtain estimates of the IC_{50}. However, because there was some variation in the potency of dequalinium during the course of the study, equieffective molar ratios (EMR; relative to dequalinium) were obtained by simultaneous nonlinear least squares fitting of the data with the Hill equation. It is these values which have been used for the comparison between compounds. It should be noted that the compounds were applied in a continuously flowing solution to isolated cells, so that differences in depletion as a concequence of variation in lipophilicity are unlikely to have been a complicating factor.

Although relatively simple, this assay relies on Ca^{2+} influx during the action potential to activate the SK_{Ca} channels, and the potency of any compound interfering with this influx may be overestimated. Dequalinium itself is a highly selective blocker of the SK_{Ca} channel, with no detectable effect on Ca^{2+} current even at the relatively high concentration of 10 μM.[32] As most of the compounds tested in the present work have a similar bis-cationic structure to dequalinium, an action on Ca^{2+} channels seems unlikely. Nevertheless, because of the indirectness of the assay, test concentrations of more than 10–30 μM were generally avoided. The time course of the onset of the blocking action provided an additional criterion since dequalinium and all but two of the compounds tested acted rapidly, within 90 s. The two exceptions were the amphipathic monocations **1** and **2** which were clearly less selective in their actions on sympathetic neurones.

Results and Discussion

Despite being a relatively simple molecule, dequalinium is the most potent nonpeptidic blocker of the SK_{Ca} channel so far described.[31] It is more active than many other bis-quaternary compounds (such as atracurium, tubocurarine, and pancuronium; Figure 1) in which the positive charge is carried by alkylammonium groups.[27] It is also approximately 500 times more potent than a simple structural analogue, decamethonium (Figure 1), in which the positive charges are carried by two trimethylammonium groups.[27]

In view of these findings, it seemed important to address the questions of the need for two quinolinium groups and of their role. The answer to the first question would establish whether our structural analogues should have one or two quinolinium groups, and the answer(s) to the second should reveal the explanation for the importance of the charge being carried by a quinolinium rather than an alkylammonium group and should also guide our thinking in designing more potent blockers of the SK_{Ca} channel.

We therefore started by removing one quinolinium group from the molecule of dequalinium to provide compound **1** (Table 1). Although the drop in activity that results from this change appears rather small to account for the loss of a binding site, the biological test result for **1** does not reflect pure SK_{Ca} channel blocking activity, for at least two reasons. Firstly, **1** slowed the rising phase of the action potential of the neurone, and this in itself would reduce the AHP by lowering Ca^{2+} entry. Secondly, in contrast to dequalinium, the onset of the action of **1** was slow (many minutes rather than seconds), suggesting a different mechanism of action. Shortening the chain of **1** from 10 to 4 carbons provided **2** which, although it did not block the action potential of the neurone, again had a slow onset of action. It is important to note that, as for dequalinium,[32] analogues **3**, **5**, **6**, **8**, and **10**–**20** (Table 2) have a fast onset of action (complete within 90 s). It seems that **1** and **2** either bind at a different site on the SK_{Ca} channel or act via a different mechanism. However, the finding that replacement of the aminoquinolinium groups of dequalinium by the 9-amino-1,2,3,4-tetrahydroacridine group affords an equipotent compound (**12**; see below) prompted the testing of 9-amino-1,2,3,4-tetrahydroacridine (**4**) itself as another example of a compound having one instead of two positive charges. As can be seen from Tables 1 and 2, **12** is substantially more potent than **4**. It should be noted that the inactivity of **4** can neither be attributed to the lack of a positive charge, since the compound is protonated at physiological pH as its pK_a is 9.95,[38] nor to the lack of a quaternary nitrogen, since it is shown later in the discussion that nonquaternary compounds (**8** and **20**) are active as blockers of the SK_{Ca}

Table 2.

Compd	Structure					$IC_{50} \pm SD$¶	EMR†±SD	n*
				A				
5	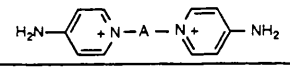			$(CH_2)_{10}$		35 ± 6	33 ± 13	7
6				Acetylene#		6 ± 0.8	4.7 ± 1.6	4
			R⁴		R⁵			
7	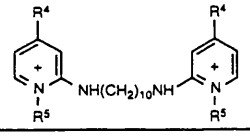		NO_2		O⁻	>> 30	>> 30	4
8			NH_2		H	5.5 ± 0.7	5 ± 1.8	3
9	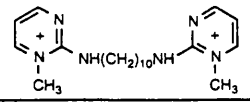					>> 10	>> 10	5
		R⁶	R⁷	R⁸	B			
Deq	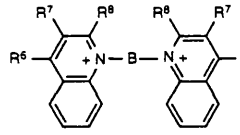	NH_2	H	CH_3	$(CH_2)_{10}$	0.74 ± 0.05	1	18
10		NH_2	H	CH_3	Acetylene#	1.6 ± 0.3	2.4 ± 0.9	3
11		H	H	H	$(CH_2)_{10}$	21 ± 5	15 ± 7.9	5
12		NH_2	CH_2CH_2—CH_2CH_2		$(CH_2)_{10}$	1 ± 0.2	0.9 ± 0.7	5
				R⁹	C			
13	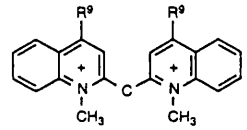			H	$(CH_2)_{10}$	72 ± 15	130 ± 34	6
14				OCH_3	$(CH_2)_{10}$	9.5 ± 3.5	27 ± 9	3
15				H	$(CH_2)_{12}$	21 ± 15	33 ± 10	4
					R¹⁰			
16	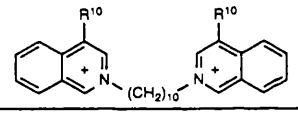				H	25 ± 5	80 ± 42	5
17					Br	4.7 ± 0.9	7.6 ± 3.1	5
					R¹¹			
18	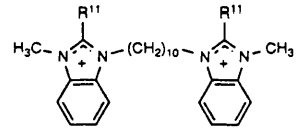				H	16 ± 5.6	77 ± 23	4
19					CH_3	> 10	> 10	4
20	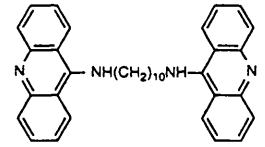					6.7 ± 0.4	12.2 ± 4.9	3

¶ In μM.

† For definition of EMR see footnote to Table I.

* Number of neurones tested.

Acetylene = $-(CH_2)_3C{\equiv}CC{\equiv}C(CH_2)_3-$

> Insufficient activity at this concentration to determine IC_{50}.

>> No activity up to this concentration.

channel. However, some ambiguity concerning the validity of the comparison of **4** with **12** may arise from the absence of an alkyl chain R^1 in compound **4**. This, combined with the uncertain mechanism of action of the other monoquaternary compounds (**1** and **2**), suggested that attention should be focused on bis-charged compounds for potency, consistency, and obtaining comparable and interpretable results.

Replacement of one quinolinium group of dequalinium by the triethyl ammonium group to give **3** resulted in a 20-fold drop in potency (relative to dequalinium), confirming that the properties of both of the charged groups are critical. It could also be concluded on comparing **3** with **1** that the introduction of a second charge to the latter restores the dequalinium-type pharmacological profile, as **3** has a fast onset of action and does not interfere with the action potential of the neurone. Focusing on those differences between the triethylammonium and quinolinium groups which might account for the superiority of the latter, it is evident that the charge distribution is very different and that enhanced delocalization via the resonance effect of the amino group in the case of dequalinium may be of significance (Figure 2). The flatness of the ring could also contribute through, for example, π-stacking if there were appropriately situated side chains of aromatic amino acids in the channel. Indeed, quinolinium cations have been shown to bind more strongly than alkylammonium cations to artificial receptors containing aromatic rings.[39] Although the structure of the SK_{Ca} channel is not known, there appears to be remarkable conservation of aromatic amino acids close to or in the

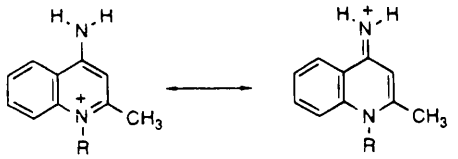

Figure 2. Two of the canonical structures contributing to aminoquinolinium resonance.

pore-forming areas of the proteins of the structures which have been proposed for the ATP-regulated,[4] inward rectifier,[3] voltage-dependent,[40] and high-conductance Ca^{2+}-activated[5] K^+ channels. Further evidence on the importance of aromatic amino acids in the binding of K^+ channel blockers is provided by the finding that TEA blocks tetrameric voltage-dependent K^+ channels by binding at a site consisting of four aromatic amino acids, one being contributed from each of the four subunits.[8,9]

On the other hand, the preference for the quinolinium over the triethylammonium group could arise from a more favorable electrostatic interaction with anionic sites on the channel, and this in turn may be due to a more favorable charge distribution. Although, conventionally, the positive charge is shown localized on the quaternary nitrogen in the structure of the quinolinium and triethylammonium groups, it is actually mainly distributed over the hydrogen atoms. To identify any differences in charge distribution between the two groups, the partial charges for two model compounds, namely, 4-amino-1,2-dimethylquinolinium and methyltriethylammonium, were examined (Figure 3). The choice of the two model compounds was based on the assumption that the two charged groups in the bisquaternary blockers, which are separated by 10 carbons and cannot therefore interact inductively or mesomerically, do not interact through space i.e., the two charged groups are treated as being isolated. To simplify the problem, the aliphatic chain was replaced by methyl. Although the former has slightly different electronic properties in terms of its inductive and hyperconjugation effects compared with the latter, the errors introduced are expected to be largely the same in the case of the quinolinium and triethylammonium groups so that the results should be comparable. The charges were obtained by a semiempirical molecular orbital calculation using the MOPAC package, with the AM1 Hamiltonian[41] and performing Mulliken population analysis.

It can be seen in Figure 3 that in the quinolinium group the positive charge is mainly distributed over carbon atoms 2, 4, and 8a and the hydrogen atoms of the two methyl and amino groups, with all aromatic hydrogen atoms carrying substantial positive charges. The fact that the carbon atoms of positions 2, 4, and 8a are positively charged is in qualitative agreement with the conventional depiction of delocalization that results from resonance structures for the quinolinium group. On the other hand, the positive charge of the triethylammonium group is distributed over its hydrogen atoms, with the methylene groups directly attached to the quaternary nitrogen atom being more positively charged than the three terminal methyl groups. The charge distribution differences observed between the two groups may account for the difference in the potencies of dequalinium and **3**, but it is not clear that this is necessarily so.

Alternatively, the electrostatic interaction may involve matching parts of the electric fields of the two interacting species, which have oposite signs, rather than matching point charges. It is likely that the interaction with the receptor is at an anionic site, in which case the electrostatic potential maps of the molecules should provide a better representation of what the receptor actually "sees" of the molecule. These are shown in Figure 4. The electrostatic potential energy map of the triethylammonium group corresponds to one of the low-energy conformations of the group. Clearly, there are considerable differences in the two maps. The field around the methyltriethylammonium is more spherical in shape, while the one around the quinolinium group is more ring shaped and arises from the positively charged hydrogen atoms of the heterocycle. There is no buildup of positive charge above and below the plane of the quinolinium ring. It should also be noted that the shape of the positive field around the quinolinium group is "fixed" since all atoms that give rise to the field occupy strictly defined positions relative to each other. This is not the case with the field of the triethylammonium group because of the conformational mobility of the three ethyl groups.

The advantageous interaction resulting from a ring-shaped charge distribution might be related to the existence of rings of negative charge in the pore region of many ion channels.[42] These result from the negatively charged side chains of amino acids, one being contributed from each subunit of the channel, arranged in a circular fashion, pointing toward the center of the pore, thus forming a negative "wall" at that point. One can envisage the positive ring of the quinolinium group complementing the negative ring of the channel. In this way, the plane of the quinoline would be perpendicular to the longitudal axis of the channel pore and the compound would obstruct the flow of K^+ through the channel, thus acting as a blocker. On the other hand, the spherical (and smaller) field of the triethylammonium group would be a poor match to the ring-shaped field of the channel, yielding an interaction of lower strength. The conformational mobility of the ethyl groups could further weaken the interaction either directly, by varying the electrostatic field of the molecule, or indirectly, by introducing unfavorable entropic factors. Although, as mentioned in the introductory section, the structure of the SK_{Ca} channel is not known, this represents a resonable hypothesis explaining the observed more favorable binding of the quinolinium compared with the triethylammonium groups, particularly since all K^+ channel types that have been cloned so far have negatively charged amino acids in the sequence of the putative pore-forming region of the protein.[3-5,40]

Removal of the fused benzene ring to provide a pyridinium compound (**5**; Table 2) results in substantial loss of potency, and this may be due to reduction in the area of the flat π-electron system and/or altered charge distribution. As far as the latter is concerned, the size of the positively charged ring in the electrostatic potential energy map of the compound is smaller than in the case of the quinoline. To increase rigidity of the linking aliphatic chain of this compound in order to force the charged rings to occupy more strictly defined positions in space relative to each other, triple bonds were

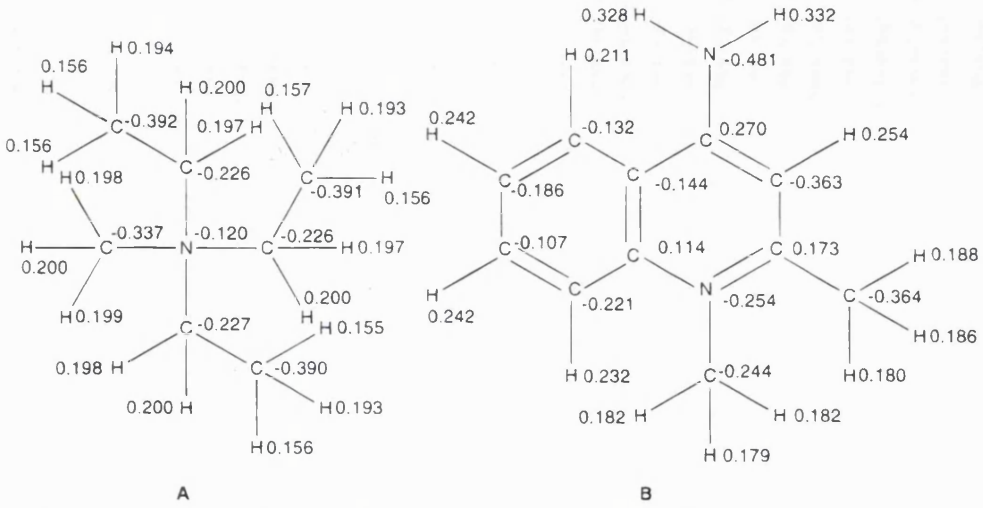

Figure 3. Partial charges on the atoms of two model compounds: methyltriethylammonium (A) and 4-amino-1,2-dimethylquinolinium (B).

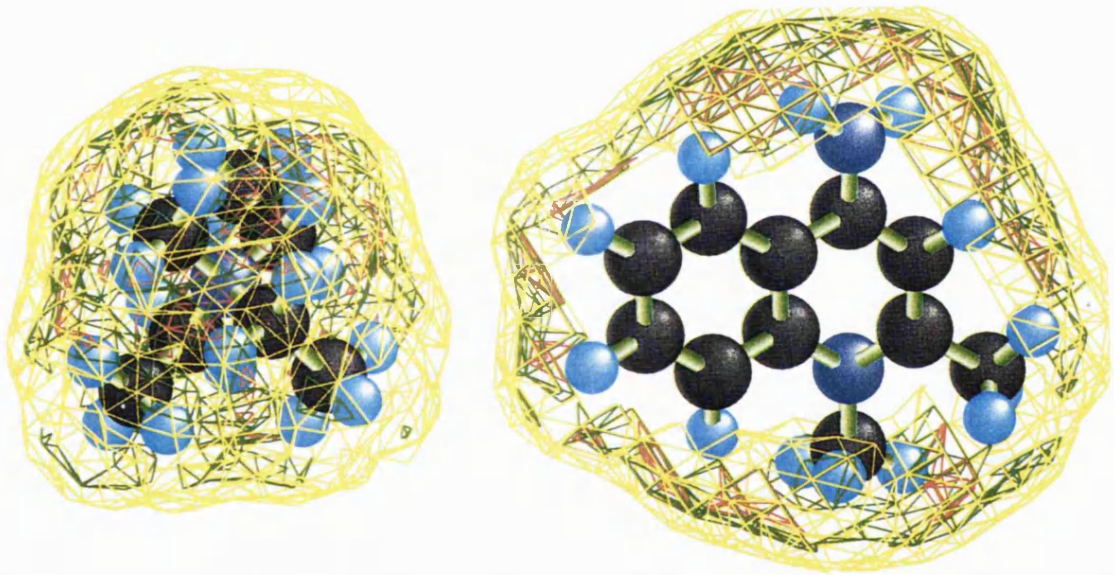

Figure 4. Electrostatic potential energy maps of the two model compounds of Figure 3. Contours were calculated at 30 (yellow), 40 (green), and 50 (red) kcal/mol using Sybyl 6.0. The molecules were minimized with AM1. Atoms are colored black (carbon), ultramarine (nitrogen), and turquoise (hydrogen).

introduced (**6**; Table 2), and this resulted in a 6-fold increase in potency. Motivated by this finding, the chain of dequalinium was analogously constrained by making **10**. However, this did not provide the expected increase in activity but rather a small decrease.

Experimenting further with the pyridine compound **5**, a second amino group at position 2 was introduced and the two rings were linked via this group (**8**). This compound is not a quaternary ammonium salt, but its p*K*a is sufficiently high (p*K*a of 2,4-diaminopyridine[43] = 9.52) for the rings to be protonated and, hence, charged at physiological pH. The resulting 6-fold increase in activity may be due to the greater delocalization effected by the second amino group, suggesting once again that charge delocalization is an important feature for potent blockade of the channel. As a speculative structural modification, **7** (an intermediate in the synthesis of **8**) was also tested, but it proved to be completely inactive at concentrations up to 30 μM.

As mentioned in the introductory section, it is believed that the arginine residues of apamin and in particular the guanidinium groups are crucial for activity. To bridge apamin with the dequalinium-like compounds, **9** was synthesized in which a guanidinium-type group is partially incorporated into a heterocyclic ring to provide an aminopyrimidinium structure. This compound was less potent than **5**. Since there seemed to be no advantage with the pyridine compounds, attention was refocused on the quinoline series.

Since charge delocalization appears to be an important factor, its contribution was tested by reducing its extent and removing the NH_2 group of dequalinium to give **11**; this resulted in considerable loss of potency, adding further evidence in support of the argument. To investigate an alternative position for the aliphatic chain in joining the two quinoline rings, some representative compounds were made. Moving the linking point of **11** from position 1 to position 2 (**13**) resulted in further loss of potency, possibly due to changes in conformation. Introduction of a methoxy group at position 4 of the quinoline rings of **13** improved activity by a factor of 5 (**14**), possibly due to increased delocal-

ization of the charge. Adding two more methylene groups to the 10-methylene chain of **13** also produced a similar increase in potency (**15**).

Replacement of the quinoline ring of **11** by the isoquinoline ring results in **16** which is 5 times less potent than **11**. Introduction of a bromine atom at position 4 of the isoquinoline (**17**) provided almost an order of magnitude increase in activity compared with **16**.

Assuming that the nitrogen of the amino group of dequalinium serves to delocalize the positive charge, it seemed appropriate to examine the importance of it being exocyclic. Hence, the benzimidazole compound **18** was synthesized, in which the exocyclic nitrogen of dequalinium has been incorporated into the ring, while keeping its ability to delocalize the charge. This compound is considerably less potent than dequalinium. It is even 5 times less potent than **11** and half as potent as **5**. Adding a methyl group at position 2 of the benzimidazole (**19**) did not alter potency significantly.

To explore further the nature of the charged heterocycle, two acridine analogues (**20** and **12**) were synthesized. In the case of **20**, we were unable to obtain a direct comparison with dequalinium because 9-aminoacridine failed to react with 1,10-diiododecane, as mentioned in the Chemistry section. However, **20**, in which the rings are joined by the exocyclic rather than the endocyclic nitrogens, is active but some 10 times less potent than dequalinium. On the other hand, **12** is equipotent with dequalinium, suggesting the binding site can accommodate a tricyclic structure and the reduced potency of **20** is not due to the size of the heterocycle.

Conclusion

From the results presented above, a number of conclusions can be drawn. It seems that the presence of two charged groups and the properties of both these groups are important for SK_{Ca} channel blocking activity in the dequalinium analogues. The present results have allowed us to develop a hypothetical model for the interaction of the charged part of the molecules examined with the channel. It is based on the differences in electrostatic potential energy maps, which could account for the tighter binding of the quinolinium compared with the triethylammonium groups. In particular, it seems that there is a need for a ring-shaped positive electrostatic field around the charged part of the molecule for blockade of the SK_{Ca} channel.

Furthermore, it appears that the blocking potency of the compounds correlates qualitatively with the degree of the delocalization of the positive charge within a series having the same heterocycle and also between compounds bearing different heterocycles. There may also be some dependence of activity on the extent of the flat π-electron system of the heterocyclic ring. Furthermore, it has been demonstrated that the quinolinium rings of dequalinium can be replaced by other heterocyclic cations to give active compounds. The binding site must therefore possess steric tolerance since compounds having monocyclic, bicyclic, or tricyclic heterocycles can be accommodated. In addition to the above, it has been shown that the rings do not necessarily have to be permanently charged, since non-quaternary compounds, basic enough to be protonated at physiological pH, are relatively potent blockers.

Experimental Section

Melting points (mp) were obtained on an Electrothermal melting point apparatus and are uncorrected. Infrared (IR) spectra were run on a Perkin-Elmer 983 spectrophotometer. Nuclear magnetic resonance (NMR) spectra were recorded on a Varian XL-200 (200 MHz) or VXR-400 (400 MHz) spectrometer, and chemical shifts (ppm) are reported relative to the solvent peak ($CHCl_3$ in $CDCl_3$ at 7.24 ppm and DMSO in DMSO-d_6 at 2.49 ppm) or relative to TMS. Signals are designated as follows: s, singlet; s_{br}, broad singlet; d, doublet; dd, doublet of doublets; t, triplet; q, quadruplet; quint, quintet; m, multiplet. Mass spectra were run on a ZAB SE or VG 7070H spectrometer. Analytical reverse phase high-performance liquid chromatography (HPLC) was performed on either a Gilson or Shimadzu HPLC apparatus with a UV detector at 215 or 254 nm and a Kromasil C18 7 μm (K) or Lichrosorb RP SELECT B 7 μm (L) column. Isocratic elutions using solvent mixtures of A = water + 0.1% TFA and B = MeOH + 0.1% TFA or C = water + 0.5% sodium salt of hexanesulfonic acid + 0.5% orthophosphoric acid and D = MeOH + 0.5% sodium salt of hexanesulfonic acid + 0.5% orthophosphoric acid were performed unless otherwise stated. The ratio of A:B or C:D is indicated for each individual compound. The flow rate was 1 mL/min.

1-Decanyl-2-methyl-4-aminoquinolinium Iodide (1). A solution of 4-aminoquinaldine (1 g, 6.3 mmol) and 1-iododecane (1.66 g, 6.3 mmol) in 4-methyl-2-pentanol (30 mL) was heated under reflux for 80 h. After cooling the solvent was removed in vacuo, and the resulting red oil was purified by column chromatography on silica gel using 10% MeOH in EtOAc. This gave a solid which was recrystallized from hot water to give fine white needles (0.12 g, 4.5%): mp = 196.1−196.6 °C; ^{1}H NMR (400 MHz, DMSO-d_6) δ 0.85 (m, 2 H, -CH_2-), 1.25 (m, 13 H, -CH_2-), 1.43 (m, 2 H, -CH_2-), 1.47 (m, 2 H, -CH_2-), 2.73 (s, 3 H, quinoline-CH_3), 4.45 (t, J = 8 Hz, 2 H, -CH_2-N), 6.73 (s, 1 H, quinoline-H_3), 7.72 (t, J = 9 Hz, 1 H, quinoline-H_6 or -H_7), 8.01 (t, J = 9 Hz, 1 H, quinoline-H_7 or -H_6), 8.14 (d, J = 9 Hz, 1 H, quinoline-H_5 or -H_8), 8.44 (d, J = 9 Hz, 1 H, quinoline-H_8 or -H_5), 8.78 (s_{br}, 2 H, NH_2); HPLC column L, flow 0.75 mL/min, C:D = 20:80, major peak at 9.26 min representing 96.9% of the absorption at 254 nm. Anal. ($C_{20}H_{31}N_2I\cdot H_2O$) C, H, N.

1-Butyl-2-methyl-4-aminoquinolinium Iodide (2). 4-Aminoquinaldine (0.5 g, 3.2 mmol) was dissolved in MEK (20 mL) and treated with 1-iodobutane (5 mL, 40 mmol) under reflux for 70 h. This gave a creamy white precipitate which was collected by vacuum filtration, washed with MEK and then EtOAc, and dried. Recrystallization from a mixture of iPrOH and MeOH afforded creamy colored platelet crystals (0.51 g, 47%): mp 151 °C; ^{1}H NMR (400 MHz, CD_3OD) δ 1.05 (t, J = 7.4 Hz, 3 H, -CH_2CH_3), 1.58 (sextet, J = 7.6 Hz, 2 H, -CH_2CH_3), 1.84 (quint, J = 7.7 Hz, 2 H, -$CH_2CH_2CH_3$), 2.78 (s, 3 H, quinoline-CH_3), 4.52 (t, J = 7.9 Hz, 2 H, -CH_2N), 6.79 (s, 1 H, quinoline-H_3), 7.70 (t, 1 H, quinoline-H_6 or -H_7), 8.03 (t, 1 H, quinoline-H_7 or -H_6), 8.11 (d, 1 H, quinoline-H_5 or -H_8), 8.33 (d, 1 H, quinoline-H_8 or -H_5); HPLC column L, C:D = 50:50, major peak at 8.38 min representing 99.4% of the absorption at 215 nm. Anal. ($C_{14}H_{19}N_2I$) C, H, N, I.

1,1,1-Triethyl-1-(10-iododecan-1-yl)ammonium Iodide (3a). 1,10-Diiododecane (1 g, 2.54 mmol) was dissolved in MEK (20 mL) and treated with triethylamine (0.175 mL, 1.25 mmol) under reflux for 24 h. The mixture was allowed to cool and a further portion of triethylamine (0.175 mL, 1.25 mmol) added; the mixture was heated under reflux for a further 72 h. The white precipitate was removed by vacuum filtration and shown to be 1,1′-(decane-1,10-diyl)bis(1,1,1-triethylammonium) diiodide by NMR, MS, and elemental analysis (data not shown). The filtrate was evaporated in vacuo to yield a yellow oil (0.9 g) which was purified by column chromatography on silica gel using EtOAc to remove the unreacted 1,10-diiododecane and 1% aqueous NH_3 in MeOH to give the product as a pale yellow oil (0.252 g, 24%): MS (FAB, MNOBA matrix) $(M + I)^+$ 494, M^+ 368, fragments at m/z 240, 226, 212, 198, 184, 170, 156, 142, 128, 114, 100.

1-[10-(*N,N,N*-Triethylammonium-1-yl)decan-1-yl]-2-methyl-4-aminoquinolinium Diiodide (3). 1,1,1-Triethyl-1-(10-iododecan-1-yl)ammonium iodide (0.252 g, 0.685 mmol) was dissolved in 4-methyl-2-pentanol (25 mL) and treated with 4-aminoquinaldine (0.15 g, 0.95 mmol) at 80 °C for 36 h. The temperature was then raised to 120 °C for a further 90 h. The solid precipitate was collected by vacuum filtration, washed with MEK, and dried to give the product which was characterized as a white powder (0.03 g, 6.7%): mp 226–229 °C dec; ^{1}H NMR (400 MHz, CD_3OD) δ 1.34–1.90 (m, 23 H, -CH_2- and -CH_3), 2.82 (s, 3 H, quinoline-CH_3), 3.24 (m, 2 H, $Et_3N^+CH_2$), 3.36 (m, 8 H, -CH_2-), 4.56 (t, J = 7.7 Hz, 2 H, -CH_2-$N_{quinoline}$), 6.82 (s, 1 H, quinoline-H_3), 7.75 (t, 1 H, quinoline-H_6 or -H_7), 8.07 (t, 1 H, quinoline-H_7 or -H_6), 8.16 (d, 1 H, quinoline-H_5 or -H_8), 8.38 (d, 1 H, quinoline-H_8 or -H_5); HPLC column L, C:D = 40:60, major peak at 4.48 min representing 98.7% of the absorption at 215 nm. Anal. ($C_{26}H_{45}N_3I_2$) H, N; C: calcd, 47.78; found, 47.07. I: calcd, 38.83; found, 40.16.

1,1′-(Decane-1,10-diyl)bis(4-aminopyridinium) Diiodide[44] (5). 4-Aminopyridine (4 g, 42 mmol) was dissolved in 4-methyl-2-pentanol (75 mL) and treated with 1,10-diiododecane (8.7 g, 22 mmol) under reflux with stirring for 1 h. After cooling to room temperature, a creamy white solid precipitated from the solution. This was collected by vacuum filtration and washed thoroughly with water and then acetone. After drying, the solid was recrystallized from hot MeOH to yield creamy colored microneedles of product (7.09 g, 55.4% yield): mp = 249–251 °C; ^{1}H NMR (60 MHz, DMSO-d_6) δ 1.20 (s, 12 H, -CH_2-), 1.70 (m, 4 H, -CH_2-), 4.10 (t, J = 5 Hz, 4 H, -CH_2-N), 6.79 (d, J = 7 Hz, 4 H, pyridine-H_3 and -H_5), 8.17 (d, J = 7 Hz, 4 H, pyridine-H_2 and -H_6), 7.95 (s, 4 H, NH_2, disappears with D_2O); HPLC column L, linear gradient elution with C:D = 80:20 at 0 min to C:D = 40:60 at 20 min, major peak at 30.11 min representing 98.6% of the absorption at 254 nm. Anal. ($C_{20}H_{32}N_4I_2$) C, H, N; I: calcd, 43.60; found, 45.40.

1-(4-Pentyn-1-yl)-4-aminopyridinium Chloride (6a). 4-Aminopyridine (0.5 g, 5.3 mmol) was dissolved in MEK (20 mL) and treated with 5-chloro-1-pentyne (1.06 mL, 10 mmol) under reflux for 28 h. After the mixture had cooled to room temperature, the precipitate was collected by vacuum filtration and then purified by column chromatography on silica gel using 50% MeOH in EtOAc. This gave a colorless gum which solidified on standing (0.151 g, 15% yield): mp = 139.5–141 °C; ^{1}H NMR (200 MHz, DMSO-d_6) δ 2.00 (m, 2 H, -CH_2-), 2.25 (m, 2 H, -CH_2-), 2.88 (t, J = 2 Hz, 1 H, C≡CH), 4.08 (t, J = 6 Hz, 2 H, N-CH_2), 6.63 (d, J = 7 Hz, 2 H, pyridine-H_3 and -H_5), 7.79 (d, J = 7 Hz, 2 H, pyridine-H_2 and -H_6), 8.11 (s, 2 H, NH_2).

1,1′-(Deca-4,6-diyne-1,10-diyl)bis(4-aminopyridinium) Dichloride Dihydrate (6). 1-(4-Pentyn-1-yl)-4-aminopyridinium chloride (1.3 g, 6.63 mmol) and a saturated solution of finely powdered $(AcO)_2Cu$ (1.725 g, 9.48 mmol) in 60 mL of pyridine:MeOH (1:1) were heated under reflux for 24 h. The solvents were removed in vacuo, and the green solid was dried in vacuo. This was purified by column chromatography on silica gel using 50% MeOH in EtOAc which was increased to 80% toward the end of the procedure. The product was isolated as a yellow-green needle-like material. This was dissolved in the minimum amount of MeOH, and iPrOH was added until the solution turned cloudy. After filtration, Et_2O was added dropwise to the filtrate to precipitate the product. The solvents were removed in vacuo, and the resultant pale yellow solid rigorously was dried under vacuum at 70 °C and then dissolved in water and treated with H_2SO_4 (a few drops) and H_2S gas for 30 min. Decolorizing charcoal was added, and the mixture was stirred for 10 min. After filtration the filtrate was neutralized with Na_2CO_3 and the solvents were removed in vacuo. This gave a solid material which was twice dissolved in iPrOH and concentrated to dryness to azeotropically remove water and then dissolved in hot iPrOH, and the insoluble Na_2SO_4 and Na_2CO_3 were removed by filtration. The solvents were removed in vacuo from the filtrate to give a sticky gum. This was treated with dry Et_2O and scratched until a powder formed. The Et_2O was removed in vacuo and the proceedure repeated with fresh Et_2O until all the gum had solidified (0.2 g, 19%): mp 115 °C; ^{1}H NMR (400 MHz, DMSO-d_6) δ 2.00 (quint, 4 H, -CH_2-), 2.38 (t, 4 H, -CH_2-), 4.05 (t, 4 H, N-CH_2-), 6.52 (d, 4 H, pyridine-H_3 and -H_5), 7.72 (d, 4 H, pyridine-H_2 and -H_6), 8.00 (s_{br}, 4 H, NH_2); ^{13}C NMR (100 MHz, DMSO-d_6) δ 15.4, 28.5, 56.1, 65.5, 76.7, 109.3, 142.0, 158.8; HPLC column L, linear gradient elution with C:D = 70:30 at 0 min to C:D = 20:80 at 30 min, major peak at 18.09 min representing 99.2% of the absorption at 254 nm. Anal. ($C_{20}H_{24}N_4Cl_2 \cdot 2H_2O$) C, H; N: calcd, 13.11; found, 12.57.

2,2′-*N,N′*-(Decane-1,10-diyl)bis(4-nitro-2-aminopyridine 1-oxide) (7). A solution of 2-chloro-4-nitropyridine 1-oxide[45] (0.5 g, 0.28 mmol) in EtOH (50 mL) containing 1,-10-diaminodecane (0.25 g, 0.14 mmol) was heated under reflux for 4 h. The EtOH was removed in vacuo to yield an orange solid which was a mixture of products and starting materials (TLC). This was purified by column chromatography on silica gel using EtOAc until the starting materials had been eluted and then using MeOH to give two compounds. The first was identified as the desired product and obtained as a mixture of the free base and the dihydrochloride salt. Total conversion to the free base was achieved by basification of a solution of the mixture in water with aqueous NH_3 and extraction with EtOAc. The yield of the pure free base was 0.192 g (31%): mp 126.5–127 °C; ^{1}H NMR (200 MHz, $CDCl_3$) δ 1.35–1.75 (m, 16 H, -CH_2-), 3.36 (q, J = 7 Hz, 4 H, N-CH_2-), 6.97 (t_{br}, 2 H, NH), 7.39 (m, 4 H, pyridine-H_5 and -H_6), 8.26 (m, 2 H, pyridine-H_3); HPLC column L, MeOH:EtOAc = 20:80, major peak at 6.87 min representing 99.6% of the absorption at 254 nm. Anal. ($C_{20}H_{28}N_6O_6$) C, H; N: calcd, 18.75; found, 18.00.

2,2′-*N,N′*-(Decane-1,10-diyl)bis(2,4-diaminopyridine) (8). 2,2′-*N,N′*-(Decane-1,10-diyl)bis(4-nitro-2-aminopyridine 1-oxide) (0.26 g) was dissolved in MeOH (100 mL) and treated with 10% Pd/C (0.5 g) in a Parr low-pressure hydrogenation apparatus at 50 psi of hydrogen for 11.5 h. The catalyst was filtered off, and the filtrate was evaporated in vacuo to give a colorless gum. This was purified by column chromatography on silica gel using 1% NH_4OH in MeOH. The product (0.061 g, 30% yield) was recrystallized from MeOH to yield a white, microcrystalline material: mp 140–142 °C; ^{1}H NMR (400 MHz, DMSO-d_6) δ 1.25 (m, 12 H, -CH_2-), 1.45 (quint, J = 6 Hz, 4 H, -CH_2-), 3.03 (q, J = 7 Hz, 4 H, N-CH_2-), 5.46 (s, 4 H, NH_2), 5.50 (d, J = 2 Hz, 2 H, pyridine-H_3), 5.74 (m, 4 H, pyridine-H_5 and NH), 7.45 (d, J = 6 Hz, 2 H, pyridine-H_6); HPLC column L, flow 0.75 mL/min, C:D = 35:65, major peak at 5.91 min representing 93.5% of the absorption at 254 nm. Anal. ($C_{20}H_{32}N_6 \cdot H_2O$) H; C: calcd, 64.14; found, 65.41. N: calcd, 22.44; found, 21.84.

2,2′-*N,N′*-(Decane-1,10-diyl)bis(2-aminopyrimidine) (9a). 2-Chloropyrimidine (1 g, 8.73 mmol), 1,10-diaminodecane (0.752 g, 4.37 mmol), and Et_3N (2 mL, 14.35 mmol) were dissolved in 40 mL of absolute EtOH and heated under reflux for 30 h. After the solution had cooled to room temperature, MeOH was added to the solution and the white precipitate formed was collected by vacuum filtration and washed with MeOH to yield pure product. The filtrate was concentrated to dryness, and the resulting solid formed was basified with dilute KOH solution until the solution was strongly alkaline and extracted with 5 × 50 mL CH_2Cl_2. After drying (Na_2SO_4) the CH_2Cl_2 was removed in vacuo to give a redish oil which was recrystallized from MeOH to yield white crystals (total: 0.973 g, 68%): mp 107–108 °C; ^{1}H NMR (400 MHz, $CDCl_3$, TMS) δ 1.29 (m, 12 H, -CH_2-), 1.62 (quint, 4 H, -CH_2-), 3.39 (td, J_1 = 5.8 Hz, J_2 = 7.2 Hz, 4 H, N-CH_2-), 5.18 (s_{br}, 2 H, NH), 6.50 (t, J = 4.8 Hz, 2 H, pyrimidine-H_5), 8.27 (d, J = 4.7 Hz, 4 H, pyrimidine-H_4 and -H_6); HPLC column K, A:B = 50:50, major peak at 12.12 min representing 97.7% of the absorption at 215 nm. Anal. ($C_{18}H_{28}N_6 \cdot 0.2CH_3OH$) C, H, N.

2,2′-*N,N′*-(Decane-1,10-diyl)bis(1-methyl-2-aminopyrimidinium) Diiodide (9). 2,2′-*N,N′*-(Decane-1,10-diyl)bis(2-aminopyrimidine) (0.2 g, 0.61 mmol) and MeI (3 mL, 48.2 mmol) were dissolved in MEK and heated under reflux under argon for 14 h. A creamy precipitate formed which was collected by vacuum filtration and washed extensively with MEK (0.328 g, 88%): mp 182–184 °C dec; ^{1}H NMR (400 MHz, DMSO-d_6, TMS) δ 1.26 (m, 12 H, -CH_2-), 1.58 (m, 4 H, -CH_2-), 3.50 (q, 4 H, N-CH_2-), 3.72 (s, 6 H, -CH_3), 7.08 (dd, J_1 = 4.4 Hz, J_2 = 6.5 Hz, 2 H, pyrimidine-H_5), 8.61 (dd, J_1 = 2.1 Hz, J_2

= 6.5 Hz, 2 H, pyrimidine-H_4), 8.74 (t_{br}, 2 H, NH), 8.88 (dd, J_1 = 4.4 Hz, J_2 = 2.1 Hz, 2 H, pyrimidine-H_6); HPLC column K, linear gradient elution with A:B = 45:55 at 0 min to A:B = 10:90 at 15 min, major peak at 4.46 min representing 100% of the absorption at 254 nm. Anal. ($C_{20}H_{34}N_6I_2$) C, H, N.

1-(4-Pentyn-1-yl)-2-methyl-4-aminoquinolinium Iodide (10a). 4-Aminoquinaldine (0.7 g, 4.42 mmol) and 5-iodo-1-pentyne[48] were dissolved in 25 mL of hot diisobutyl ketone, and the solution was heated to 120–140 °C under argon for 96 h. The reaction mixture was cooled to room temperature and the dark solid collected by filtration and dried under vacuum. This was dissolved in MeOH, adsorbed onto silica, and chromatographed using 10% MeOH in EtOAc. The fractions containing the product were combined, and the solvents removed in vacuo to yield a dark red oil (1.1 g, 70.6%) which was recrystallized from MeOH–Et_2O to yield a pink solid: mp = 193–195 °C; ^{1}H NMR (400 MHz, DMSO-d_6) δ 1.92 (quint, 2 H, -CH_2-), 2.42 (t_{br}, 2 H, -CH_2-), 2.73 (s, 3 H, -CH_3), 2.97 (s, 1 H, ≡CH), 4.52 (t, J = 8.2 Hz, 2 H, N^+-CH_2-), 6.71 (s, 1 H, quinoline-H_3), 7.72 (t, J = 7.6 Hz, 1 H, quinoline-H_6 or -H_7), 8.02 (t, J = 7.6 Hz, 1 H, quinoline-H_7 or -H_6), 8.19 (d, J = 8.9 Hz, 1 H, quinoline-H_5 or -H_8), 8.43 (d, J = 8.1 Hz, 1 H, quinoline-H_8 or -H_5), 8.84 (d_{br}, 2 H, NH_2). Anal. ($C_{15}H_{17}N_2I$·0.25 H_2O) C, H, N; I: calcd, 35.57; found, 34.98.

1,1′-(Deca-4,6-diyne-1,10-diyl)bis(4-amino-2-methylquinolinium) Diiodide Hydrate (10). TMEDA (0.5 g, 4.3 mmol) and CuCl (0.42 g, 4.25 mmol) were dispersed with vigorous stirring in 100 mL of iPrOH. The solution turned deep blue and some solid remained undissolved. After the solid had precipitated, 2 mL of the supernatant solution were added to a solution of 1-(4-pentyn-1-yl)-2-methyl-4-aminoquinolinium iodide (0.1 g, 0.284 mmol) in a mixture of iPrOH:MeOH 4:1. The solution was rapidly decolourized. O_2 was bubbled through with vigorous stirring for 2 h while the reaction mixture was kept in a water bath at 40 °C. The bubbling of O_2 was stopped, and the solution was stirred vigorously for another 48 h. The reaction mixture was concentrated to a small volume; the creamy precipitate formed was collected, washed with MeOH, and dried in vacuo (0.07 g, 70%): mp 295–297 °C dec; ^{1}H NMR (400 MHz, DMSO-d_6) δ 1.95 (q, 4 H, -CH_2-), 2.58 (t, J = 6.9 Hz, 4 H, -CH_2-), 2.73 (s, 6 H, -CH_3), 4.50 (t, J = 8.1 Hz, 4 H, N^+-CH_2-), 6.71 (s, 2 H, quinoline-H_3), 7.72 (t, J = 7.6 Hz, 2 H, quinoline-H_6 or -H_7), 8.01 (t, J = 8.5 Hz, 2 H, quinoline-H_7 or -H_6), 8.18 (d, J = 9.0 Hz, 2 H, quinoline-H_5 or -H_8), 8.43 (d, J = 8.4 Hz, 2 H, quinoline-H_8 or -H_5), 8.85 (d, 2 H, NH_2); HPLC column K, A:B = 55:45, major peak at 13.67 min representing 95% of the absorption at 215 nm. Anal. ($C_{30}H_{32}N_4I_2$·1.25H_2O) C, H, N; I: calcd, 35.01; found, 33.44.

1,1′-(Decane-1,10-diyl)bis(quinolinium) diiodide[46] (11): HPLC column L, C:D = 40:60, major peak at 5.26 min representing 99.5% of the absorption at 220 nm.

1,1′-(Decane-1,10-diyl)bis(9-amino-1,2,3,4-tetrahydroacridinium) dibromide[47] hydrate (12): HPLC column L, C:D = 25:75, major peak at 6.61 min representing 98.2% of the absorption at 254 nm.

2,2′-(Decane-1,10-diyl)bis(quinoline) (13a). Na (1.966 g, 85.52 mmol) was dispersed in liquid NH_3 containing a catalytic amount of $Fe(NO_3)_3$ under argon. When the dark blue color of the suspension turned gray, quinaldine (11.638 g, 81.28 mmol) was added and the reaction mixture was stirred for 1 h. 1,8-Diiodooctane (14.87 g, 40.63 mmol) was then gradualy added, and the NH_3 was allowed to evaporate overnight. Water was added to the residue and the aqueous phase extracted with Et_2O. The extracts were combined, dried (Na_2SO_4), and rotay evaporated to dryness to yield an oil which was dissolved in the minimum ammount of petroleum ether at 40–60 °C and kept at −20 °C overnight. The solid mass that had formed was allowed to warm to room temperature, filtered, and the yellow solid obtained was washed with the solvent and dried (1.984 g, 12.3%). This contained some quinaldine (TLC); hence it was recrystallized from MeOH. Large, orange crystals came out of solution, which were collected and dried. However, the compound was still impure; therefore, it was purified by column chromatography on silica gel using petroleum ether:EtOAc (3:1). It was isolated as yellow crystals which were dried in vacuo (1.03 g): mp 96–97 °C; ^{1}H NMR (400 MHz, $CDCl_3$, TMS) δ 1.27–1.42 (m, 12 H, -CH_2-), 1.80 (quint, 4 H, -CH_2-), 2.96 (t, J = 7.9 Hz, 4 H, quinoline-CH_2-), 7.29 (d, J = 8.4 Hz, 2 H, quinoline-H_3), 7.48 (t, J = 6.9 Hz, 2 H, quinoline-H_6 or -H_7), 7.68 (t, J = 7.0 Hz, 2 H, quinoline-H_7 or -H_6), 7.77 (d, J = 8.1 Hz, 2 H, quinoline-H_5 or -H_8), 8.03–8.07 (d, d, 4 H, quinoline-H_8 or -H_5, quinoline-H_4); HPLC column K, A:B = 50:50, major peak at 14.76 min representing 100% of the absorption at 215 nm. Anal. ($C_{28}H_{32}N_2$·0.1H_2O) C, H, N.

2,2′-(Decane-1,10-diyl)bis(1-methylquinolinium) Diiodide Hydrate (13). 2,2′-(Decane-1,10-diyl)bis(quinoline) (0.3 g, 0.757 mmol) and MeI (2 mL, 32.13 mmol) were dissolved in MEK, and the solution was heated under reflux for 33 h. More MeI was added after 6 h (1 mL, 16.07 mmol) and after 16 h (2 mL, 32.13 mmol). The reaction mixture was filtered hot, and the yellow solid collected was dried. Four recrystallizations from MeOH were needed to get an analyticaly pure sample for testing. At the last two, care was taken to allow the material to crystallize only for 30 min at room temperature. The crystals collected were washed with hot MeOH (0.119 g, 23%): mp = 234 °C dec; ^{1}H NMR (400 MHz, DMSO-d_6, TMS) 1.31 (m, 8 H, -CH_2-), 1.45 (m, 4 H, -CH_2-), 1.76 (quint, 4 H, -CH_2-), 3.36 (t, J = 7.9 Hz, 4 H, quinoline-CH_2-), 4.48 (s, 6 H, N^+-CH_3), 8.00 (t, J = 7.5 Hz, 2 H, quinoline-H_6 or -H_7), 8.11 (d, J = 8.7 Hz, 2 H, quinoline-H_3), 8.23 (td, J_1 = 1.5 Hz, J_2 = 8.1 Hz, 2 H, quinoline-H_7 or -H_6), 8.40 (d, J = 8.1 Hz, 2 H, quinoline-H_5 or -H_8), 8.57 (d, J = 9.1 Hz, 2 H, quinoline-H_8 or -H_5), 9.11 (d, J = 8.7 Hz, 2 H, quinoline-H_4); HPLC column K, A:B = 50:50, major peak at 4.92 min representing 97.3% of the absorption at 215 nm. Anal. ($C_{30}H_{38}N_2I_2$·H_2O) C, H, N.

2,2′-(Decane-1,10-diyl)bis(4-methoxyquinoline) (14a). Na (0.42 g, 18.27 mmol) was dispersed in aproximately 150 mL of liquid NH_3, under argon, containing a catalytic ammount of ferric nitrate. When the initially dark blue suspension had turned gray, 4-methoxy-2-methylquinoline[49] (3 g, 17.32 mmol) was added and the dark red reaction mixture was stirred for 1 h. Then, 1,8-diiodooctane (3.128 g, 8.54 mmol) was added slowly. After 1 h of stirring, no reaction had taken place (TLC); therefore, 90 mL of dry DMF was added, and the solution was stirred overnight. The reaction was quenched by adding water, and the solvents were removed in vacuo at 35 °C. Water was added to the residue, and it was extracted with Et_2O. The extracts were combined and dried (Na_2SO_4) and the solvent removed in vacuo. The residue consisted mainly of product and 4-methoxyquinaldine, which were separated by column chromatography on silica gel using CH_2Cl_2:EtOAc (2:1). The product was recrystallized from MeOH to yield small, white-grayish crystals (1.1 g, 28%): mp 88–89 °C; ^{1}H NMR (200 MHz, $CDCl_3$) δ 1.29–1.42 (m, 12 H, -CH_2-), 1.80 (quint, J = 7.4 Hz, 4 H, -CH_2-), 2.94 (t, J = 7.9 Hz, 4 H, quinoline-CH_2-), 4.04 (s, 6 H, OCH_3), 6.64 (s, 2 H, quinoline-H_3), 7.44 (t, J = 7.1 Hz, 2 H, quinoline-H_6 or -H_7), 7.66 (t, J = 7.1 Hz, 2 H, quinoline-H_7 or -H_6), 7.99 (d, J = 8.5 Hz, 2 H, quinoline-H_5 or -H_8), 8.14 (dd, J_1 = 1.5 Hz, J_2 = 8.3 Hz, 2 H, quinoline-H_8 or -H_5); HPLC column K, A:B = 45:55, major peak at 18.02 min representing 98.8% of the absorption at 215 nm. Anal. ($C_{30}H_{36}N_2O_2$·4H_2O) C, H, N.

2,2′-(Decane-1,10-diyl)bis(1-methyl-4-methoxyquinolinium) Diiodide (14). 2,2′-(Decane-1,10-diyl)bis(4-methoxyquinoline) (0.2 g, 0.44 mmol) and MeI (2 mL, 32.13 mmol) were dissolved in 20 mL of MEK, and the solution was heated under reflux for 12 h under argon. The white precipitate that formed was collected by filtration, washed with solvent, and dried in vacuo. A single recrystallization from CH_2Cl_2 afforded pure material (0.167 g, 51.5%): mp 186–188 °C; ^{1}H NMR (400 MHz, DMSO-d_6, TMS) 1.33 (m, 8 H, -CH_2-), 1.47 (m, 4 H, -CH_2-), 1.74 (m, 4 H, -CH_2-), 3.28 (t, J = 8.1 Hz, 4 H, quinoline-CH_2), 4.30 (s, 12 H, OCH_3 and NCH_3), 7.62 (s, 2 H, quinoline-H_3), 7.91 (t, J = 7.2 Hz, 2 H, quinoline-H_6 or -H_7), 8.17 (t, J = 7.1 Hz, 2 H, quinoline-H_7 or -H_6), 8.38–8.45 (d, d, 4 H, quinoline-H_5, and -H_8); HPLC column K, A:B = 45:55, major peak at 8.16 min representing 100% of the absorption at 215 nm. Anal. ($C_{32}H_{42}N_2O_2I_2$) H, N; C: calcd, 51.90; found, 51.44.

2,2′-(Dodecane-1,12-diyl)bis(quinoline) Hemihydrate (15a). To a solution of LDA (23.05 mmol) in THF at −78 °C

was added quinaldine (3 g, 20.95 mmol) over a period of 15 min. The solution was stirred at −78 °C for 1 h. 1,10-Diiododecane (3.144 g, 10.47 mmol) was then added, and the solution was allowed to warm gradually to room temperature and stirred for 18 h. The reaction was quenched with MeOH, and the mixture was concentrated to dryness, diluted with water, and extracted with $CHCl_3$. The extracts were dried (Na_2SO_4) and rotary evaporated to dryness to yield a yellow solid. This was recrystallized from MeOH to give pale yellow crystals (3.46 g, 78%): mp 98−100 °C; ^{1}H NMR (400 MHz, $CDCl_3$) δ 1.25 (m, 16 H, -CH_2-), 1.80 (quint, 4 H, -CH_2-), 2.96 (t, 4 H, quinoline-CH_2), 7.30 (d, J = 8.5 Hz, 2 H, quinoline-H_3), 7.47 (t, J = 7.5 Hz, 2 H, quinoline-H_6 or -H_7), 7.66 (t, J = 7.6 Hz, 2 H, quinoline-H_7 or -H_6), 7.77 (d, J = 8.1 Hz, 2 H, quinoline-H_5 or -H_8), 8.05 (d, d, 4 H, quinoline-H_4, -H_8 or -H_5); HPLC column K, A:B = 35:65, major peak at 6.32 min representing 100% of the absorption at 215 nm. Anal. ($C_{30}H_{36}N_2$·0.5H_2O) C, H, N.

2,2′-(Dodecane-1,12-diyl)bis(1-methylquinolinium) Diiodide (15). 2,2′-(Dodecane-1,12-diyl)bis(quinoline) (0.5 g, 1.18 mmol) and MeI (2 mL, 32.13 mmol) were dissolved in MEK, and the solution was heated under reflux for 72 h under argon, more portions of MeI (2 mL) being added after 12, 24, 36, 48, and 60 h. The yellow solid formed was collected by filtration and washed with the solvent and Et_2O. This was recrystallized twice from absolute EtOH to yield yellow crystals (0.7 g, 84%): mp = 172−174 °C; ^{1}H NMR (400 MHz, DMSO-d_6) δ 1.28 (m, 12 H, -CH_2-), 1.46 (m, 4 H, -CH_2-), 1.77 (quint, 4 H, -CH_2-), 3.38 (t, J = 8 Hz, 4 H, quinoline-CH_2), 4.52 (s, 6 H, -CH_3), 8.01 (td, J_1 = 7.6 Hz, J_2 = 0.7 Hz, 2 H, quinoline-H_6 or -H_7), 8.12 (d, J = 8.6 Hz, 2 H, quinoline-H_3), 8.24 (td, J_1 = 7.7 Hz, J_2 = 1.4 Hz, 2 H, quinoline-H_7 or -H_6), 8.41 (d, J = 8.1 Hz, 2 H, quinoline-H_5 or -H_8), 8.59 (d, J = 9 Hz, 2 H, quinoline-H_8 or -H_5), 9.13 (d, J = 8.6 Hz, 2 H, quinoline-H_4); HPLC column L, A:B = 50:50, major peak at 17.42 min representing 100% of the absorption at 215 nm. Anal. ($C_{32}H_{42}N_2I_2$) C, H, N.

2,2′-(Decane-1,10-diyl)bis(isoquinolinium) Diiodide[46] (16): HPLC column K, A:B = 50:50, major peak at 5.2 min representing 98.9% of the absorption at 254 nm.

1,1′-(Decane-1,10-diyl)bis(4-bromoisoquinolinium) Diiodide (17). A solution of 4-bromoisoquinoline (3 g, 14.4 mmol) in MEK (100 mL) was treated with 1,10-diiododecane (2.84 g, 7.2 mmol) and heated under reflux with stirring for 96 h. After cooling the precipitate was collected by vacuum filtration and recrystallised twice from MeOH to give golden yellowish crystals (2 g, 2.5 mmol, 34.7%): mp 241−243 °C; ^{1}H NMR (400 MHz, DMSO-d_6) δ 1.26−1.31 (m, 12 H, -CH_2-), 2.03 (m, 4 H, -CH_2-), 4.69 (t, J = 7.5 Hz, 4 H, N-CH_2), 8.18 (ddd, J_1 = 1.4 Hz, J_2 = 6.7 Hz, J_3 = 8.1 Hz, 2 H, isoquinoline-H_6 or -H_7), 8.38−8.44 (m, 4 H, isoquinoline), 8.57 (d, J = 8.3 Hz, 2 H, isoquinoline-H_5 or -H_8), 9.34 (d, J = 1 Hz, 2 H, isoquinoline-H_3), 10.23 (s, 2 H, isoquinoline-H_1); HPLC column K, A:B = 50:50, major peak at 7.1 min representing 96.8% of the absorption at 254 nm. Anal. ($C_{28}H_{32}N_2Br_2I_2$) C, H, N.

1,1′-(Decane-1,10-diyl)bis(1*H*-benzimidazole) (18a). To a suspension of benzimidazole (1 g, 8.47 mmol) in THF at −78 °C, was added 5.3 mL (8.48 mmol) of a 1.6 M solution of nBuLi in hexanes. The resultant solution was stirred for 30 min and then allowed to warm to room temperature. 1,10-Diiododecane (1.668 g, 4.23 mmol) was added, and the solution was heated under reflux for 36 h under argon. MeOH was then added, and the solvents were removed in vacuo to yield an oil. This was purified by column chromatography on silica gel using EtOAc:MeOH (10:1). The product (R_f = 0.3) was obtained as a yellow solid. This was dispersed in 50 mL of hot water, and EtOH was added until the solution was clear. On cooling to room temperature, a yellow oil came out of solution. The supernatant was decanted into another flask, excess of water was added dropwise to it while scratching the walls of the flask, and the suspension was placed in the refridgerator for 5 h. The white precipitate was collected by filtration, washed well with water, and dried in vacuo at 40 °C (60% yield): mp 87 °C; ^{1}H NMR (400 MHz, $CDCl_3$) δ 1.22−1.29 (m, 12 H, -CH_2-), 1.86 (m, 4 H, -CH_2-), 4.16 (t, J = 7 Hz, 4 H, NCH_2), 7.26−7.31 (m, 4 H, benzimidazole-H_5, H_6), 7.40 (dd, J_1 = 6.9 Hz, J_2 = 2.5 Hz, 2 H, benzimidazole-H_4 or -H_7), 7.81 (dd, J_1 = 6.8 Hz, J_2 = 2 Hz, 2 H, benzimidazole-H_7 or -H_4), 7.89 (s, 2 H, benzimidazole-H_2); ^{13}C NMR (100 MHz, $CDCl_3$) δ 26.7, 29.0, 29.2, 29.7, 45.1, 109.6, 120.3, 122.0, 122.8, 133.7, 142.9, 143.8; MS (FAB, MNOBA matrix) $[M + H]^+$ 375, fragments at m/z 257, 243, 229, 215, 201, 187, 173, 159, 145, 131, 119; HPLC column K, A:B = 55:45, major peak at 10.44 min representing 99.9% of the absorption at 215 nm. Anal. ($C_{24}H_{30}N_4$·0.2H_2O) C, H, N.

1,1′-(Decane-1,10-diyl)bis(3-methylbenzimidazolium) Diiodide Hemihydrate (18). 1,1′-(Decane-1,10-diyl)bis(1*H*-benzimidazole) (0.2 g, 0.53 mmol) and MeI (1 mL, 16.06 mmol) were dissolved in 15 mL MEK and heated under reflux for 36 h, more MeI (1 mL) being added after 12 h. The white solid that formed was collected by filtration, washed extensively with solvent, and dried (0.332 g, 95%): mp 204−205 °C; ^{1}H NMR (400 MHz, DMSO-d_6) δ 1.24−1.30 (m, 12 H, -CH_2-), 1.88 (m, 4 H, -CH_2-), 4.08 (s, 6 H, CH_3), 4.47 (t, J = 7.1 Hz, 4 H, N-CH_2), 7.69−7.73 (m, 4 H, benzimidazole), 8.02−8.04 (m, 2 H, benzimidazole), 8.08−8.10 (m, 2 H, benzimidazole), 9.72 (s, 2 H, benzimidazole-H_2); HPLC column K, A:B = 55:45, major peak at 11.91 min representing 99.2% of the absorption at 215 nm. Anal. ($C_{26}H_{36}N_4I_2$·0.5H_2O) C, H, N.

1,1′-(Decane-1,10-diyl)bis(2-methylbenzimidazole) (19a). To a suspension of 2-methylbenzimidazole (1 g, 7.57 mmol) in THF (70 mL) at −78 °C was added a 1.6 M solution of nBuLi in hexanes (5 mL, 7.95 mmol) dropwise, and the mixture was stirred at −78 °C for 30 min. Then, a solution of 1,10-diiododecane (1.49 g, 3.78 mmol) in THF was added, and the mixture was warmed to room temperature and then heated under reflux for 36 h under Ar. After the solution had cooled to room temperature, MeOH was added and the solvents were removed in vacuo to yield an oil. This was partitioned between water (50 mL) and $CHCl_3$ (40 mL), and the water phase was further extracted with 40 mL $CHCl_3$. The extracts were combined and dried (Na_2SO_4), and the solvent was removed in vacuo to yield an oil. This was purified by column chromatography on silica gel using petroleum ether:EtOAc (10:1). The product (R_f = 0.25) was isolated as a white solid which was dissolved in $CHCl_3$ and filtered to remove any silica and the solvent removed in vacuo to yield a white solid (1.444 g, 95%): mp 101−102 °C; ^{1}H NMR (200 MHz, $CDCl_3$, TMS,) δ 1.23−1.31 (m, 12 H, CH_2), 1.78 (m, 4 H, CH_2), 2.60 (s, 6 H, CH_3), 4.09 (t, J = 7.1 Hz, 4 H, N-CH_2), 7.20−7.30 (m, 6 H, Ar), 7.67−7.72 (m, 2 H, Ar). Anal. ($C_{26}H_{34}N_4$·0.2H_2O) C, H, N.

1,1′-(Decane-1,10-diyl)bis(2,3-dimethylbenzimidazolium) Diiodide (19). 1,1′-(Decane-1,10-diyl)bis(2-methylbenzimidazole) (0.2 g, 0.497 mmol) and MeI (1 mL, 16.06 mmol) were dissolved in MEK and heated under reflux for 36 h under Ar, more MeI (1 mL) being added after 24 h. After cooling to room temperature, the solid formed was collected by filtration and washed extensively with MEK. This was recrystallized from MeOH, but the sample obtained was less pure (by HPLC). It was suspected that it decomposed on heating; therefore, it was recrystallized again from approximately 25 mL of MeOH with gentle heating (0.2 g, 59%): mp 274−276 °C; ^{1}H NMR (400 MHz, DMSO-d_6) δ 1.23−1.32 (m, 12 H, CH_2), 1.74 (quint, 4 H, CH_2), 2.88 (s, 6 H, CH_3), 3.98 (s, 6 H, N-CH_3), 4.47 (t, J = 7.4 Hz, 4 H, N-CH_2), 7.62−7.64 (m, 4 H, Ar), 7.98−8.02 (m, 4 H, Ar); HPLC column K, A:B = 50:50, major peak at 4.62 min representing 97.8% of the absorption at 215 nm. Anal. ($C_{28}H_{40}N_4I_2$·0.2H_2O) C, H, N.

1,10-Bis[*N*-(Acridin-9-yl)amino]decane dihydrochloride dihydrate[50] (20): HPLC column L, flow 0.75 mL/min, A:B = 35:65, major peak at 10 min representing 96% of the absorption at 215 nm.

Acknowledgment. This work was supported by the Wellcome Trust (including Fellowships to C.A.D. and P.M.D.).

References

(1) Watson, S.; Girdlestone, D. *Trends Pharmacol. Sci. Receptor Ion Channel Nomenclature Suppl.* **1994**, 5th ed, pp 44−47.

(2) Pongs, O. Structural basis of voltage-gated K^+ channel pharmacology. *Trends Pharmacol. Sci.* **1992**, *13*, 359–365.
(3) Kubo, Y.; Baldwin, T. J.; Jan, Y. N.; Jan, L. Y. Primary structure and functional expression of a mouse inward rectifier potassium channel. *Nature* **1993**, *362*, 127–133.
(4) Ho, K.; Nichols, C. G.; Lederer, W. J.; Lytton, J.; Vassilev, P. M.; Kanazirska, M. V.; Hebert, S. C. Cloning and expression of an inwardly rectifying ATP-regulated potassium channel. *Nature* **1993**, *362*, 31–38.
(5) Butler, A.; Tsunoda, S.; McCobb, D. P.; Wei, A.; Salkoff, L. *mSlo*, a complex mouse gene encoding "Maxi" calcium-activated potassium channels. *Science* **1993**, *261*, 221–224.
(6) Garcia-Calvo, M.; Knaus, H.-G.; McManus, O. B.; Giangiacomo, K. M.; Kaczorowski, G. J.; Garcia, M. L. Purification and reconstitution of the high-conductance, calcium-activated potassium channel from tracheal smooth muscle. *J. Biol. Chem.* **1994**, *269*, 676–682.
(7) Knaus, H.-G.; Folander, K.; Garcia-Calvo, M.; Garcia, M. L.; Kaczorowski, G. J.; Smith, M.; Swanson, R. Primary sequence and immunological characterization of b-subunit of high conductance Ca^{2+}-activated K^+ channel from smooth muscle. *J. Biol. Chem.* **1994**, *269*, 17274–17278.
(8) Heginbotham, L.; MacKinnon, R. The aromatic binding site for tetraethylammonium ion on potassium channels. *Neuron* **1992**, *8*, 483–491.
(9) Kavanaugh, M. P.; Hurst, R. S.; Yakel, J.; Varnum, M. D.; Adelman, J. P.; North, R. A. Multiple subunits of a voltage-dependent potassium channel contribute to the binding site for tetraethylammonium. *Neuron* **1992**, *8*, 493–497.
(10) Stong, P. N. Potassium channel toxins. *Pharmacol. Ther.* **1990**, *46*, 137–162.
(11) Cook, N. S. The pharmacology of potassium channels and their therapeutic potential. *Trends Pharmacol. Sci.* **1988**, *9*, 21–28.
(12) Robertson, D. W.; Steinberg, M. I. Potassium channel modulators: scientific applications and therapeutic promise. *J. Med. Chem.* **1990**, *33*, 1529–1541.
(13) Haylett, D. G.; Jenkinson, D. H. Calcium-activated potassium channels. In *Potassium Channels*; Cook, N. S., Ed.; Ellis Horwood: Chichester, 1990; pp 70–95.
(14) Lazdunski, M.; Romey, G.; Schmid-Antomarchi, H.; Renaud, J. F.; Mourre, C.; Hugues, M.; Fosset, M. The apamin-sensitive Ca^{2+}-dependent K^+ channel: Molecular properties, differentiation, involvement in muscle disease, and endogenous ligands in mammalian brain. *Handb. Exp. Pharmacol.* **1988**, *83*, 135–145.
(15) Banks, B. E. C.; Brown, C.; Burgess, G. M.; Burnstock, G.; Claret, M.; Cocks, T. M.; Jenkinson, D. H. Apamin blocks certain neurotransmitter-induced increases in potassium permeability. *Nature* **1979**, *282*, 415–417.
(16) Burgess, G. M.; Claret, M.; Jenkinson, D. H. Effects of quinine and apamin on the calcium-dependent potassium permeability of mammalian hepatocytes and red cells. *J. Physiol. (London)* **1981**, *317*, 67–90.
(17) Lazdunski, M. Apamin, a neurotoxin specific for one class of Ca^{2+}-dependent K^+ channels. *Cell Calcium* **1983**, *4*, 421–428.
(18) Demonchaux, P.; Ganellin, C. R.; Dunn, P. M.; Haylett, D. G.; Jenkinson, D. H. Search for the pharmacophore of the K^+ channel blocker, apamin. *Eur. J. Med. Chem.* **1991**, *26*, 915–920.
(19) Ferrero, J. D.; Cocks, T.; Burnstock, G. A comparison between ATP and bradykinin as possible mediators of the responces of smooth muscle to non-adrenergic non-cholinergic nerves. *Eur. J. Pharmacol.* **1980**, *63*, 295–302.
(20) Brown, C. M.; Burnstock, G. Evidence in support of the P_1/P_2 purinoceptor hypothesis in the guinea-pig taenia coli. *Br. J. Pharmacol.* **1981**, *73*, 617–624.
(21) Gater, P. R.; Haylett, D. G.; Jenkinson, D. H. Neuromuscular blocking agents inhibit receptor-mediated increases in the potassium permeability of intestinal smooth muscle. *Br. J. Pharmacol.* **1985**, *86*, 861–868.
(22) Nohmi, M.; Kuba, K. (+)-Tubocurarine blocks Ca^{2+}-dependent K^+ channel of the bullfrog sympathetic ganglion cell. *Brain Res.* **1984**, *301*, 146–148.
(23) Pennefather, P.; Lancaster, B.; Adams, P. R.; Nicoll, R. A. Two distinct Ca-activated K currents in bullfrog sympathetic ganglion cells. *Proc. Natl. Acad. Sci. U.S.A.* **1985**, *82*, 3040–3044.
(24) Fosset, M.; Schmid-Antomarchi, H.; Hughes, M.; Romey, G.; Lazdunski, M. The presence in pig brain of an endogenous equivalent of apamin, the bee venom peptide that specifically blocks Ca^{2+}-dependent K^+ channels. *Proc. Natl. Acad. Sci. U.S.A.* **1984**, *81*, 7228–7232.
(25) Renaud, J. F.; Desnuelle, C.; Schmid-Antomarchi, H.; Hughes, M.; Serratrice, G.; Lazdunski, M. Fxpression of apamin receptor in muscles of patients with myotonic muscular dystrophy. *Nature* **1986**, *319*, 678–680.
(26) Behrens, M. I.; Vergara, C. Increase of apamin receptors in sceletal muscle induced by colchicine: possible role in myotonia. *Am. J. Physiol.* **1992**, *263*, C794–C802.
(27) Cook, N. S.; Haylett, D. G. Effects of apamin, quinine and neuromuscular blockers on calcium-activated potassium channels in guinea pig hepatocytes. *J. Physiol.* **1985**, *358*, 373–394.
(28) Jenkinson, D. H.; Haylett, D. G.; Cook, N. S. Calcium-activated potassium channels in liver cells. *Cell Calcium* **1983**, *4*, 429–437.
(29) Nohmi, M.; Kiba, K. (+)-Tubocurarine blocks Ca^{2+}-dependent K^+ channel of the bullfrog sympathetic ganglion cell. *Brain Res.* **1984**, *301*, 146–148.
(30) Babbs, M.; Collier, H. O. J.; Austin, W. C.; Potter, M. D.; Taylor, E. P. Salts of decamethylene-bis-4-aminoquinaldinium ("Dequadin") a new antimicrobial agent. *J. Pharm. Pharmacol.* **1956**, *8*, 110–119.
(31) Castle, N. A.; Haylett, D. G.; Morgan, J. M.; Jenkinson, D. H. Dequalinium; a potent inhibitor of apamin-sensitive K^+ channels in hepatocytes and of nicotinic responses in skeletal muscle. *Eur. J. Pharmacol.* **1993**, *236*, 201–207.
(32) Dunn, P. M. Dequalinium, a selective blocker of the slow afterhyperpolarization in rat sympathetic neurones in culture. *Eur. J. Pharmacol.* **1994**, *252*, 189–194.
(33) Part of this work was presented as a preliminary communication at the British Pharmacological Society Meeting, University of Glasgow, Glasgow, July 10–12, 1991. Abstract published in: Dunn, P. M.; Davis, C. M.; Ganellin, C. R.; Haylett, D. G.; Morgan, J. M.; Jenkinson, D. H. Potassium channel blocking activity of dequalinium analogues in guinea-pig hepatocytes and rat sympathetic neurones. *Br. J. Pharmacol.* **1991**, *104*, 165P.
(34) Campbell, I. O.; Englinton, G. Diphenyl diacetylene. In *Organic Synthesis*; Wiley: New York **1973**; Collect. Vol. V, pp 517–520.
(35) Hay, A. S. Oxidative coupling of acetylenes. II. *J. Org. Chem.* **1962**, *27*, 3320–3321.
(36) Persico, F.; wuest, J. D. Use of hydrogen bonds to control molecular aggregation. Behavior of a self-complementary dipyridone designed to self-replicate. *J. Org. Chem.* **1993**, *58*, 95–99.
(37) Kalatzis, E. Kinetics of the hydrolytic deamination of *N*-heteroaromatic amines in aqueous alkaline solutions. *J. Chem. Soc. B* **1969**, 96–104.
(38) Albert, A. Acridine syntheses and reactions. Part VI. A new dehalogenation of 9-chloroacridine and its derivatives. Further acridine ionization constants and ultraviolet spectra. *J. Chem. Soc.* **1965**, 4653–4657.
(39) Kearney, P. C.; Mizoue, L. S.; Kumpf, R. A.; Forman, J. E.; McCurdy, A.; Dougherty, D. A. Molecular recognition in aqueous media. New binding studies provide further insight into the cation-π interaction and related phenomena. *J. Am. Chem. Soc.* **1993**, *115*, 9907–9919.
(40) Kavanaugh, M. P.; Varnum, M. D.; Osborne, P. B.; Christie, M. J.; Busch, A. E.; Adelman, J. P.; North, R. A. Interaction between tetraethylammonium and amino acid residues in the pore of cloned voltage-dependent potassium channels. *J. Biol. Chem.* **1991**, *266*, 7583–7587.
(41) Dewar, M. J. S.; Zoebisch, E. G.; Healy, E. F.; Stewart, J. J. P. AM1: A new general purpose quantum mechanical molecular model. *J. Am. Chem. Soc.* **1985**, *107*, 3902–3909.
(42) Imoto, K.; Busch, C.; Sakmann, B.; Mishina, M.; Konno, T.; Nakai, J.; Bujo, H.; Mori, Y.; Fukuda, K.; Numa, S. Rings of negatively charged amino acids determine the acetylcholine receptor channel conductance. *Nature* **1988**, *335*, 645-648.
(43) Rauckman, B. S.; Roth, B. 2.4-Diamino-5-benzylpyrimidines and analogues as antibacterial agents. 3. C-Benzylation of aminopyridines with phenolic mannich bases. Synthesis of 1- and 3-deaza analogues of trimethoprim. *J. Med. Chem.* **1980**, *23*, 384–391.
(44) Austin, W. C.; Lunts, L. H. C.; Potter, M. D.; Taylor, E. P. Chemotherapeutic properties of some new quaternary ammonium salts. *J. Pharm. Pharmacol.* **1959**, *11*, 80–93.
(45) Brown, E. V. Preparation and reactions of 2-nitropyridine-1-oxides. *J. Am. Chem. Soc.* **1957**, *79*, 3565–3566.
(46) Taylor, E. P. Synthetic neuromuscular blocking agents. Part I. Heterocyclic decamethylenebis(quaternary ammonium salts). *J. Chem. Soc.* **1951**, 1150–1157.
(47) Boehringer, C. H. Neth. Appl. 6,611,621, 1967; *Chem. Abstr.* **1968**, *68*, 49470w.
(48) Jackson, P. M.; Moody, C. J.; Shah, P. Preparation and Diels-Alder reactivity of thieno[2,3-c]- and thieno[3,2-c]pyran-3-ones, stable 2,3-dimethylenethiophene derivatives; synthesis of benzothiophenes. *J. Chem. Soc., Perkin Trans. 1* **1990**, *11*, 2909–2918.
(49) Conrad, M.; Limpach, L. Ueber das c-Oxychinaldin und dessen derivate. (On 4-hydroxyquinaldin and its derivatives.) *Chem. Ber.* **1887**, *20*, 948–959.
(50) Deshpande, S. M.; Singh, A. K. Synthesis of some N,N'-bis-(9-acridino)-a,z-diaminoalkanes dihydrochloride as potential antibacterial, antitubercular and antileprotics. *Chem. Pharm. Bull.* **1972**, *20*, 206–208.

JM9405755

Pergamon

Bioorganic & Medicinal Chemistry Letters, Vol. 5, No. 6, pp. 559-562, 1995

0960-894X/95 $9.50+0.00

0960-894X(95)00073-9

SYNTHESIS AND QSAR OF DEQUALINIUM ANALOGUES AS K+ CHANNEL BLOCKERS. INVESTIGATIONS ON THE ROLE OF THE 4-AMINO GROUP.

Dimitrios Galanakis,[1] Carole A. Davis,[1] Benedicto Del Rey Herrero,[1] C. Robin Ganellin,*[1]
Philip M. Dunn[2] and Donald H. Jenkinson[2]

Departments of [1]Chemistry and [2]Pharmacology, University College London, 20 Gordon Street, London WC1H 0AJ, U.K..

Abstract: Dequalinium (**1**) is a potent and selective non-peptidic blocker of the SK_{Ca} channel. The contribution of the 4-amino group to activity was investigated by replacing it by other groups R^4. The size or lipophilicity of R^4 was found to be unimportant and a good correlation was obtained between σ_R for R^4 and the blocking potency of the analogues, suggesting that the role of the NH_2 group is electronic.

Introduction. In recent years there has been an increasing interest in compounds that modulate K^+ channels as potential therapeutic agents.[1,2] With at least 20 subtypes described to date,[3] most of them need pharmacological exploration. One of the least well studied subtypes is that of small conductance Ca^{2+} - activated K^+ (SK_{Ca}) channels.[4,5] SK_{Ca} channels have been implicated in myotonic muscular dystrophy.[6,7] Dequalinium (**1**), a bis-quinolinium compound that has been used for many years as an antiseptic,[8] has recently been shown to be a potent and selective non - peptidic blocker of the SK_{Ca} channel.[9,10] This compound therefore constitutes a useful lead for the development of more potent blockers to assist investigations of the physiological and pathophysiological role of the SK_{Ca} channels. We have therefore initiated studies towards identifying the pharmacophore of dequalinium for SK_{Ca} channel blockade.[11,12]

Synthesis. Two structural features of dequalinium that merit examination are the 2-methyl and 4-amino groups. Hence analogues have been synthesised in which these have been removed or replaced by other groups to probe their potential contribution to blocking activity. The compounds for this study (**Table 1**) were synthesised via **Scheme 1**. Substituent R^4 was introduced via a nucleophilic displacement of the chlorine atom of 4-chloroquinoline and the resulting intermediates were reacted with 1,10-diiododecane either in MEK or in 4-methylpentan-2-ol to yield the final products **2** - **8**.

Biological testing. The SK_{Ca} blocking action of the compounds was assessed from their ability to inhibit the after - hyperpolarisation (AHP) in cultured rat sympathetic neurones as described previously.[10] Each compound was tested at 2 to 4 concentrations on at least three cells and dequalinium was also tested on the same cells as a reference compound. The Hill equation was fitted to the data to obtain estimates of the IC_{50} (**Table 1**). However, because there was some variation in the potency of dequalinium during the course of the study, equi - effective molar ratios (EMR: relative to dequalinium) were obtained by simultaneous non linear least squares fitting of the data with the Hill equation. It is these values which have been used for the comparison between compounds, bearing in mind that the smaller the value of EMR the more potent is the compound.[13]

Discussion of results. It is clear that the contribution of the 2-methyl group of dequalinium is very small since its removal does not result in much loss of potency (compound **2**). On the other hand, the 4-amino group seems to be important as the desamino analogue[12] **8** is an order of magnitude less potent than **2**. The NH_2 group is an excellent H-bond donor particularly since it participates in the delocalisation of the ring charge and, hence, carries a fractional positive charge which makes the hydrogens more acidic. However, it clearly does not act as an H-bond donor since its replacement by the NMe_2 group (compound **3**) does not result in loss of potency. On the other hand, it is unlikely that it acts as a H-bond acceptor, as its lone pair of electrons is involved in the delocalisation of the ring charge and is not readily available for H-bonding.

Scheme 1[a]

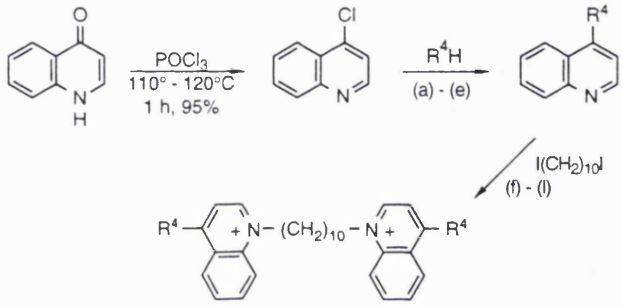

[a]Methods: (a) $R^4 = NH_2$, dry NH_3 (gas)/PhOH, 180°C, 4 h, 99%; (b) $R^4 = NMe_2$, Me_2NH·HCl, 170°C, 30 min, 76%; (c) $R^4 = NHPh$, $PhNH_2$/glacial AcOH, reflux, 3 h, 86%; (d) $R^4 = OPh$, PhOH/KOH, 125° - 130°C, 1 h, 100%; (e) $R^4 = NHCOCH_3$, 4-aminoquinoline made under (a) was acetylated using Ac_2O/pyridine, 80°C, 24 h, 100%; (f) **2**, 4-methylpentan-2-ol, reflux, 2.5 h, 59%; (g) **3**, 4-methylpentan-2-ol, reflux, 22 h, 17%; (h) **4**, methyl ethyl ketone (MEK), reflux, 96 h, 82%; (i) **5**, 4-methylpentan-2-ol, reflux, 30 h, 71%; (j) **6**, MEK, reflux, 96 h, 16%; (k) **7**, MEK, reflux, 96 h, 25%; (l) **8**, see ref. 12.

The importance of the delocalisation of the charge was examined by replacing the NH_2 group by other groups having different electronic properties (**Table 1**). It should be noted that all the substituents used have an overall electron releasing effect or are neutral. This was because quinolines with electron withdrawing substituents at position 4 are very weak nucleophiles and we were unable to alkylate the ring nitrogen in the final quaternization step (**Scheme 1**). The 2-methyl was also removed to facilitate the synthesis. From **Table 1** it is evident that there is no correlation between the size or lipophilicity (as expressed by the sum of the hydrophobic fragmental constants[14] Σf) of R^4 with EMR. However, it is also clear that the more electron releasing is R^4 the more potent is the compound. This trend can be quantified using the Hammett constant for "para" substitution[15] σ_p and the correlation equation that results is **1**:

$$pEMR = -1.16\ (\pm 0.38)\ \sigma_p - 1.05\ (\pm 0.17) \qquad \mathbf{1}$$
$$n = 7,\ r = -0.80,\ s = 0.317$$

where n is the number of compounds, r is the correlation coefficient and s is the standard deviation.

Table 1. Structure, biological results and parameter values for the compounds.

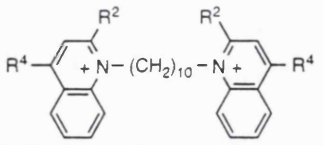

Compd	R^4	R^2	Σf[1]	σ_P[2]	σ_I[3]	σ_R[4]	pEMR[5]	EMR[6]±SD	$IC_{50} \pm SD$[7]	n[8]
1	NH_2	CH_3	—	—	—	—	0	1	0.74 ± 0.05	18
2	NH_2	H	-0.842	-0.66	0.17	-0.80	-0.11	1.3 ± 0.5	1.4 ± 0.3	4
3	NMe_2	H	0.473	-0.83	0.17	-0.88	-0.15	1.4 ± 0.6	1.4 ± 0.3	3
4	NHPh	H	0.893	-0.40	0.30	-0.86	-0.53	3.4 ± 1.8	2.4 ± 0.5	8
5	$NHCOCH_3$	H	-0.589	0.00	0.28	-0.35	-0.74	5.5 ± 1.0	4.5 ± 0.3	3
6	OPh	H	1.401	-0.03	0.40	-0.48	-0.81	6.5 ± 1.9	2.7 ± 1.6	5
7	CH_3	H	0.701	-0.17	-0.01	-0.16	-1.41	26 ± 14	15 ± 3.8	3
8	H	H	0.182	0.00	0.00	0.00	-1.18	15 ± 7.9	21 ± 5.0	4

[1] Σf: sum of hydrophobic fragmental constants for substituent R^4 (ref. 14). [2] σ_P: Hammett constant for "para" substitution (ref. 15). [3] σ_I: Electronic parameter for inductive effects (ref. 16). [4] σ_R: Electronic parameter for resonance effects (ref. 16). [5] pEMR: -log(EMR). [6] EMR: equi - effective molar ratio: the ratio of the concentration of the test compound and of dequalinium that cause 50% inhibition of the AHP, as determined in the same experiment. [7] In μM. [8] Number of cells tested.

Equation **1** is only a moderate correlation at first glance. It should be noted, however, that σ_P is a descriptor of the *overall* electronic effect of R^4. When this is separated into its inductive and resonance components as represented by σ_I[16] and σ_R[16] respectively interesting correlations result:

$$pEMR = 1.43\ (\pm 1.27)\ \sigma_I - 0.97\ (\pm 0.30) \qquad \mathbf{2}$$
$$n = 7,\ r = 0.45,\ s = 0.477$$

$$pEMR = -1.25\ (\pm 0.26)\ \sigma_R - 1.33\ (\pm 0.16) \qquad \mathbf{3}$$
$$n = 7,\ r = -0.90,\ s = 0.228$$

The blocking potency of the compounds does not correlate with the inductive effect of R^4 but correlates well with its resonance effect. This is consistent with conventional chemical concepts. R^4 is "para" to the positively charged ring nitrogen and is in direct conjugation with it. Therefore, it is likely that the inductive effect of R^4 only operates to a small extent from such a distance, while its resonance effect, being less dependent on distance, would become the dominant factor. The greater resonance effect of R^4 would obviously cause better delocalisation of the positive charge. A plot of pEMR vs σ_R is shown in **Figure 1**.

In conclusion, the 2-methyl group of dequalinium is not important for SK_{Ca} channel blocking activity whereas the 4-amino group makes a substantial contribution. The latter acts neither as a H-bond donor nor as a H-bond acceptor but its replacement by other groups and QSAR on the resultant compounds suggests that its role is electronic via delocalisation of the positive charge of the quinolinium ring.

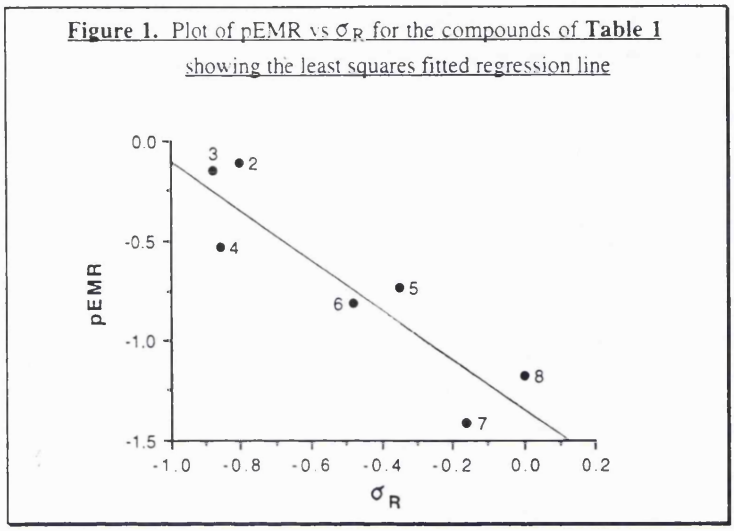

Figure 1. Plot of pEMR vs σ_R for the compounds of **Table 1** showing the least squares fitted regression line

Acknowledgment: This work was supported by the Wellcome Trust (including Fellowships to CAD and PMD).

References and Notes:

1. Cook, N. S. *Trends Pharm. Sci.* **1988**, *9*, 21 - 28.
2. Robertson, D. W.; Steinberg, M. I. *J. Med. Chem.* **1990**, *33*, 1529 - 1541.
3. Watson, S.; Girdlestone, D. *Trends Pharm. Sci. Receptor and Ion Channel Nomenclature Supplement* **1994**, 5th Edition, pp 44 - 47.
4. Haylett, D. G.; Jenkinson, D. H. *Potassium Channels*; Cook, N. S., Ed.; Ellis Horwood Limited: Chichester, 1990; pp. 70 - 95.
5. Lazdunski, M.; Romey, G.; Schmid - Antomarchi, H.; Renaud, J. F.; Mourre, C.; Hugues, M.; Fosset, M. *Hbk. Exp. Pharmacol.* **1988**, *83*, 135 - 145.
6. Renaud, J. F.; Desnuelle, C.; Schmid - Antomarchi, H.; Hugues, M.; Serratrice, G.; Lazdunski, M. *Nature* **1986**, *319*, 678 - 680.
7. Behrens, M. I.; Vergara, C. *Am. J. Physiol.* **1992**, *263*, C794 - C802.
8. Babbs, M.; Collier, H. O. J.; Austin, W. C.; Potter, M. D.; Taylor, E. P. *J. Pharm. Pharmacol.* **1956**, *8*, 110 - 119.
9. Castle, N. A.; Haylett, D. G.; Morgan, J. M.; Jenkinson, D. H. *Eur. J. Pharmacol.* **1993**, *236*, 201 - 207.
10. Dunn, P. M. *Eur. J. Pharmacol.* **1994**, *252*, 189 - 194.
11. Dunn, P. M.; Davis, C. M.; Ganellin, C. R.; Haylett, D. G.; Morgan, J. M.; Jenkinson, D. H. *Br. J. Pharmacol.* **1991**, *104*, 165P.
12. Galanakis, D.; Davis, C.A.; Del Rey Herrero, B.; Ganellin, C.R.; Dunn, P.M.; Jenkinson, D.H. *J. Med. Chem.* **1995**, in press.
13. The compounds appear to be a biologically homogeneous set. Although their selectivity has not been tested systematically, none of them produced obvious broadening of the action potential suggesting that, like dequalinium, they have little effect on other K^+ channels.
14. Rekker, R. F.; de Kort, H. M. *Eur. J. Med. Chem.* **1979**, *14*, 479 - 488.
15. Hansch, C.; Leo, A. *Substituent constants for correlation analysis in chemistry and biology*; Wiley: New York, 1979; pp. 1-8.
16. Charton, M. *Prog. Phys. Org. Chem.* **1981**, *13*, 119 - 251.

(*Received in Belgium* 24 *November* 1994; *accepted* 16 *January* 1995)